

**Ethylene-responsive transcription factors orchestrating  
AM-dependent fatty acid biosynthesis act in complexes  
with Nuclear Factor-Y TFs  
and the key AM regulator RAM1**

Von der Naturwissenschaftlichen Fakultät der  
Gottfried Wilhelm Leibniz Universität Hannover

zur Erlangung des Grades  
Doktorin der Naturwissenschaften (Dr. rer. nat.)

genehmigte Dissertation  
von  
Lisa Hartung, M. Sc.

2021

Referent: Prof. Dr. rer. nat. Helge Küster

Korreferent: Dr. rer. nat. Sascha Offermann

Tag der Promotion: 17.06.2021

## Abstract

The formation and establishment of an arbuscular mycorrhiza (AM) symbiosis between the legume plant *Medicago truncatula* and the soil fungus *Rhizophagus irregularis* is directed by a set of defined genes undergoing transcriptional reprogramming. Along with other groups of transcription factor (TF) genes, *ETHYLENE-RESPONSIVE FACTOR* genes (*ERFs*) showed transcriptional up- or downregulation during AM, indicating a role during this symbiosis. More precisely, recent publications showed that three ERF TFs (*WRI5A*, *WRI5B* and *WRI5C*) play a role in the regulation of AM-dependent fatty acid (FA) biosynthesis and suggested regulatory networks containing ERF TFs in addition to the GRAS TF MtRAM1 as upstream regulators of this process. Nevertheless, these results could not answer the questions, how the stated regulatory networks mediate AM-dependent FA biosynthesis, which factors are included, and which are the direct regulatory targets of TFs involved.

To shed light on these questions, seven AM-upregulated ERF TF genes (*WRI5A*, *WRI5B*, *WRI5C*, *460730*, *15867*, *21492* and *25005*) were analyzed in this thesis.

Reporter gene studies in mycorrhized wild-type, *ram1-1* (mutated in a gene encoding the GRAS TF MtRAM1) and *pt4-2* (mutated in the AM-specific phosphate transporter gene *MtPT4*) roots revealed that all seven *ERF* TF candidate genes are linked to an arbusculated cell with a functioning nutritional exchange. Moreover, gene silencing of selected *ERF* TF genes via RNA-interference (RNAi) revealed downregulation of AM marker genes encoding MtPT4 and MtRAM1 as well as on genes belonging to the AM-dependent FA biosynthesis. Gene silencing additionally showed the downregulation of other selected ERF TF genes, suggesting that the encoded TFs regulate each other.

Interaction studies using Yeast-1-Hybrid (Y1H) revealed a direct regulation of promoters regulating genes encoding components of the AM-dependent FA biosynthesis, while Yeast-2-Hybrid (Y2H) and Bimolecular Fluorescence Complementation (BiFC) studies added regulatory ERF TF-RAM1 and ERF TF-NUCLEAR-FACTOR-Y (NF-Y) complexes to these regulatory networks. In conclusion, data obtained in this thesis therefore indicate complex regulatory networks of ERF TFs, RAM1 and NF-Y that orchestrate AM-dependent FA biosynthesis, allowing insights into the regulation of AM in *M. truncatula*.

**Keywords:** Arbuscular mycorrhiza, symbiosis, ERF transcription factors, RAM1, AM-dependent fatty acid biosynthesis

## Zusammenfassung

Der Aufbau und die Etablierung der arbuskulären Mykorrhiza (AM) Symbiose zwischen *Medicago truncatula* und *Rhizophagus irregularis* wird durch eine definierte Gruppe von Genen, die transkriptionell umprogrammiert werden, gezielt gelenkt. Neben anderen Familien von Transkriptions Faktor (TF) Genen gehören auch *ETHYLEN RESPONSIVE (ERF)* TF Gene zu AM-abhängig regulierten TF Genen. Dies deutet auf eine Rolle der ERF TF Gene während der AM hin. In vorangegangenen Publikationen konnte gezeigt werden, dass neben dem AM-Regulator RAM1 (ein GRAS TF) drei ERF TFs (WRI5A, WRI5B und WRI5C) eine wichtige Rolle während der AM-abhängigen Fettsäure (FS) Biosynthese spielen. Diese Daten weisen auf regulatorische Netzwerke während der AM-abhängigen FS Biosynthese hin, konnten aber bisher nicht Fragen nach den genauen Zielen der regulatorischen TFs beantworten.

Um diese Fragen zu klären, wurden sieben AM-hochregulierte ERF TF Gene (*WRI5A*, *WRI5B*, *WRI5C*, *460730*, *15867*, *21492* und *25005*) in der vorliegenden Dissertation analysiert. Reporter-gen-Analysen in mykorrhizierten Wildtyp, *ram1-1* und *pt4-2* mutierten Wurzeln zeigen, dass die Genexpression aller sieben *ERF* TF Gene von einer Arbuskelhaltigen Zelle mit funktionierendem Nährstoff-Austausch abhängig ist. Des Weiteren führte das *silencing* einiger *ERF* TF Kandidatengene durch RNA-Interferenz (RNAi) zur Herunterregulierung von AM-Markergenen wie *MtPT4* und *MtRam1* sowie von Genen, die Komponenten der AM-abhängigen FA Biosynthese codieren. Ebenso konnten Effekte auf andere *ERF* TF Kandidatengene gezeigt werden, was darauf schließen lässt, dass ERF TFs sich gegenseitig regulieren.

*Yeast-1-Hybrid* (Y1H) Interaktionsstudien konnten eine direkte Interaktion von Promotoren von Genen, die Komponenten der AM-abhängigen FS Biosynthese codieren mit verschiedenen ERF TFs, sowie die gegenseitige Interaktion mit Promotoren von *ERF* TF Genen nachweisen. Zusätzlich zeigten Y2H und *Bimolecular Fluorescence Complementation* (BiFC) Studien, dass ERF TFs in regulatorischen Komplexen mit TFs der *Nuclear-Factor-Y* (NF-Y) Familie und MtRAM1 ihre Funktion ausüben. Basierend auf den Resultaten dieser Doktorarbeit wird die AM-abhängige FS Biosynthese in *M. truncatula* daher von ERF-RAM1 bzw. ERF-NF-Y Komplexen reguliert.

**Schlüsselwörter:** Arbuskuläre Mykorrhiza, Symbiose, ERF Transkriptionsfaktoren, RAM1, AM-abhängige Fettsäure-Biosynthese

## Table of Content

<b>Abstract</b> .....	<b>3</b>
<b>Zusammenfassung</b> .....	<b>4</b>
<b>Introduction</b> .....	<b>7</b>
The model plant <i>Medicago truncatula</i> can establish an arbuscular mycorrhiza symbiosis with the soil fungus <i>Rhizophagus irregularis</i> .....	7
AM formation and establishment in <i>M. truncatula</i> underlies major transcriptional reprogramming.....	9
AM dependent fatty acid biosynthesis is crucial for AMF lipid nourishment .....	12
ERF TFs play a role in different biological conditions including symbiosis .....	15
Three different <i>cis</i> -regulatory elements are known to mediate binding and thereby regulation via ERF TFs.....	18
ERF TFs can build heterodimers with members of the GRAS TF family.....	20
CCAAT-box-binding TFs can interact with ERF TFs on a protein-protein level.....	22
ERF TFs regulate AM-dependent nutritional exchange .....	24
<b>Aim of this thesis</b> .....	<b>28</b>
<b>Material and Methods</b> .....	<b>29</b>
Material .....	29
Strains .....	29
Primer/ Oligonucleotides .....	30
Plasmids.....	36
Media, antibiotics, and supplements .....	44
Methods .....	52
Molecular biological work with bacteria.....	52
Plant work.....	61
Histochemical analysis of <i>M. truncatula</i> .....	62
Yeast work.....	66
<b>Results</b> .....	<b>70</b>
Seven AM-related <i>ERF</i> candidate genes show upregulation during the time course of AM development .....	70
Seven AM-related <i>ERF</i> TF genes are specifically expressed in arbuscule-containing cells.....	75
<i>WRI5A</i> , <i>WRI5B</i> , <i>WRI5C</i> , <i>460730</i> and <i>15867</i> expressions depend on nutritional exchange of mature, active arbuscules .....	79
<i>ERF</i> TF genes show diverging expression patterns, delimiting <i>WRI5A</i> , <i>WRI5B</i> , <i>WRI5C</i> and <i>25005</i> from the other candidate genes .....	83

## Table of Content

---

RNAi knockdowns targeting <i>ERF</i> TF genes reveal effects on mycorrhization and AM-dependent FA biosynthesis genes .....	85
Phenotyping of RNAi roots showed only slight effects on the fungal morphology .....	88
Y1H approaches reveal that <i>ERF</i> TFs and RAM1 regulate promoters of <i>ERF</i> TF and genes belonging to the FA biosynthesis .....	93
Autoactivity tests reveal that all Y1H bait strains can be used for Y1H studies .....	94
The promoter of <i>15867</i> and <i>21492</i> are targeted by <i>ERF</i> TFs and RAM1 in a Y1H approach.....	96
Shortened promoter fragments of <i>p460730</i> and <i>p15867</i> reveal the promoter length needed to provide expression of <i>460730</i> and <i>15867</i> genes .....	99
Genes of the FA biosynthesis are regulated via promoter binding of <i>ERF</i> TF in an Y1H approach.....	106
In Y2H studies, <i>ERF</i> TFs interact with either NF-Y subunits or RAM1 .....	109
Bait strains expressing the proteins RAM1, <i>460730</i> , <i>15867</i> and <i>21492</i> display autoactivation .....	109
<i>ERF</i> TFs interact with AM-upregulated members of the NF-Y TFs .....	112
AM-upregulated NF-Y subunits A and B are involved in the regulation of FA biosynthesis .....	118
<i>ERF</i> TFs do not interact with NF-Y TFs via known protein interacting domains .....	120
RAM1 forms a heterodimer with either WRI5A or WRI5C in Y2H and BiFC approaches .....	122
<b>Discussion .....</b>	<b>127</b>
Seven <i>ERF</i> TFs play a role in the regulatory network of AM-dependent FA biosynthesis .....	127
Expression of AM-upregulated <i>ERF</i> TF genes is dependent on a functioning arbuscule .....	128
Seven AM-upregulated TFs form regulatory networks of <i>ERF</i> TFs.....	130
<i>ERF</i> TFs directly control each other as well as genes of the AM-dependent FA biosynthesis .....	132
<i>ERF</i> TF interact with NF-Ys and RAM1 on a protein-protein level .....	135
<i>ERF</i> TFs, together with RAM1 and NF-Y TFs, conjointly regulate AM-dependent FA biosynthesis in <i>M. truncatula</i> .....	138
<b>References .....</b>	<b>141</b>
Theses .....	159
<b>Abbreviations.....</b>	<b>160</b>
<b>Acknowledgement .....</b>	<b>164</b>
<b>Curriculum Vitae .....</b>	<b>165</b>
<b>Publication list .....</b>	<b>166</b>

---

## Introduction

### **The model plant *Medicago truncatula* can establish an arbuscular mycorrhiza symbiosis with the soil fungus *Rhizophagus irregularis***

The word symbioses, originating from the ancient greek word σύν (together) βίος (living), was originally defined as the interaction of two individuals living in close contact to each other (de Bary, 1879; Gemoll, 1908). In nature, a multitude of varying symbiotic communities can be found, classified as parasitic, commensalistic and mutualistic.

Parasitism is characterised as a relationship of two different species where one partner lives on or in a host even harming it, whereas commensalism describes a form of symbiosis where one partner benefits and the other partner is neither harmed nor benefits from the partnership (Poulin, 2007; Wilson, 1975). A mutualistic symbiosis, also referred to as reciprocal altruism, is defined as a partnership between two species, both benefitting from it. This may either be in an obligate or facultative manner or a mixture of both types (Paracer & Ahmadjian, 1986). A large group of mutualistic symbiosis is the mycorrhiza symbiosis, derived from the greek words *mykes* = fungus and *rhiza* = root, first described and named by Albert Bernhard Frank (Frank, 1885). He observed symbiotic systems between fungi and trees which are restricted to the apoplast of the outer cortex, covering roots with hyphae, displaying an Ectomycorrhizal (ECM) form of mycorrhiza. Besides ECM, further forms of mycorrhiza exist, the most prominent forms being the Arbuscular Mycorrhiza (AM), originating from the latin word *arbuscula* for tree, and the Ericoid Mycorrhiza (ERM) (Cairney, 2000), defined by the resulting fungus – plant structure and the taxonomic groups of participating plants and fungi (Figure 1).

The earliest form of mycorrhiza is probably the AM, which evolved 450 – 500 million years ago, followed by the ECM (200 million years ago) and the ERM (100 million years ago), nowadays appearing together in 90 % of all terrestrial land plants. The goal of these mutualistic types of symbiosis is a bidirectional exchange of carbon (in the form of hexoses and lipids) and mineral nutrients, possibly adjoined by further benefits like abiotic stress and pathogen resistance (Daniell et al., 1999; Govindarajulu et al., 2005; Harrison & Buuren, 1995; Trépanier et al., 2005).

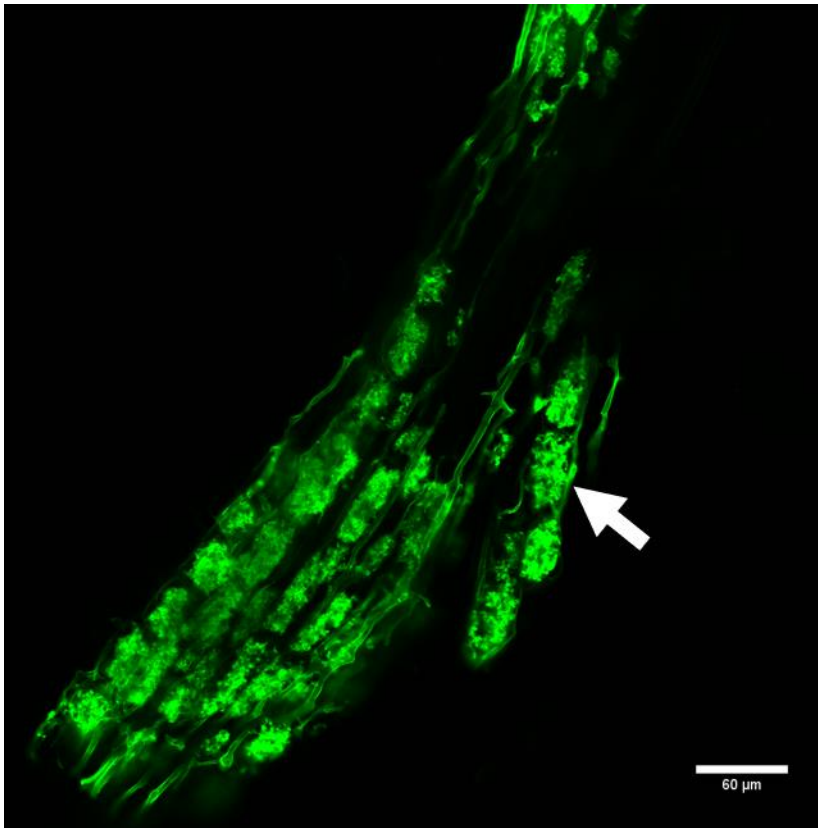


**Figure 1: Arbusculated *M. truncatula* wild type root, revealing the "tree-like" structure of AMF.** The white arrow points towards an arbuscule filling a root cortex cell.

Mostly angiosperms, but also pteridophytes, gametophytes and some lower plants like mosses and lycopods can establish an AM symbiosis (Cairney, 2000). In contrast to this large group of possible AM host plant orders, Arbuscular Mycorrhiza Fungi (AMF) exclusively belong to the monophyletic phylum Glomeromycota (Schwarzott & Walker, 2001). So far, only 150 Glomales are described (Morton & Benny, 1990).

Exemplary for AM symbiosis is the association between the Fabaceae *Medicago truncatula* and the AMF *Rhizophagus irregularis*. During this whole symbiosis, plant root cells of *M. truncatula* undergo huge transcriptomical and physiological changes. *M. truncatula* is a diploid, autogamous and self-fertilising Fabaceae, that is Mediterranean-originated, preferring semi-arid growth conditions (Barker et al., 1990). The plant's genome size is 450 Mb. Its relatively short generation time as well as *Agrobacterium*-transformable root systems and further well-established methods of molecular biology make it a suitable model legume to study bacterial and fungal symbiosis. *M. truncatula* is also able to form a rhizobial symbiosis with *Sinorhizobium meliloti*.



## **AM formation and establishment in *M. truncatula* underlies major transcriptional reprogramming**

During AM symbiosis, the plant undergoes various physiological and transcriptional adjustments to organize the entering of AMF into the root cells and the establishment of a reciprocal nutritional exchange. This exchange, being the very core of the symbiosis, leads to the plant supplying organic carbons in form of sugars and lipids, and receiving inorganic Pi and nitrogen from the fungus (Govindarajulu et al., 2005; Harrison & Buuren, 1995). The Pi homeostasis of the plant thereby plays a determining role for the establishment and maintenance of the symbiosis, in which low levels of Pi lead to the release of strigolactones in the rhizosphere and further AM colonization, whereas high Pi levels reduce arbuscule development (Floss et al., 2013; Liu et al., 2011; Yoneyama et al., 2007) (Figure 2).

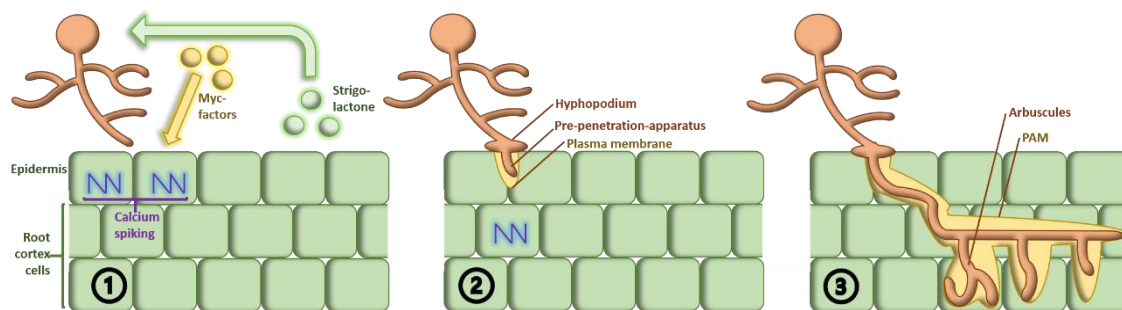


**Figure 2: AM establishment and first arbuscule formation.** 1. Strigolactones released by plant cells (due to a lack of phosphate) induce germination and hyphal branching of AMF. Perception of these plant strigolactones by the AMF leads to secretion of Myc-factors e.g. (Lipo) Chitooligosaccharides, ((L)COs) activating the symbiosis signaling pathway by triggering calcium oscillations. 2. AMF attaches to epidermal cells via a hyphopodium, allowing fungal hyphae to grow inside the plant. This growth is directed by a cluster of cytoskeleton and ER, the Pre-Penetration Apparatus (PPA). Fungal colonization inside the plant is accompanied by the simultaneously growing Peri-Arbuscular Membrane (PAM) built by the host. 3. The inner cortex is colonized by the AMF through hyphal growth. Finally, this leads to the formation of arbuscules in inner root cortical cells (adapted from Oldroyd, 2013).

The “mutual communication” between AMF and *M. truncatula* via strigolactones and other diffusible molecules like Myc-COs/LCOs plays a major role during AM formation and hyphopodium establishment (Bucher et al., 2014; Czaja et al., 2012; Gutjahr & Parniske, 2013; Hohnjec et al., 2015). On the fungal site, perception of strigolactones leads to hyphal branching and growth towards the symbiosis partner. When the AMF cells physically contact the plant root cells, they differentiate and form hyphopodia to attach to the epidermis (Bonfante & Genre, 2010). Hyphae then penetrate the epidermal cells that form a so called Pre-Penetration-Apparatus (PPA), a cytoplasmic bridge across the vacuole filled with endoplasmic reticulum (ER), cytoskeleton and surrounded by a plasma membrane (Genre et al., 2005, 2013). Thereby, the fungus is able to enter the root and grows towards the cortex, accompanied by intracellular structures similar to the PPA.

## Introduction

---

Fungal growth within *M. truncatula* is also conducted by the Peri-Arbuscular Membrane (PAM) that surrounds the developing arbuscules (Gutjahr & Parniske, 2013). Further branching of arbuscules leads to clusters of actin filaments and microtubules around arbuscule branches (Balestrini et al., 1992; Blancaflor et al., 2001; Carling & Brown, 1982). These clusters are probably important for the fragmentation of the plant vacuole, nuclear movement, vesicle trafficking and protein localization.

The PAM is directly connected to the plant cytoplasm and builds, as well as the developing arbuscules, an interface for nutritional exchange via transporters integrated into this membrane (Breuillin-Sessoms et al., 2015; M. J. Harrison, 2002; Kobae et al., 2010; Kobae & Hata, 2010; Luginbuehl et al., 2017; Zhang et al., 2010). Between fungal plasma membrane and PAM, nutrients are transported through the Peri-Arbuscular Space (PAS) via vesicle formations spanning the whole PAS from fungal membrane to the PAM (Ivanov et al., 2019).

Besides clarification of the physiological reorganization of *M. truncatula* root cells, various approaches to analyze the transcriptional changes were made via RNAseq, GeneChip hybridization or quantitative reverse transcriptase Real Time Polymerase Chain Reaction (qRT-PCR) experiments (Fiorilli et al., 2009; Gaude et al., 2012; Gomez et al., 2009; Hoge Kamp & Küster, 2013, Luginbuehl et al., 2017). The resulting profiles revealed a high number of genes activated during AM. Those genes are either active during all stages of mycorrhization or induced in specific stages of AM in different species (Handa et al., 2015; Hoge Kamp et al., 2011; Hohnjec et al., 2015). Up- or downregulation of genes during AM were, amongst others, found in groups of transcription factors (TFs), transporter genes and genes of the plant metabolite biosynthesis e.g. the lipid biosynthesis (Gaude et al., 2012; Hoge Kamp et al., 2011; Hoge Kamp & Küster, 2013; Rich et al., 2015; Xue et al., 2015).

During AM, transcriptomical reprogramming of *M. truncatula* starts with the perception of Myc-LCOs which triggers the Common Symbiotic Signal Pathway (CSSP) via calcium spiking (Chabaud et al., 2011; Genre et al., 2013; Kosuta et al., 2008; Kosuta et al., 2003; Kuhn et al., 2010; Maillet et al., 2011; Mukherjee & Ané, 2011; Oláh et al., 2005) (Figure 3 A). Calcium spiking then leads to the release of a nuclear-localized CALCIUM AND CADMODULIN-DEPENDENT KINASE (CCaMK) from autoinhibition. Interaction with and phosphorylation of a DNA-BINDING COILED-COIL DOMAIN-CONTAINING TRANSCRIPTION FACTOR (CYCLOPS) leads to the activation of other genes important for AM establishment like *REDUCED ARBUSCULAR MYCORRHIZA 1 (RAM1)* (Sun et al., 2015). *Ram1-1* mutant lines fail to build high-order branches of fungal arbuscules and show reduced AMF colonization (Park et al., 2015; Pimprikar et al., 2016; Rich et al., 2015; Xue et al., 2015). These data suggest that RAM1 acts upstream of a pathway that regulates arbuscular branching as well as many other important AM-associated processes.

## Introduction

Expression of *RAM1* starts at stage II of the arbuscule development, where arbuscule trunks are built (Figure 3 B).

In *M. truncatula*, *RAM1* is required for the expression of further AM-specific genes e.g. *M. TRUNCATULA PHOSPHATE TRANSPORTER 4 (MtPT4)* encoding an phosphate transporter active during AM or members of the AM-dependent lipid biosynthesis like *REDUCED ARBUSCULAR MYCORRHIZA 2 (RAM2)* or *FAT REQUIRED FOR ARBUSCULAR MYCORRHIZA SYMBIOSIS (FatM)* (Jiang et al., 2017; Keymer et al., 2017; Luginbuehl et al., 2017; Park et al., 2015; Pimprikar et al., 2016). *MtPT4* expression is induced during stage III –the so called bird foot stage- where low-order branches of the arbuscule are formed. The *MtPT4* transporter protein is exclusively localized at the PAM of fine-branched arbuscules which underlines its function as a phosphate transporter from the PAS into the plant (Pumplin et al., 2012; Pumplin & Harrison, 2009). A loss of *MtPT4* function leads to the premature death of arbuscules (Javot et al., 2007).

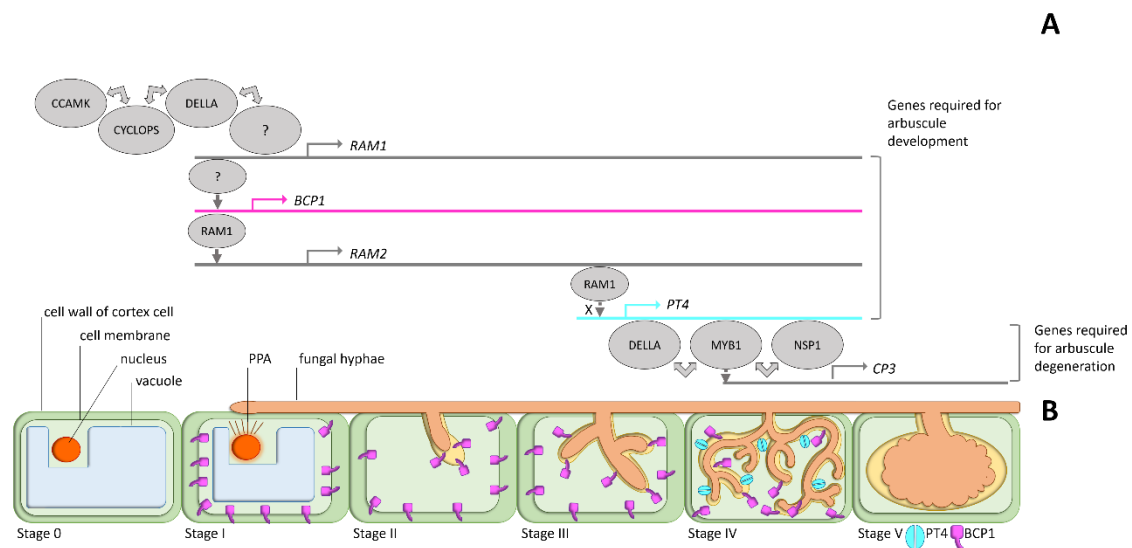


**Figure 3: Physiological transformation of cortex cells during AM stages with corresponding transcriptomical changes. (A)** Different genes play a role during arbuscule development and degeneration. Transcriptional regulation of *RAM1* via the CCaMK-CYCLOPS-DELLA complex leads to the activation of some *RAM1* downstream target genes like *RAM2* and *PT4*, which are all necessary for the fatty acid biosynthesis and the phosphate pathway during AM. Whereas *RAM2* and *PT4* is directly regulated by *RAM1*, *PT4* is regulated by additional factors – not only *RAM1* – indicated by the X. The dotted line at the *PT4* regulation indicates that it remains unclear if *RAM1* directly binds to the *PT4* promoter. Unlike *RAM2* and *PT4*, the *BLUE COPPER PROTEIN 1 (BCP1)* is independent of *RAM1* and important for AM initiation. *M. truncatula* cells containing arbuscules experience a life cycle in which the arbuscule is degenerated after a few days. This last step also requires a set of genes, exemplary shown with the regulation of *CYSTEIN PROTEASE 3 (CP3)* via *MYELOBLASTOSIS 1 (MYB1)*, *NODULATION SIGNALING PATHWAY 1 (NSP1)* and *DELLA*. **(B)** Inner cortex cells of the plant root containing arbuscules undergo a certain lifecycle characterised in 6 stages (0 – VI). (0) cortical cell before PPA formation, (I) PPA formation, (II) arbuscule trunk formation, (III) formation of low-order branches, (IV) mature arbuscule, (V) arbuscule degradation. During this process, AM-specific genes are activated at different stages, regulating different parts of the arbuscular development. Genes required for the regulation of this development can be split in two groups: Genes needed for arbuscule development and genes involved in arbuscule degeneration. *RAM2* and *RAM1* are activated at early stages (I and II) and are required until stage IV. The *RAM1*-dependent expression of *PT4* starts at stage III and lasts until stage IV. *CP3* activation begins with stage IV and stays until the arbuscule is degenerated (adapted from Pimprikar & Gutjahr, 2018).

**AM dependent fatty acid biosynthesis is crucial for AMF lipid nourishment**

Since the Pi homeostasis of plants plays a special role during establishment and maintenance of AM, the already mentioned MtPT4 is crucial for a functioning AM. *MtPT4* belongs to a large family of phosphate transporter genes (Pht1 family), divided into four subfamilies: I, II, III and IV. Whereas members of subfamily IV are not mycorrhiza-induced and subfamilies II and III are only partial mycorrhiza-inducible, members of subfamily I are exclusively expressed during AM (Loth-Pereda et al., 2011; Nagy et al., 2005; Walder et al., 2015). The gene *MtPT4*, as well as its homologues *Lotus japonicus PT4* (*LjPT4*), *Zea mays PT6* (*ZmPT6*) or *Oryza sativa PT11* (*OsPT11*) are all included in the subfamily I, revealing impaired mycorrhiza and dysfunctional AM-dependent phosphate-uptake when disrupted (Javot et al., 2007; Xue et al., 2018; Yang et al., 2012) (Figure 4). The encoded phosphate transporters are all located in the PAM, controlling Pi influx from the Periarbuscular Interface (PAI) into the arbusculated cortex cells. The driving force for this influx is a proton gradient generated via the symporter H<sup>+</sup>ATPase encoded by the *mycorrhiza-inducible H<sup>+</sup>ATPase* (*HA1*) gene in *M. truncatula*, *L. japonicus* and other mycorrhized plant species. HA1 is essential for phosphate delivery and arbuscular development in species like *M. truncatula* or *O. sativa* (Bucher, 2007).

As well as phosphate nutritioning of the plant, provision of fatty acids also plays a central role for AMF since the fungus is packed with vesicles, hyphae and spores containing lipids. In contrast to earlier models, where carbohydrates, delivered by the host plants, were thought to be converted into lipids by AMF, it has been lately proposed that AMF are directly supplied with long-chain fatty acids (FA) (Kamel et al., 2017; Trépanier et al., 2005; Wewer et al., 2014). This idea is based on the finding that AMF lack the ability to synthesize long-chain FAs *de novo* because of a missing fatty acid synthase (FAS) that can be found in other eukaryotes (Ropars et al., 2016; Tang et al., 2016; Tisserant et al., 2013). Thus, AMF are dependent on their host plant for FA supply. In addition, a linear pathway for *de novo* FA biosynthesis has been stated, that provides long-chain FAs to the fungus during mycorrhizal colonization (Bravo et al., 2017; Jiang et al., 2017; Keymer et al., 2017; Luginbuehl et al., 2017) (Figure 4).

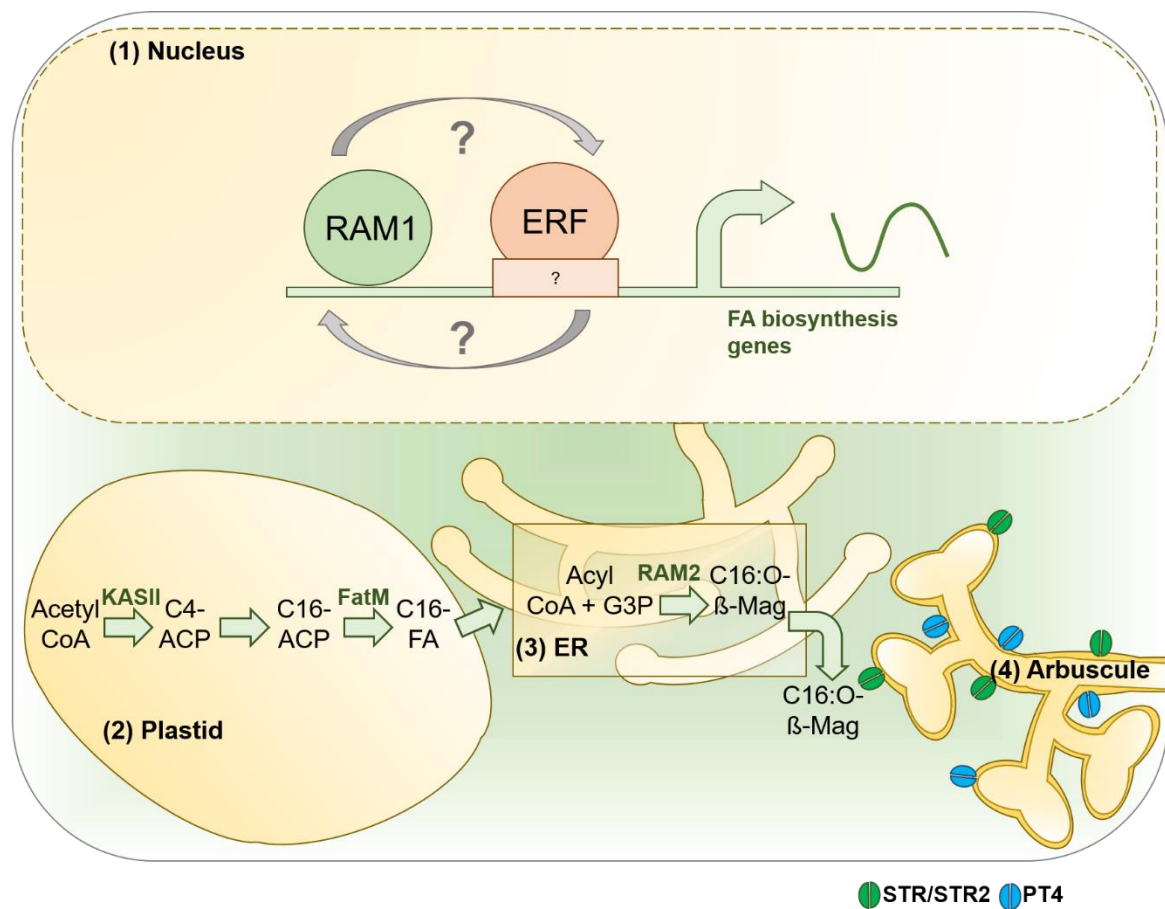


**Figure 4: The FA biosynthesis is AM-dependent.** (1) ERF TFs as well as the GRAS TF RAM1 regulate FA biosynthesis genes in the nucleus (Luginbuehl et al., 2017; Jiang et al., 2018). (2) In the plastids, RAM1 induces the  $\alpha$ -KETO-ACYL CARRIER PROTEIN (ACP) SYNTHASE (KAS) III that elongates C2:0-ACP to C4:0-ACP. C4:0-ACP is extended to C16:0-ACP by DISORGANIZED ARBUSCULE (DIS) (Keymer et al., 2017). The AM-specific acyl thioesterase FatM then releases C16:0 from its carrier ACP and the FA is exported to the cytosol, conjugated to CoA and transported to the Endoplasmic Reticulum (ER). (3) In the ER, the RAM2-encoded GLYCEROL-3-PHOSPHATE ACYL TRANSFERASE (GPAT) attaches C16:0-FA to the second carbon of glycerol-3-phosphate to form C16:0 MONOACYLGLYCEROL (C16:0  $\beta$ -MAG). (4) C16:0  $\beta$ -MAG is then exported to the Periarbuscular Interface (PAI) by STUNTED ARBUSCULE/ STUNTED ARBUSCULE 2 (STR/STR2), two members of the ATP BINDING CASSETTE TRANSPORTER SUBFAMILY G (ABCG) (Bravo et al., 2017; Jiang et al., 2017; Keymer et al., 2017). C16:0-FAs can be imported into the fungal cytosol and e.g., be converted into Triacylglycerol (TAG). Import mechanisms into the fungal cytosol remain widely unclear (adapted from Choi et al., 2018).

In this pathway, the AM-specific transcription factor RAM1 plays a major role, inducing an early step of FA elongation and acting upstream of important structural genes like *RAM2* or *FatM* (Luginbuehl et al., 2017). A whole-genome sequencing approach, using RNA isolated from mycorrhized *ram1-1* mutant versus mycorrhized Wildtype (WT) roots, not only revealed the RAM1 dependency of those FA biosynthesis regulators but also showed the

## Introduction

---

dependency of three ERF TFs, WRINKLED 5 ETHYLENE-RESPONSIVE FACTORS (WRI5 ERF TFs), WRI5A, B and C (Luginbuehl et al., 2017).

**ERF TFs play a role in different biological conditions including symbiosis**

ERF TFs genes belong to the *APETALA 2 (AP2)/ ERF* gene family of plant specific transcription factors. This family consists of five subfamilies, classified in accordance to a shared DNA binding domain and its repetitions (Sakuma et al., 2002). The five subfamilies contain the following groups: *AP2*, *ERF*, *DEHYDRATION-RESPONSIVE ELEMENT-BINDING PROTEIN/ C-REPEAT BINDING FACTOR (DREB/CBF)*, *RELATED TO ABSISIC ACID 3/ VIVIRAOUS 1 (RAV)* and *SOLOSIT* (Sakuma et al., 2002). The ERF TF subfamily functions during abiotic and biotic stress responses to pathogens or drought, heat and salt stress.

These stress conditions and the role of ERF TFs in conjunction with ethylene is very well studied in *A. thaliana* (Cheng et al., 2013; Zhao & Schaller, 2004). Studies, dealing with this topic, revealed that the plant hormone ethylene is a key mediator in the stress signaling and response pathway. Increasing levels of ethylene trigger the ethylene signaling pathway which finally leads to the activation of ERF TFs binding either to DRE-elements as a reaction to abiotic stress or to the GCC-box (AGCCGCC motive) during pathogen stress (Chen et al., 2005; Gao et al., 2003; Huang et al., 2003; Ju et al., 2012; Kendrick & Chang, 2008; Kieber et al., 1993; Lacey & Binder, 2014; Solano et al., 1998). The binding of ERF TFs either to a DRE-element or to a GCC-box results in an activation of stress response genes corresponding to the actual stress condition.

Abiotic stress response via ERF TFs binding to DRE-elements is not only known in *A. thaliana*, but also in several other plant species, including *Glycine max*, *Capsicum annum* and *Nicotiana tabacum* (Lee et al., 2004; Wu et al., 2007; Zhang et al., 2009).

Response to abiotic and biotic stress in *M. truncatula* is likewise mediated by members of the ERF TF family including WXP1, a factor involved in drought stress response by enhancing cuticular waxes or ETHYLENE RESPONSE FACTOR REQUIRED FOR NODULE DIFFERENTIATION (MtEFD) (Moreau et al., 2014; Zhang et al., 2005). Interestingly, MtEFD positively effects pathogen susceptibility of *Ralstonia solanoceum* on the one hand, and controls nodule differentiation and number during nodule symbiosis with *S. meliloti*, on the other (Vernie et al., 2008). The model pathway to regulate pathogenic interaction between *R. solanoceum* and *M. truncatula* hereby very much resembles the regulatory pathway of nodule symbiosis including cytokinins and the CYTOKININ RESPONSE 1 FACTOR (MtCRE1) (Laffont et al., 2015; Moreau et al., 2014). The suggested double function of MtEFD in pathogen susceptibility and nodule symbiosis regulation is a fitting example for the close connection of pathogen and symbiosis response regulation, the latter, amongst others, being regulated by ERF TFs in *M. truncatula*.

## Introduction

Besides MtEFD, three other ERF TFs called ERF REQUIRED FOR NODULATION 1, 2 and 3 (ERN1, 2, 3) are known to regulate rhizobial symbiosis by binding NF-boxes (Andriankaja et al., 2007; Cerri et al., 2012; Cerri et al., 2017; Middleton et al., 2007). The exact regulatory mechanism of these three genes in early signaling and infection stages is very well understood, revealing transcriptional activation of genes like *Mt EARLY NODULIN 11* (*MtENOD11*) by ERN1 and ERN2 in reaction to Nod Factor (NF) signaling (Figure 5). In opposite to this, ERN3 acts as a repressor, controlling *MtENOD11* expression before and during rhizobial infection in cells adjacent to root hair infections. Interestingly, transcriptional activation of *MtENOD11* via the NF-box requires a GCC-like motive, which underlines the central role of the GCC-box for transcriptional regulation via ERF TFs.

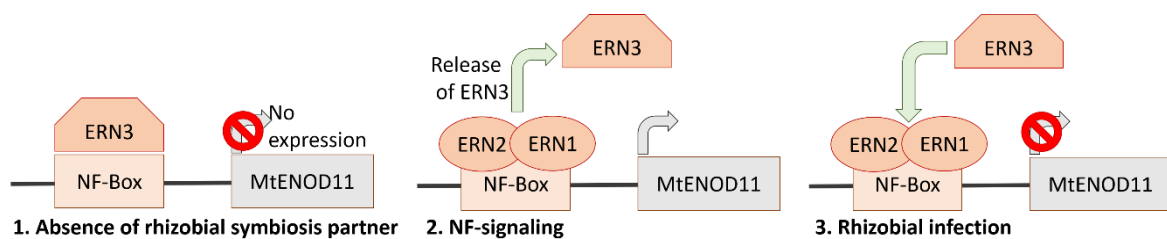


**Figure 5: ERF TFs ERN1, ERN2 and ERN3 control nodule symbiosis via a *cis*-regulatory element on the promoter of *MtENOD11*.** 1. In the absence of a rhizobial symbiosis partner, the expression of *MtENOD11* is repressed through ERN3 binding to the NF-box. 2. When NF-signalling by a nearby *Rhizobium* starts, ERN3 is released from the NF-box, *ERN2* and *ERN1* expression is upregulated and the two TFs bind to the NF-box, thereby conveying transcriptional activation of *MtENOD11*. 3. During progressing rhizobial infection, *ERN3* expression is upregulated again, resulting in ERN3 replacing ERN1 and 2 as binding partners at the NF-box. This leads to the transcriptional repression of *MtENOD11* (adapted from Andriankaja et al., 2007).

Further studies revealed that ERN1 and ERN2, although showing overlapping expression patterns and being close homologues, control divergent parts of rhizobial infection, revealing a regulatory network of these ERF TFs during rhizobial symbiosis (Cerri et al., 2012; Cerri et al., 2017) (Figure 6).



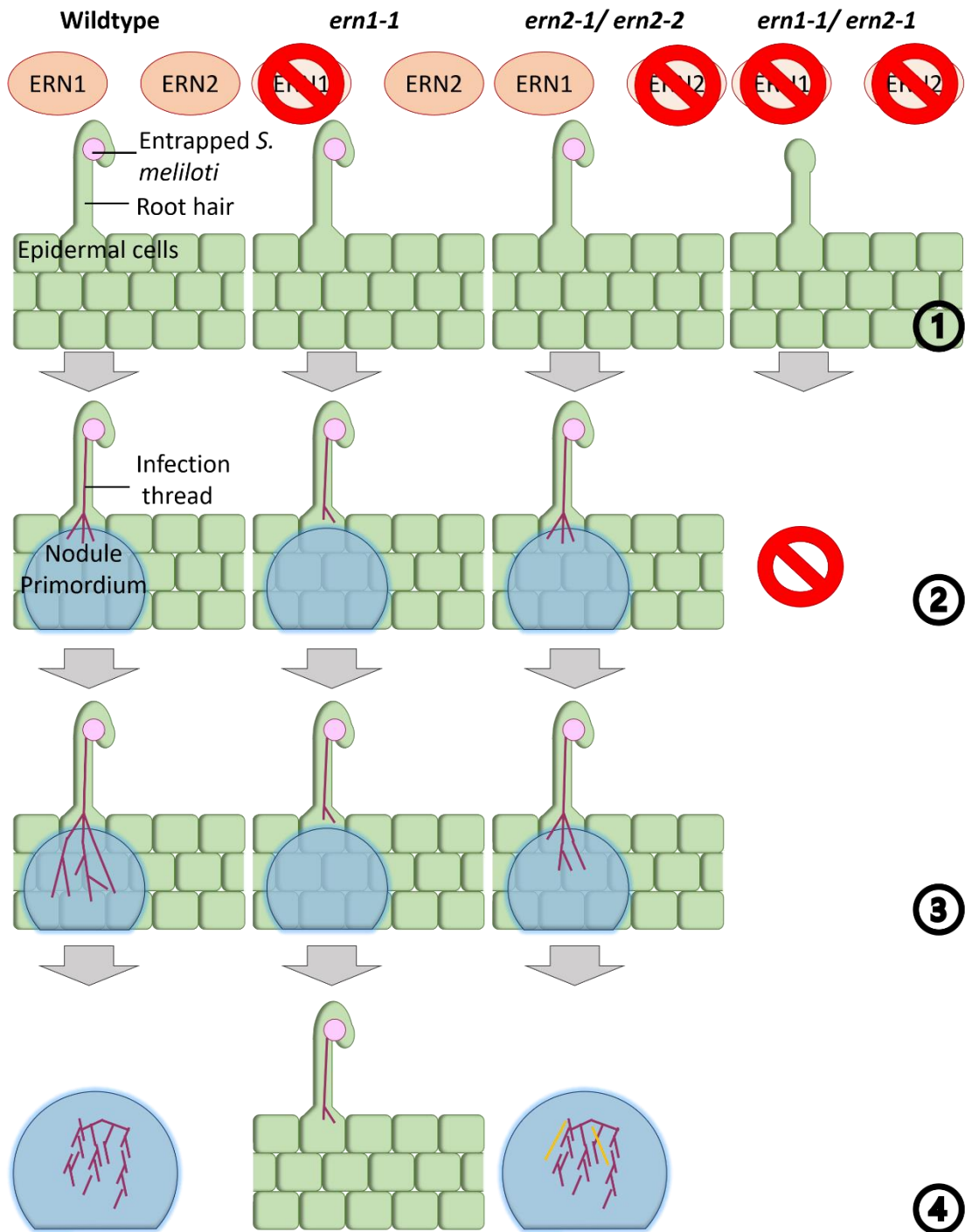


**Figure 6: The ERF TFs ERN1 and ERN2 display different functions in the regulation of rhizobial symbiosis in *M. truncatula*.** 1. In the wild type, with functioning ERN1 and ERN2, as well as in the *ern1-2*, *ern2-1/ern2-2* mutant lines, root hairs are built due to NF-signalling, entrapping rhizobial bacteria by swelling at the tip. The double mutant line *ern1-1/ern2-1* fails to initiate root hair infection followed by nodule development. 2. ERN1 alone is sufficient for the progression of the infection thread (shown as purple lines) (see: *ern2-1/ern2-2*) whereas ERN2 (*ern1-1* mutant line) alone is not able to provide proper root hair colonization and nodule organogenesis. Mutant lines missing functional ERN1 arrest at this step. 3. In contrast to the wild type, *ern2-1/ern2-2* mutant lines are less efficient in root colonization. 4. Compared to the wild type, mutant lines missing ERN2 show signs of premature nodule senescence (shown with yellow lines) (adapted from Cerri et al., 2016).

---

### **Three different *cis*-regulatory elements are known to mediate binding and thereby regulation via ERF TFs**

To control regulatory targets during the various abiotic and biotic stress responses, ERF-TFs can bind to different *cis*-regulatory elements on their target promoters. These elements are conserved among different plant species including *A. thaliana*, *L. japonicus* or *M. truncatula* (Allen et al., 1995; Cerri et al., 2012; Hao et al., 1998; Jiang et al., 2018; Xue et al., 2018; Yamasaki et al., 2013). So far, three important elements are known: the GCC-box, the AW-box and the CTTC motive. The AP2/ERF GCC-BOX BINDING DOMAIN (GBD) consists of ca. 60 Amino Acids (AA) folding into three antiparallel  $\beta$ -sheets followed by one  $\alpha$ -helix (Allen et al., 1995; Yamasaki et al., 2013). These 60 AAs are highly conserved among members of the AP2/ ERF TF family. The arrangement of the secondary structural elements resembles zinc fingers, but in contrast to those, DNA-binding via GBD is conveyed by  $\beta$ -sheets and not the  $\alpha$ -helix motive. ERF TF genes can contain one or more GDB binding motifs. The GBD binding to the GCC-box and the following regulation of target genes was first identified in *A. thaliana* ERF TFs, but also exists in e.g. *M. truncatula* ERN2 (Allen et al., 1998; Cerri et al., 2016). As mentioned above, studies showed that ERN2 is an important regulator of rhizobial symbiosis (Andriankaja et al., 2007; Cerri et al., 2012, 2016; Middleton et al., 2007). Point mutations in the thereby used *ern2-1* mutant line targeted a conserved C-terminal Threonine in the third  $\beta$ -sheet of the *M. truncatula* GBD, leading to the loss of a crucial hydrogen bond and therefore to an unstable binding to the targeted GCC-box (Cerri et al., 2016). Comparative modelling of the same point mutation in the *AtERF1* GBD displayed a similar result, underlining the conservation of this motive in different plant species.

Similar to the GBD and its target the GCC-box, ERF TFs binding to the AW-box can be found in *A. thaliana* as well as in *M. truncatula* (Jiang et al., 2018; Maeo et al., 2009). The conserved AW-box motive 5'-[CnTnG]<sub>n</sub>[CG]-3' could be identified in the promoter of many ERF TF target genes. In *A. thaliana*, target genes of *AtWRI1* involved in FA synthesis during seed development including a pyruvate kinase (PI-Pk $\beta$ 1), an acetyl CoA carboxylase (BCCP2) and ketoacyl- acyl carrier protein synthase (KASI) contained an AW-box motive on their promoters. The AW-box motifs present on those promoters were located at the transcription start site (TSS) on the 5' Untranslated Region (UTR). It can either be bound by *M. truncatula* WRI5A in the *pSTR* or *pPT4* or by *L. japonicus* CBX1 to regulate expression of FA biosynthesis genes. Apart from the AW-box, regulation of *LjpPt4* via CBX1 is also mediated by the CTTC motive (Xue et al., 2018).

In contrast to the GCC-box and the AW-box, the CTTC motive mediated ERF TF regulation could exclusively be found in *L. japonicus*. Nevertheless, the identified core motive 5'-

## Introduction

---

**CTTCTTGTTCT**- 3' (nucleotides crucial for binding emphasized in bold letters) could be identified in *PT4*-homologues of several other plant species showing activation by CBX1. To put it in a nutshell, the data presented so far on either the AW-box, the GCC-box motive and the CTTC motive indicate conserved binding motifs for FA synthesis regulation and phosphate uptake via ERF TFs. Besides the very-well studied targets of WRI5A and the exact regulation of those, the regulation by further ERF TFs in *M. truncatula* remains elusive.

### **ERF TFs can build heterodimers with members of the GRAS TF family**

The already mentioned TF RAM1 belongs to a large family of plant specific TFs, the GIBBERELLIN-INSENSITIVE (GAI), REPRESSOR OF GAL1-3 (RGA) OR SCARECROW (SCR) (GRAS) TFs (Di Lorenzo et al., 1996; Peng et al., 1997; Raikhel, 1992). This family of TFs is characterized by the conserved GRAS domain motive localized in the C-terminal region that was first analyzed in *A. thaliana* (Pysh et al., 1999) (Figure 7).



**Figure 7: Five domains are conserved in the GRAS TF family.** The C-terminus of the GRAS TF family consists of LEUCINE HEPTADE REPEATS I and II (LHRI and LHRII), which flank VHIID, followed by a PFYRE and a SAW domain. LHRs might mediate multimerization of GRAS proteins. The N-terminus is highly variable, although often containing domains conserved within GRAS TF subfamilies like DELLA or SCARECROW LIKE (SCL). Putative NUCLEAR LOCALIZATION SEQUENCES (NLSs) can be found in SCLs and other GRAS protein domains. Figure not to scale (adapted from Pysh et al., 2002).

The GRAS TF family is further divided into eight subfamilies, often classified by common binding motifs in the N-terminus. This large family of TFs can be found in various plant species like *A. thaliana*, *L. japonicus*, *M. truncatula* and *O. sativa* (Heckmann et al., 2006; Kaló et al., 2005; Lee et al., 2006; Tian et al., 2004; Tong et al., 2009). GRAS TFs are regulators of many different abiotic and biotic stress responses also regulating rhizobial as well as AM symbiosis in *M. truncatula* and *L. japonicus* (Czaja et al., 2012; Floss et al., 2013; Gobbato et al., 2012; Maillet et al., 2011; Xue et al., 2015).

Rhizobial symbiosis is conducted by two GRAS TFs NSP1 and NSP2, which are able to form homo- and heterodimers (Czaja et al., 2012; Hirsch et al., 2009; Maillet et al., 2011). Activated by CCaMK, these two TFs form a heterodimer allowing NSP1 to bind *pENOD11*. Interestingly, NSP2 not only functions in rhizobial, but also in AM symbiosis, where it is known to dimerize with RAM1 to induce the *RAM2* encoded GPAT in order to initiate AM-dependent FA biosynthesis together with the biosynthesis of cutin and suberin (Gobbato et al., 2012; Xue et al., 2015). Besides dimerization with NSP2, RAM1 is also able to dimerize with AM-upregulated REQUIRED FOR ARBUSCULE DEVELOPMENT 1 (RAD1) in *L. japonicus* and DELLA-INTERACTING PROTEIN 1 (DIP1) from *O. sativa* (Xue et al., 2015). The RAD1-RAM1 interaction in *L. japonicus* is an important part of AM regulation, since *Ljrad1* mutant lines display a reduced number and accelerated degeneration of arbuscules (Park et al., 2015). The DIP1-RAM1 interaction, along with the NSP2-RAM1 and the RAD1-RAM1 heterodimers show, that GRAS TFs are part of a complex regulatory network with RAM1 playing a major role in the regulation of AM. These examples further show, that RAM1 is not able to bind to its target DNA alone, but instead needs a dimerization partner. During AM-dependent FA biosynthesis, RAM1 and the WRIs are placed at a similar

## Introduction

---

regulatory position, but the connection between these TFs remains unclear (Jiang et al., 2018; Luginbuehl et al., 2017; Xue et al., 2018).

In this context, it is worth mentioning that GRAS TFs and members of the AP2/ERF TF group are known to heterodimerize in order to control wound defenses and responses as well as chitin induction in *A. thaliana* (Heyman et al., 2016, 2018; Son et al., 2012) (Figure 8). There are various examples for AP2/ERF-GRAS dimers, including *At*ERF114 and *At*ERF115, that belong to the special subfamily X of the EREB/ DREB family of ERF TFs. The X subfamily is characterized by one AP2 binding domain and a conserved AA motive. Binding of ERF TFs to their wound defense and response target genes is mediated by GRAS TFs. GRAS TFs hereby do not directly bind to the target promoter (Gao et al., 2004, 2015). Instead, they post transcriptionally control the regulation of the target gene via recruitment of histone-modifying enzymes like *A.t.* HISTONE DEACETYLASE 19 (*At*HDA19) (Gao et al., 2004, 2015; Zhou et al., 2005).

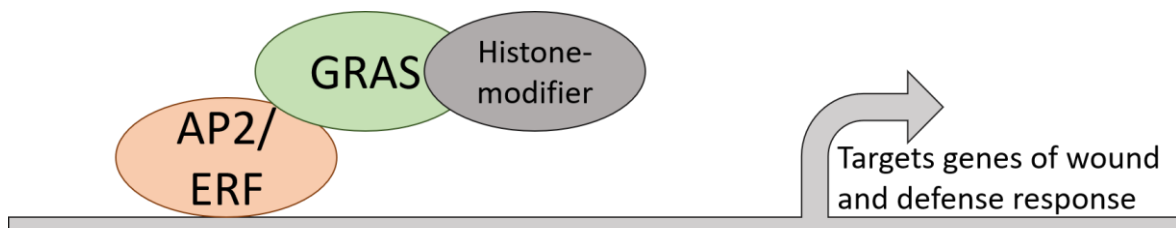


**Figure 8: AP2/ERF TFs and GRAS TFs heterodimerize to regulate wound defense.** Current regulatory model of wound defense in *A. thaliana*, showing the heterodimerization of ERF TFs and GRAS TFs. ERF TFs then bind the promoter of their target genes, whereas GRAS TFs are thought to recruit histone-modifier for posttranscriptional regulation (adapted from Heyman et al., 2018).

These examples show that a potential dimerization between ERF TFs and GRAS TFs is possible and might also be true for RAM1 and the WRIs to regulate lipid biosynthesis during AM.

---

**CCAAT-box-binding TFs can interact with ERF TFs on a protein-protein level**

Similar to GRAS TFs, CCAAT-BOX-BINDING TFs (CBFs), also referred to as NUCLEAR FACTOR Y (NF-Y), are equally known to interact with ERF TFs (Laloum et al., 2013; Zhiguo et al., 2018). In contrast to ERF and GRAS TFs, NF-Y TFs exist in all higher eukaryotes, including yeast, plants and mammals and are involved in the regulation of many different processes like FA biosynthesis, stress response and endosperm development in plants (Combiere et al., 2006; Forsburg & Guarente, 1989; Mantovani, 1999; Rangan et al., 1996; Roder et al., 1997; Schweizer et al., 2002; Siefers et al., 2009; Vernie et al., 2008; Xu et al., 2016; Zhiguo et al., 2018).

Notably, NF-Y TFs consist of three different subunits: NF-YA, B and C, which need to build a heterotrimeric complex in order to function as a TF and regulate downstream target genes (Coustry et al., 1996; Gnesutta et al., 2017; Laloum et al., 2013; Sinha et al., 1996). The stepwise assembly of this heteromer starts with the dimerization of the B- and C-subunit in the cytoplasm (Romier et al., 2003; Sinha et al., 1996; Xing et al., 1994). The B-C dimer is then transported into the nucleus, where a NF-YA subunit can bind to the complex. The added NF-YA subunit mediates binding to a CCAAT-box motive on target promoters via the CCT-motive in the so called A2 domain. Proteins, that share a CCT-motive similar to the A2 domain can replace NF-YA in the heterotrimer (Wenkel et al., 2006).

The contact between the NF-YA subunit and the B-C dimer is stabilized by an  $\alpha$ -helix motive, referred to as A1 domain on the NF-YA AA sequence (Mantovanis et al., 1994; Xing et al., 1994). NF-Ys can act as repressors or activators and often regulate their target genes through posttranscriptional modifications (Caretto et al., 1999; Dolfini et al., 2012; Donati et al., 2008; Gatta & Mantovani, 2011, 2013). Interestingly, NF-YB and C-subunits resemble the core histone fold motive of H2B in structure and AA sequence (Dolfini et al., 2012).

In mammals, only one gene for each subunits exists, whereas in plants whole genome duplications and single gene tandem duplications led to a variety of encoded NF-Y subunits (Maere et al., 2005). This variety of NF-Ys in plants results in a structural and functional diversification of NF-Ys, even causing phylogenetically related subgroups of NF-Ys that fulfil specified regulatory tasks (Baudin et al., 2015; Xie et al., 2008).

NF-Ys not only build heterotrimeric complexes, but even establish tetrameric complexes with a fourth binding partner, potentially via an  $\alpha$ -helix motive of the NF-YB or C subunit (Romier et al., 2003). In *O. sativa*, this fourth subunit is an ERF TF, regulating endosperm development conjointly with OsNF-YA8 and a B- and C-subunit (Bai et al., 2016; Sun et al., 2014; Zhiguo et al., 2018) (Figure 9).

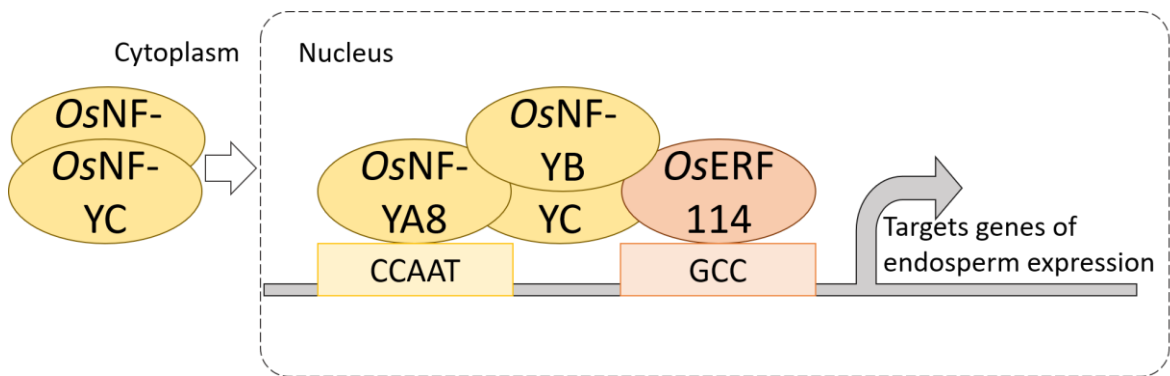


**Figure 9: Endosperm development in *O. sativa* is regulated by a tetrameric complex of NF-Ys and OsERF114.** Dimerization of two B- and C-subunits leads to the transport of the complex into the nucleus. Here, addition of the OsNF-YA8 subunit and OsERF114 results in the expression of target genes. OsERF114 binding to the target promoter is mediated by binding to a GCC-box, whereas OsNF-YA8 binds the CCAAT-motive via its CCT domain (adapted from Zhigou et al., 2018).

In *A. thaliana* and *Z. mays*, ERF TFs and NF-Ys are known to be important regulators of oil accumulation in seeds (Baud et al., 2007; Cernac & Benning, 2004; Lotan et al., 1998; Maeo et al., 2009; Mu et al., 2008; Santos-Mendoza et al., 2008; Shen et al., 2010). Overexpression of *AtWRI1* and the NF-Y TF *AtLEC1* leads to higher TAG levels. When overexpressed, *ZmLEC1* overexpression equally results in an increase in seed oil production, but additionally reduces germination and growth. Co-overexpressing *ZmWRI1* uncouples the unwanted effects of *ZmLEC1* and augments seed oil production on his parts, too. NF-Ys do not only regulate FA biosynthesis in plants but also in mammals, which possibly points to a conserved role of NF-Ys in FA biosynthesis regulation, similar to ERF TFs (Rangan et al., 1996; Roder et al., 1997; Schweizer et al., 2002).

NF-Ys also regulate ERF TFs by binding to their promoters, thereby regulating the gene's expression (Laloum et al., 2013). An example for this is the regulation of rhizobial infection in *M. truncatula* via ERN1 and its binding to the *pENOD11* (Andriankaja et al., 2007; Cerri et al., 2012; Hirsch et al., 2009; Laloum et al., 2013; Middleton et al., 2007). *ERN1* expression, in turn, is regulated by the redundantly functioning NF-Y A1 and 2, which directly bind to *pERN1*.

During AM symbiosis in *M. truncatula*, three NF-Y genes are significantly upregulated and encode the B-subunit CBF3 (NF-Y B7) and the two C-subunits CBF1 (NF-Y C6) and CBF2 (NF-Y C11) (Czaja et al., 2012; Hoge Kamp et al., 2011). The promoters of *CBF1* and 2 accompany fungal infection from the first physical contact on, indicating a function of the two NF-Ys during the whole AM. Nevertheless, the potential targets and further binding partners of NF-Ys remain widely unclear and need further examination. Considering the fact that NF-Y TFs are known to interact with ERF TFs on a protein-protein level, it would be worth investigating these interactions in the *M. truncatula* AM symbiosis.

### **ERF TFs regulate AM-dependent nutritional exchange**

In contrast to the well-established function of ERF TFs in the rhizobial symbiosis, the regulatory tasks of ERF TFs during AM are only partially understood. Nevertheless, due to more recent findings it is clear that the three ERF TFs *WRI5A*, *WRI5B* and *WRI5C* play an important role during AM-dependent nutritional exchange of C16-FA and phosphate transport (Jiang et al., 2017; Liu et al., 2020; Luginbuehl et al., 2017; Xue et al., 2018). *WRI5* TF genes were first linked to the FA biosynthesis via phylogenetic analyses, based on their homology to the *AtWRI1* gene (Cernac & Benning, 2004; Focks & Benning, 1998; Luginbuehl et al., 2017). The name WRINKLED is derived from the *A. thaliana wri1* mutant line which displays wrinkled, incompletely filled seeds lacking the essential function of *AtWRI1* controlling seed metabolism pathway from sucrose import to oil storage and accumulation in seeds. Like their *A. thaliana* homologue, *WRI5A*, *B* and *C* positively induce TAG production (Jiang et al., 2018; Luginbuehl et al., 2017). Together with the finding that *WRI5A*, *B* and *C* as well as *FatM*, *RAM2* and *ABCG3* are not expressed in mycorrhized *ram1-1* roots compared to colonized wild type roots, it was stated that *WRI5* TFs must play a role in the AM-dependent FA biosynthesis.

Overexpression studies of *WRI5A* and *RAM1* in mycorrhized *M. truncatula* roots underline these results and indicate a regulatory role of both *WRI5A* and *RAM1* during this FA biosynthesis (Jiang et al., 2018). Interestingly, in both cases overexpression led to an activation of *RAM2*, *FatM*, and *MtPT4*. The *RAM1*-overexpression construct additionally activated *WRI5A*, *B* and *C* expression, whereas roots containing the *WRI5A* construct displayed enhanced *RAM1* expression as well as transcriptional activation of *STR* and an increased level of C16:0 FAs.

*M. truncatula* transient knockdown or stable mutant lines of *WRI5A* display a lower amount of fully developed arbuscules as well as decreased overall colonization by the AMF. The overall effects on the AMF were stronger in the RNAi knockdown lines compared to the stable *wri5a* mutant line indicating only a partial loss-of-function mutation. The Tnt1-insertion relatively close to the stop codon in the *wri5a* mutant line, in contrast to the more upstream positioned RNAi constructs, might be an explanation for this reduced mycorrhizal phenotype. Even stronger effects on fungal colonization could be observed in a triple RNAi knockdown construct of *WRI5A*, *WRI5B* and *WRI5C*. This triple knockdown also led to a downregulation of *RAM1*, *STR* and *MtPT4* expression. Besides the *WRI5A* phenotype, *M. truncatula* roots containing an amirRNA construct of *WRI5B*, also referred to as *ERF1*, revealed a decreased overall AM colonization and truncated arbuscules (Devers et al., 2013). In summary, recent findings on *WRI5* TFs suggest that *RAM1* and *WRI5A* act in a positive feedback loop by enhancing each other's expression resulting in upregulation of



target genes belonging to the AM-dependent phosphate transport and FA biosynthesis. The suggested role of the WRI5s TFs during AM-dependent lipid biosynthesis as well as the regulatory function of *AtWRI1* in TAG production indicates a conserved role of ERF TFs in the regulation of TAG production (Jiang et al., 2018; Luginbuehl et al., 2017).

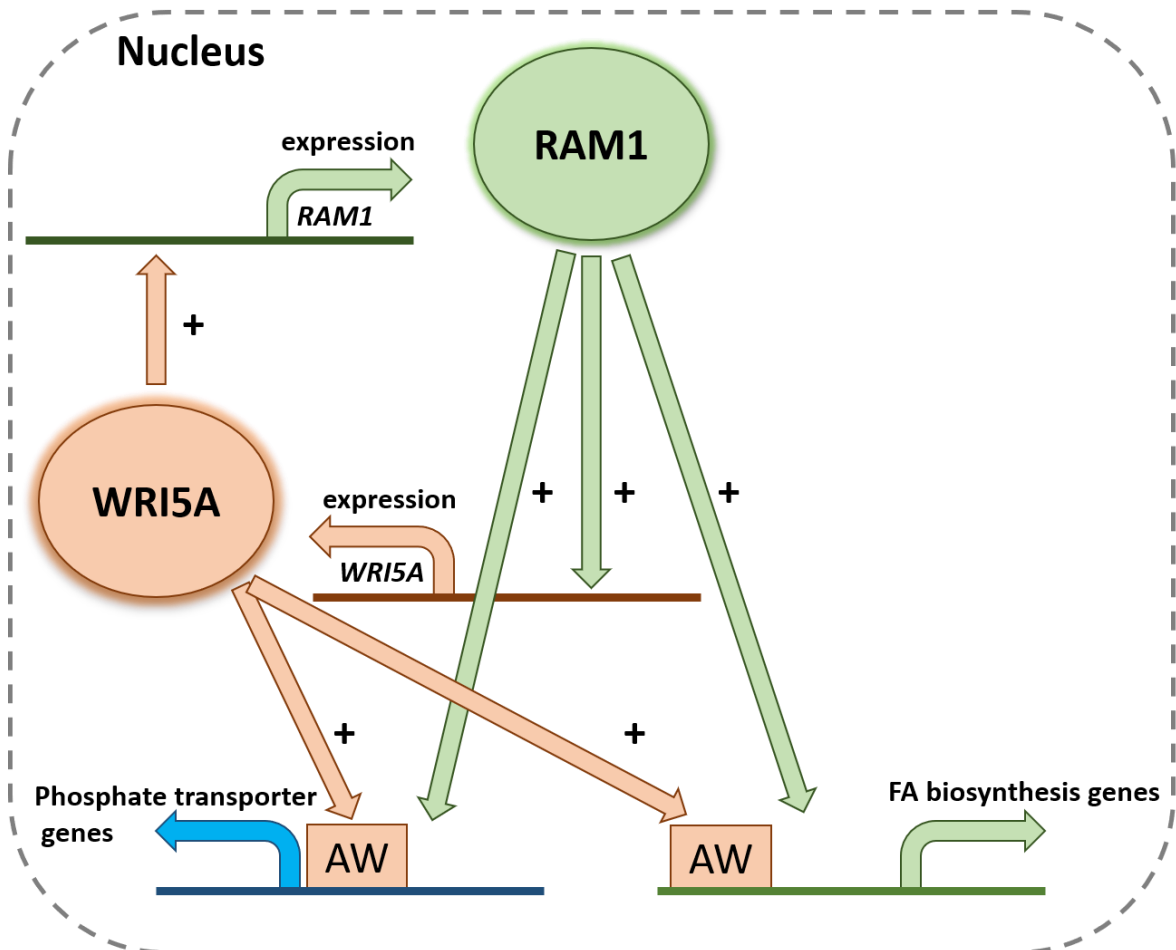


**Figure 10: WRI5A and RAM1 interact in a positive feedback loop to regulate FA biosynthesis and phosphate transport in arbusculated cells.** Transcriptional activation of *RAM1* induces *WRI5A* expression. *WRI5A* in turn activates *RAM1*. Both *RAM1* and *WRI5A* upregulate expression of genes related to the AM-dependent phosphate transport e.g., *MtPT4* or of the AM-dependent FA biosynthesis genes *RAM2*, *FatM* or *STR*. These -indirect or direct- targets of the two TFs often contain an AW-box motive, potentially mediating *WRI5A* binding.

Yeast-1-Hybrid (Y1H), transactivation assays in *N. benthamiana* leaves and ChIP-seq followed by qRT-PCR revealed a direct regulation of *STR* regulation via *WRI5A* binding to the *STR*-promoter (*pSTR*) (Jiang et al., 2018) (Figure 10). Two ASML1 WRI1 (AW)-box motifs in the 250 bp region upstream of the ATG seem to be crucial for *WRI5A* binding, which could be likewise shown for the binding of *WRI5A* to *pMtPT4*. AW-box motifs could be found on *pPK*, *pKASII*, *pKAR*, *pFatM*, *pRAM2* and *pMthA1*. *WRI5A* could induce expression of *KAR*, *FatM*, and *RAM2* in *in planta* transactivation assays in *N. benthamiana* leaves suggesting a direct regulation of these genes by *WRI5A* via the AW-box. Since

## Introduction

---

*pRAM1* lacks an AW-box motive, *WRI5A* might only indirectly enhance *RAM1* expression. *WRI5B* and *WRI5C* could also transactivate *pMtPT4* but only *WRI5B* further activated *pSTR* in *N. benthamiana* leaves.

Regulation of AM-dependent phosphate uptake via AW-box binding by an ERF TF is not only known in *M. truncatula* AM, but also during mycorrhizal symbiosis in *L. japonicus*, during which an ERF TF, the CTTC MOTIF BINDING TF 1 (*CBX1*) mediates *LjPT4* activation via binding to the promoters' AW-box and CTTC motive (Liu et al., 2020; Xue et al., 2018). Regulation of the *pLjPT4*'s CTTC motive by *CBX1* binding was analyzed using ChIP-seq. Electromobility Shift Assay (EMSA) as well as transactivation assays in hairy roots and cell suspension with *CBX1* and its potential target *pLjPT4* showed that the CTTC is important, but not crucial for *LjPT4* expression and also revealed the promoters' AW-box as the other *cis*-regulatory motive mediating transcriptional *LjPT4* activation. Overexpression of *CBX1* as well as the already mentioned transactivation assays further exposed direct regulatory targets like *LjRAM2* and *LjHA1*. Besides those genes, *CBX1* was also able to activate *PT4* homologues from other plants including *MtPT4*. These findings suggest a conserved regulation of *cis*-regulatory elements like the AW-box or the CTTC motive via *CBX1* and its orthologues. *Cbx1* mutants displayed a reduced overall mycorrhization and less arbusculated cells in *L. japonicus* roots. Additional qRT-PCR experiments of *cbx1* mutant lines disclosed decreased AM marker gene expression of *LjHA1*, *LjPT4* and *LjRAM2*. Reduced but not totally diminished expression levels of marker genes indicate a redundantly functioning gene, probably *LjRAM1*, although it remains unclear whether *CBX1* and *LjRAM1* act in cooperative or independent manner or if *CBX1* even acts downstream of *LjRAM1*. Fitting with the strong arbuscular phenotype of *cbx1* is the cellular expression of *CBX1*, being activated exclusively in mycorrhized roots. Not surprisingly, the TF *CBX1* can be localized in the nucleus.

As well as the *M. truncatula* homologues *WRI5A*, *WRI5B* and *WRI5C* and *AtWRI1*, overexpression of *CBX1* similarly leads to increased TAG production in tobacco leaves. Interestingly, overexpressing *CBX1* also induces activation of *WRI5A*, *WRI5B* and *WRI5C*. To summarize, the ERF TF *CBX1* is one of the major regulators of AM symbiosis in *L. japonicus*. By binding the *cis*-regulatory AW-box and CTTC motive, it conducts AM-dependent FA biosynthesis and phosphate uptake.

Surprisingly, phylogenetic studies revealed that *WRI5A*, *WRI5B* and *WRI5C* are not the *M. truncatula* ERF TFs genes closest related to *CBX1*. Indeed, two other ERF TFs, *Medtr2g460730.1* and *Medtr4g130270.1* are even closer related to *CBX1*. Nevertheless, the regulation of mycorrhizal symbiosis in *M. truncatula* by these two factors is known to a lesser extent, when compared to the role of either *WRI5A*, *B* and *C*.

## Introduction

---

In a genome-wide profiling approach with whole *M. truncatula* roots, additional ERF TF genes besides *WR15A* and *B* were identified to be upregulated during AM, including *Medtr4g130270.1* as well as the so far not mentioned *Medtr6g012970.1* and *Medtr7g011630.1* (Hogekamp et al., 2011). Via laser microdissection followed by qRT-PCR, the cell-specific expression of these genes could be localized, revealing arbuscule-correlated expression for *M. truncatula* ERF genes (Gaude et al., 2012; Hogekamp & Küster, 2013). These data clearly suggest that more ERF TFs act as AM symbiosis regulators in *M. truncatula*. Given the high number of *ERF* TF genes upregulated during AM, it is possible that they function redundantly.

## **Aim of this thesis**

The described studies on the ERF TFs WRI5A, B and C in *M. truncatula* as well as potential orthologues in *L. japonicus* like CBX1, strongly indicate a regulatory role of these genes during AM-dependent FA biosynthesis (Jiang et al., 2018; Luginbuehl et al., 2017; Xue et al., 2018). Although some regulatory targets and the related binding motifs of WRI5A could be identified, the exact role of WRI5A, as well as the -potentially redundant- ERF TF WRI5B and WRI5C as well as other AM-activated ERF TF genes widely remains unclear and will be further analysed in this thesis. Additionally, the connection between the WRI5A, WRI5B, WRI5C and MtRAM1 TFs during the regulation of AM-dependent FA biosynthesis is equally unsolved and will be investigated.

The strategy of this thesis is therefore to examine the role of AM-related ERF TFs for the AM symbiosis in *M. truncatula* via *in situ* studies of gene expression and functional genomics approaches. The aim of this thesis is to shed light on the regulatory networks these AM-regulators are involved in and thus contribute to a deeper understanding of their relevance for AM symbiosis. To fulfil this, potential target genes regulated by these ERF TF candidates must be identified. Since ERF TFs are not only known to directly bind DNA (Allen et al., 1998; Hao et al., 1998; Jiang et al., 2018; Xue et al., 2018), but also interact on the protein level with TFs from the GRAS (Heyman et al., 2016, 2018) or NF-Y families (Bai et al., 2016; Sun et al., 2014; Zhiguo et al., 2018), potential heterodimerization partners will be analysed using various types of protein-protein interaction studies.

## Material and Methods

### Material

#### Strains

Table 1: Bacterial strains.

strain	reference/ supplier
<i>Escherichia coli</i> DH5 $\alpha$ mcr'	(Grant et al., 1990)
<i>Agrobacterium rhizogenes</i> Arqua 1	(Quandt et al., 1993)
One Shot OmniMAX 2T1 <sup>R</sup> chemically competent <i>Escherichia coli</i>	Invitrogen, Karlsruhe, Germany

Table 2: *M. truncatula* strains.

strain	reference/ supplier
<i>Medicago truncatula</i> Gaertn. Jemalong A17	Thierry Huguet; INRA, Toulouse, France
<i>Medicago truncatula</i> R108	(Hoffmann et al., 1997)
<i>Medicago truncatula</i> ram1-1 A17	Giles, BIC, UK
<i>Medicago truncatula</i> pt4-2 A17	Maria Harrison, Boyce Thompson Institute, USA

Table 3: Fungal spores used for mycorrhization

strain	reference/ supplier
<i>Rhizophagus irregularis</i> DAOM197198	PremierTech, Rivière-du-Loup, Canada

Table 4: Yeast strains used for Y1H and Y2H.

strain	genotype	reference/ supplier
<i>Saccharomyces cerevisiae</i> Y187	<i>Mata, ura3-52, his3-200, ade2-101, trp1-901, leu2-3, 112, gal4<math>\Delta</math>, gal80<math>\Delta</math>, met-, URA3:GAL1<sub>UAS</sub>-Gal1<sub>TATA</sub>-LacZ, Mel1</i>	Clontech Laboratories, Fitchburg, USA
<i>Saccharomyces cerevisiae</i> Y2HGold	<i>Mata, trp1-901, leu2-3, 112, ura3-52, his3-200, gal4<math>\Delta</math>, gal80<math>\Delta</math>, LYS2::GAL1<sub>UAS</sub>-Gal1<sub>TATA</sub>-Ade2 URA3::MEL1<sub>UAS</sub>-Mel1<sub>TATA</sub> AUR1-C MEL1</i>	Clontech Laboratories, Fitchburg, USA
<i>Saccharomyces cerevisiae</i> YM4271	<i>Mata ura3-52 his<math>\Delta</math>200 ade2-101 lys2-801 leu2-3 leu2-112 trp1-901 gal4<math>\Delta</math>512 gal80<math>\Delta</math>538 ade5::hisG</i>	ATCC (LGC)

## Material and Methods

### Primer/ Oligonucleotides

**Table 5: Primers used for amplification of *M. truncatula* AP2/ERF promoter sequences.** Sequence parts written in small letters indicate artificially added restriction sites or primer extensions, native promoter sequences are written in capital letters.

number	Mtr. /Medtr number of gene	Primer name	Sequence (5'-3')	Cloning site	Partner Primer
6	<i>Mtr.21492.1.S1_at</i>	p21492_2168_Eco-h	aaagaattcATGAGTATGAGCCATAGTAA	<i>EcoRI</i>	8
8	<i>Mtr.21492.1.S1_at</i>	p21492_3029_Hind-r	aaaaagcttATTTATATGTGAAGGGA GAG	<i>HindIII</i>	6
12	<i>Mtr.1449.1.S1_at</i>	pWRI5a_Eco_h	cccgaattcTAGATATGAATCATGCTA ACTCGT	<i>EcoRI</i>	13
13	<i>Mtr.1449.1.S1_at</i>	pWRI5a_Hind_r	cccaagcttATTGATCAATACTCTTCA CTTTCT	<i>HindIII</i>	12
14	<i>Mtr.158671.1.S1_at</i>	p15867_Sma_h	aaaccgggTGTGACATCACAGAACT GAGG	<i>SmaI</i>	15
15	<i>Mtr.158671.1.S1_at</i>	p15867_Sma_r	aaaccgggTGGAAAAAAAAGAAG TGTA	<i>SmaI</i>	14
16	<i>Mtr.25005.1.S1_at</i>	p25005_Eco_h	cccgaattcGAGAGTGACATTGGATC AAC	<i>EcoRI</i>	17
17	<i>Mtr.25005.1.S1_at</i>	p25005_Pst_r	gggctcagTGATTTTCCTTCATAAG TAA	<i>PstI</i>	16
18	<i>Medtr2g460730.1</i>	pMedtr460730_Eco_h	cccgaattcTAATTGGCTAACAATAAG AA	<i>EcoRI</i>	19
19	<i>Medtr2g460730.1</i>	pMedtr460730_Hind_r	cccaagcttTGGAAAACAAAAGATGA ATA	<i>HindIII</i>	18
20	<i>Medtr2g460730.1</i>	pWRI5c_for_SphI	aaagcatgcCATGACAAGTCCACAGC TGT	<i>SphI</i>	21
21	<i>Medtr2g460730.1</i>	pWRI5c_rev_EcoRI	aaagaattcTTCTCCAATGAACTGTG TCT	<i>EcoRI</i>	20
22	<i>Medtr2g460730.1</i>	p460730_1kB_for	aaagaattcCGGATAGGCTCAAACCTG GTC	<i>EcoRI</i>	23
23	<i>Medtr2g460730.1</i>	p460730_250bp_for	aaagaattcCCGGTTGAAAGCCACAT AAC	<i>EcoRI</i>	22
24	<i>Medtr2g460730.1</i>	p460730_ohneGCC_for	aaagaattcTATATGTAATGTAATGAA AT	<i>EcoRI</i>	25
25	<i>Mtr.158671.1.S1_at</i>	p15867_1kB_Sma_for	aaaccgggCGCTACTGTTTGAGCG TTGA	<i>SmaI</i>	24
26	<i>Mtr.158671.1.S1_at</i>	p15867_250bp_Eco_for	aaagaattcGATTTTACAGACGGCCA CAAA	<i>EcoRI</i>	27
27	<i>Mtr.158671.1.S1_at</i>	p15867_ohneGCC_Eco_for	aaagaattcACCCCATTCTTAGCCC ATC	<i>EcoRI</i>	26
28	<i>Mtr.158671.1.S1_at</i>	p15867_Hind_rev	aaaaagcttTGGAAAAAAAAGAAGT GTA	<i>HindIII</i>	29
29	<i>Medtr2g460730.1</i>	p460730_pGC_C_for	aaagaattcAGAAGCAACCATTCTA AGC	<i>EcoRI</i>	28

## Material and Methods

**Table 6: Primers used for amplification of the RNAi-constructs.** Small letters indicate the attB-sites needed for Gateway cloning; capital letters are the genomic *M. truncatula* sequence.

number	Mtr./Medtr number of gene	Primer name	sequence (5'-3')	Partner Primer	Amplification successful?
1	<i>Mtr.21492.1.S1_at</i>	21492_RNAi1_f	ggggacaagttgtacaaaaaagcaggctgcTTCACCTCAC TCTCCCTTCAC	2	yes
2	<i>Mtr.21492.1.S1_at</i>	21492_RNAi1_r	ggggaccactttgtacaagaagctgggtcACCATGCTTC CTTCTTCAACTG	1	yes
3	<i>Mtr.21492.1.S1_at</i>	21492_RNAi2_f	ggggacaagttgtacaaaaaagcaggctgcTTCACCTCAC TCTCCCTTCAC	4	yes
4	<i>Mtr.21492.1.S1_at</i>	21492_RNAi2_r	ggggaccactttgtacaagaagctgggtcGCCAACAAAT CTCTTTCCG	3	yes
5	<i>Mtr.21492.1.S1_at</i>	21492_RNAi3_f	ggggacaagttgtacaaaaaagcaggctgcTGAGCCTTC AATGATTAGAG	6	yes
6	<i>Mtr.21492.1.S1_at</i>	21492_RNAi3_r	ggggaccactttgtacaagaagctgggtcGATCAGAAATT CCTCTTCC	5	yes
7	<i>Mtr.21492.1.S1_at</i>	21492_RNAi4_f	ggggacaagttgtacaaaaaagcaggctgcGAAGAAGAT GGTGGATGAG	8	yes
8	<i>Mtr.21492.1.S1_at</i>	21492_RNAi4_r	ggggaccactttgtacaagaagctgggtcCAAATAGGAG GAAGATCAAGTG	7	Yes
9	<i>Mtr.1449.1.S1_at</i>	1449_RNAi1_f	ggggacaagttgtacaaaaaagcaggctgcTGTGAAATC TGAACCTAAGTCCA	10	yes
10	<i>Mtr.1449.1.S1_at</i>	1449_RNAi1_r	ggggaccactttgtacaagaagctgggtgCTTCTCTTCAC AGTGGTTGCA	9	yes
11	<i>Mtr.1449.1.S1_at</i>	1449_RNAi2_f	ggggacaagttgtacaaaaaagcaggctgcACACCGAAC CTCAACCTTC	12	yes
12	<i>Mtr.1449.1.S1_at</i>	1449_RNAi2_r	ggggaccactttgtacaagaagctgggtgAATCTGGTTT GCTGCAAGGA	11	yes
13	<i>Mtr.1449.1.S1_at</i>	1449_RNAi3_f	ggggacaagttgtacaaaaaagcaggctgcAGAAGGGAT TGCAGGGGTTT	14	yes
14	<i>Mtr.1449.1.S1_at</i>	1449_RNAi3_r	ggggaccactttgtacaagaagctgggtgAGAAGGTCAC AGTGAAGGA	13	yes
15	<i>Mtr.25005.1.S1_at</i>	25005_RNAi1_f	ggggacaagttgtacaaaaaagcaggctgcACACCAATC AGAGACACCCA	16	yes
16	<i>Mtr.25005.1.S1_at</i>	25005_RNAi1_r	ggggaccactttgtacaagaagctgggtgACCTCATTCC ATTCCTTGATTGT	15	yes
17	<i>Medtr2g460730.1</i>	460370_RNAi1_f	ggggacaagttgtacaaaaaagcaggctgcGGCGAAACT ATCACAACAGCA	18	yes
18	<i>Medtr2g460730.1</i>	460370_RNAi1_r	ggggaccactttgtacaagaagctgggtgTGGGACACTT CTCCTTGTCT	17	yes
19	<i>Medtr2g460730.1</i>	460370_RNAi2_f	ggggacaagttgtacaaaaaagcaggctgcGCTGCTGAT TTATCCCCAACA	20	yes
20	<i>Medtr2g460730.1</i>	460370_RNAi2_r	ggggaccactttgtacaagaagctgggtgCTGAATCAAAT AAAGGTGGCACA	19	yes
21	<i>Mtr.15867.1.S1_at</i>	15867_RNAi1_f	ggggacaagttgtacaaaaaagcaggctgcACCCATTC CTTAGCCCATC	22	yes
22	<i>Mtr.15867.1.S1_at</i>	15867_RNAi1_r	ggggaccactttgtacaagaagctgggtgTCCTCGTCCG TTTTGCTTTG	21	yes
23	<i>Mtr.15867.1.S1_at</i>	15867_RNAi2_f	ggggacaagttgtacaaaaaagcaggctgcACCCAAGAA GAAGCAGCTACA	24	yes

## Material and Methods

**Table 7: Primers used for RT-PCR measurements.**

number	Mtr. /Medtr number of gene	Primer name	sequence (5'-3')	Partner Primer
1	<i>Mtr.21492.1.S1_at</i>	ERF_21492_(f)	AGTTTTGAATCGTGTTTAACC	2
2	<i>Mtr.21492.1.S1_at</i>	ERF_21492_(r)	CATTCTCTTCATAACAGCTCT	1
3	<i>Mtr.25005.1.S1_at</i>	ERF_25005_(f)	CAAATTGACTGCATTACAAGT	4
4	<i>Mtr.25005.1.S1_at</i>	ERF_25005_(r)	TCTTAGCATTGAAGACTCATC	3
5	<i>Mtr.25005.1.S1_at</i>	ERF_25005_2(f)	ACACTGGTTGAAGACATTAAT	6
6	<i>Mtr.25005.1.S1_at</i>	ERF_25005_2(r)	TCTTCAGCTGTATCAAAAGTT	5
7	<i>Mtr.21492.1.S1_at</i>	ERF_21492_2(f)	ACTCTTGTTCCTCCTTTTCTT	8
8	<i>Mtr.21492.1.S1_at</i>	ERF_21492_2(r)	GGTTAAACACGATTCAAAAC	7
9	<i>Medtr2g460730.1</i>	ERF_460730_(f)	GAATATCGAGGACTTAATGCT	10
10	<i>Medtr2g460730.1</i>	ERF_460730_(r)	TTGATGATTGAAGCAAAAGAC	9
11	<i>Mtr.1449.1.S1_at</i>	ERF_1449_(f)	CTCTTGCAAGTTGAAAATACA	12
12	<i>Mtr.1449.1.S1_at</i>	ERF_1449_(r)	GGATTGCATAGTTCCATGATA	11
13	<i>Medtr1g040500.1</i>	MtRam2_RT_for	GATCACTCCTACCAATGAAAT	14
14	<i>Medtr1g040500.1</i>	MtRam2_RT_rev	TAGGAAGATAGGGTCAAGTAG	13
15	<i>Mtr..46362.1.S1_at</i>	MtErf1_RT_for	TGTGTTTAGGAAAGAGTCAA	16
16	<i>Mtr..46362.1.S1_at</i>	MtErf1_RT_rev	AATCTTGAGCTTCTCTTTGAA	15
17	<i>Medtr7g027190.1</i>	MtRam1_RT_for	CATTACTACTCCGCAATTTTC	18
18	<i>Medtr7g027190.1</i>	MtRam1_RT_rev	CAACAAACAACCTTTATCCTC	17
19	<i>Mtr.15867.1.S1_at</i>	Mtr.15867.1.S1_at_hin	GGACAATGAAATATCACTCAA	20
20	<i>Mtr.15867.1.S1_at</i>	Mtr.15867.1.S1_at_rev	CCACCATTTCTTAAACTTAG	19
21	<i>GW088233.1</i>	Gi_a-Tub_for	TGTCCAACCGTTTTAAAGT	22
22	<i>GW088233.1</i>	Gi_a-Tub_rev	AAAGCACGTTTGGCGTACAT	21
23	<i>Medtr1g028600.1</i>	MtPT4f	TCGCGCGCCATGTTTGTGT	24
24	<i>Medtr1g028600.1</i>	MtPT4r	GCGAAGAAGAATGTTAGCCC	23
25	<i>Medtr1g109110.1</i>	MtFatM_for	TTGAGCAAAGGCCAATAAGGT	26
26	<i>Medtr1g109110.1</i>	MtFatM_rev	CTATGTAGAAAATGGACATGTAG	25
27	<i>Medtr6g021805.1</i>	MtTefa_f	AAGCTAGGAGGTATTGACAAG	28
28	<i>Medtr6g021805.1</i>	MtTefa_r	ACTGTGCAGTAGTACTTGGTG	27
29	<i>Mtr.52071.1.S1.at</i>	Mtr.52071-h	CCAACATTGTGAGTGGTAGA	30
30	<i>Mtr.52071.1.S1.at</i>	Mtr.52071-r	CTTCAACTTCTCCTTGCTCT	29



## Material and Methods

**Table 8: Primers used for Y1H promoter (bait) fragments.** Small letters indicate the attB-sites needed for Gateway cloning; capital letters are the genomic *M. truncatula* sequence.

number	Mtr./Medtr-number of gene	Primer name	sequence (5'-3')	Partner Primer	Amplification successful?
1	<i>Mtr.15867.1.S1_at</i>	Y1H-15867-for	ggggacaagttgtacaaaaagcaggcTGCTTGACA TCACAGAACTGAGG	2	yes
2	<i>Mtr.15867.1.S1_at</i>	Y1H-15867-rev	ggggaccactttgtacaagaaagctgggtcTGGAAAAA AAAGAAGTGTA	1	yes
3	<i>Mtr.25005.1.S1_at</i>	Y1H-25005-for	ggggacaagttgtacaaaaagcaggcTGCGAGAGT GACATTGGATCAAC	4	no
4	<i>Mtr.25005.1.S1_at</i>	Y1H-25005-rev	ggggaccactttgtacaagaaagctgggtcTGATTTTCC TTCATAAGTAA	3	no
5	<i>Mtr.1449.1.S1_at</i>	Y1H-1449-for	ggggacaagttgtacaaaaagcaggcTGCTAGATA TGAATCATGCTAACTCGT	6	no
6	<i>Mtr.1449.1.S1_at</i>	Y1H-1449-rev	ggggaccactttgtacaagaaagctgggtcATTGATCAA TACTCTTCACCTTCT	5	no
7	<i>Medtr2g460730.1</i>	Y1H-460730-for	ggggacaagttgtacaaaaagcaggcTGCTAATTG GCTAACATAAGAA	8	yes
8	<i>Medtr2g460730.1</i>	Y1H-460730-rev	ggggaccactttgtacaagaaagctgggtcTGGAAAAC AAAAGATGAAT	7	yes
9	<i>Mtr..46362.1.S1_at</i>	Y1H-Erf1-for	ggggacaagttgtacaaaaagcaggcTGCTCCTTG CCTCTAGTTTGTC	10	yes
10	<i>Mtr..46362.1.S1_at</i>	Y1H-Erf1-rev	ggggaccactttgtacaagaaagctgggtcAAATTTCTT GTATTTATTTG	9	yes
11	<i>Mtr.21492.1.S1_at</i>	Y1H-21492-for	ggggacaagttgtacaaaaagcaggcTGCATGAGT ATGAGCCATAGTAA	12	yes
12	<i>Mtr.21492.1.S1_at</i>	Y1H-21492-rev	ggggaccactttgtacaagaaagctgggtcTATTTATAT GTGAAGGGAGAG	11	yes
13	<i>Medtr1g109110.1</i>	Y1H-FatM-for	ggggacaagttgtacaaaaagcaggcTGCGTTCAT ACTCTCGTGATTGCCA	14	yes
14	<i>Medtr1g109110.1</i>	Y1H-FatM-rev	ggggaccactttgtacaagaaagctgggtcGTTCTGTT CCTTTTTTTATTTTTCACTTTC	13	yes
15	<i>Medtr4g096690.1</i>	Y1H-KASII-for	ggggacaagttgtacaaaaagcaggcTGCGAACTC TAGCATTTGATCGA	16	yes
16	<i>Medtr4g096690.1</i>	Y1H-KASII-rev	ggggaccactttgtacaagaaagctgggtcTGTGTTTGT TGAAATGACGGA	15	yes
17	<i>Medtr7g027190.1</i>	Y1H-RAM1-for	ggggacaagttgtacaaaaagcaggcTGCTCCCTT TTCTTGCTTTTTTACCACC	18	yes
18	<i>Medtr7g027190.1</i>	Y1H-RAM1-rev	ggggaccactttgtacaagaaagctgggtcTTTTTTCCC ACCCTTTTTTATTTG	17	yes
19	<i>Medtr1g040500.1</i>	Y1H-RAM2-for	ggggacaagttgtacaaaaagcaggcTGCATTGCC GGTGGGATAAACAC	20	yes
20	<i>Medtr1g040500.1</i>	Y1H-RAM2-rev	ggggaccactttgtacaagaaagctgggtcGGTGATGA TGGTGATTTCTTCT	19	yes
21	<i>Medtr4g093845.1</i>	Y1H-ABCG-for	ggggacaagttgtacaaaaagcaggcTGCGGTCTA TTAATTACCGATGACAAA	22	yes
22	<i>Medtr4g093845.1</i>	Y1H-ABCG-rev	ggggaccactttgtacaagaaagctgggtcGTCAGTGA ACTAATTGGTGATCATC	21	yes

## Material and Methods

**Table 9: Primer used for amplification of *M. truncatula* CDS of AP2/ERF genes for Y2H.** Capital letters indicate the native gene sequence whereas small letters indicate added restriction sites.

number	Mtr./Medtr- number of gene	Primer name	sequence (5'-3')	Partner Primer
1	<i>Mtr.1449.1.S1_at/ Medtr8g468920.1</i>	Y2H_1449_ Smal_rev	aaaacccgggTCAGTTAGAAATGTTGGAAGG	2
2	<i>Mtr.1449.1.S1_at/ Medtr8g468920.1</i>	Y2H_1449_ Smal_for	aaaacccgggATGGAGGAGGTTTCCAATGTG	1
3	<i>Medtr2g460730.1</i>	Y2H_460730_ Smal_rev	aaaacccgggCTAGACCTTTAAGCATAGATC	4
4	<i>Medtr2g460730.1</i>	Y2H_460730_ Smal_for	aaaacccgggGATGGCGAAACTATCACAAACAG	3
5	<i>Mtr.21492.1.S1_at</i>	Y2H_21492_ Smal_forward	ggggcccgggATGGCAAGGAAGAGAAAGGTT	6
6	<i>Mtr.21492.1.S1_at</i>	Y2H_21492_ Smal_reverse	ggggcccgggGAAAATGGTTCATTCAATTAG	5
7	<i>Mtr.25005.1.S1_at</i>	Y2H_25005_ Smal_forward	ggggcccgggATGACAAGAAAGAGAAAGATT	8
8	<i>Mtr.25005.1.S1_at</i>	Y2H_25005_ Smal_reverse	ggggcccgggGATGATACATACAACCTGTAA	7
9	<i>Mtr..46362.1.S1_at</i>	Y2H_ERF1_ Smal_forward	aaaacccgggATGGCAATGTTGATAGAAAAC	10
10	<i>Mtr..46362.1.S1_at</i>	Y2H_ERF1_ Smal_reverse	aaaacccgggTTATTGTCCAAAATTTAAGTA	9
11	<i>Medtr6g011490.1</i>	Y2H_WRI5C_ Smal_forward	ggggcccgggATGGAAATGATGATGAAGGAA	12
12	<i>Medtr6g011490.1</i>	Y2H_WRI5C_ Smal_reverse	ggggcccgggCTAAGGTGTCCATTGGGGTTT	11
13	<i>Mtr.15867.1.S1_at</i>	Y2H_15867_ Smal_forward	ggggcccgggATGGCGAAAAAATCGCAGAAG	14
14	<i>Mtr.15867.1.S1_at</i>	Y2H_15867_ Smal_reverse	ggggcccgggGAGGGTGCTGAGGTTTTATAG	13

## Material and Methods

**Table 10: Primer used for amplification of *M. truncatula* CDS of AP2/ERF genes for BiFC.** Capital letters indicate the native gene sequence whereas small letters indicate added restriction sites.

number	Mtr./Medtr- number of gene	Primer name	sequence (5'-3')	Partner Primer
1	<i>Mtr.1449.1.S1_at/Medtr8g468920.1</i>	WRI5A_BiFc_for	ggggacaagttgtacaagcaggctacATGGAGGAGGT TTCCAATGTG	2
2	<i>Mtr.1449.1.S1_at/Medtr8g468920.1</i>	WRI5A_BiFc_rev	ggggaccactttgtacaagaaagctgggtAGTTAGAAATGT TGGAAGG	1
3	<i>Mtr.25005.1.S1_at</i>	Y2H_25005_Smal_forward	ggggacaagttgtacaagcaggctacATGACAAGAAAG AGAAAGATT	4
4	<i>Mtr.25005.1.S1_at</i>	Y2H_25005_Smal_reverse	ggggaccactttgtacaagaaagctgggtACAGGTTGTAT GTATCATT	3
5	<i>Mtr..46362.1.S1_at</i>	WRI5B_BiFc_for	ggggacaagttgtacaagcaggctacATGGCAATGTTG ATAGAAAAC	6
6	<i>Mtr..46362.1.S1_at</i>	WRI5B_BiFc_rev	ggggaccactttgtacaagaaagctgggtATTGTCCAAAAT TTAAGTA	5
7	<i>Medtr6g011490.1</i>	WRI5C_BiFc_for	ggggacaagttgtacaagcaggctacATGGAATGATG ATGAAGGAA	8
8	<i>Medtr6g011490.1</i>	WRI5c_BiFc_rev	ggggaccactttgtacaagaaagctgggtAAGGTGTCCAT TGGGGTTT	7

## Material and Methods

### Plasmids

**Table 11: Cloned promoter-gus constructs.** Promoter sequences amplified in this table were cloned using (Table 5):

Clone	Strain	Resistance	Plasmid size [kb]	Origin of the plasmide/ insert, used restriction enzymes
<i>pK18:p21492_kurz</i>	<i>E. coli DH5 alpha mcr</i>	Kan 50	3,5	<i>pK18</i> -derivative, promoter (-955/-94) of MtERF-TF ( <i>Medtr6g012970.1/Mtr.21492.1.S1_at</i> ), 862 bp native size. Cloned into <i>pK18</i> via <i>EcoRI/HindIII</i> . Primer #6 and #8 (TAB. 2)
<i>pgusInt:p21492_kurz-GUS</i>	<i>E. coli DH5 alpha mcr</i>	Amp 100	6,3	<i>pgusInt</i> -derivative promoter (-955/-94) of MtERF-TF ( <i>Medtr6g012970/Mtr.21492.1.S1_at</i> ), 862 bp native size. Cloned via <i>EcoRI/HindIII</i> .
<i>pRR:p21492_kurz-GUS</i>	<i>E. coli DH5 alpha mcr</i>	Kan 50	13,21	<i>pRR</i> -derivative, cloned promoter (-955/-94) of MtERF-TF ( <i>Medtr6g012970/Mtr.21492.1.S1_at</i> ), 862 bp native size + 2,35 size of <i>gus</i> -cassette. Cloned via <i>BglII/BamHI</i> .
<i>pRR:p21492_kurz-GUS</i>	<i>A. rhizogenes: Arqua 1</i>	Strep 600/ Kan 100	13,21	<i>pRR</i> -derivative, cloned promoter (-955/-94) of MtERF-TF ( <i>Medtr6g012970/Mtr.21492.1.S1_at</i> ), 862 bp native size + 2,35 size of <i>gus</i> -cassette. Cloned via <i>BglII/BamHI</i> .
<i>pK18:p15867</i>	<i>E. coli DH5 alpha</i>	Kan 50	4,9	<i>pK18</i> -derivative, promoter (-2296/-1) of MtERF-TF ( <i>Mtr.15867.1.S1_at</i> ), 2295 bp native size. Cloned into <i>pK18</i> via <i>SmaI</i> . Primer #14 and #15 (TAB. 2)
<i>pgusInt:p15867</i>	<i>E. coli DH5 alpha</i>	Amp 100	7,7	<i>pgusInt</i> -derivative promoter (-2296/-1) of MtERF-TF ( <i>Mtr.15867.1.S1_at</i> ), 2295 bp native size. Cloned via <i>SmaI</i> .
<i>pRR:p15867</i>	<i>E. coli DH5 alpha</i>	Kan 50	15,82	<i>pRR</i> -derivative, cloned promoter (-2296/-1) of MtERF-TF ( <i>Mtr.15867.1.S1_at</i> ), 2295 bp native size + 2,35 size of <i>gus</i> -cassette. Cloned via <i>BglII/XbaI</i> .
<i>pRR:p15867</i>	<i>A. rhizogenes: Arqua 1</i>	Strep 600/ Kan 100	15,82	<i>pRR</i> -derivative, cloned promoter (-2296/-1) of MtERF-TF ( <i>Mtr.15867.1.S1_at</i> ), 2295 bp native size + 2,35 size of <i>gus</i> -cassette. Cloned via <i>BglII/XbaI</i> .
<i>pK18:p460730</i>	<i>E. coli DH5 alpha</i>	Kan 50	4,2	<i>pK18</i> -derivative, promoter (-1512/+1) of MtERF-TF ( <i>Medtr2g460730.1</i> ), 1513 bp native size. Cloned into <i>pK18</i> via <i>EcoRI/HindIII</i> . Primer #18 and #19 (TAB. 2)
<i>pgusInt:p460730</i>	<i>E. coli DH5 alpha</i>	Amp 100	6,9	<i>pgusInt</i> -derivative promoter (-1512/+1) of MtERF-TF ( <i>Medtr2g460730.1</i> ), 1513 bp native size. Cloned via <i>EcoRI/HindIII</i> .
<i>pRR:p460730</i>	<i>E. coli DH5 alpha</i>	Kan 50	15,04	<i>pRR</i> -derivative, cloned promoter (-1512/+1) of MtERF-TF ( <i>Medtr2g460730.1</i> ), 1513 bp native size + 2,35 size of <i>gus</i> -cassette. Cloned via <i>BglII/XbaI</i> .
<i>pRR:p460730</i>	<i>A. rhizogenes: Arqua 1</i>	Strep 600/ Kan 100	15,04	<i>pRR</i> -derivative, cloned promoter (-1512/+1) of MtERF-TF ( <i>Medtr2g460730.1</i> ), 1513 bp native size + 2,35 size of <i>gus</i> -cassette. Cloned via <i>BglII/XbaI</i> .
<i>pK18:p1449</i>	<i>E. coli DH5 alpha</i>	Kan 50	5,1	<i>pK18</i> -derivative, promoter (-2460/+2) of MtERF-TF ( <i>Mtr.1449.1.S1_at</i> ), 2462 bp native size. Cloned into <i>pK18</i> via <i>EcoRI/HindIII</i> . Primer #12 and #13 (TAB. 2)
<i>pgusInt:p1449</i>	<i>E. coli DH5 alpha</i>	Amp 100	7,9	<i>pgusInt</i> -derivative, promoter (-2460/+2) of MtERF-TF ( <i>Mtr.1449.1.S1_at</i> ), 2462 bp native size. Cloned into <i>pK18</i> via <i>EcoRI/HindIII</i> .
<i>pRR:p1449</i>	<i>E. coli DH5 alpha</i>	Kan 50	15,98	<i>pRR</i> -derivative, cloned promoter (-2460/+2) of MtERF-TF ( <i>Mtr.1449.1.S1_at</i> ), 2462 bp native size + 2.35 kb size of <i>gus</i> -cassette. Cloned via <i>BglII/BamHI</i> .
<i>pRR:p1449</i>	<i>A. rhizogenes: Arqua 1</i>	Strep 600/ Kan 100	15,98	<i>pRR</i> -derivative, cloned promoter (-2460/+2) of MtERF-TF ( <i>Mtr.1449.1.S1_at</i> ), 2462 bp native size + 2.35 kb size of <i>gus</i> -cassette. Cloned via <i>BglII/BamHI</i> .
<i>pK18:p25005</i>	<i>E. coli DH5 alpha</i>	Kan 50	4,7	<i>pK18</i> -derivative, promoter (-2000/+1) of MtERF-TF ( <i>Mtr.25005.1.S1_at</i> ), 2001 bp native size. Cloned into <i>pK18</i> via <i>EcoRI/PstI</i> . Primer #12 and #13 (TAB. 2)
<i>pgusInt:p25005</i>	<i>E. coli DH5 alpha</i>	Amp 100	7,4	<i>pgusInt</i> -derivative promoter (-2000/+1) of MtERF-TF ( <i>Medtr2g460730.1</i> ), 2001 bp native size. Cloned via <i>EcoRI/PstI</i> .
<i>pRR:p25005</i>	<i>E. coli DH5 alpha</i>	Kan 50	15,52	<i>pRR</i> -derivative promoter (-2000/+1) of MtERF-TF ( <i>Medtr2g460730.1</i> ), 2001 bp native size + 2.35 kb size of <i>gus</i> cassette. Cloned via <i>BglII/BamHI</i> .
<i>pRR:p25005</i>	<i>A. rhizogenes: Arqua 1</i>	Strep 600/ Kan 100	15,52	<i>pRR</i> -derivative promoter (-2000/+1) of MtERF-TF ( <i>Medtr2g460730.1</i> ), 2001 bp native size + 2.35 kb size of <i>gus</i> cassette. Cloned via <i>BglII/BamHI</i> .

promoter-gus constructs cloned by Agnes Krüger (A. Krüger; bachelor thesis; 2019; LUH):

## Material and Methods

<i>pK18:pWRI5c</i>	<i>E.coli DH5 alpha</i>	Kan 50	5	<i>pK18</i> -derivative, promoter (-2280/-1) of MtERF-TF ( <i>Medtr6g011490.1</i> ), 2279 bp native size. Cloned into <i>pK18</i> via <i>SphI/EcoRI</i> . Primer #20 and #21 (TAB. 2)
<i>pGUS:pWRI5c</i>	<i>E.coli DH5 alpha</i>	Amp 100	7,7	<i>pgusInt</i> -derivative promoter (-2280/-1) of MtERF-TF ( <i>Medtr6g011490.1</i> ), 2280 bp native size. Cloned via <i>SphI/EcoRI</i> .
<i>pRR:pWRI5c-gus</i>	<i>E.coli DH5 alpha</i>	Kan 50	18,2	<i>pRR</i> -derivative promoter (-2280/-1) of MtERF-TF ( <i>Medtr6g011490.1</i> ), 2280 bp native size + 2.35 kb size of <i>gus</i> cassette. Cloned via <i>SpeI</i> .
<i>pRR:pWRI5c-gus</i>	<i>A. rhizogenes: Arqua 1</i>	Strep 600/ Kan 100	18,2	<i>pRR</i> -derivative promoter (-2280/-1) of MtERF-TF ( <i>Medtr6g011490.1</i> ), 2280 bp native size + 2.35 kb size of <i>gus</i> cassette. Cloned via <i>SpeI</i> .
<i>pK18:p460730_1Kb</i>	<i>E.coli DH5 alpha</i>	Kan 50	3,7	<i>pK18</i> -derivative, promoter (-1046/+1) of MtERF-TF ( <i>Medtr2g460730.1</i> ), 1047 bp native size. Cloned into <i>pK18</i> via <i>EcoRI/HindIII</i> . Primer #22 and #19 (TAB. 2)
<i>pK18:p460730_250bp</i>	<i>E.coli DH5 alpha</i>	Kan 50	2,9	<i>pK18</i> -derivative, promoter (-255/+1) of MtERF-TF ( <i>Medtr2g460730.1</i> ), 256 bp native size. Cloned into <i>pK18</i> via <i>EcoRI/HindIII</i> . Primer #23 and #19 (TAB. 2)
<i>pK18:p460730_ohneGCC</i>	<i>E.coli DH5 alpha</i>	Kan 50	2,8	<i>pK18</i> -derivative, promoter (-135/+1) of MtERF-TF ( <i>Medtr2g460730.1</i> ), 136 bp native size. Cloned into <i>pK18</i> via <i>EcoRI/HindIII</i> . Primer #24 and #19 (TAB. 2)
<i>pK18:p15867_1kB</i>	<i>E.coli DH5 alpha</i>	Kan 50	2,9	<i>pK18</i> -derivative, promoter (-999/-1) of MtERF-TF ( <i>Mtr.15867.1.S1_at</i> ), 999 bp native size. Cloned into <i>pK18</i> via <i>SmaI</i> . Primer #25 and #15 (TAB. 2)
<i>pK18:p15867_250bp</i>	<i>E.coli DH5 alpha</i>	Kan 50	3,7	<i>pK18</i> -derivative, promoter (-250/-1) of MtERF-TF ( <i>Mtr.15867.1.S1_at</i> ), 250 bp native size. Cloned into <i>pK18</i> via <i>EcoRI/HindIII</i> . Primer #26 and #15 (TAB. 2)
<i>pK18:p15867_ohneGCC</i>	<i>E.coli DH5 alpha</i>	Kan 50	2,9	<i>pK18</i> -derivative, promoter (-176/-1) of MtERF-TF ( <i>Mtr.15867.1.S1_at</i> ), 176 bp native size. Cloned into <i>pK18</i> via <i>EcoRI/HindIII</i> . Primer #27 and #15 (TAB. 2)
<i>pK18:p460730_pGCC</i>	<i>E.coli DH5 alpha</i>	Kan 50	2,8	<i>pK18</i> -derivative, promoter (-249/+1) of MtERF-TF ( <i>Medtr2g460730.1</i> ), 250 bp native size. Cloned into <i>pK18</i> via <i>EcoRI/HindIII</i> . Primer #29 and #19 (TAB. 2)
<i>pgusInt:p460730_1kB</i>	<i>E.coli DH5 alpha</i>	Amp 100	6,4	<i>pgusInt</i> -derivative, promoter (-1046/+1) of MtERF-TF ( <i>Medtr2g460730.1</i> ), 1047 bp native size. Cloned into <i>pgusInt</i> via <i>EcoRI/HindIII</i> .
<i>pgusInt:p460730_250bp</i>	<i>E.coli DH5 alpha</i>	Amp 100	5,7	<i>pgusInt</i> -derivative, promoter (-255/+1) of MtERF-TF ( <i>Medtr2g460730.1</i> ), 256 bp native size. Cloned into <i>pgusInt</i> via <i>EcoRI/HindIII</i> .
<i>pgusInt:p460730_ohneGCC_for</i>	<i>E.coli DH5 alpha</i>	Amp 100	5,6	<i>pgusInt</i> -derivative, promoter (-135/+1) of MtERF-TF ( <i>Medtr2g460730.1</i> ), 136 bp native size. Cloned into <i>pgusInt</i> via <i>EcoRI/HindIII</i> .
<i>pgusInt:p15867_1kBr</i>	<i>E.coli DH5 alpha</i>	Amp 100	6,4	<i>pgusInt</i> -derivative, promoter (-999/-1) of MtERF-TF ( <i>Mtr.15867.1.S1_at</i> ), 999 bp native size. Cloned into <i>pgusInt</i> via <i>SmaI</i> .
<i>pgusInt:p15867_250bp</i>	<i>E.coli DH5 alpha</i>	Amp 100	5,7	<i>pgusInt</i> -derivative, promoter (-250/-1) of MtERF-TF ( <i>Mtr.15867.1.S1_at</i> ), 250 bp native size. Cloned into <i>pgusInt</i> via <i>EcoRI/HindIII</i> .
<i>pgusInt:p15867_ohneGCC</i>	<i>E.coli DH5 alpha</i>	Amp 100	5,6	<i>pgusInt</i> -derivative, promoter (-176/-1) of MtERF-TF ( <i>Mtr.15867.1.S1_at</i> ), 176 bp native size. Cloned into <i>pgusInt</i> via <i>EcoRI/HindIII</i> .
<i>pgusInt:p460730_pGCC</i>	<i>E.coli DH5 alpha</i>	Amp 100	5,7	<i>pgusInt</i> -derivative, promoter (-249/+1) of MtERF-TF ( <i>Medtr2g460730.1</i> ), 250 bp native size. Cloned into <i>pgusInt</i> via <i>EcoRI/HindIII</i> .
<i>pRR:p460730_1kB</i>	<i>E.coli DH5 alpha</i>	Kan 50	17	<i>pRR</i> -derivative, promoter (-1046/+1) of MtERF-TF ( <i>Medtr2g460730.1</i> ), 1047 bp native size + 2.35 kb size of <i>gus</i> cassette. Cloned into <i>pRR</i> via <i>SpeI</i> .
<i>pRR:p460730_250bp</i>	<i>E.coli DH5 alpha</i>	Kan 50	16	<i>pRR</i> -derivative, promoter (-255/+1) of MtERF-TF ( <i>Medtr2g460730.1</i> ), 256 bp native size + 2.35 kb size of <i>gus</i> cassette. Cloned into <i>pRR</i> via <i>SpeI</i> .
<i>pRR:p460730_ohneGCC</i>	<i>E.coli DH5 alpha</i>	Kan 50	16	<i>pRR</i> -derivative, promoter (-135/+1) of MtERF-TF ( <i>Medtr2g460730.1</i> ), 136 bp native size + 2.35 kb size of <i>gus</i> cassette. Cloned into <i>pRR</i> via <i>SpeI</i> .
<i>pRR:p15867_1kB</i>	<i>E.coli DH5 alpha</i>	Kan 50	17	<i>pRR</i> -derivative, promoter (-999/-1) of MtERF-TF ( <i>Mtr.15867.1.S1_at</i> ), 999 bp native size + 2.35 kb size of <i>gus</i> cassette. Cloned into <i>pRR</i> via <i>SpeI</i> .
<i>pRR:p15867_250b</i>	<i>E.coli DH5 alpha</i>	Kan 50	16	<i>pRR</i> -derivative, promoter (-250/-1) of MtERF-TF ( <i>Mtr.15867.1.S1_at</i> ), 250 bp native size + 2.35 kb size of <i>gus</i> cassette. Cloned into <i>pRR</i> via <i>SpeI</i> .
<i>pRR:p15867_ohneGCC</i>	<i>E.coli DH5 alpha</i>	Kan 50	16	<i>pRR</i> -derivative, promoter (-176/-1) of MtERF-TF ( <i>Mtr.15867.1.S1_at</i> ), 176 bp native size + 2.35 kb size of <i>gus</i> cassette. Cloned into <i>pRR</i> via <i>SpeI</i> .
<i>pRR:p460730_pGCC</i>	<i>E.coli DH5 alpha</i>	Kan 50	16	<i>pRR</i> -derivative, promoter (-249/+1) of MtERF-TF ( <i>Medtr2g460730.1</i> ), 250 bp native size + 2.35 kb size of <i>gus</i> cassette. Cloned into <i>pRR</i> via <i>SpeI</i> .

## Material and Methods

pRR: p460730_1kB	A. rhizogenes: Arqua 1	Strep 600/ Kan 100	17	pRR-derivative, promoter (-1046/+1) of MtERF-TF ( <i>Medtr2g460730.1</i> ), 1047 bp native size + 2.35 kb size of <i>gus</i> cassette. Cloned into pRR via <i>SpeI</i> .
pRR: p460730_250bp	A. rhizogenes: Arqua 1	Strep 600/ Kan 100	16	pRR-derivative, promoter (-255/+1) of MtERF-TF ( <i>Medtr2g460730.1</i> ), 256 bp native size + 2.35 kb size of <i>gus</i> cassette. Cloned into pRR via <i>SpeI</i> .
pRR: p460730_ohneGCCr	A. rhizogenes: Arqua 1	Strep 600/ Kan 100	16	pRR-derivative, promoter (-135/+1) of MtERF-TF ( <i>Medtr2g460730.1</i> ), 136 bp native size + 2.35 kb size of <i>gus</i> cassette. Cloned into pRR via <i>SpeI</i> .
pRR:p15867_1kB_Sma_for	A. rhizogenes: Arqua 1	Strep 600/ Kan 100	17	pRR-derivative, promoter (-999/-1) of MtERF-TF ( <i>Mtr.15867.1.S1_at</i> ), 999 bp native size + 2.35 kb size of <i>gus</i> cassette. Cloned into pRR via <i>SpeI</i> .
pRR:p15867_250bp	A. rhizogenes: Arqua 1	Strep 600/ Kan 100	16	pRR-derivative, promoter (-250/-1) of MtERF-TF ( <i>Mtr.15867.1.S1_at</i> ), 250 bp native size + 2.35 kb size of <i>gus</i> cassette. Cloned into pRR via <i>SpeI</i> .
pRR:p15867_ohneGCC	A. rhizogenes: Arqua 1	Strep 600/ Kan 100	16	pRR-derivative, promoter (-176/-1) of MtERF-TF ( <i>Mtr.15867.1.S1_at</i> ), 176 bp native size + 2.35 kb size of <i>gus</i> cassette. Cloned into pRR via <i>SpeI</i> .
pRR: p460730_pGCC	A. rhizogenes: Arqua 1	Strep 600/ Kan 100	16	pRR-derivative, promoter (-249/+1) of MtERF-TF ( <i>Medtr2g460730.1</i> ), 250 bp native size + 2.35 kb size of <i>gus</i> cassette. Cloned into pRR via <i>SpeI</i> .
promoter- <i>gus</i> constructs designed and cloned by Phil Pallok (P. Pallok master thesis; 2013; LUH):				
pRR:p46362- <i>gus</i>	A. rhizogenes: Arqua 1	Strep 600/ Kan 100	17,3	pRR-derivative; promoter (-1/-1492) of MtERF TF ( <i>Mtr.46362.1.S1_at</i> ) 1492 bp native size + 2.35 kb size of <i>gus</i> -cassette. Cloned into pRR via <i>SpeI</i> .

**Table 12: Cloned RNAi-constructs.** Gene sequences amplified in this table were cloned using primers (Table 6).

Clone	Strain	Resistance	Plasmid size [kb]	Origin of the plasmid, Insert
pDonor:RNAiNr1_Mtr21492	<i>E. coli</i> DH5 <i>alpha mcr</i>	Kan 50	2,6	pDONR-derivative, contains Mtr.21492.1.S1_s_at (ERF-TF) RNAi-fragment (-121/+50), cloned with BP-Reaction
pDonor:RNAiNr2_Mtr21492	<i>E. coli</i> DH5 <i>alpha mcr</i>	Kan 50	2,6	pDONR-derivative, contains Mtr.21492.1.S1_s_at (ERF-TF) RNAi-fragment (-121/+120), cloned with BP-Reaction, from ATG to a homologous region of Mtr. 25005 (ERF-TF)
pDonor:RNAiNr3_Mtr21492	<i>E. coli</i> DH5 <i>alpha mcr</i>	Kan 50	2,5	pDONR-derivative, contains Mtr.21492.1.S1_s_at (ERF-TF) RNAi-fragment (+878/+1024), cloned with BP-Reaction, over a homologous region of Mtr. 25005 (ERF-TF)
pDonor:RNAiNr4_Mtr21492	<i>E. coli</i> DH5 <i>alpha mcr</i>	Kan50	2,5	pDONR-derivative, contains Mtr.21492.1.S1_s_at (ERF-TF) RNAi-Fragment (+1073/+1199), cloned with BP-Reaction
pK7GWIWG2:RNAiNr1_Mtr21492	Omnimax	Strep 600/Spec 100	13,9	pK7GWIWG2-derivative; contains fragment of 171 bp (-121/+50) of Mtr.21492.1.S1_s_at (ERF-TF) flanked with attB sites, cloned with LR-Reaction
pK7GWIWG2:RNAiNr2_Mtr21492	Omnimax	Strep 600/Spec 100	14	pK7GWIWG2-derivative; contains fragment of 241 bp (-121/+120) of Mtr.21492.1.S1_s_at (ERF-TF) flanked with attB sites, cloned with LR-Reaction, from ATG over a homologous region of Mtr. 25005 (ERF-TF)
pK7GWIWG2:RNAiNr3_Mtr21492	Omnimax	Strep 600/Spec 100	13,8	pK7GWIWG2-derivative; contains fragment of 146 bp (+878/+1024) of Mtr.21492.1.S1_s_at (ERF-TF) flanked with attB sites, cloned with LR-Reaction, from ATG over a homologous region of Mtr. 25005 (ERF-TF)
pK7GWIWG2:RNAiNr4_Mtr21492	Omnimax	Strep 600/Spec 100	13,8	pK7GWIWG2-derivative; contains fragment of 171 bp (+1073/+1199) of Mtr.21492.1.S1_s_at (ERF-TF) flanked with attB sites, cloned with LR-Reaction
pK7GWIWG2:RNAiNr1_Mtr21492	A. rhizogenes: Arqua 1	Spec 100/Strep 600	ca. 13,9	pK7GWIWG2-derivative; contains fragment of 171 bp (-121/+50) of Mtr.21492.1.S1_s_at (ERF-TF) flanked with attB sites, cloned with LR-Reaction
pK7GWIWG2:RNAiNr1_Mtr21492	A. rhizogenes: Arqua 1	Spec 100/Strep 600	ca. 13,9	pK7GWIWG2-derivative; contains fragment of 171 bp (-121/+50) of Mtr.21492.1.S1_s_at (ERF-TF) flanked with attB sites, cloned with LR-Reaction
pK7GWIWG2:RNAiNr2_Mtr21493	A. rhizogenes: Arqua 1	Spec 100/Strep 600	ca. 14	pK7GWIWG2-derivative; contains fragment of 241 bp (-121/+120) of Mtr.21492.1.S1_s_at (ERF-TF) flanked with attB sites, cloned with LR-Reaction, from ATG over a homologous region of Mtr. 25005 (ERF-TF)

## Material and Methods

pK7GWIWG2:RNAiNr3_Mtr21494	<i>A. rhizogenes</i> : <i>Arqua 1</i>	Spec 100/Strep 600	ca. 13,8	pK7GWIWG2-derivative; contains fragment of 146 bp (+878/+1024) of Mtr.21492.1.S1_s_at (ERF-TF) flanked with attB sites, cloned with LR-Reaction, from ATG over a homologous region of Mtr. 25005 (ERF-TF)
pK7GWIWG2:RNAiNr4_Mtr21495	<i>A. rhizogenes</i> : <i>Arqua 1</i>	Spec 100/Strep 600	ca. 13,8	pK7GWIWG2-derivative; contains fragment of 171 bp (+1073/+1199) of Mtr.21492.1.S1_s_at (ERF-TF) flanked with attB sites, cloned with LR-Reaction
pDonor:RNAi_158_67_2	<i>E.coli DH5 alpha</i>	Kan 50	2,62	pDONR-derivative, contains fragment of 223 bp (+2550/+2772) of Mtr.15867.1.S1_s_at (ERF-TF) cloned with BP reaction
pDonor:RNAi_144_9_1	<i>E.coli DH5 alpha</i>	Kan 50	2,59	pDONR-derivative, contains fragment of 192 bp (+18/+209) of Mtr.1449.1.S1_s_at (ERF-TF) cloned with BP reaction
pDonor:RNAi_144_9_2	<i>E.coli DH5 alpha</i>	Kan 50	2,57	pDONR-derivative, contains fragment of 171 bp (+2483/+2653) of Mtr.1449.1.S1_s_at (ERF-TF) cloned with BP reaction
pDonor:RNAi_144_9_3	<i>E.coli DH5 alpha</i>	Kan 50	2,68	pDONR-derivative, contains fragment of 281 bp (+2763/+3043) of Mtr.1449.1.S1_s_at (ERF-TF) cloned with BP reaction
pDonor:RNAi_460_730_1	<i>E.coli DH5 alpha</i>	Kan 50	2,52	pDONR-derivative, contains fragment of 120 bp (-3/+118) of Medtr2g460730.1 (ERF-TF) cloned with BP reaction
pDonor:RNAi_460_730_2	<i>E.coli DH5 alpha</i>	Kan 50	2,56	pDONR-derivative, contains fragment of 160 bp (+2909/+3068) of Medtr2g460730.1 (ERF-TF) cloned with BP reaction
pK7GW:RNAi_158_67_2	<i>Omnimax</i>	Spec50/Chloro15	ca. 14,1	pK7GWIWG2-derivative; contains fragment of 223 bp (+2550/+2772) of Mtr.15867.1.S1_s_at (ERF-TF) flanked with attB sites, cloned with LR-Reaction
pK7GW:RNAi_460_730_1	<i>Omnimax</i>	Spec50/Chloro15	ca. 13,8	pK7GWIWG2-derivative; contains fragment of 120 bp (-3/+118) of Medtr2g460730.1 (ERF-TF) flanked with attB sites, cloned with LR-Reaction
pK7GW:RNAi_460_730_2	<i>Omnimax</i>	Spec50/Chloro15	ca. 13,8	pK7GWIWG2-derivative; contains fragment of 160 bp (+2909/+3068) of Medtr2g460730.1 (ERF-TF) flanked with attB sites, cloned with LR-Reaction
pK7GW:RNAi_158_67_2	<i>A. rhizogenes</i> : <i>Arqua 1</i>	Spec 100/Strep 600	ca. 14,1	pK7GWIWG2-derivative; contains fragment of 223 bp (+2550/+2772) of Mtr.15867.1.S1_s_at (ERF-TF) flanked with attB sites, cloned with LR-Reaction
pK7GW:RNAi_144_9_3	<i>Omnimax</i>	Spec50/Chloro15	ca. 13,8	pK7GWIWG2-derivative; contains fragment of 281 bp (+2763/+3043) of Mtr.1449.1.S1_s_at (ERF-TF) flanked with attB sites, cloned with LR-Reaction
pK7GW:RNAi_460_730_1	<i>A. rhizogenes</i> : <i>Arqua 1</i>	Spec 100/Strep 600	ca. 13,8	pK7GWIWG2-derivative; contains fragment of 120 bp (-3/+118) of Medtr2g460730.1 (ERF-TF) flanked with attB sites, cloned with LR-Reaction
pK7GW:RNAi_460_730_2	<i>A. rhizogenes</i> : <i>Arqua 1</i>	Spec 100/Strep 600	ca. 13,8	pK7GWIWG2-derivative; contains fragment of 160 bp (+2909/+3068) of Medtr2g460730.1 (ERF-TF) flanked with attB sites, cloned with LR-Reaction
pDonor:RNAi_250_05_1	<i>E.coli DH5 alpha</i>	Kan 50	2,696	pDONR-derivative, contains fragment of 299 bp (-219/+77) of Mtr.25005.1.S1_s_at (ERF-TF) cloned with BP reaction
pDonor:RNAi_158_67_1	<i>E.coli DH5 alpha</i>	Kan 50	2,682	pDONR-derivative, contains fragment of 285 bp (-176/+106) of Mtr.15867.1.S1_s_at (ERF-TF) cloned with BP reaction
pK7GW:RNAi_144_9_2	<i>Omnimax</i>	Spec50/Chloro15	14,042	pK7GWIWG2-derivative; contains fragment of 171 bp (+2483/+2653) of Mtr.1449.1.S1_s_at (ERF-TF) flanked with attB sites, cloned with LR-Reaction
pK7GW:RNAi_158_67_1	<i>Omnimax</i>	Spec50/Chloro15	14,27	pK7GWIWG2-derivative; contains fragment of 285 bp (-176/+106) of Mtr.15867.1.S1_s_at (ERF-TF) flanked with attB sites, cloned with LR-Reaction
pK7GW:RNAi_250_05_1	<i>Omnimax</i>	Spec50/Chloro15	14,298	pK7GWIWG2-derivative; contains fragment of 299 bp (-219/+77) of Mtr.25005.1.S1_s_at (ERF-TF) flanked with attB sites, cloned with LR-Reaction
pK7GW:RNAi_144_9_2	<i>A. rhizogenes</i> : <i>Arqua 1</i>	Spec 100/Strep 600	14,042	pK7GWIWG2-derivative; contains fragment of 171 bp (+2483/+2653) of Mtr.1449.1.S1_s_at (ERF-TF) flanked with attB sites, cloned with LR-Reaction
pK7GW:RNAi_144_9_3	<i>A. rhizogenes</i> : <i>Arqua 1</i>	Spec 100/Strep 600	14,262	pK7GWIWG2-derivative; contains fragment of 281 bp (+2763/+3043) of Mtr.1449.1.S1_s_at (ERF-TF) flanked with attB sites, cloned with LR-Reaction
pK7GW:RNAi_158_67_1	<i>A. rhizogenes</i> : <i>Arqua 1</i>	Spec 100/Strep 600	14,27	pK7GWIWG2-derivative; contains fragment of 285 bp (-176/+106) of Mtr.15867.1.S1_s_at (ERF-TF) flanked with attB sites, cloned with LR-Reaction
pK7GW:RNAi_250_05_1	<i>A. rhizogenes</i> : <i>Arqua 1</i>	Spec 100/Strep 600	14,298	pK7GWIWG2-derivative; contains fragment of 299 bp (-219/+77) of Mtr.25005.1.S1_s_at (ERF-TF) flanked with attB sites, cloned with LR-Reaction
pK7GW:RNAi_144_9_1	<i>Omnimax</i>	Spec50/Chloro15	ca. 13,9	pK7GWIWG2-derivative; contains fragment of 192 bp (+18/+209) of Mtr.1449.1.S1_s_at (ERF-TF) flanked with attB sites, cloned with LR-Reaction
pK7GW:RNAi_144_9_1_IS	<i>Omnimax</i>	Spec50/Chloro15	ca. 13,9	pK7GWIWG2-derivative; contains fragment of 192 bp (+18/+209) of Mtr.1449.1.S1_s_at (ERF-TF) flanked with attB sites, cloned with LR-Reaction, intron of pK7GW is switched in this construct
pK7GW:RNAi_144_9_1	<i>A. rhizogenes</i> : <i>Arqua 1</i>	Spec 100/Strep 600	ca. 13,9	pK7GWIWG2-derivative; contains fragment of 192 bp (+18/+209) of Mtr.1449.1.S1_s_at (ERF-TF) flanked with attB sites, cloned with LR-Reaction

## Material and Methods

pK7GW:RNAi_144_9_1_IS	A. rhizogenes: Arqua 1	Spec 100/ Strep 600	ca. 13,9	pK7GW/WG2-derivative; contains fragment of 192 bp (+18/+209) of Mtr.1449.1.S1_s_at (ERF-TF) flanked with attB sites, cloned with LR-Reaction, intron of pK7GW is switched in this construct
-----------------------	------------------------	---------------------	----------	---

**Table 13: Cloned promoter-constructs for Y1H.** Promoter sequences amplified in this table were cloned using (Table 8).

Clone	Strain	Resistance	Plasmid size [kb]	Origin of the plasmid, Insert
pDonr:p15867	<i>E.coli</i> DH5 alpha	Kan 50	4,6	pDONR-derivative, contains fragment of 2296 bp (-2296/-1) of Mtr.15867.1.S1_s_at (ERF-TF) cloned with BP reaction
pMWR#2:p15867	<i>E.coli</i> DH5 alpha	Amp 100	7,9	pMWR#2-derivative, contains fragment of 2296 bp (-2296/-1) of Mtr.15867.1.S1_s_at (ERF-TF) cloned with LR reaction
pMWR#3:p15867	<i>E.coli</i> DH5 alpha	Amp 100	10,6	pMWR#3-derivative, contains fragment of 2296 bp (-2296/-1) of Mtr.15867.1.S1_s_at (ERF-TF) cloned with LR reaction
pDonr:p21492	<i>E.coli</i> DH5 alpha	Kan 50	3,6	pDONR-derivative, contains fragment of 862 bp (-955/-94) of Mtr.21492.1.S1_s_at (ERF-TF) cloned with BP reaction
pMWR#2:p21492	<i>E.coli</i> DH5 alpha	Amp 100	6,5	pMWR#2-derivative, contains fragment of 862 bp (-955/-94) of Mtr.21492.1.S1_s_at (ERF-TF) cloned with LR reaction
pMWR#3:p21492	<i>E.coli</i> DH5 alpha	Amp 100	9,4	pMWR#3-derivative, contains fragment of 862 bp (-955/-94) of Mtr.21492.1.S1_s_at (ERF-TF) cloned with LR reaction
pDonr:p460730	<i>E.coli</i> DH5 alpha	Kan 50	4,1	pDONR-derivative, contains fragment of 1513 bp (-1513/-1) of Medtr2g460730.1 (ERF-TF) cloned with BP reaction
pMWR#2:p460730	<i>E.coli</i> DH5 alpha	Amp 100	7,1	pMWR#2-derivative, contains fragment of 1513 bp (-1513/-1) of Medtr2g460730.1 (ERF-TF) cloned with LR reaction
pMWR#3:p460730	<i>E.coli</i> DH5 alpha	Amp 100	9,9	pMWR#3-derivative, contains fragment of 1513 bp (-1513/-1) of Medtr2g460730.1 (ERF-TF) cloned with LR reaction
pDonr:pRAM1	<i>E.coli</i> DH5 alpha	Kan 50	5,3	pDONR-derivative, contains fragment of 2453 bp (-2453/-1) of Medtr7g027190.1 (ERF-TF) cloned with BP reaction
pMWR#2:pRAM1	<i>E.coli</i> DH5 alpha	Amp 100	8,1	pMWR#2-derivative, contains fragment of 2453 bp (-2453/-1) of Medtr7g027190.1 (ERF-TF) cloned with LR reaction
pMWR#3:pRAM1	<i>E.coli</i> DH5 alpha	Amp 100	10,9	pMWR#3-derivative, contains fragment of 2453 bp (-2453/-1) of Medtr7g027190.1 (ERF-TF) cloned with LR reaction
pDonr:pSTR	<i>E.coli</i> DH5 alpha	Kan 50	4,7	pDONR-derivative, contains fragment of 257 bp (-257/-1) of Medtr8g107450.1 (ERF-TF) cloned with BP reaction
pMWR#2:pSTR	<i>E.coli</i> DH5 alpha	Amp 100	7,6	pMWR#2-derivative, contains fragment of 257 bp (-257/-1) of Medtr8g107450.1 (ERF-TF) cloned with LR reaction
pMWR#3:pSTR	<i>E.coli</i> DH5 alpha	Amp 100	10,4	pMWR#3-derivative, contains fragment of 257 bp (-257/-1) of Medtr8g107450.1 (ERF-TF) cloned with LR reaction
pDonr:pFatM	<i>E.coli</i> DH5 alpha	Kan 50	3,7	pDONR-derivative, contains fragment of 1108 bp (-1108/-1) of Medtr1g109110.1 (ERF-TF) cloned with BP reaction
pMWR#2:pFatM	<i>E.coli</i> DH5 alpha	Amp 100	6,7	pMWR#2-derivative, contains fragment of 1108 bp (-1108/-1) of Medtr1g109110.1 (ERF-TF) cloned with LR reaction
pMWR#3:pFatM	<i>E.coli</i> DH5 alpha	Amp 100	9,5	pMWR#3-derivative, contains fragment of 1108 bp (-1108/-1) of Medtr1g109110.1 (ERF-TF) cloned with LR reaction
pDonr:pKASII	<i>E.coli</i> DH5 alpha	Kan 50	3,6	pDONR-derivative, contains fragment of 985 bp (-985/-1) of Medtr4g096690.1 (ERF-TF) cloned with BP reaction
pMWR#2:pKASII	<i>E.coli</i> DH5 alpha	Amp 100	6,5	pMWR#2-derivative, contains fragment of 985 bp (-985/-1) of Medtr4g096690.1 (ERF-TF) cloned with LR reaction
pMWR#3:pKASII	<i>E.coli</i> DH5 alpha	Amp 100	9,4	pMWR#3-derivative, contains fragment of 985 bp (-985/-1) of Medtr4g096690.1 (ERF-TF) cloned with LR reaction
constructs derived from BSc thesis of Agnes Krüger, 2020:				
pDonr:p460730_250bp	<i>E.coli</i> DH5 alpha	Kan 50	3,1	pDONR-derivative, contains fragment of 256 bp (-255/+1) of Medtr2g460730.1 (ERF-TF) cloned with BP reaction
pDonr:p460730_ohneGCC	<i>E.coli</i> DH5 alpha	Amp 100	3	pDONR-derivative, contains fragment of 136 bp (-135/+1) of Medtr2g460730.1 (ERF-TF) cloned with BP reaction
pMWR#2:p460730_250bp	<i>E.coli</i> DH5 alpha	Amp 100	5,9	pMWR#2-derivative, contains fragment of 256 bp (-255/+1) of Medtr2g460730.1 (ERF-TF) cloned with LR reaction
pMWR#3:p460730_250bp	<i>E.coli</i> DH5 alpha	Amp 100	8,7	pMWR#3-derivative, contains fragment of 256 bp (-255/+1) of Medtr2g460730.1 (ERF-TF) cloned with LR reaction
pMWR#2:p460730_ohneGCC	<i>E.coli</i> DH5 alpha	Kan 50	5,7	pMWR#2-derivative, contains fragment of 136 bp (-135/+1) of Medtr2g460730.1 (ERF-TF) cloned with LR reaction
pMWR#3:p460730_ohneGCC	<i>E.coli</i> DH5 alpha	Amp 100	8,5	pMWR#3-derivative, contains fragment of 136 bp (-135/+1) of Medtr2g460730.1 (ERF-TF) cloned with LR reaction



## Material and Methods

**Table 14: Cloned Y2H constructs.** Constructs were cloned using (Table 9).

Clone	Strain	Resistance	Plasmid size [kb]	Origin of the plasmid, Insert
pGBKT:25005#1	<i>E.coli DH5 alpha</i>	Kan 50	8,7	CDS of <i>Mtr.25005.1.S1_at (Medtr7g011630.1)</i> cloned with Smal into pGBKT, native length of CDS 1392 bp
pGADT:25005#4	<i>E.coli DH5 alpha</i>	Amp 100	9,4	CDS of <i>Mtr.25005.1.S1_at (Medtr7g011630.1)</i> cloned with Smal into pGADT, native length of CDS 1392 bp
pGBKT:21492#3	<i>E.coli DH5 alpha</i>	Kan 50	8,6	CDS of <i>Mtr.21492.1.S1_at (Medtr6g012970.1)</i> cloned with Smal into pGBKT, native length of CDS 1236 bp
pGADT:21492#1	<i>E.coli DH5 alpha</i>	Amp 100	9,3	CDS of <i>Mtr.21492.1.S1_at (Medtr6g012970.1)</i> cloned with Smal into pGADT, native length of CDS 1236 bp
pGADT:ERF1#7	<i>E.coli DH5 alpha</i>	Amp 100	9,2	CDS of <i>Mtr.46362.1.S1_at (Medtr7g009410.1)</i> cloned with Smal into pGADT, native length of CDS 1188 bp
pGBKT:ERF1#6	<i>E.coli DH5 alpha</i>	Kan 50	8,5	CDS of <i>Mtr.46362.1.S1_at (Medtr7g009410.1)</i> cloned with Smal into pGBKT, native length of CDS 1188 bp
pGADT:WRI5A#6	<i>E.coli DH5 alpha</i>	Amp 100	9,2	CDS of <i>Mtr.1449.1.S1_at (Medtr8g468920.1)</i> cloned with Smal into pGADT, native length of CDS 1221 bp
pGBKT:WRI5A#18	<i>E.coli DH5 alpha</i>	Kan 50	8,5	CDS of <i>Mtr.1449.1.S1_at (Medtr8g468920.1)</i> cloned with Smal into pGBKT, native length of CDS 1221 bp
pGADT:460730#2	<i>E.coli DH5 alpha</i>	Amp 100	9,1	CDS of <i>Medtr2g460730.1</i> cloned with Smal into pGADT, native length of CDS 1101 bp
pGBKT:460730#3	<i>E.coli DH5 alpha</i>	Kan 50	8,4	CDS of <i>Medtr2g460730.1</i> cloned with Smal into pGBKT, native length of CDS 1101 bp
pGADT:15867#20	<i>E.coli DH5 alpha</i>	Amp 100	9,1	CDS of <i>Mtr.15867.1.S1_at (Medtr4g130270.1)</i> cloned with Smal into pGADT, native length of CDS 1091 bp
pGBKT:15867#1	<i>E.coli DH5 alpha</i>	Kan 50	8,4	CDS of <i>Mtr.15867.1.S1_at (Medtr4g130270.1)</i> cloned with Smal into pGBKT, native length of CDS 1091 bp
pGADT:WRI5C#24	<i>E.coli DH5 alpha</i>	Amp 100	9,2	CDS of <i>Medtr6g011490.1</i> cloned with Smal into pGADT, native length of CDS 1196 bp
pGBKT:WRI5C#9	<i>E.coli DH5 alpha</i>	Kan 50	8,5	CDS of <i>Medtr6g011490.1</i> cloned with Smal into pGBKT, native length of CDS 1196 bp

**Table 15: Coconstructed strains used as Y1H baits.**

Clone	Strain	Resistance	Origin of the plasmid, Insert
pMWR:p15867	<i>S. cerevisiae</i> YM4271	HIS/URA	pMWR-derivative, contains fragment of 2296 bp (2296/-1) of <i>Mtr.15867.1.S1_s_at (ERF-TF)</i>
pMWR:p21492	<i>S. cerevisiae</i> YM4271	HIS/URA	pMWR-derivative, contains fragment of 862 bp (955/-94) of <i>Mtr.21492.1.S1_s_at (ERF-TF)</i>
pMWR:pSTR	<i>S. cerevisiae</i> YM4271	HIS/URA	pMWR-derivative, contains fragment of 257 bp (257/-1) of <i>Medtr8g107450.1 (ERF-TF)</i>
pMWR:pFatM	<i>S. cerevisiae</i> YM4271	HIS/URA	pMWR-derivative, contains fragment of 1108 bp (1108/-1) of <i>Medtr1g109110.1 (ERF-TF)</i>
pMWR:pKASII	<i>S. cerevisiae</i> YM4271	HIS/URA	pMWR-derivative, contains fragment of 985 bp (985/-1) of <i>Medtr4g096690.1 (ERF-TF)</i>
pMWR:p460730_250bp	<i>S. cerevisiae</i> YM4271	HIS/URA	pMWR-derivative, contains fragment of 256 bp (255/+1) of <i>Medtr2g460730.1 (ERF-TF)</i>
pMWR:p460730_ohneGCC	<i>S. cerevisiae</i> YM4271	HIS/URA	pMWR-derivative, contains fragment of 136 bp (135/+1) of <i>Medtr2g460730.1 (ERF-TF)</i>

**Table 16: Cloned yeast strains used for Y2H.**

Clone	Strain	Resistance	Plasmid size [kb]	Origin of the plasmid, Insert
pGBKT:25005#1	<i>S. cerevisiae</i> Y2H Gold	TRP	8,7	CDS of <i>Mtr.25005.1.S1_at (Medtr7g011630.1)</i> cloned with Smal into pGBKT, native length of CDS 1392 bp
pGADT:25005#4	Y187 ( <i>S. cerevisiae</i> )	LEU	9,4	CDS of <i>Mtr.25005.1.S1_at (Medtr7g011630.1)</i> cloned with Smal into pGADT, native length of CDS 1392 bp
pGBKT:21492#3	<i>S. cerevisiae</i> Y2H Gold	TRP	8,6	CDS of <i>Mtr.21492.1.S1_at (Medtr6g012970.1)</i> cloned with Smal into pGBKT, native length of CDS 1236 bp
pGADT:21492#1	Y187 ( <i>S. cerevisiae</i> )	LEU	9,3	CDS of <i>Mtr.21492.1.S1_at (Medtr6g012970.1)</i> cloned with Smal into pGADT, native length of CDS 1236 bp
pGADT:ERF1#7	Y187 ( <i>S. cerevisiae</i> )	LEU	9,2	CDS of <i>Mtr.46362.1.S1_at (Medtr7g009410.1)</i> cloned with Smal into pGADT, native length of CDS 1188 bp

## Material and Methods

pGBKT:ERF1#6	<i>S. cerevisiae</i> Y2H Gold	TRP	8,5	CDS of <i>Mtr.46362.1.S1_at (Medtr7g009410.1)</i> cloned with <i>SmaI</i> into pGBKT , native length of CDS 1188 bp
pGADT:WRI5A#6	Y187 ( <i>S. cerevisiae</i> )	LEU	9,2	CDS of <i>Mtr.1449.1.S1_at (Medtr8g468920.1)</i> cloned with <i>SmaI</i> into pGADT, native length of CDS 1221 bp
pGBKT:WRI5A#18	<i>S. cerevisiae</i> Y2H Gold	TRP	8,5	CDS of <i>Mtr.1449.1.S1_at (Medtr8g468920.1)</i> cloned with <i>SmaI</i> into pGBKT, native length of CDS 1221 bp
pGADT:460730#2	Y187 ( <i>S. cerevisiae</i> )	LEU	9,1	CDS of <i>Medtr2g460730.1</i> cloned with <i>SmaI</i> into pGADT, native length of CDS 1101 bp
pGBKT:460730#3	<i>S. cerevisiae</i> Y2H Gold	TRP	8,4	CDS of <i>Medtr2g460730.1</i> cloned with <i>SmaI</i> into pGBKT, native length of CDS 1101 bp
pGADT:15867#20	Y187 ( <i>S. cerevisiae</i> )	LEU	9,1	CDS of <i>Mtr.15867.1.S1_at (Medtr4g130270.1)</i> cloned with <i>SmaI</i> into pGADT, native length of CDS 1091 bp
pGBKT:15867#1	<i>S. cerevisiae</i> Y2H Gold	TRP	8,4	CDS of <i>Mtr.15867.1.S1_at (Medtr4g130270.1)</i> cloned with <i>SmaI</i> into pGBKT, native length of CDS 1091 bp
pGADT:WRI5C#24	Y187 ( <i>S. cerevisiae</i> )	LEU	9,2	CDS of <i>Medtr6g011490.1</i> cloned with <i>SmaI</i> into pGADT, native length of CDS 1196 bp
pGBKT:WRI5C#9	<i>S. cerevisiae</i> Y2H Gold	TRP	8,5	CDS of <i>Medtr6g011490.1</i> cloned with <i>SmaI</i> into pGBKT, native length of CDS 1196 bp
constructs cloned by Steven Krüger (unpublished data)				
pGADT:NFYA1	Y187 ( <i>S. cerevisiae</i> )	LEU	9	Y2H-prey vector containing <i>MtNF-YA1</i> CDS (999bp), cloned from <i>pk18:NF-YA1</i> via <i>SmaI</i> -restriction sites in-frame into pGADT7 AD. ( <i>Medtr1g056530.1/Mtr.43750.1.S1_at</i> )
pGADT:NFYA2	Y187 ( <i>S. cerevisiae</i> )	LEU	9	Y2H-prey vector containing <i>MtNF-YA2</i> CDS (1002bp), cloned from <i>pk18:NF-YA2</i> via <i>SmaI</i> -restriction sites in-frame into pGADT7 AD. ( <i>Medtr7g106450.1/Mtr.1584.1.S1_at</i> )
pGADT:NFYA3	Y187 ( <i>S. cerevisiae</i> )	LEU	8,7	Y2H-prey vector containing <i>MtNF-YA3</i> CDS (708bp), cloned from <i>pk18:NF-YA3</i> via <i>SmaI</i> -restriction sites in-frame into pGADT7 AD. ( <i>Medtr2g041090.1/Mtr.42674.1.S1_at</i> )
pGADT:NFYA4	Y187 ( <i>S. cerevisiae</i> )	LEU	9,04	Y2H-prey vector containing <i>MtNF-YA4</i> CDS (1044bp), cloned from <i>pk18:NF-YA4</i> via <i>SmaI</i> -restriction sites in-frame into pGADT7 AD. ( <i>Medtr2g099490.1/Mtr.13830.1.S1_s_at</i> )
pGADT:NFYA5	Y187 ( <i>S. cerevisiae</i> )	LEU	9	Y2H-prey vector containing <i>MtNF-YA5</i> CDS (990bp) cloned into pGADT7-AD. ( <i>Medtr3g061510.1/Mtr.40999.1.S1_at</i> )
pGADT:NFYA6	Y187 ( <i>S. cerevisiae</i> )	LEU	8,6	Y2H-prey vector containing <i>MtNF-YA6</i> CDS (624bp), cloned from <i>pk18:NF-YA6</i> via <i>SmaI</i> -restriction sites in-frame into pGADT7 AD. ( <i>Medtr2g030170.1/Mtr.44133.1.S1_at</i> )
pGADT:NFYA7	Y187 ( <i>S. cerevisiae</i> )	LEU	8,9	Y2H-prey vector containing <i>MtNF-YA7</i> CDS (915bp), cloned from <i>pk18:NF-YA7</i> via <i>SmaI</i> -restriction sites in-frame into pGADT7 AD. ( <i>Medtr8g037270.1/Mtr.5583.1.S1_at</i> )
pGADT:NFYA8	Y187 ( <i>S. cerevisiae</i> )	LEU	8,9	Y2H-prey vector containing <i>MtNF-YA8</i> CDS (903bp), cloned from <i>pk18:NF-YA8</i> via <i>SmaI</i> -restriction sites in-frame into pGADT7 AD. ( <i>Medtr8g019540.1/Mtr.34979.1.S1_at</i> )
pGADT:Cbf1	Y187 ( <i>S. cerevisiae</i> )	LEU	8,36	Y2H prey vector for <i>MtCbf1</i> cds(0/360) cloned via <i>NdeI/BamHI (Mtr.51511.1.S1_at)</i>
pGADT:Cbf2	Y187 ( <i>S. cerevisiae</i> )	LEU	8,35	Y2H prey vector for <i>MtCbf2</i> cds(0/354) cloned via <i>NdeI/BamHI (Mtr.16863.1.S1_at)</i>
pGADT:Cbf3	Y187 ( <i>S. cerevisiae</i> )	LEU	8,6	Y2H prey vector for <i>MtCbf3</i> cds(0/609) cloned via <i>EcoRI/BamHI</i> , deletion leads to ~10 altered AA at the end of the sequence ( <i>Mtr.4282.1.S1_at</i> )
constructs cloned by Rico Hartmann, 2018 (phd thesis)				
pGADT7:MtGras1	Y187 ( <i>S. cerevisiae</i> )	LEU	ca. 9,3 kb	CDS of GRAS1 ( <i>Medtr3g022830/Mtr.7264.1.S1_at</i> ) cloned with <i>SmaI</i> into pGADT, native length of CDS 1332 bp
pGADT7:MtGras4	Y187 ( <i>S. cerevisiae</i> )	LEU	ca. 9,4 kb	CDS of GRAS4 ( <i>Medtr7g109580.1/Mtr.31955.1.S1_at</i> ) cloned with <i>SmaI</i> into pGADT, native length of CDS 1671 bp
pGADT7:MtGras5	Y187 ( <i>S. cerevisiae</i> )	LEU	ca. 9,4 kb	CDS of GRAS5 ( <i>Medtr2g089100/Mtr.47463.1.S1_at</i> ) cloned with <i>SmaI</i> into pGADT, native length of CDS 1407 bp

## Material and Methods

pGADT7:MtGras6	Y187 ( <i>S. cerevisiae</i> )	LEU	ca. 9,4 kb	CDS of GRAS6 ( <i>Medtr1g069725/Mtr.31955.1.S1_at</i> ) cloned with SmaI into pGADT, native length of CDS 1377 bp
pGADT7:MtGras7	Y187 ( <i>S. cerevisiae</i> )	LEU	ca. 9,4 kb	CDS of GRAS7 ( <i>Medtr1g086970/Mtr.24642.1.S1_at</i> ) cloned with SmaI into pGADT, native length of CDS 1443 bp
pGADT7:MtGras8	Y187 ( <i>S. cerevisiae</i> )	LEU	ca. 9,4 kb	CDS of GRAS8 ( <i>Medtr4g104020/Mtr.36004.1.S1_at</i> ) cloned with SmaI into pGADT, native length of CDS 1566 bp
pGADT7:MtGras9	Y187 ( <i>S. cerevisiae</i> )	LEU	ca. 9,5 kb	CDS of GRAS9 ( <i>Medtr8g093070.1/Mtr.45911.1.S1_at</i> ) cloned with SmaI into pGADT, native length of CDS 1524 bp
pGADT7:MtRam1	Y187 ( <i>S. cerevisiae</i> )	LEU	ca. 10 kb	CDS of RAM1 ( <i>Medtr7g027190/Mtr.11244.1.S1_at</i> ) cloned with SmaI into pGADT, native length of CDS 2033 bp

**Table 17: cloned BIFC constructs**

Clone	Strain	Resistance	Plasmid size [kb]	Origin of the plasmid, Insert
pDonor:WRI5A	<i>E. coli DH5 alpha mcr</i>	Kan50	3,8	pDONR-derivative with the CDS of WRI5A (1221 bp) ( <i>Mtr.1449.1.S1_at/Medtr8g468920.1</i> ),
pDonor:WRI5B	<i>E. coli DH5 alpha mcr</i>	Kan50	3,8	pDONR-derivative with the CDS of WRI5B (1188 bp) ( <i>Mtr.46362.1.S1_at/Medtr7g009410.1</i> ),
pDonor:WRI5C	<i>E. coli DH5 alpha mcr</i>	Kan50	3,8	pDONR-derivative with the CDS of WRI5C (1196 bp) ( <i>Medtr6g011490.1</i> )
pDonor:25005	<i>E. coli DH5 alpha mcr</i>	Kan50	4	pDONR-derivative with the CDS of <i>Mtr.25005.1.S1_at</i> ( <i>Medtr7g011630.1</i> (1392 bp),
pSPYCE:WRI5A	<i>E. coli DH5 alpha mcr</i>	Rif100 Genta15 Kan50	13	pSPYCE:35s-GW-derivative with the CDS of WRI5A (1221 bp) ( <i>Mtr.1449.1.S1_at/Medtr8g468920.1</i> ), integrated over a LR-Reaction to obtain a fusion of WRI5A with the C-Terminus of an eYFP
pSPYNE:WRI5A	<i>E. coli DH5 alpha mcr</i>	Rif100 Genta15 Kan50	13	pSPYNE:35s-GW-derivative with the CDS of WRI5A (1221 bp) ( <i>Mtr.1449.1.S1_at/Medtr8g468920.1</i> ), integrated over a LR-Reaction to obtain a fusion of WRI5A with the N-Terminus of an eYFP
pSPYCE:WRI5B	<i>E. coli DH5 alpha mcr</i>	Rif100 Genta15 Kan50	13	pSPYCE:35s-GW-derivative with the CDS of WRI5B (1188 bp) ( <i>Mtr.46362.1.S1_at/Medtr7g009410.1</i> ), integrated over a LR-Reaction to obtain a fusion of WRI5B with the C-Terminus of an eYFP
pSPYNE:WRI5B	<i>E. coli DH5 alpha mcr</i>	Rif100 Genta15 Kan50	13	pSPYNE:35s-GW-derivative with the CDS of WRI5B (1188 bp) ( <i>Mtr.46362.1.S1_at/Medtr7g009410.1</i> ), integrated over a LR-Reaction to obtain a fusion of WRI5B with the N-Terminus of an eYFP
pSPYCE:WRI5C	<i>E. coli DH5 alpha mcr</i>	Rif100 Genta15 Kan50	13	pSPYCE:35s-GW-derivative with the CDS of WRI5C (1196 bp) ( <i>Medtr6g011490.1</i> ), integrated over a LR-Reaction to obtain a fusion of WRI5C with the C-Terminus of an eYFP
pSPYNE:WRI5C	<i>E. coli DH5 alpha mcr</i>	Rif100 Genta15 Kan50	13	pSPYNE:35s-GW-derivative with the CDS of WRI5C (1196 bp) ( <i>Medtr6g011490.1</i> ), integrated over a LR-Reaction to obtain a fusion of WRI5C with the N-Terminus of an eYFP
pSPYCE:25005	<i>E. coli DH5 alpha mcr</i>	Rif100 Genta15 Kan50	13	pSPYCE:35s-GW-derivative with the CDS of <i>Mtr.25005.1.S1_at</i> ( <i>Medtr7g011630.1</i> (1392 bp), integrated over a LR-Reaction to obtain a fusion of 25005 with the C-Terminus of an eYFP
pSPYNE:25005	<i>E. coli DH5 alpha mcr</i>	Rif100 Genta15 Kan50	13	pSPYNE:35s-GW-derivative with the CDS of <i>Mtr.25005.1.S1_at</i> ( <i>Medtr7g011630.1</i> (1392 bp), integrated over a LR-Reaction to obtain a fusion of 25005 with the N-Terminus of an eYFP
pSPYCE:WRI5A	<i>A.tumefaciens</i> GV3101	Rif100 Genta15 Kan50	13	pSPYCE:35s-GW-derivative with the CDS of WRI5A (1221 bp) ( <i>Mtr.1449.1.S1_at/Medtr8g468920.1</i> ), to obtain a fusion of WRI5A with the C-Terminus of an eYFP
pSPYNE:WRI5A	<i>A.tumefaciens</i> GV3101	Rif100 Genta15 Kan50	13	pSPYNE:35s-GW-derivative with the CDS of WRI5A (1221 bp) ( <i>Mtr.1449.1.S1_at/Medtr8g468920.1</i> ), to obtain a fusion of WRI5A with the N-Terminus of an eYFP
pSPYCE:WRI5B	<i>A.tumefaciens</i> GV3101	Rif100 Genta15 Kan50	13	pSPYCE:35s-GW-derivative with the CDS of WRI5B (1188 bp) ( <i>Mtr.46362.1.S1_at/Medtr7g009410.1</i> ), to obtain a fusion of WRI5B with the C-Terminus of an eYFP
pSPYNE:WRI5B	<i>A.tumefaciens</i> GV3101	Rif100 Genta15 Kan50	13	pSPYNE:35s-GW-derivative with the CDS of WRI5B (1188 bp) ( <i>Mtr.46362.1.S1_at/Medtr7g009410.1</i> ), to obtain a fusion of WRI5B with the N-Terminus of an eYFP
pSPYCE:WRI5C	<i>A.tumefaciens</i> GV3101	Rif100 Genta15 Kan50	13	pSPYCE:35s-GW-derivative with the CDS of WRI5C (1196 bp) ( <i>Medtr6g011490.1</i> ) to obtain a fusion of WRI5C with the C-Terminus of an eYFP

## Material and Methods

<i>pSPYNE:WRI5C</i>	<i>A.tumefaciens</i> GV3101	Rif100 Genta15 Kan50	13	<i>pSPYNE:35s-GW</i> -derivative with the CDS of <i>WRI5C</i> (1196 bp) ( <i>Medtr6g011490.1</i> ), obtain a fusion of <i>WRI5C</i> with the N-Terminus of an eYFP
<i>pSPYCE:25005</i>	<i>A.tumefaciens</i> GV3101	Rif100 Genta15 Kan50	13	<i>pSPYCE:35s-GW</i> -derivative with the CDS of <i>Mtr.25005.1.S1_at</i> ( <i>Medtr7g011630.1</i> (1392 bp), to obtain a fusion of <i>25005</i> with the C-Terminus of an eYFP
<i>pSPYNE:25005</i>	<i>A.tumefaciens</i> GV3101	Rif100 Genta15 Kan50	13	<i>pSPYNE:35s-GW</i> -derivative with the CDS of <i>Mtr.25005.1.S1_at</i> ( <i>Medtr7g011630.1</i> (1392 bp), to obtain a fusion of <i>25005</i> with the N-Terminus of an eYFP
constructs cloned by Steven Krüger (unpublished data)				
<i>pSPYNE:Nf-YA4</i>	<i>A.tumefaciens</i> GV3101	Rif100 Genta15 Kan50	14kb	<i>pSPYNE:35s-GW</i> -derivative with the CDS of <i>Nf-YA4</i> (1044 bp) ( <i>Medtr2g099490.1/ Mtr.13830.1.S1_s_at</i> ), to obtain a fusion of <i>Nf-YA4</i> with the N-Terminus of an eYFP.
<i>pSPYCE:Nf-YA4</i>	<i>A.tumefaciens</i> GV3101	Rif100 Genta15 Kan50	14kb	<i>pSPYCE:35s-GW</i> -derivative with the CDS of <i>Nf-YA4</i> (1044 bp) ( <i>Medtr2g099490.1/ Mtr.13830.1.S1_s_at</i> ), to obtain a fusion of <i>Nf-YA4</i> with the C-Terminus of an eYFP.
<i>pSPYNE:Nf-YA7</i>	<i>A.tumefaciens</i> GV3101	Rif100 Genta15 Kan50	14kb	<i>pSPYNE:35s-GW</i> -derivative with the CDS of <i>Nf-YA7</i> (915 bp) ( <i>Medtr8g037270.1/ Mtr.5583.1.S1_at</i> ), to obtain a fusion of <i>Nf-YA7</i> with the N-Terminus of an eYFP.
<i>pSPYCE:Nf-YA7</i>	<i>A.tumefaciens</i> GV3101	Rif100 Genta15 Kan50	14kb	<i>pSPYCE:35s-GW</i> -derivative with the CDS of <i>Nf-YA7</i> (915 bp) ( <i>Medtr8g037270.1/ Mtr.5583.1.S1_at</i> ), to obtain a fusion of <i>Nf-YA7</i> with the C-Terminus of an eYFP.
<i>pSPYNE:Nf-YA2</i>	<i>A.tumefaciens</i> GV3101	Rif100 Genta15 Kan50	14kb	<i>pSPYNE:35s-GW</i> -derivative with the CDS of <i>Nf-YA2</i> (1002 bp) ( <i>Medtr7g106450.1/ Mtr.1584.1.S1_at</i> ), to obtain a fusion of <i>Nf-YA2</i> with the N-Terminus of an eYFP.
<i>pSPYCE:Nf-YA2</i>	<i>A.tumefaciens</i> GV3101	Rif100 Genta15 Kan50	14kb	<i>pSPYCE:35s-GW</i> -derivative with the CDS of <i>Nf-YA2</i> (1002 bp) ( <i>Medtr7g106450.1/ Mtr.1584.1.S1_at</i> ), to obtain a fusion of <i>Nf-YA2</i> with the C-Terminus of an eYFP
<i>pSPYNE:Cbf3</i>	<i>A.tumefaciens</i> GV3101	Rif100 Genta15 Kan50	14kb	<i>pSPYNE:35s-GW</i> -derivative with the CDS of <i>CBF3</i> (609 bp) ( <i>Mtr.4282.1.S1_at</i> ), to obtain a fusion of <i>CBF3</i> with the N-Terminus of an eYFP
<i>pSPYCE:Cbf3</i>	<i>A.tumefaciens</i> GV3101	Rif100 Genta15 Kan50	14kb	<i>pSPYCE:35s-GW</i> -derivative with the CDS of <i>CBF3</i> (609 bp) ( <i>Mtr.4282.1.S1_at</i> ), to obtain a fusion of <i>CBF3</i> with the C-Terminus of an eYFP
cloned by Arne Petersen (unpublished data)				
<i>pSPYCE:MtRam1</i>	<i>A.tumefaciens</i> GV3101	Rif100 Genta15 Kan50	14,1	<i>pSPYCE:35s-GW</i> -derivative with the CDS of <i>MtRAM1</i> ( <i>Medtr7g027190.1</i> ), to obtain a fusion of <i>MtRAM1</i> with the N-Terminus of an eYFP.
<i>pSPYNE:MtRam1</i>	<i>A.tumefaciens</i> GV3101	Rif100 Genta15 Kan50	14,1	<i>pSPYNE:35s-GW</i> -derivative with the CDS of <i>MtRAM1</i> ( <i>Medtr7g027190.1</i> ), to obtain a fusion of <i>MtRAM1</i> with the N-Terminus of an eYFP.

## Media, antibiotics, and supplements

### Growth media for bacteria, yeast, and plants

Table 18: Growth media for bacteria, yeast, and plants.

media	compound	concentration
<b>LB-media</b>	tryptone	10 g/l
	yeast extract	5 g/l
	NaCl	5 g/l
adjust to pH 7,4		
<b>LBG-media</b>	tryptone	10 g/l
	yeast extract	5 g/l
	NaCl	5 g/l
	glucose	1 g/l
adjust to pH 7,4		
<b>TY-media</b>	tryptone	5 g/l
	yeast extract	3 g/l
	CaCl <sub>2</sub> x H <sub>2</sub> O	0,7 g/l
adjust to pH 7,2		
<b>PA-media</b>	antibiotic media no. 3	17,5 g/l
<b>SOC-media</b>	tryptone	20 g/l

## Material and Methods

	yeast extract	5 g/l
	NaCl	0,58 g/l
	KCl (250 mM)	10 ml/l
<b>YPDA</b>		
<b>SC</b>		
<b>phytoagar</b>		

## Antibiotics and supplements

Table 19: Antibiotics and supplements.

antibiotic	abbreviation	final concentration	diluted in
Agar		15g/l	
Ampicillin	AMP	100 µg/ml	sterile H <sub>2</sub> O *
Kanamycin	KAN	50 µg/ml	sterile H <sub>2</sub> O *
Streptomycin	STREP	600 µg/ml	sterile H <sub>2</sub> O *
X-Gal		25 mg/ml	N,N-Dimethylformamid
Isopropyl-β-D-1-thiogalactopyranoside	IPTG	25 mg/ml	sterile H <sub>2</sub> O *
X-Gluc		50 mg/ml	N,N-Dimethylformamid

## Buffers and solutions

Table 20: Buffers and solutions.

buffer	compound	final concentration
Tbf1-buffer	RbCl	100 mM
	2(N-Morpholino)ethanesulfonacid	10 mM
	CaCl <sub>2</sub> x 2 H <sub>2</sub> O	10 mM
	MnCl <sub>2</sub> x 2 H <sub>2</sub> O	50 mM
adjust to pH 6		
Tbf2-buffer	MOPS	10 mM
	CaCl <sub>2</sub> x 2 H <sub>2</sub> O	75 mM
	RbCl	10 mM
	glycerol (87 %)	15 % (v/v)
adjust to pH 6,5		
PS-buffer	Na <sub>2</sub> H <sub>2</sub> PO <sub>4</sub> x 2 H <sub>2</sub> O	7 g/l
	NaCl	5 g/l
	KH <sub>2</sub> PO <sub>4</sub>	3 g/l
adjust to pH 7,0		
P1-buffer	Tris-Cl	50 mM
	EDTA	10 mM
adjust to pH 8,0 with HCl		
P2-buffer	NaOH	200 mM
	SDS	1 % (v/v)
P3-buffer	kalium acetate	2,55 M
adjust to pH 4,8 with glacial acetic acid		
TE-buffer	Tris-HCl (pH 8)	10 mM
	EDTA (pH 8)	1 mM

## Material and Methods

10 x TA restriction buffer	K-acetate	660 mM
	Tris-HCl	330 mM
	MgCl <sub>2</sub>	100 mM
	Dithiothreitol (DTT)	5 mM
	bovine serum albumin	1 mg/ml
adjust to 7,5 pH with glacial acetic acid		
TCM-buffer	CaCl <sub>2</sub>	10 mM
	MgCl <sub>2</sub>	10 mM
	Tris-HCl	10 mM
adjust to pH 7,5		
1 x TAE buffer (gelelectrophoresis)	Tris-HCl	40 mM
	Na-acetate	10 mM
	EDTA	1 mM
adjust to pH 7,8 with glacial acetic acid		
BPB/ glycerol solution	glycerol	87 %
	TA-buffer	
	brom phenole blue (BPB)	
1 % agarose		0,01 g /ml
TrisHCl/ NaCl-buffer	Tris-HCl	100 mM
	NaCl	50 mM
adjust to pH 7,0 with HCl		
K-Ferri/Ferrocyanid	K-Ferricyanid	100 mM
	K-Ferrocyanid	100 mM
X-Gluc stock solution	5-Bromo-4-Cloro-3-Indolyl/ $\beta$ -D-glucoside)	25 mg X-Gluc in 500 $\mu$ l N,N-Dimethylformamid
GUS staining solution	Tris-HCl/ NaCl buffer	96 %
	K-Ferri/Ferrocyanid solution	2 %
	X-Gluc	2 %
Na-phosphate-buffer	NaH <sub>2</sub> PO <sub>4</sub> (pH 4,2)	0,5 mM
	Na <sub>2</sub> HPO <sub>4</sub> (pH 9,5)	0,5 mM
adjust to pH 7,5		
$\frac{1}{2}$ strength Hoagland's solution	Ca(NO <sub>3</sub> ) <sub>2</sub> x 4 H <sub>2</sub> O (1 M)	2,5 mM
	KNO <sub>3</sub> (1 M)	2,5 mM
	MgSO <sub>4</sub> x 7 H <sub>2</sub> O	1 mM
	NaFe EDTA	50 $\mu$ M
	KH <sub>2</sub> PO <sub>4</sub>	20 $\mu$ M
	micronutrient solution	
	- Na <sub>2</sub> MoO <sub>4</sub> x 2 H <sub>2</sub> O	0,2 $\mu$ M
	- H <sub>3</sub> BO <sub>3</sub>	10 $\mu$ M
	- NiCl <sub>2</sub> x 6 H <sub>2</sub> O	0,2 $\mu$ M
	- ZnSO <sub>4</sub> x 7 H <sub>2</sub> O	1 $\mu$ M
	- MnCl <sub>2</sub> x 2 H <sub>2</sub> O	2 $\mu$ M
	- CuSO <sub>4</sub> x 5 H <sub>2</sub> O	0,5 $\mu$ M
	- CoCl <sub>2</sub> x 6 H <sub>2</sub> O	0,2 $\mu$ M
adjust to pH 6,3 – 6,5 (with 10 % KOH)		

## Material and Methods

### Enzymes

Table 21: Enzymes.

enzyme	supplier
<i>ApaI</i>	
<i>BamHI</i>	
<i>BglII</i>	
<i>BseRI</i>	
BP Clonase	
<i>Clal</i>	
<i>DraI</i>	
<i>EcoRI</i>	
<i>EcoRV</i>	
<i>HindIII</i>	
Klenow-Fragment (10 U/μl)	Fermentas, St. Leon-Rot, Germany
<i>KpnI</i>	
LR Clonase	
<i>NcoI</i>	
<i>NdeI</i>	
<i>NsiI</i>	
Phusion HF Polymerase	Finnzymes, Vantaa, France
<i>PstI</i>	
RNAse A	SERVA Electrophoresis, Heidelberg, Germany
<i>SalI</i>	
shrimp alkaline phosphatase (1 U/μL)	Fermentas, St. Leon-Rot, Germany
<i>SacI</i>	
<i>SmaI</i>	
<i>SpeI</i>	
<i>SphI</i>	
SuperScript RT III	Invitrogen, Karlsruhe, Germany
T4-DNA ligase (1 U/μl)	Fermentas, St. Leon-Rot, Germany
<i>XbaI</i>	
<i>XhoI</i>	
<i>XmaI</i>	

### Kits

Table 22: Comercial kits.

kits	supplier
<i>NucleoSpin Extract II Kit</i>	Macherey-Nagel, Düren, Germany
<i>QIAprep Spin Miniprep Kit</i>	Qiagen, Hilden, Germany
<i>RNeasy Plant Mini Kit</i>	Qiagen, Hilden, Germany
<i>SensiFAST<sup>TM</sup> Sybr No-ROX One-Step Kit</i>	Bioline, Luckenwalde, Germany
<i>Superscript RT III Kit</i>	Invitrogen, Karlsruhe, Germany
<i>DNAseI, RNAse free</i>	Thermo Scientific
<i>DNeasy Plant Mini Kit</i>	Qiagen, Hilden, Germany
<i>Matchmaker Gold yeast Two Hybrid System</i>	Clontech Laboratories, Inc., Takara Bio Company, Mount View, USA

## Material and Methods

### Chemicals

Table 23: Used chemicals.

chemicals	supplier
acetetic acid	Roth, Karlsruhe, Germany
agar agar	Invitrogen, Karlsruhe, Germany
Agarose PeqGold	Peqlab, Erlangen, Germany
Antibiotic Medium No.3	Oxoid, Wesel, Germany
brome-phenolic-blue (BPB)	Merck, Darmstadt, Germany
bovine serumalbumin (BSA)	Serva, Heidelberg, Germany
Ca(NO <sub>3</sub> ) <sub>2</sub> x 4 H <sub>2</sub> O	Roth, Karlsruhe, Germany
CaCl <sub>2</sub> x 2 H <sub>2</sub> O	Merck, Darmstadt, Germany
CoCl <sub>2</sub> x 6 H <sub>2</sub> O	Sigma Aldrich, München, Germany
CuSO <sub>4</sub> x 5 H <sub>2</sub> O	Sigma Aldrich, München, Germany
DEPC-treated H <sub>2</sub> O	Roth, Karlsruhe, Germany
desoxy-nucleosidetriphosphates (dNTP's)	Fermentas, St. Leon-Rot, Germany
Dithiothreitol (DTT)	Sigma Aldrich, München, Germany
ethylendiamintetraacetate acid (EDTA)	Merck, Darmstadt, Germany
ethanole	Merck, Darmstadt, Germany
ethidium bromide	Roth, Karlsruhe, Germany
GeneRuler DNA ladders (50 bp, 100 bp and 1kB)	Thermo Fisher Scientific, Waltham, Massachusetts, US A
glycerine	AppliChem, Darmstadt, Germany
H <sub>2</sub> SO <sub>4</sub>	Roth, Karlsruhe, Germany
H <sub>3</sub> BO <sub>3</sub>	Sigma Aldrich, München, Germany
HCl	Roth, Karlsruhe, Germany
ink	Sheaffer, Shelton, Connecticut, USA
IPTG	Roth, Karlsruhe, Germany
isopropanole	Roth, Karlsruhe, Germany
K <sub>2</sub> HPO <sub>4</sub>	Merck, Darmstadt, Germany
KCl	Merck, Darmstadt, Germany
K-Ferricyanide	Sigma Aldrich, München, Germany
K-Ferrocyanide	Sigma Aldrich, München, Germany
KNO <sub>3</sub>	Sigma Aldrich, München, Germany
KOH	Roth, Karlsruhe, Germany
Morpholinoethansulfonacetate (MES)	SERVA Electrophoresis, Heidelberg, Germany
MgCl <sub>2</sub> x 6 H <sub>2</sub> O	Merck, Darmstadt, Germany
MgSO <sub>4</sub> x 7 H <sub>2</sub> O	Merck, Darmstadt, Germany
MnCl <sub>2</sub> x 2 H <sub>2</sub> O	Merck, Darmstadt, Germany
MnSO <sub>4</sub> x H <sub>2</sub> O	Sigma, Taufkirchen, Germany
3-Morpholinopropane-1-sulfonicacid (MOPS)	AppliChem, Darmstadt, Germany
N,N-dimethylformamide	Merck, Darmstadt, Germany
N <sub>2</sub>	Linde, Pullach, Germany
Na <sub>2</sub> HPO <sub>4</sub> x 2 H <sub>2</sub> O	Merck, Darmstadt, Germany
Na <sub>2</sub> MoO <sub>4</sub> x 2 H <sub>2</sub> O	Sigma Aldrich, München, Germany
NaCl	Sigma Aldrich, München, Germany
NaClO	Carl Roth, Karlsruhe, Germany
NaFeEDTA	Sigma Aldrich, München, Germany



## Material and Methods

Natriumacetate	Merck, Darmstadt, Germany
NaOH	Merck, Darmstadt, Germany
NiCl <sub>2</sub> x 6 H <sub>2</sub> O	Roth, Karlsruhe, Germany
phytoagar	Duchefa, Haarlem, NL
polyethyleneglycole (PEG)	Serva Electrophoresis, Heidelberg, Germany
potassium-acetate	Merck, Darmstadt, Germany
RbCl	Merck, Darmstadt, Germany
sodium-dodecyl-sulfate (SDS)	Serva, Heidelberg, Germany
β-Mercaptoethanole	Sigma Aldrich, München, Germany
tryptone	Ooxid, Wesel, Germany
Tween 20	Merck, Darmstadt, Germany
yeast extract	Ooxid, Wesel, Germany
ZnSO <sub>4</sub> x 7 H <sub>2</sub> O	Merck, Darmstadt, Germany

## Expendable material

Table 24: Expendable materials.

expendable materials	supplier
1.5 ml reaction vessels	Sarstedt, Nümbrecht, Germany
1.5 mL reaction vessels (RNase-free)	Carl Roth, Karlsruhe, Germany
1.5/ 2 ml-Reaktionsgefäß (safe lock)	Eppendorf, Hamburg, Germany
13 mL-Reaktionsgefäß	Greiner, Kremsmünster, Austria
96 plates for real-time PCR	Biozym, Hess. Oldendorf, Germany
centrifuge vessels (15/50 ml)	Greiner, Kremsmünster, Austria
cover lids	Roth, Karlsruhe, Germany
cuvettes	Sarstedt, Nümbrecht, Germany
cuvettes for electroporation	Peqlab, Erlangen, Germany
FastPrep-Tubes	MP Biomedicals, Santa Ana, Canada
filter	Sarstedt, Nümbrecht, Germany
filter paper	Whatman, Dassel, Germany
glas pipettes	Brand, Wertheim/Main, Germany
glas vessels	Schott, Mainz, Germany
gloves	Ansell, München, Germany
Lysing Matrix D	MP Biomedicals, USA
nitril gloves	Ansell, Richmond, Australia
nitril gloves	StarLab, Hamburg, Germany
object slides	Roth, Karlsruhe, Germany
optical cover folia for Real-time PCR	Biozym, Hess. Oldendorf, Germany
Parafilm	Bemis NA, Neenah, Wisconsin, USA
Pasteur pipettes	Brand, Wertheim/Main, Germany
PCR-tubes	Sarstedt, Nümbrecht, Germany
petri-dish (12 x 12 cm)	Novodirekt, Kehl, Germany
petri-dish (9 cm)	Greiner, Kremsmünster, Austria
pipetting tips (10, 100, 1000 µl)	Eppendorf, Sarstedt, Germany
pipetting tips with filter (10, 100, 1250 µl)	Biozym, Hess. Oldendorf, Germany
pipetting tips with filter (10, 100, 1250 µl)	StarLab, Hamburg, Germany
PP-tubes (13, 15, 50 ml)	Greiner bio-one, Frickenhausen, Germany
Razor blades	ScienceServices, München, Germany
RNase-free reaction vessels (1.5 ml)	Roth, Karlsruhe, Germany

## Material and Methods

scalpel	B. Braun, Melsungen, Germany
Seramis	Seramis, Mogendorf, Germany
serologic single use pipetting tips (10 ml)	Roth, Karlsruhe, Germany
single use syringe(5 ml)	Sigma Aldrich, München, Germany
syringe	BD Medical, Franklin Lakes, New Jersey, USA
wipes	Kimberley-Clark, Koblenz

## Material and Methods

### Equipment

**Table 25: Equipment used in this thesis.**

equipment	supplier
Autoclave WX150	Systec, Wettengel, Germany
Cleanbench HERASafe K518	Thermo, Langenselbold, Germany
climate cupboard KPS 1700	Weisshaar, Bad Salzungen, Germany
Confocal laser microscope TCS SP8 MP	Leica, Soehnle, Germany
Cooling centrifuge 5810 R with the rotors HL 030 and A-4-62	Eppendorf, Hamburg, Germany
Device for homogenizing tissues FastPrep®-24	MP Biomedicals, Santa Ana, Canada
Digital camera XC50	Olympus, Tokyo, Japan
electroporator Cellject Uno	Thermo, Langenselbold, Germany
fluorescence-binocular EL6000	Leica, Soehnle, Germany
fluorescence-mikroskop Axio observer. Z1	Carl Zeiss, Oberkochen/Jena, Germany
gel documentation station UV Solo	Biometra, Göttingen, Germany
Heating block Thriller	Peqlab, Erlangen, Germany
Hitzeschrank/Sterilisator T 6420	Thermo, Langenselbold, Germany
incubation cupboard B6	Thermo, Langenselbold, Germany
millipore-pump Arium®611 UV	Sartorius, Göttingen, Germany
Nanodrop 2000	Thermo, Langenselbold, Germany
on table centrifuge 5424	Eppendorf, Sarstedt, Germany
PCR machine Mastercycler pro S	Eppendorf, Hamburg, Germany
pH-meter Basic Meter PB-11	Sartorius, Göttingen, Germany
Photometer BioPhotometer plus	Eppendorf, Hamburg, Germany
Plant cultivation chamber JC-ESC 300	Johnson Controls, Milwaukee, Wisconsin, USA
Real-time PCR-machine Mastercycler realplex <sup>2</sup>	Eppendorf, Hamburg, Germany
Shaker device Certomat® IS	Shaker device Certomat® IS
Transilluminator	Biometra, Göttingen, Germany
Vibratome VT1000S	Leica, Soehnle, Germany
Vortex M53 basic	IKA, Staufen, Germany
water bath 1002, 1003	GFL, Burgwedel, Germany
Weighting machine Extend	Sartorius, Göttingen, Germany

### Software and internet tools

**Table 26: Software, internet tools and homepages.**

Name or tool	Provider or website/ link
CLC Main Workbench 7.0.3	CLC bio (QIAGEN), 2008 -2013
Fiji (ImageJ 1.51r)	Wayne Rasband, National Institute of Health, USA
Microsoft Office	Microsoft, 2016
Nanodrop 2000	Thermo Fisher Scientific 2009 – 2014
Realplex 2.2	Eppendorf, 2005 – 2008, Sarstedt, Germany
InterProScan	<a href="http://www.ebi.ac.uk/Tools/pfa/iprscan/">http://www.ebi.ac.uk/Tools/pfa/iprscan/</a>
National Center for Biotechnology Information	<a href="http://www.ncbi.nlm.nih.gov/">http://www.ncbi.nlm.nih.gov/</a>

## Material and Methods

Medicago truncatula Gene Expression Atlas V3	<a href="https://mtgea.noble.org/v3/">https://mtgea.noble.org/v3/</a>
Medicago truncatula Genome Database v4.0	<a href="http://www.medicagogenome.org/">http://www.medicagogenome.org/</a>
Mtsspb (RNAseq Daten)	(Luginbuehl et al., 2017)
Primer3 web tool	<a href="https://primer3.ut.ee/">https://primer3.ut.ee/</a>
JCVI	<a href="https://www.jcvi.org/">https://www.jcvi.org/</a>

## **Methods**

### **Molecular biological work with bacteria**

#### Growing and Conservation of Bacterial Strains

*E. coli* strains are either grown on liquid or solid PA- or LB-media containing additional antibiotics for selection. Single colonies are incubated for at least 12 h (overnight). Incubation of *A. rhizogenes* strains lasts 48 h and is performed in either solid or liquid TY-media with additional antibiotic markers.

To store bacterial strains containing produced plasmids, glycerol cultures are used. These liquid cultures either contain 0,5 ml LB- or TY-media, depending on the bacterial strain resuspended. Afterwards 0,6 ml glycerol (87 % stock solution) is added, the stocks are briefly mixed and directly stored at -20 °C.

#### Generation of competent *E. coli* cells for heat shock-transformation

Since *E. coli* bacteria are not able to incorporate plasmid DNA naturally, they must be prepared via rubidium-chloride treatment. Hence, a rotating, non-selective *E. coli* DH5 $\alpha$ mc $r$  liquid culture is incubated at 37 °C overnight. This culture consists of 10  $\mu$ l of the *E. coli* glycerol culture in 10 ml LB-media. 2 ml of this overnight culture are each transferred into 1000 ml shaking flasks, mixed with 200 ml LB-media respectively and incubated at 300 rpm and 37 °C. All following steps must be performed on ice and under sterile conditions (clean bench).

As soon as the shaking cultures reach an OD<sub>580</sub> at 0,6 the culture is distributed in 50 ml reaction tubes and centrifuged for 15 min at 2000 rpm. The centrifuge must be cooled down to 4 °C before. After centrifugation, the supernatant can be thrown away. Bacterial cells are carefully resuspended in cooled Tbf1-buffer and incubated on ice for 15 min. After centrifugation and supernatant removal the cells are resuspended in cooled Tbf2-buffer. 100  $\mu$ l fractions of the resuspended bacterial cells are transferred to 1,5 ml reaction tubes and immediately stored at -80°C.

#### Generation of competent *A. rhizogenes* cells for electroporation

Transformation via electroporation causes holes in the transformed bacteria's' membrane due to an electrical pulse. This allows the incorporation of free, recombinant (plasmid) DNA

## Material and Methods

---

by the bacterial cells. To enable bacteria for an electroporation transformation a precedingly treatment with glycerol is needed.

A selective starter culture consisting of 10 ml TY-media and an *A. rhizogenes*-colony is incubated at 30 °C (rotating). Then 200 ml TY-media are inoculated with 2 ml of the starter culture at 30 °C until an OD<sub>600</sub> of 0,6 - 0,8 is reached. The culture is cooled on ice. Subsequent, the culture is centrifuged for 10 min at 2000 rpm and 4 °C, the supernatant is removed, and the bacterial cells are washed in 50 ml water containing 10 % glycerol. Washing steps are repeated 3 times consecutively. Afterwards, the supernatant is removed, and the bacterial cells are resuspended in 4 ml of 10 % glycerol. 50 – 100 µl of the competent cells are fractioned and stored at -80 °C.

### Agarose gel electrophoresis

Agarose gel electrophoresis is a method to detect e.g., mixtures of DNA or RNA molecules and separate them in an agarose gel matrix by their length. To prepare agarose gels, TAE buffer containing (mostly) 1 % agarose are heated in the microwave until the boiling point is almost reached. The liquid gel is added on an electrophoresis tray and polymerates in this tray. Furthermore, a gel comb is added at one site of the liquid gel to provide wells that can later be used to load the gel with DNA or RNA molecules.

During polymerization, the gel matrix forms pores which sizes depend on the amount of agarose added to the buffer. If the gel is set, the comb can be removed, and the gel must be coated with TAE buffer. 3 – 5 µl of DNA or RNA samples are mixed with loading buffer, a buffer that contains either glycerol or sucrose to dense the sample as well as dyes like bromophenol or xylene cyanole to observe the later progress of the samples in the gel matrix. Samples are applied on the coated gel matrix afterwards. Due to the higher density, the samples sink to the ground of the prepared wells. A DNA marker, containing a mixture of DNA fragments of a defined length and loading buffer, should equally added to a well as an internal standard.

A voltage between 100 – 120 V is applied to the gel chamber containing the coated and loaded gel. Since DNA and RNA are overall negatively charged, the molecules progress through the gel matrix from the cathode to the anode in the resulting electric field. Because of the pores in the gel matrix bigger DNA or RNA molecules move slower than smaller molecules and are therefore separated by their size.

After enough progression, marked by the added bromophenol or xylene cyanole bands, the voltage is switched off and the gel matrix with the samples and the marker can be incubated at least 2 min in an ethidium bromide bath. Ethidium bromide intercalates with the major grooves of the DNA and fluoresces under UV light provided by e.g., a transilluminator. DNA or RNA fragments on the gel can be documented in the transilluminator by photos.

## Material and Methods

---

### Measurements of nucleic acid concentrations

Quality and quantity of RNA, plasmid or genomic DNA can be controlled by photometric measurements via *Nanodrop*. To do so, 1  $\mu$ l of each sample is applied to the measuring table, compared to a precedingly applied reference (mostly the elution buffer previously used for the sample preparation). The DNA's or RNA's maxima of absorption are at 260 nm whereas proteins absorb at 280 nm and phenolic compounds at 230 nm. To check the impurity of DNA or RNA absorption quotients of 260/ 280 nm or 230/280 nm are calculated by the *Nanodrop*. The closer these calculated values are to 2, the purer is the controlled DNA or RNA sampled.

### Amplification of DNA strands via Polymerase Chain Reaction (PCR)

PCR is a method to amplify specific DNA fragments and multiply them from a template DNA e.g., genomic DNA of *M. truncatula*. To perform this method, the 5' and 3' ends of the fragment of interest must be known. Oligonucleotides, called primers, framing the DNA fragment of interest must be designed to amplify the DNA region of interest between them. Those primers consist of a part complementary to the template in the 5' to 3' direction with a length of 18 to 25 bp and sometimes a non-target specific part. The latter located at the 5' sites of the primers contain restriction or recombination sites for the following cloning of the fragments into vectors. Besides the two primers (Phusion) polymerase with the corresponding enzymatic buffer, desoxy-nucleosidetriphosphates (dNTPs), template DNA or if applicable template plasmid and sterile water are needed (Table 27).

## Material and Methods

**Table 27: Standard PCR reaction in a 50 µl reaction.**

compound	volume [µl]	final concentration
Phusion Hot Start II polymerase (5 U/ µl)	0,5	2,5 U
Phusion polymerase buffer hf (5 x)	10	1 x
Forward primer (100 mM)	0,25	0,5 mM
Reverse primer (100 mM)	0,25	0,5 mM
dNTPs (10 mM each)	1	0,2 mM
Template DNA or plasmid	variable	variable
<i>add. 50 µl sterile Water</i>		

The amplification of the fragment of interest is performed by 6 defined steps, that are repeated 34 times. In each cycle, the fragment copies are doubled (Table 28).

**Table 28: Standard PCR program.** The initial denaturation (1) separates hydrogen bonds between the whole double-stranded genomic template material, whereas the following and shorter denaturation (2) separates the hydrogen bonds in the newly polymerised double-stranded fragment-of-interest. The annealing (3) step enables primer binding to the complementary template parts, which then allows the polymerization (4) of the fragment in 5' to 3' direction mediated by the (Phusion) polymerase and the integration of free dNTPs. After the final polymerization (5), the program arrests at 4 °C (6) to store the PCR amplicates properly. Asterisks (\*) indicate variability in length and temperature of step (2) and (3). The length of (2) and (3) differ depending on the length of the amplified fragment whereas the temperature of (3) varies depending on the melting temperature of the used primers.

	step	time	temperature [°C]	
1	Initial denaturation	5 min	98	
2	Denaturation*	30 s	98	} 34 repetitions
3	Annealing*	30 s	60	
4	Polymerization	30 s	72	
5	Final polymerization	5 min	72	
6	Cooling	hold	4	

### Real-time Reverse Transcriptase (RT) PCR

Real-time RT PCR was used to analyse isolated RNA from e.g., transgenic roots containing knockdown constructs. Therefore, primers using the following conditions were designed with Primer3web (<http://primer3.ut.ee/>): T<sub>m</sub>: min = 52 °C, opt= 53 °C, max= 54 °C; product size: 250 – 350 bp; primer length: min= 18 bp, opt= 21 bp, max= 24 bp (

## Material and Methods

Table 7). RT PCR were performed using the *Sensifast Sybr No-ROX One-Step Kit* (Table 29).

**Table 29: Standard RT PCR reaction.**

compound	volume [ $\mu$ l]	final concentration
Primer mixture (2,5 $\mu$ M)	4	0,2 $\mu$ M/ $\mu$ l)
Template RNA (1 ng/ $\mu$ l)	5	0,2 ng/ $\mu$ l
Sensifast mix (2 x)	10	1 x
RNAse inhibitor	0,4	
Reverse transcriptase	0,2	
add. 20 $\mu$ l DPEC-treated water		

The real-time RT PCR was performed in the *Real-time PCR-machine Mastercycler realplex<sup>2</sup>* (Table 30) in 96 well plates. On each RT PCR run, the translation-elongation factor *MtTef $\alpha$*  was measured and later used for normalization. Each biological replicate was measured in three technical replicates. Average values of the three technical replicates were used to calculate gene expression level via the  $2^{-\Delta C_t}$  method ( $\Delta C_t = C_{t_{\text{gene}}} - C_{t_{MtTef\alpha}}$ ). Statistical significance was determined with a two-tailed student's t-test using *MS Excel 2016*.

**Table 30: Standard real-time RT PCR program.**

	step	time	temperature [ $^{\circ}$ C]	
1	reverse transcription	10 min	45	
2	polymerase activation	2 min	95	
2	denaturation	5 s	95	} 40 repetitions
3	annealing	10 s	55	
4	elongation	8 s	72	
5	final polymerization	5 min	72	
6	cooling	hold	4	

## Sequencing

To finally check cloned DNA constructs, *Sanger* sequencing was performed. The sequencing reaction itself was performed by *Microsynth Seqlab* and samples were prepared accordingly to the laboratory's manual (Table 31).

**Table 31: Sequencing reaction.**

compound	volume [ $\mu$ l]	final concentration
plasmid DNA	variable	80 ng/ $\mu$ l
sequencing primer	1	2 pmol/ $\mu$ l
add. 15 $\mu$ l sterile water		



### Cloning

Gel extraction of DNA via *Nucleo Spin II Kit*

With the *Nucleo Spin II Kit* DNA fragments can be purified either directly from a performed PCR reaction or from an agarose gel piece containing the fragment of interest. The latter is especially important when a performed PCR reaction not only results in the fragment of interest but in a mixture of amplicates also containing mis-amplifications with the wrong length. If this is the case, the PCR reaction is applied on an agarose gel. Thereby the first gel lane contains a DNA marker, the second a small amount of the PCR reaction (2 – 5 µl) as reference lanes and on the following lanes larger amounts of the PCR product (10 – 15 µl) are applied for isolation. After the gel electrophoretic separation of the different DNA bands, gel lanes 1 and 2 are separated from the rest of the agarose gel and stained in an ethidium bromide bath to make the DNA bands visible.

In the transilluminator the PCR band of interest is marked by a cut at the right height. This mark is used as a reference to cut out the PCR fragment of interest for isolation blindly from the gel and transfer the agarose gel pieces into 1,5 ml reaction tubes. The remaining gel is stained in the ethidium bromide bath and checked, together with the already stained lane 1 and 2, in the transilluminator for proper cutting out of the fragment of interest. The reaction tubes containing the agarose gel pieces must be weighted to determine the weight of the gel pieces.

The following purification of the DNA fragments was performed with the *Nucleospin II Kit* accordingly to the manufacturers' instructions. Successful purification can be checked by agarose gel electrophoresis subsequently.

Blue-white selection via *lacZ* gene

Since the pK18 vector, often used as an entry vector in this work, contains a *lacZ* gene that can be disrupted by the insertion of a cloned DNA fragment this can be used to select on positive pK18 clones. Thus, 30 µl of X-Gal (25 mg/ml) are mixed with 30 µl IPTG (25 mg/ml) and are distributed on selective media plates. Transformed *E. coli* are spread over the media plate and the plates are incubated at 37 °C overnight. Blue and white single colonies should appear after incubation whereat the white colonies contain a plasmid with an insert integration at the *lacZ* gene and were further analysed.

Enzymatic restriction of DNA

Double stranded DNA can be restricted by restriction endonucleases that cut DNA at a specific recognition site. For this work, mostly type II restriction enzymes were used, which cut in palindromic recognition sites. The restriction can either lead to blunt ends or sticky ends, depending on the used enzyme. In this work, restriction enzymes where either used

## Material and Methods

---

to prepare recombinant DNA for cloning or to characterise produced constructs. A typical restriction reaction consists of the double stranded DNA that must be restricted, restriction enzyme, TA restriction buffer and sterile water (Table 32). The reactions were incubated in conformance with the manual instruction.

**Table 32: Standard restriction reaction.** For usual restriction reactions, a 20 µl approach was used. The volume of DNA applied to the reaction was estimated by gel electrophoresis.

compound	volume [µl]	final concentration
restriction enzyme (10 U/ µl)	1	0,5 U/ µl
TA restriction buffer (10 x)	2	1 x
DNA	variable	variable
add. 20 µl sterile water		

Filling of 5'-DNA ends to blunt ends via the Klenow-fragment

The *Klenow*-fragment is the big subunit of the polymerase I that can be used to fill single stranded 5' overhangs and thereby generates double stranded DNA with blunt ends. This method can therefore be used if the restriction sites of an insert are not compatible with the destination vector e.g., during subcloning. A reaction with the *Klenow*-fragment contains the enzyme itself, the corresponding buffer, restricted DNA, and sterile water (Table 33). The reaction is incubated at 37 °C for 15 min. Afterwards 1 µl of ethylenediaminetetraacetate (EDTA, 200 mM), a chelating agent that binds divalent cations like Mg<sup>2+</sup> and therefore stops the ongoing *Klenow* reaction. The *Klenow*-fragment is inactivated at 75 °C for 10 min. The restricted DNA fragment with filled 5' overhangs was purified with the *Nucleospin II Kit* before further use.

**Table 33: Standard *Klenow* reaction.** The usual reaction amounted 20 µl, applied DNA was estimated via agarose gel electrophoresis before.

compound	volume [µl]	final concentration
<i>Klenow</i> -fragment (1 U/ µl)	1	0,05 U/ µl
<i>Klenow</i> buffer (10 x)	2	1 x
restricted DNA	variable	variable
add. 20 µl sterile water		

Dephosphorylation of cloning vectors

To avoid religation of a restricted vector before ligation with an insert, the vector can be dephosphorylated. This reaction is mediated by the alkaline phosphatase, an enzyme that removes 5'-phosphate groups from the ends of linearized vectors. The method therefore increases the chance of a subsequently ligation of an insert with the vector. Dephosphorylation reactions contain a linearized vector, Shrimp Alkaline phosphatase (SAP), SAP buffer and sterile water (Table 34). The reaction was either incubated 15 min

## Material and Methods

at 37 °C (sticky end restriction) or 1 h at 37 °C (blunt end restriction). The SAP was inactivated at 70 °C for 15 min.

**Table 34: Standard dephosphorylation reaction.** A 20 µl reaction approach was used for the dephosphorylation of linearized vectors. The applied volume of the linearized vector was estimated with a preceding agarose gel electrophoresis.

compound	volume [µl]	final concentration
SAP (1 U/ µl)	1	0,05 U/ µl
SAP buffer (10 x)	2	1 x
linearized vector	variable	variable
<i>add. 20 µl sterile water</i>		

Ligation of insert and vector

3'-OH and 5'-phosphate groups of vector and insert are covalently linked with the help of the T4-ligase enzyme. This method is used for the ligation of the vector with the corresponding insert of interest. A ligation reaction contains the T4-ligase enzyme, ligase buffer, insert, vector and sterile water (Table 35).

The ligation reaction is performed in a ligation can overnight, decreasing the reaction temperature from about 18 °C to 8 °C. Reaction temperatures must be chosen in accordance with the length of the used insert.

**Table 35: Standard ligation reaction.** A 20 µl reaction approach was used for the ligation reaction. Asterisks (\*) indicate that the amount of vector and insert DNA should be in a 1:3 relation. To estimate proper vector and insert amount, an agarose gel electrophoresis with both compounds is performed precedingly.

compound	volume [µl]	final concentration
T4-ligase (1 U/ µl)	1	0,05 U/ µl
T4-ligase buffer (10 x)	2	1 x
dephosphorylated, linearized, vector DNA	*	*
restricted insert DNA	*	*
<i>add. 20 µl sterile water</i>		

Generation of RNAi- or rather Y1H (Yeast- one- hybrid) via Gateway-cloning

To obtain either RNAi (targeting *ERF* TF genes) or Y1H-bait constructs, gene-fragments or promoter were cloned into the entry vector pDONRTM221 (Gateway®-System, Invitrogen, Karlsruhe, Germany), using the BP clonase reaction. The LR clonase reaction was used for cloning into the destination vector *pK7GWIWG2* or the *pMWR*, respectively.

Isolation of *E. coli* plasmid DNA via HB Lysis

To perform test restrictions of bacterial clones containing plasmids and therefore allow screening for correct clones, the plasmid isolation via HB lysis was used (Becker *et al.*, 1993). For this plasmid isolation, single colonies of bacteria were picked and spread on selective media plates as little squares. Usually, 12 colonies were incubated on one plate

## Material and Methods

---

overnight at 37 °C. Then, the bacterial colonies are resuspended in 200 µl HB1-buffer and 200 µl HB2-buffer is added. After mixing 200 µl of HB3-buffer is added followed by a new mixing. After a centrifugation step at 14500 rpm at 10 min the supernatant is applied on 500 µl isopropanol and mixed by repeated inversion. Subsequently the samples are centrifuged at 13000 rpm for 20 min. The supernatant is carefully removed, and the pellet is washed with 500 µl 70 % (v/v) EtOH. Following this, the samples are centrifuged at 13000 rpm for 2 min. Afterwards the supernatant is removed, and the pellets are dried until the alcohol is evaporated. Then the pellets can be resuspended in 50 µl TE-buffer. Further analysis of the plasmid DNA like test restrictions and agarose gel electrophoresis can be performed subsequently.

Isolation of bacterial plasmid DNA via *QIAprep Spin mini-Kit*.

Plasmid DNA used for sequencing or further cloning was isolated via the *QIAprep Spin mini-Kit*. Isolations were performed in accordance with the manufacturers' manual.

Isolation of bacterial plasmid DNA from *A. rhizogenes*

Since isolations of *A. rhizogenes* plasmids are more difficult than *E. coli* plasmid isolations, this protocol is like the HB lysis protocol followed by a plasmid isolation with the *QIAprep Spin mini-Kit*.

50 ml of a selective overnight culture incubated at 30 °C is centrifuged at 14000 rpm for 10 min. Supernatant is removed and the pellet is resuspended in HB1-buffer. 2 ml of HB2- and HB3-buffer are added consecutively with mixing steps between each addition. The reaction is centrifuged for 20 min at 4000 rpm followed by the transfer of the supernatant to 5 ml of 100 % (v/v) isopropanol. Afterwards the samples are centrifuged for 20 min at 4000 rpm, supernatant is removed, and the pellet is washed with 5 ml of 70 % (v/v) EtOH. After a third centrifugation step for 2 min at 4000 rpm the supernatant is removed, and the pellet is dried until the alcohol is evaporated.

Subsequently, the pellet is resuspended in buffer P1 from the *QIAprep Spin mini-Kit* and a plasmid isolation in accordance with the manual of the kit is performed.

Transformation of *E. coli* cells via heat shock

Competent, rubidium-chloride treated *E. coli* bacteria can incorporate recombinant plasmid DNA via heat shock. Therefore 100 µl aliquots of competent bacteria are thawed on ice and mixed with 50 µl TCM-buffer and 5 – 10 µl of the ligation reaction (or a suitable amount of plasmid DNA) and incubated on ice for 30 min. The subsequent heat shock of the cells is performed at 42 °C for 1 min and 15 s and immediately stored on ice for 5 min afterwards. 1 ml of liquid LB-media is added to the transformation reaction followed by rotating incubation at 37 °C for 1 h. To grow transformed single colonies, the transformation reaction

## Material and Methods

---

must be spread on selective media plates (in a dilution series). The media plates incubate at 37 °C overnight and single colonies can be harvested from the plates.

Transformation of *A. rhizogenes* cells via electroporation

To transform *A. rhizogenes* cells via electroporation, aliquots with competent bacteria are thawed on ice. 5 µl of the ligation reaction (or a suitable amount of plasmid DNA) are added and transferred to a cooled electroporation cuvette. Any moist must be removed from the outside of the cuvette before the electric impulse of 1200 V is induced to the sample. 1 ml LBG-media is directly added to the transformation reaction and the whole reaction is transferred to a 1,5 ml reaction tube. Lastly, the transformation reaction is incubated 2 – 4 h at 30 °C (rotating) and then spread on selective TY-media and incubated at 30 °C. Single colonies can be observed after approximately 48 h.

## Plant work

### Scarification and sterilisation of *M. truncatula*

*M. truncatula* seeds are enclosed by the *testa*, a layer impermeable to water. This layer protects the seeds from early germination. To achieve simultaneous germination of a seed batch, the *testa* is perforated mechanically and chemically during scarification.

*M. truncatula* seeds are coated with 95 – 98 % (v/v) sulphuric acid and incubated for 10 – 15 min with simultaneously repeated inversion until small brown dots appear on the *testa*. Sulphuric acid is removed, and sterile water is added. The seeds are quickly inverted, and the water is removed immediately. Following this, three washing steps with sterile water are consecutively performed with inversion of the seeds for at least 1 min. After the last washing step, the seeds are treated with 2 % (v/w) sodium hypochloride for 2 min and followed by three washing steps with sterile water. The seeds are coated with water and incubated for 2 – 4 h in the phyto cabinet. After incubation, the seeds are placed on phytoagar and incubated for 4 days in the dark at 4 °C. This is followed by an incubation in the phyto chamber in the dark and 1 day exposed to the light of the phyto chamber.

### Growing of *M. truncatula*

*M. truncatula* seeds were grown in a climate chamber (relative humidity: 60 %; photosynthetic photon flux: 150 µmol m<sup>2</sup>s<sup>-1</sup>) under a 16 h light (22 °C) and 8 h dark regime. R108 plants carrying a *tnt1* insertion in an *ERF* gene were grown in a lab room at room temperature and under natural light conditions during spring 2019. In rare cases the phyto cabinet (Klimaschrank KPS 1700 Weisshaar, Bad Salzuflen, Germany) with a relative humidity of 60 % and photosynthetic photon flux: 150 µmol m<sup>2</sup>s<sup>-1</sup>. The phyto cabinet is equally driven under a 16 h light and an 8 h dark regime using Osram FLUORA neon tubes (Osram, Munich, Germany) at 22 °C.

## Material and Methods

---

Plants were either nourished with  $\frac{1}{2}$  strength Hoagland's solution, sterile water from the tap or sterile water from the tap mixed with desalted water.

### Root transformation of *M. truncatula* via *A. rhizogenes*

To obtain transgenic *M. truncatula* roots, roots were inoculated with *A. rhizogenes*. Before inoculation bacteria are grown on selective media plates for 2 days at 30 °C and *M. truncatula* seedlings must be scarified and must show a thickened hypocotyl part. Bacteria are transferred into 6 – 10 ml PS-buffer and resuspended. The bacterial suspension is pulled up in an insulin syringe and injected into the thick hypocotyl part. Plants are potted into a tray filled with *Seramis*. Thereby it is important to leave the injection site uncovered and eventually moisten this area again with bacterial suspension. Finally, the tray is covered with a wet transparent cover to provide humidity. The plants are incubated in the dark at 19 °C overnight and relocated to the climate chamber. If the plants show transgenic hairy roots at the injection site, roots must be covered with *Seramis*. Humidity provided by covering must last until 2 - 3 weeks. After approximately 4 weeks, plants can be screened for DsRed (or other) fluorescence indicating transgenic roots.

### Mycorrhization of *M. truncatula*

In this thesis *M. truncatula* roots were exclusively mycorrhized with the AMF *R. irregularis*. Therefore roots are inoculated with 1000 sterile spores (in 0,5 ml liquid) per root and incubated for 3 - 4 h in the dark. Afterwards the plants are potted in *Seramis* moistened with  $\frac{1}{2}$  strength Hoagland's solution (containing  $\text{KH}_2\text{PO}_4$ ). Remaining spore suspension is added to the plant pots. Roots are colonized by the AMF after 2 – 3 weeks. Successful colonization of *M. truncatula* can be checked by ink-staining or staining with *WGA-Alexa Fluor 488*.

### Calculation of mycorrhization rates via *Gridline intersection*

Arbuscles, hyphae and other fungal structures were counted using *Gridline intersection* (Brundrett et al., 1996).

## **Histochemical analysis of *M. truncatula***

### Detection of *DsRed* reporter gene activity

The reporter gene *DsRed* was used as a marker for transgenic hairy roots induced during this work. The DsRed protein fluoresces at 583 nm (excitation at 556 nm). Roots were screened for transgenicity under the fluorescence binocular.

### Staining for $\beta$ -Glucoronidase gene activity (GUS)

To study promoter - and thereby gene activity – under certain conditions in root tissue e.g., mycorrhization, the  $\beta$ -glucoronidase gene activity assay (GUS staining) is used. Transgenic roots containing promoter-*gusAint* gene fusions are screened for GUS staining. Therefore,

## Material and Methods

---

roots are harvested, transferred into GUS staining-buffer, and incubated at 37 °C. Incubation lasts until the roots show adequate blue staining sufficient for later microscopical analysis and documentation (Table 36). Roots are washed and kept in sterile water at 4 °C to stop GUS staining reaction.

## Material and Methods

**Table 36: GUS staining duration of analysed promoter-*gusAint* fusion.** Promoter-*gusAint* constructs used for transgenic hairy root induction and later GUS staining analysis with their corresponding staining durations are shown.

construct used for transformation	gene corresponding to promoter- <i>gusAint</i> fusion	GUS staining duration at 37 °C [h]
<i>pRR:p21492_kurz-GUS</i>	<i>Mtr21492</i>	8 h
<i>pRR:p15867</i>	<i>Mtr15867</i>	3 – 4
<i>pRR:p460730</i>	<i>WRI1</i>	5 – 7
<i>pRR:p1449</i>	<i>WRI5a</i>	2 – 3
<i>pRR:p25005</i>	<i>Mtr25005</i>	16
<i>pRR:pWRI5c-gus</i>	<i>WRI5c</i>	3 – 6
<i>pRR:p460730_1kB</i>	<i>WRI1</i>	5 – 7
<i>pRR:p460730_250bp</i>	<i>WRI1</i>	5 – 7
<i>pRR:p460730_ohneGCC</i>	<i>WRI1</i>	5 – 7
<i>pRR:p460730_pGCC</i>	<i>WRI1</i>	5 – 7
<i>pRR:p15867_1kB</i>	<i>Mtr15867</i>	3 – 4
<i>pRR:p15867_250bp</i>	<i>Mtr15867</i>	3 – 4
<i>pRR:p15867_ohneGCC</i>	<i>Mtr15867</i>	3 – 4

### Staining of fungal structures in *M. truncatula* via WGA-ALEXA Fluor 488

WGA-Alexa Fluor 488 stains fungal structures like AMF by binding to chitin incorporated in the fungal cell wall. WGA-Alexa Fluor is excited at 488 nm and emits at 519 nm. Alexa-stained fungal structures in root tissues are observed via a fluorescent binocular or confocal laser scanning microscope. This method was used to phenotype RNAi roots or counterstain roots after GUS staining.

Therefore, roots are cooked for 5 – 10 min (depending on the amount of root material) at 95 °C, followed by three washing steps with water. Water is removed and the roots are covered with Alexa staining solution and incubated at RT overnight in the dark. The staining solution is removed, and the samples are stored in water at 4 °C.

### Ink staining of fungal structures

The efficiency of mycorrhization differs due to the used mycorrhization method and fungal spores. Hence, mycorrhization rates were checked in control roots before harvesting. Therefore, control roots are cut into 1 to 2 cm fragments and transferred into a reaction tube containing 1 ml of 10 % KOH (w/v). Tubes containing roots are heated to 95 °C for 5 – 10 min (depending on the amount of root material). KOH is removed and roots are washed with water three times. 1 ml of 5 % ink solution (v/v) diluted with 8 % acetate-essence (v/v) is applied to the roots, followed by 3 min incubation at 95 °C. Samples are washed two times with 0,8 % acetate-essence (v/v) and incubated in the wash-solution for 20 min. Mycorrhization rates can be checked via binocular.



## Material and Methods

---

### Molecular biological work with plants

Isolation of plant genomic DNA via DNeasy Plant Mini Kit

With this method, plant genomic DNA can be isolated from *M. truncatula* via the *Qiagen DNeasy Plant Kit*. For this isolation either freshly harvested (e.g., young leaves, seedlings) or frozen plant material can be used. Plant material for isolation is transferred into special reaction tubes filled with beads that shear the plant material. In case of freshly harvested plant material 400 µl AP1 buffer mixed with 4 µl RNase A must be added before shearing. Shearing of the plant material is performed in the Ribolyzer at 6,5 m/s for 20 s. This is repeated for five times (or until the material looks properly sheared). Reaction tubes must be cooled down between the runs eventually to prevent overheating of the samples.

After shearing, the tubes are incubated in a water bath at 65 °C. The tubes must be inverted every 3 min. 130 µl of buffer P3 are added, samples are inverted several times and incubated on ice for 5 minutes and afterwards centrifuged at 14000 rpm for 5 min.

The supernatant of the samples is transferred to the lilac column with a collection tube and centrifuged for 2 min at 14000 rpm. Subsequently, the passage must be transferred into a new reaction tube, whereas transfer of the pellet should be avoided. Buffer AW1 is added in an amount of 1.5 % of the volume share of the supernatant. The samples are inverted and 650 µl of the samples are transferred to the white columns with corresponding reaction tubes. Columns with samples are centrifuged at 8000 rpm for 1 min, passages can be depraved, and the column must be transferred to a new collection tube. To wash off proteins and phenolic remaining 500 µl AW2 buffer must be added to the column and the column must be centrifuged at 8000 rpm for 1 min. The passage can be depraved. The washing step is repeated, and the column should be centrifuged at 14000 rpm for 2 min. The column should be transferred to a new 1.5 ml reaction tube. To elute the DNA from the column 50 µl AE buffer should be pipetted on the middle of the column. The samples must be incubated 5 min at RT and be centrifuged at 8000 rpm for 1 min. Successful DNA extraction can be checked via agarose gel electrophoresis and an UV-/VIS- spectrophotometer.

Isolation of plant RNA via *RNeasy Plant Mini Kit*

RNA was isolated with the *RNeasy Plant Mini Kit* in accordance with the manufacturer's instructions. Root tissue was disrupted using the FastPrep-24. After isolation, RNA was stored at -80 °C.

## Material and Methods

---

### Yeast work

#### Yeast cultivation

Yeast cells were either grown on liquid or solid media using YPDA or SD. For cultivation in liquid media, baffled flasks were used, and cells were incubated at 30 °C at 150 rpm. 50 µg/ml kanamycin was added to avoid bacterial contamination.

#### Storage

For yeast storage, a single yeast colony is picked from a freshly grown selective media plates and resuspended in liquid YPDA. Then 30 % sterile glycerol are added, and the stocks are stored at -80 °C.

#### Y2H

The Y2H experiments were mainly performed in accordance with the *Yeastmaker<sup>TM</sup> Yeast Transformation System 2* protocols (Clontech Laboratories, Fitchburg, USA).

cDNA synthesis from plant RNA via real-time RT PCR

Since most of the *ERF TF* genes (*WRI5a*, *WRI5b*, *WRI5c*, *WRI1*, *Mtr15867*) used in this work contain introns in their DNA sequence, cDNA synthesis from *M. truncatula* root RNA had to be performed. Because all these candidates are upregulated during AM, RNA from mycorrhized roots was used. To amplify candidate genes the *Sensifast Sybr No-ROX One-Step Kit* was used, and PCR reactions were prepared (Table 29). Since cloning via restriction sites into the bait (pGBKT) and prey (pGADT) vectors was used, primers were designed containing restriction attachment sites.

*Real-time PCR-machine Mastercycler realplex<sup>2</sup>* was used for gene amplification (Table 37).

**Table 37: RT-PCR program for cDNA synthesis.** Asterisks (\*) indicates varying annealing temperatures depending on the  $T_m$ .

	step	time	temperature [°C]	
1	reverse transcription	10 min	45	
2	polymerase activation	2 min	95	
2	denaturation	5 s	95	} 40 repetitions
3	annealing	10 s	*	
4	elongation	40 s	72	
5	final polymerization	5 min	72	
6	cooling	hold	4	

Yeast transformation

Y2H strains were transformed using an efficient transformation method (R. Hartmann; phd thesis; 2018; LUH) adapted for the usage of the *Yeastmaker<sup>TM</sup> Yeast Transformation*

## Material and Methods

---

*System 2.* The protocol is applicable for 10 yeast transformation reactions and can be scaled up or down.

The *S. cerevisiae* strains Y2H Gold and Y187 are streaked on YPDA plates and incubated at 30 °C for 3 days. A single colony is inoculated in 10 ml YPDA and incubated in a shaker at 200 rpm for 30 °C overnight. The grown yeast cells are spun down at 1000 g for 5 min and the supernatant is discarded. Cells are washed with sterile water (same amount as overnight culture). Centrifugation and washing steps are repeated and the resuspended yeast cells are fractioned into 1 ml aliquots each transformation reaction. Cells are spun down at 3500 g for 5 min and the supernatant is removed. Afterwards the yeast cells are resuspended in 100 µl freshly prepared LiAc- buffer (800 µl PEG 3350 [50 %], 200 µl LiAc [1 M], 1,5 µl β-mercaptoethanol), mixed and stored on ice for the following transformation. The carrier DNA is cooked at 99 °C for 5 min and stored on ice directly afterwards. 6 µl of carrier DNA and 100 – 200 µg of the vector DNA are added to an aliquot of competent cells. The reactions are mixed and incubated at 45 °C for 30 min (transformation reactions should be mixed every 10 min). 30 µl of the transformation reaction are spread on selective media plates and incubated at 30 °C for 3 – 5 days.

### Autoactivation test

Autoactivation of Y2H bait strains was tested in accordance with the manufacturer's instructions.

### Direct mating

To perform direct mating, bait strains and prey strains were streaked on suitable selective media plates and incubated for 3 days at 30 °C. A single colony, picked with an inoculation loop is resuspended in 700 µl YPDA. Each 20 µl bait and prey suspension are mixed with 1 ml YPDA and applied on a well plate. The mating reactions are incubated at 30 °C, 200 rpm for 24 h. Afterwards 15 µl of the mating reactions are dropped on selective media plates (DDO/ DDO/X/A/ QDO/X/A) and incubated at 30 °C for 3 – 5 days.

### Y1H

Y1H approaches were performed following a gateway-compatible Y1H system (Deplancke et al., 2004; Fuxman Bass et al., 2016a, 2016b, 2016c). This system is also consistent with prey strains from the Y2H already described.

### Generation of Bait strains

Y1H constructs were designed via *Gateway* cloning using the *pMWR#2* and *pMWR#3* (Fuxman Bass et al., 2016b) (Table 8), which are pMW plasmids containing att-sites for BP and LR recombination. After cloning constructs were digested with restriction enzymes

## Material and Methods

linearizing the constructs (1 – 4 µg plasmid) and preparing them for integration into the yeast genome (Table 38).

**Table 38: Restriction enzymes used for linearization of pMWR#2 and pMWR#3 constructs.**

vector	restriction enzymes
pMWR#2	<i>Afl</i> III, <i>Xho</i> I, <i>Nsi</i> I, <i>Bse</i> RI
pMWR#3	<i>Nco</i> I, <i>Apa</i> I, <i>Stu</i> I

The selected restriction enzyme must not cut in the DNA bait sequence. Therefore, not every restriction enzyme works for every constructed vector (Table 39).

**Table 39: Restriction enzymes used for Y1H bait vector linearization.**

Y1H bait construct	restriction enzyme used for linearization
pMWR#2:p15867	<i>Xho</i> I
pMWR#3:p15867	<i>Apa</i> I
pMWR#2:p21492	<i>Xho</i> I
pMWR#3:p21492	<i>Nco</i> I
pMWR#2:p460730	<i>Afl</i> III
pMWR#3:p460730	<i>Apa</i> I
pMWR#2:pRAM1	<i>Nsi</i> I
pMWR#3:pRAM1	<i>Nco</i> I
pMWR#2:pSTR	<i>Xho</i> I
pMWR#3:pSTR	<i>Apa</i> I
pMWR#2:pFatM	<i>Xho</i> I
pMWR#3:pFatM	<i>Apa</i> I
pMWR#2:pKASII	<i>Xho</i> I
pMWR#3:pKASII	<i>Nco</i> I
constructs derived from BSc thesis of Agnes Krüger, 2020	
pMWR#2:p460730_250bp	<i>Bse</i> RI
pMWR#3:p460730_250bp	<i>Apa</i> I
pMWR#2:p460730_ohneGCC	<i>Bse</i> RI
pMWR#3:p460730_ohneGCC	<i>Apa</i> I
pMWR#2:p460730_pGCC	<i>Bse</i> RI
pMWR#3:p460730_pGCC	<i>Apa</i> I
pMWR#2:p460730_1kB	<i>Bse</i> RI
pMWR#3:p460730_1kB	<i>Apa</i> I
pMWR#2:p15867_250bp	<i>Afl</i> III
pMWR#3:p15867_250bp	<i>Apa</i> I
pMWR#2:p15867_1kB	<i>Nsi</i> I
pMWR#3:p15867_1kB	
pMWR#2:p15867_ohneGCC	
pMWR#3:p15867_ohneGCC	<i>Apa</i> I

Bait strains were generated using the *S. cerevisiae* YM4271 strain (Fuxman Bass et al., 2016b).

## Material and Methods

---

Test DNA bait strain autoactivity (HIS autoactivity)

Since generated yeast bait strains are likely autoactivated by yeast TFs binding to the DNA bait (Deplancke et al., 2004), autoactivation of the *his* gene was tested following the provided protocols (Fuxman Bass et al., 2016b).

Colony lift colorimetric assay for  $\beta$ - Galactosidase activity

With this method, expression levels of  $\beta$ - Galactosidase an enzyme encoded by the *lacZ* gene were monitored. This assay is important to monitor autoactivation of the *lacZ* gene and later evaluation of the interaction with the prey. The assay was performed accordingly to the provided protocols (Fuxman Bass et al., 2016a).

Direct mating

Direct mating was performed as described in the Y2H section.

Zymolyase- treatment and PCR

To test constructed Y1H bait strains for correct integration into the yeast genome, the zymolase-treatment followed by PCR was used as described (Fuxman Bass et al., 2016c).

## Results

### Seven AM-related *ERF* candidate genes show upregulation during the time course of AM development

To identify *ERF* TF genes upregulated in *M. truncatula* roots during a symbiosis with the AMF *R. irregularis*, 5 different datasets were analysed: 1. GeneChip hybridizations, comparing mycorrhized vs. non-mycorrhized root systems (Hogekamp et al., 2011), 2. GeneChip hybridizations of laser microdissected cell-types in mycorrhized roots, comparing e.g. colonized with non-colonized cells (Hogekamp et al., 2011; Hogekamp & Küster, 2013), 3. GeneChip hybridizations recording an AM time course of mycorrhized roots (Hartmann; 2018), 4. RNAseq data comparing three time points of non-mycorrhized versus mycorrhized roots (Luginbuehl et al., 2017) and 5. The *Medicago truncatula* Gene Expression Atlas, containing an overview of gene expression in different tissues and under different abiotic and biotic (stress) conditions, including some of the already mentioned datasets (Hogekamp et al., 2011; Hogekamp & Küster, 2013). The seven selected candidate genes will from now on be referred to as *WRI5A*, *WRI5B*, *WRI5C*, *460730*, *15867*, *21492* and *25005* (Table 40).

**Table 40: The seven selected candidate genes with their gene names and GeneChip ID.**

Gene ID	GeneChip ID	Abbreviation	Reference in literature
<i>Medtr8g468920.1</i>	<i>Mtr.1449.1.S1_at</i>	<i>WRI5A</i>	<i>WRI5A</i> (Luginbuehl et al., 2017)
<i>Medtr7g009410.1</i>	<i>Mtr.46362.1.S1_at</i>	<i>WRI5B</i>	<i>WRI5B</i> (Luginbuehl et al., 2017); <i>ERF1</i> (Devers et al., 2013)
<i>Medtr6g011490.1</i>	No GeneChip ID	<i>WRI5C</i>	<i>WRI5C</i> (Luginbuehl et al., 2017)
<i>Medtr2g460730.1</i>	No GeneChip ID	<i>460730</i>	potential <i>CBX1</i> (in <i>L. japonicus</i> ) homologue (Xue et al., 2018)
<i>Medtr4g130270.1</i>	<i>Mtr.15867.1.S1_at</i>	<i>15867</i>	potential <i>CBX1</i> (in <i>L. japonicus</i> ) homologue (Xue et al., 2018)
<i>Medtr6g012970.1</i>	<i>Mtr.21492.1.S1_at</i>	<i>21492</i>	
<i>Medtr7g011630.1</i>	<i>Mtr.25005.1.S1_at</i>	<i>25005</i>	

Naturally, there are more *ERF* TF genes upregulated in these five datasets than the seven finally chosen candidate genes. Therefore, three different criteria were used, sorting potential candidate genes from genes not studied in this thesis. Primarily, all candidate genes must display an upregulation during AM over time, which could be derived from all 5 datasets. Secondly, genes were chosen, that were exclusively upregulated in mycorrhizal

## Results

roots, which could be best analyzed in dataset 5, and thirdly genes with an unknown function at the starting point of the thesis.

The first datasets available at the start of the thesis were datasets 1, 2, 3 and 5. Due to ongoing annotation of the *M. truncatula* genome, datasets 1, 2, 3 and 5 did not include all *ERF* TF genes, lacking e.g. *460730* and *WRI5C*, which were later obtained from datasets 3 and 4. Although different inoculation and mycorrhization techniques were used to provide datasets 1 – 4, comparative analysis of all four datasets revealed an upregulation of the seven selected *ERF* TF genes during AM (Table 41).

**Table 41: Comparative analysis of datasets 1 - 4 used to identify interesting AM-upregulated *ERF* candidate genes in *M. truncatula* roots mycorrhized with *R. irregularis*.** **1)** GeneChip hybridization, comparing mycorrhized versus non-mycorrhized roots (Myc+ vs. Myc-) harvested at 28 dpi (Hogekamp et al., 2011). Ratios between the measurements of mycorrhized and non-mycorrhized roots were built, indicating upregulation (red coloured field) of five of the seven chosen candidate genes. Grey fields indicate no available data for these candidate genes. Ratios were calculated from normalized, log<sub>2</sub>-transformed data. **2)** Laser microdissection of different root cell-types colonized by AMF, followed by RNA-isolation and qRT-PCR harvested at 28 dpi (Hogekamp et al., 2011; Hogekamp & Küster, 2013). Mycorrhization was not performed as described in the Material and Method section, but instead obtained through a leach inoculum described in the corresponding paper. The chosen inoculation method fastens AMF progression. Harvesting time points can therefore not directly be compared to dataset 1, 3 and 4. Arbusculated cells (ARB) were compared to Cortical Neighbouring Cells of mycorrhized roots (CMR), as well as Epidermal Cells (EPI) to ARB. ARB/CMR and EPI/ARB ratios are shown respectively, revealing upregulation (red fields, downregulation indicated with green) of most included candidate genes in ARB in comparison to the non-mycorrhized CMR or EPI cell-types. Only *15867* and *25005* do not reveal upregulation, instead displaying comparable expression in all cell-types. Like in dataset 1, not all candidates are included (grey fields). Ratios were calculated from normalized, log<sub>2</sub>-transformed data. **3)** GeneChip hybridization of a time course comparing mycorrhized to non-mycorrhized roots (Hartmann, 2018). Roots were harvested at 0 dpi, 28 dpi and 35 dpi, representing early to late AM stages. All candidate genes are included, showing mild (*15867*, *21492*, *25005*) to strong (*WRI5A*, *WRI5B*, *WRI5C*, *460730*) upregulation over time. **4)** RNAseq data obtained from Myc+ versus Myc- roots (Luginbuehl et al., 2017). Non-logarithmic ratios between Myc+/Myc- are given. Roots were harvested at 8 dpi, 13 dpi and 27 dpi. Importantly, roots in dataset 4 were not mycorrhized as described in the Material and Methods section. In contrast to dataset 1 – 3, roots were inoculated with spores grown in a carrot inoculum (Gobbato et al., 2012; Wang et al., 2012). The chosen inoculation method fastens the AMF progression. Harvesting time points can therefore not be directly compared to datasets 1, 2 and 3. All candidates included show upregulation over time or an early upregulation in case of *21492*.

Candidate gene	1 Myc+ vs. Myc- (log <sub>2</sub> ratio)	2 (log <sub>2</sub> ratio)		3 Myc+ (absolute expression levels)			4 Myc+ vs. Myc-		
		ARB vs. CMR	EPI vs. ARB	0 dpi	28 dpi	35 dpi	8 dpi	13 dpi	27 dpi
<i>WRI5A</i>	2,6	6,6	-6,7	3,1	6,2	6,3	0,7	9,7	13,4
<i>WRI5B</i>	5,8	1,4	-1,7	2,8	5,1	6,0	0,4	5,9	10,2
<i>WRI5C</i>	n.a.	n.a.	n.a.	3,6	6,9	6,9	5	53,5	124,3
<i>460730</i>	n.a.	n.a.	n.a.	3,6	6,5	6,2	1,4	7,6	17,2
<i>15867</i>	2,8	-0,8	-0,3	5,1	6,4	6,2	1,6	4,1	10,0
<i>21492</i>	3,5	1,7	-2,4	5,7	7,1	7,8	11,6	7,0	4,0
<i>25005</i>	1,5	0,0	-0,2	2,4	2,5	3,2	1	0,6	2,4

Due to different methodological approaches, experimenters, inoculation and varying mycorrhization conditions, datasets 1 – 4 cannot be directly compared to each other. Therefore, only general comparative analysis can be performed, at best examining and

## Results

---

directly comparing data of the different candidate genes within one dataset (Table 41). In general, *WR15A*, *WR15B*, *WR15C* and *460730* revealed the strongest upregulation over time in datasets 3 and 4 (Table 41). In comparison to *WR15A*, *WR15B* shows the highest upregulation in dataset 1, whereas *WR15A* seems to be strongly upregulated in arbusculated cells, according to dataset 2. *WR15C* and *460730* are not included in datasets 1 and 2 due to a lack of GeneChip probes. *15867* displays a level of AM-upregulation comparable to *WR15A* in dataset 1 but shows less arbuscule-upregulation than *WR15A* or *WR15B* in dataset 2. Although *15867* reveals a strong transcriptional activity over time in dataset 4, it starts at a relatively high expression level in dataset 3, in comparison to *WR15A*, *WR15B*, *WR15C* and *460730*.

*21492* equally reveals a strong upregulation in dataset 1 as well as arbuscule-upregulation according to dataset 2. In the time course studies (datasets 3 and 4), transcriptional activity of *21492* starts at a relatively high level, which points towards a certain basic expression of the gene. Progression of *21492* expression can otherwise be compared to *15867*.

*25005* displays the weakest expression in all four datasets, not showing an arbuscule-upregulation at all.

The increase of transcriptional activity, as described in datasets 3 and 4, can be best analyzed in time course diagrams. Therefore, the most recent and genome-wide RNAseq study (dataset 4) was used to visualize the already stated increasing transcriptional activity for all seven *ERF* TF candidate genes (Figure 11) (Luginbuehl et al., 2017).

Summarizing the results of datasets 1 – 4, candidate genes show an overall similar trend in all datasets revealing upregulation of all seven *M. truncatula* *ERF* TF genes in mycorrhized roots. Differing tendencies for a candidate gene in the four datasets may be explained by diverging mycorrhization approaches, harvesting timepoints and methodological differences. Given those reasons, as well as possibly contrasting levels of plant and spore fitness, further abiotic or biotic stress conditions and different experimenters, comparison of the four datasets can only reveal overall trends.



## Results

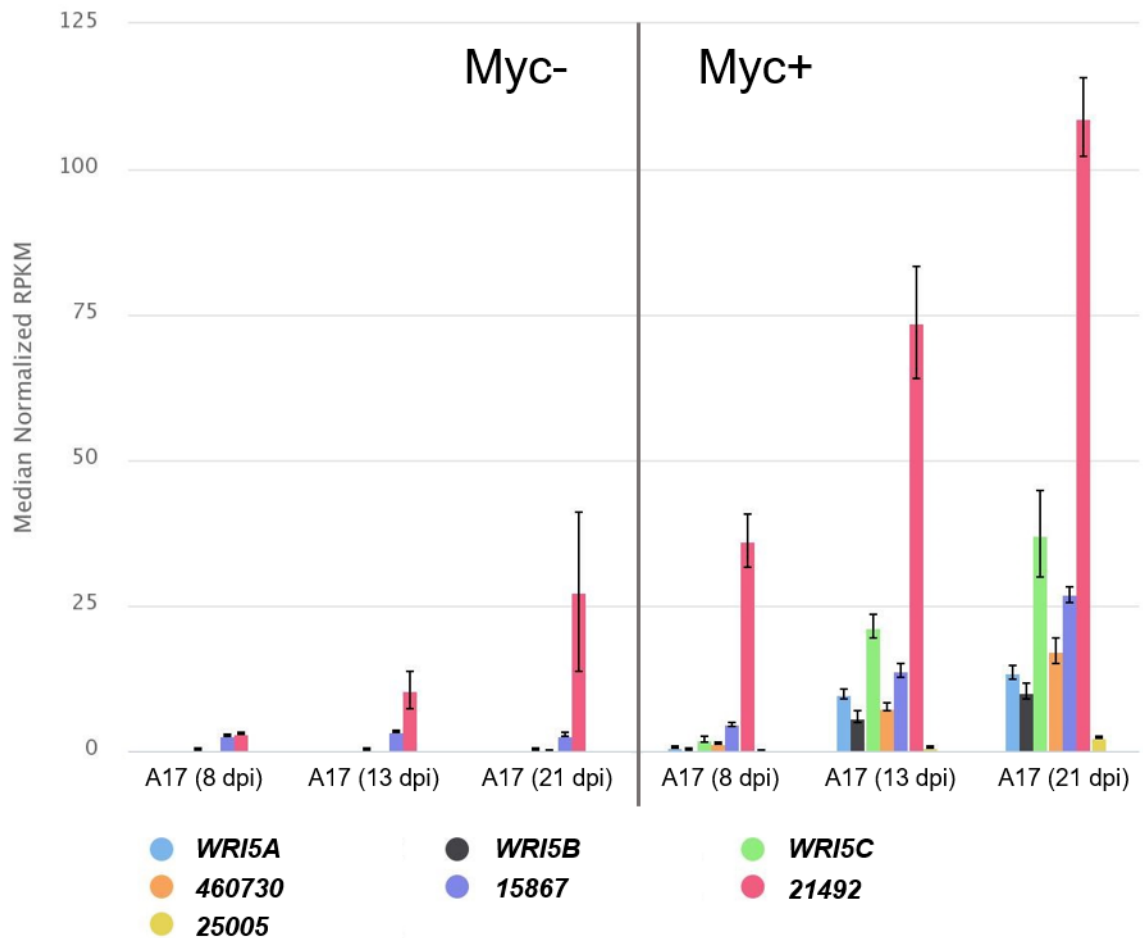


**Figure 11: RNAseq data of all *ERF* TF candidate genes in non-mycorrhized (Myc-) versus mycorrhized (Myc+) roots reveal upregulation in mycorrhized root systems over time.** Myc- and Myc+ roots were harvested at three different time points (t1= 8 dpi; t2= 13 dpi; t3= 27 dpi) using mock-inoculation for the Myc- time course, transcripts were isolated and sequenced via RNAseq (Luginbuehl et al., 2017). Data were provided as Median Normalized RPKM values. *WRI5A*, *WRI5B*, *WRI5C* as well as *460730* and *25005* show nearly no transcription in Myc- roots over time, whereas *15867* displays low and *21492* stronger transcriptional increase. All candidates display an increasing transcriptional activity in Myc+ roots over time (taken and adapted from Luginbuehl et al., 2017).

All in all, the seven *ERF* TF candidate genes showed an increased transcription in mycorrhized roots over time, although the levels of increase differ severely between the candidate genes (Figure 11). The increase of *WRI5A*, *WRI5B*, *WRI5C*, *460730* and *15867* transcription are thereby comparable to each other, whereas *25005* shows the weakest and *21492* the strongest transcriptional increase. Only two genes, *15867* and *21492* reveal marked transcriptional activity in non-mycorrhized roots. Whereas transcriptional activity of *15867* stay on a similar level over time, pointing to a basic expression of the gene under non-mycorrhized conditions, *21492* transcription increases during the time course. Strikingly, *21492* also shows the highest transcriptional activity over time in mycorrhized as well as in non-mycorrhized roots. This high increase makes it difficult to see the exact progression of the other genes' expression, especially the ones with low levels and only

## Results

mild increase like *25005*. Therefore, *21492* was left out to better analyse transcription rates of *WRI5A*, *WRI5B*, *WRI5C*, *460730*, *15867*, and *25005* (Figure 12).

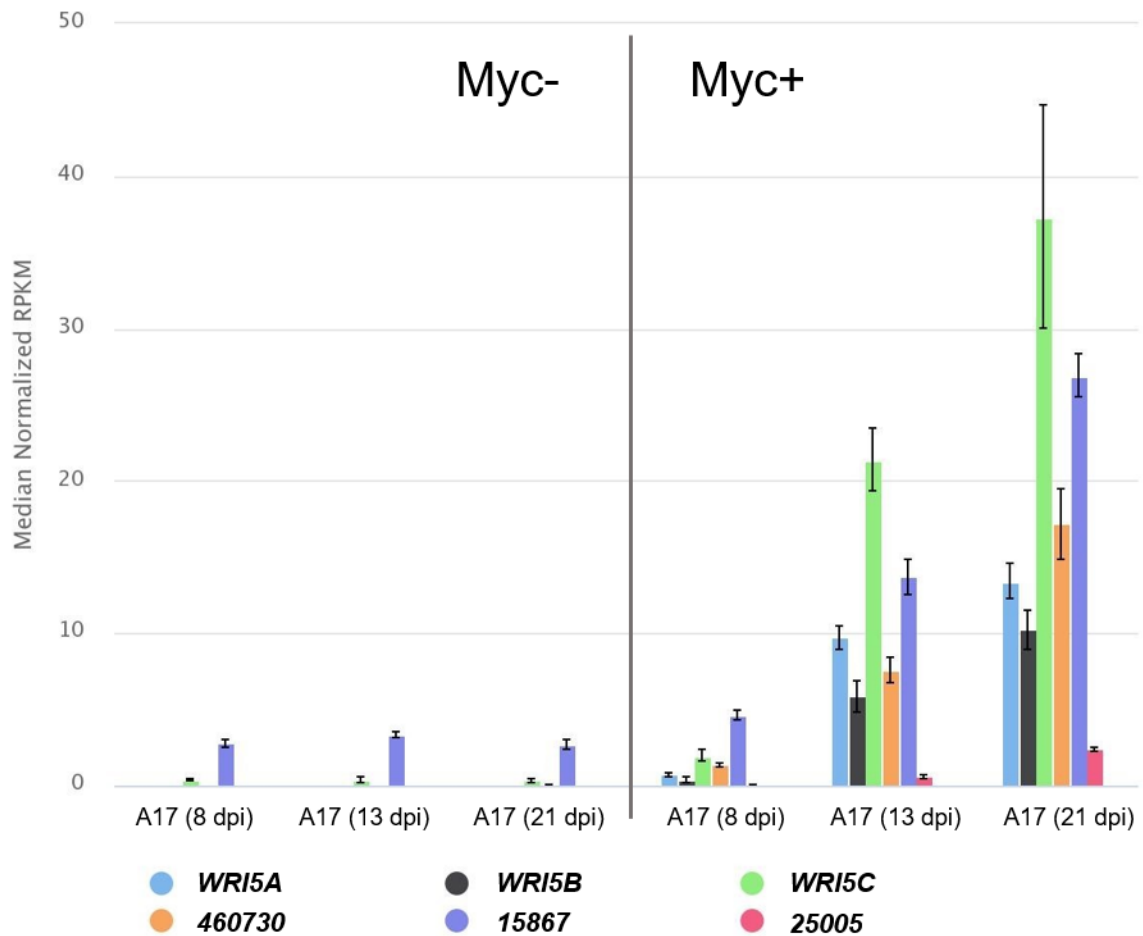


**Figure 12: RNAseq data of all *ERF* TF candidate genes in non-mycorrhizal (Myc-) versus mycorrhizal (Myc+) roots reveal upregulation.** Myc- and Myc+ roots were harvested at three different time points (t1= 8 dpi; t2= 13 dpi; t3= 27 dpi) using mock-inoculum for the Myc- time course, transcripts were isolated and sequenced via RNAseq (Luginbuehl et al., 2017). Data were provided as RPKM values. *WRI5A*, *WRI5B*, *WRI5C* as well as *460730* and *25005* show nearly no transcription in Myc- roots over time, whereas *15867* displays low rates. All candidates demonstrate increasing transcriptional activity over time in Myc+ root systems. The *ERF* TF candidate gene *21492* was left out in this figure to provide a clearer overview over the other six, less transcribed *ERF* TF candidate genes (taken and adapted from Luginbuehl et al., 2017).

To put it in a nutshell: the seven *ERF* TF genes fulfil all selection criteria (mentioned at the beginning of the chapter) and are developmentally upregulated during AM. Although dataset 2 provides first insights into a more celltype-specific expression of each gene during AM, the laser microdissection studies do not replace a more accurate insight that would be gained by *in situ* histological analysis of the candidate genes' expression. To obtain a clearer picture on the fungal structures inducing each *ERF* TF gene expression, promoter-*gus* analysis of each genes' promoter was thus performed. The results of this approach will be described in the upcoming chapter.

---

**Seven AM-related ERF TF genes are specifically expressed in arbuscule-containing cells**

To analyze, if gene activity of the seven selected *ERF* TF candidate genes really is AM-dependent and more specifically, which AMF structures induce gene expression, promoter-*gus* studies were performed, using the intron-containing  $\beta$ -glucoronidase gene *gusAint* as a reporter. Putative promoter regions were amplified (Table 5) and promoter-*gus* fusions were subsequently cloned into the binary vector *pRedRoot* (*pRR*) (Table 11).

All promoters were analyzed in *M. truncatula* A17 roots (mycorrhized roots versus non-mycorrhized roots), revealing AM-dependent activity (Figure 13). The strongest activity (staining durations 2 - 6 h) could be observed in mycorrhized roots containing *pWRI5A*, *pWRI5B* (designed and cloned by Pallokat, 2013), *pWRI5C* (cloned by Krüger; 2020), *p460730* and *p15867* reporter-gene constructs, whereas roots containing *p21492* or *p25005* constructs showed weak *gus*-staining results even after longer staining (10 – 16 h) (Table 36).

In case of *p25005*, this observation fits to the RNAseq time course (Figure 11, Figure 12), revealing low and slowly increasing AM-dependent transcript levels of *25005* over time relative to the levels of *WRI5A*, *WRI5B*, *WRI5C* and *460730*, which are steeply increasing (Luginbuehl et al., 2017).

In contrast to this analysis, the promoter activity of *p21492* is more difficult to evaluate. The amplified promoter region of *p21492* does not start directly upstream of the gene's ATG, but 93 bp upstream. Weak promoter activity can thus be explained by important promoter enhancing elements missing in this region. Furthermore, baseline expression of *21492* starts higher than the ones of *25005*, meaning that the gene is expressed to a greater extent than *25005*.

On the other hand, taking into account the existing time course of Hartmann (2018), *21492* reveals mildly rising AM-dependent expression levels over time, comparable to *25005*. This might indicate a weak induction of promoter activity even with an amplified promoter region directly starting upstream of the start codon.

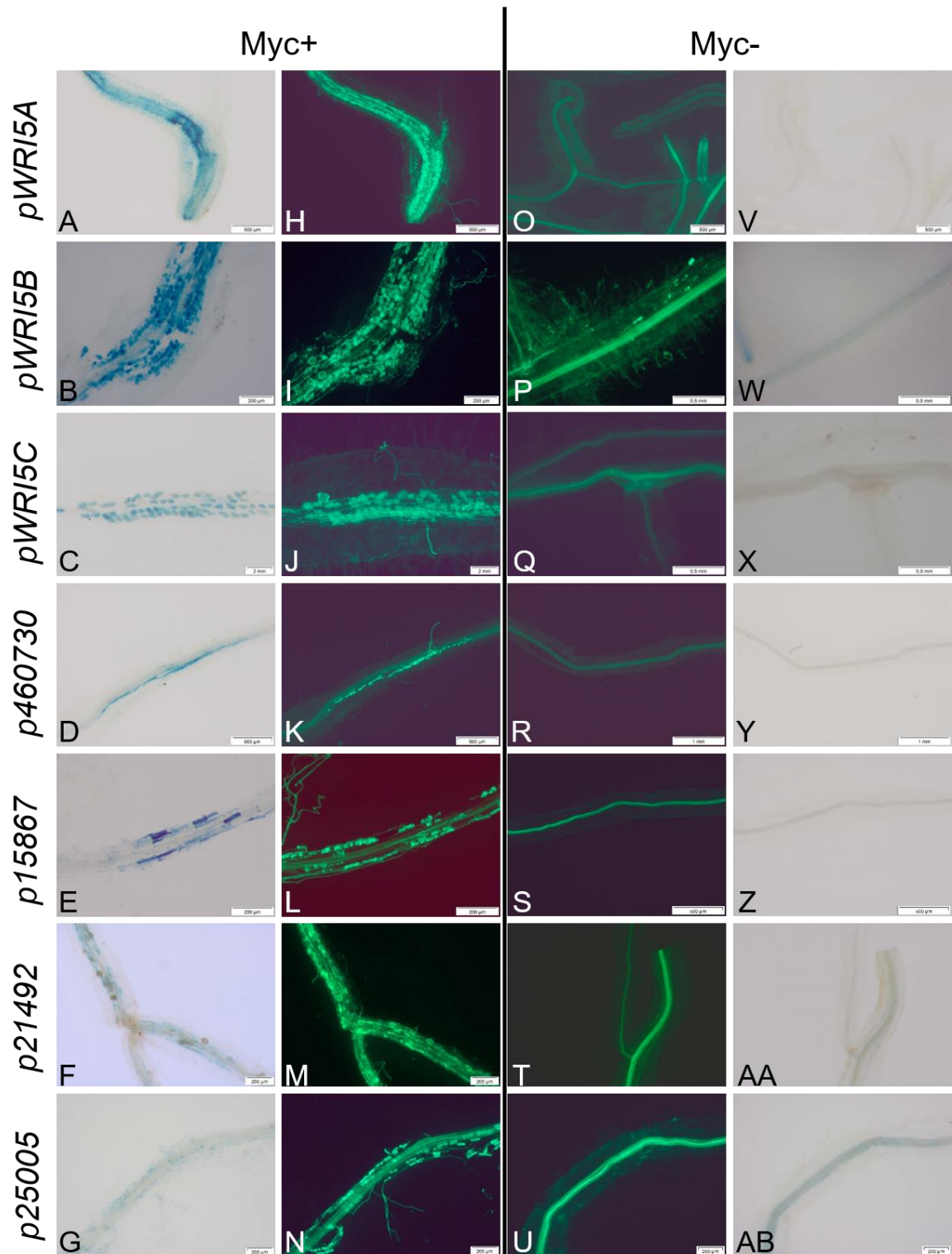


**Figure 13: Promoter activities of all *ERF* TF candidate genes can be correlated with AMF colonization.** Mycorrhized transgenic roots (Myc+, A-N), when compared with non-mycorrhized transgenic roots (Myc-, O-AB) reveal specific induction of the promoters in AMF colonized areas, always corresponding to arbuscule-containing cells. Promoter activity is restricted to the area of the inner cortical cells, where AM symbiosis mainly takes place. Myc- control roots do not reveal promoter activity. Only control roots containing the *p25005*-construct (U, AB) disclose *gus*-staining in the vascular tissue indicating background activity of the promoter. Roots were GUS-stained (A-G, V-AB) and afterwards counterstained with WGA Alexa 488 binding to fungal chitin (H-U). Roots were harvested at the following timepoints: *pWRI5A* at 35 dpi; *pWRI5B*, *p460730*, *p15867* and *p25005* at 28 dpi; *pWRI5C* at 21 dpi and *p21492* at 63 dpi. Constructs *pWRI5B* and *pWRI5C* were cloned and designed by Phil Pallokat (Pallokat, 2013) and cloned by Agnes Krüger (Krüger, 2020).

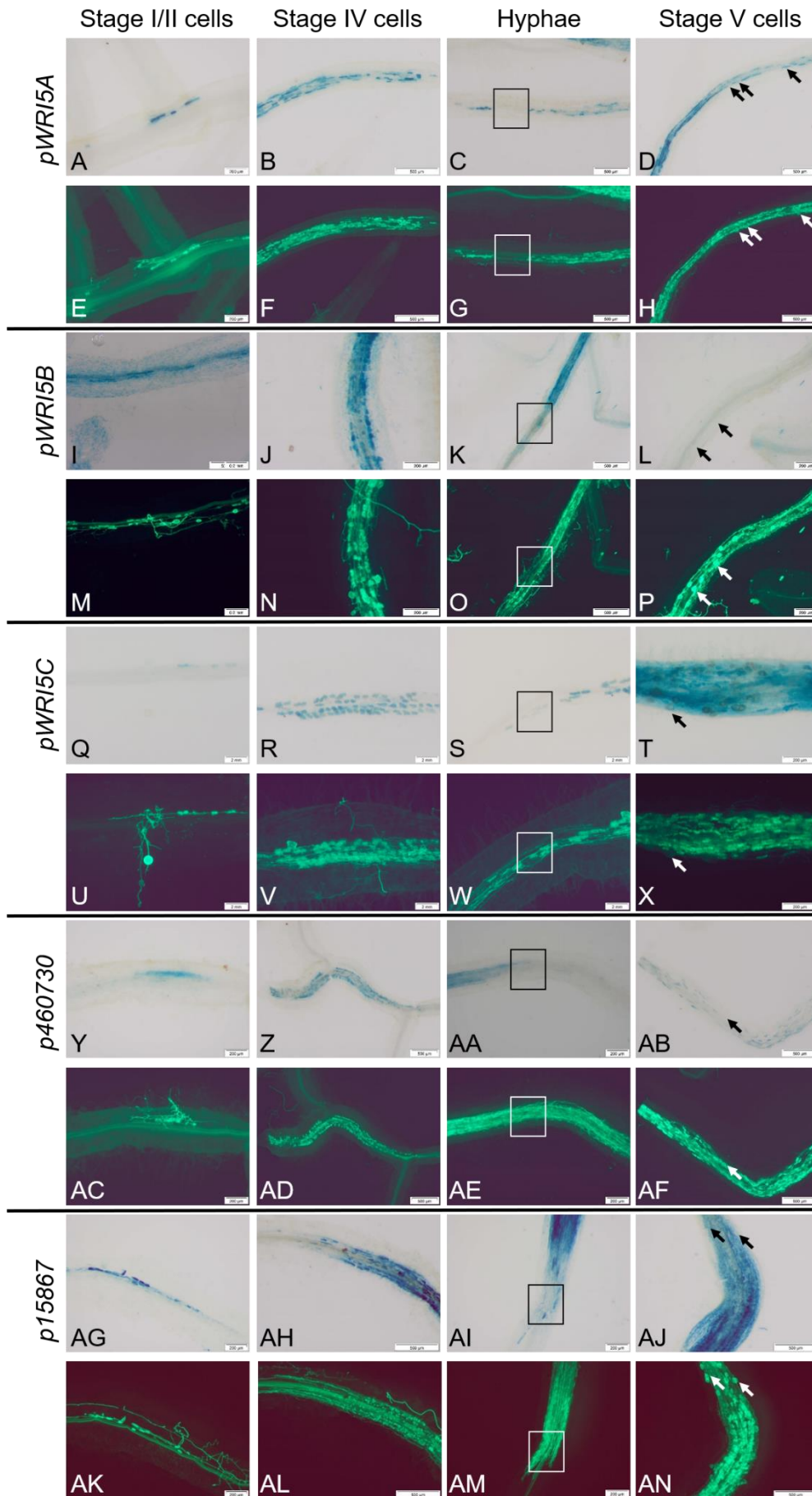
## Results

---

Exposing the strongest reporter gene expression, *pWRI5A*, *pWRI5B*, *pWRI5C*, *p460730* and *p15867* were analyzed during different AM developmental stages like hyphopodia-containing and early colonization (Stage I/II cells), highly colonized roots in younger (Stage IV cells) and older (Stage V cells) stages and hyphae-containing cells (Figure 14). In early colonization stages, all five promoters act similarly, thereby correlating promoter expression with cells containing young arbuscules. Furthermore, all promoters do not show *gus*-staining in neither appressoria-containing nor hyphae-containing cells entering the root. In later stages and hyphae-containing cells, the five promoters show differing activity. *pWRI5A*, *pWRI5B* and *p460730* do not display gene expression in cells containing hyphal structures and promoter activity seems to be absent in late AM stages, which are characterized by the appearance of vesicles.

Adjacent to the expression of those three promoters, *p15867* and *pWRI5C* demonstrate activity in late AM stages. Furthermore, expression of *15867* can also be observed in hyphae-containing cells. This suggests a *15867* function differing from *WRI5A*, *WRI5B*, *WRI5C* and *460730* or various functions in AM-dependent processes, since *p15867* also exhibits strong activity in early stages of arbuscule development.

Results



## Results

---

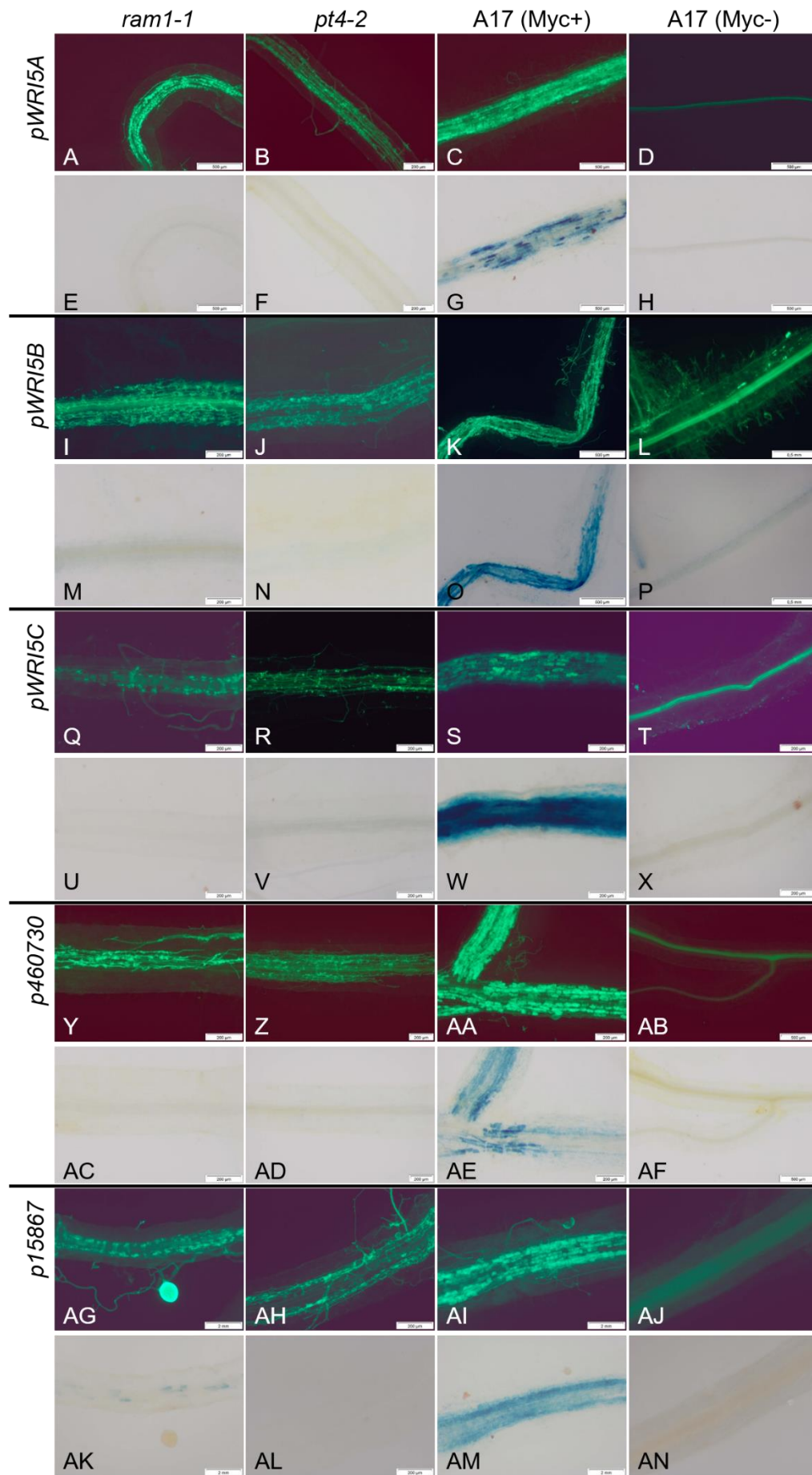
**Figure 14: Five *ERF* TF candidate genes display arbuscule-specific promoter activity.** Promoter activity of either *pWRI5A* (A-H), *pWRI5B* (I-P), *pWRI5C* (Q-X), *p460730* (Y-AF) and *p15867* (AG-AN) was analyzed during four different stages of AM development: Stage I cells (entry points and early colonization; first column of images), Stage IV cells (arbusculated cells; second column of images), hyphae-containing cells (black/ white boxes; third column of images) and Stage V cells (areas with degenerating arbuscules, characterized by increased number of vesicles, indicated by black/ white arrows; fourth column of images). In the first two columns, all seven *ERF* TF promoters show promoter activity exclusively restricted to arbuscule-containing cells, not reacting to hyphopodia-containing cells (Stage I) or hyphae entering the root. Hyphal-containing cells equally reveal no expression of neither of the candidate genes (third image column). Late stages of AM, characterized by degrading arbuscules and a high number of vesicles (arrows) do not show activation of *pWRI5A*, *pWRI5B* and *p460730*. In contrast to this, *pWRI5C-gus*- and *p15867-gus*-containing roots reveal promoter induction in this late AM stage, showing fading but still strong *gus*-staining. Roots were harvested at the following time points: *pWRI5A* 28 dpi (first column) and 35 dpi (second to fourth column); *pWRI5B* at 28 dpi; *pWRI5C* at 21 dpi (first to third column) and 49 dpi (fourth column); *p460730* at 28 dpi; *p15867* at 28 dpi. Constructs *pWRI5B* and *pWRI5C* were designed and cloned by Phil Pallokat (Pallokat, 2013) and Agnes Krüger (Krüger, 2020).

### ***WRI5A*, *WRI5B*, *WRI5C*, *460730* and *15867* expressions depend on nutritional exchange of mature, active arbuscules**

Since *RAM1* is an important regulator of arbuscule formation and FA biosynthesis (Luginbuehl et al., 2017), promoter-*gus* constructs of the five strongest activated *ERF* TF genes were expressed in mycorrhized *ram1-1* mutant roots. This approach should shed light on a potential function of the five *ERF* TF genes, which can be distinguished by a potential *RAM1*-dependency and expression downstream of this regulator. In addition to this, phosphate homeostasis is an important regulatory tool of AM, either allowing or suppressing progressing AMF colonization (Javot et al., 2007; Pumplin et al., 2012). A working AM-dependent phosphate uptake is therefore also characteristic for proper nutritional exchange in arbuscules, shortly a functioning arbuscule. Importantly, *MtPT4* expression is dependent on, but not directly regulated by *MtRAM1* (Figure 3). To analyze, whether *ERF* TF genes are dependent on a functioning arbuscule, they were furthermore analyzed in mycorrhized *pt4-2* mutant lines. Due to low promoter-*gus* activity and resulting difficulties in analyzing those roots, *p21492-gus* and *p25005-gus* expression was not studied in *ram1-1* and *pt4-2* mutants.

Plants containing the *ram1-1* mutation as well as plants accommodating a mutation in the *RAM1*-dependent *PT4* gene (*pt4-2*) were infected with *pWRI5A*, *pWRI5B* (Pallokat, 2013), *pWRI5C* (Krüger, 2020), *p460730* and *p15867* promoter-*gus* constructs (Figure 15). Promoter activity of *pWRI5A*, *pWRI5B*, *pWRI5C* and *460730* could not be observed in mycorrhized *ram1-1* and *pt4-2* lines, indicating that these *ERF* TF genes are completely dependent on *RAM1* and *PT4*. Furthermore, this reveals the necessity of a functioning arbuscule for genes expression of either of these four candidates. Contrastingly, *p15867* shows slight promoter-induction in mycorrhized *ram1-1* and - in contradiction to this - no activity in the analyzed *pt4-2* roots.

Results



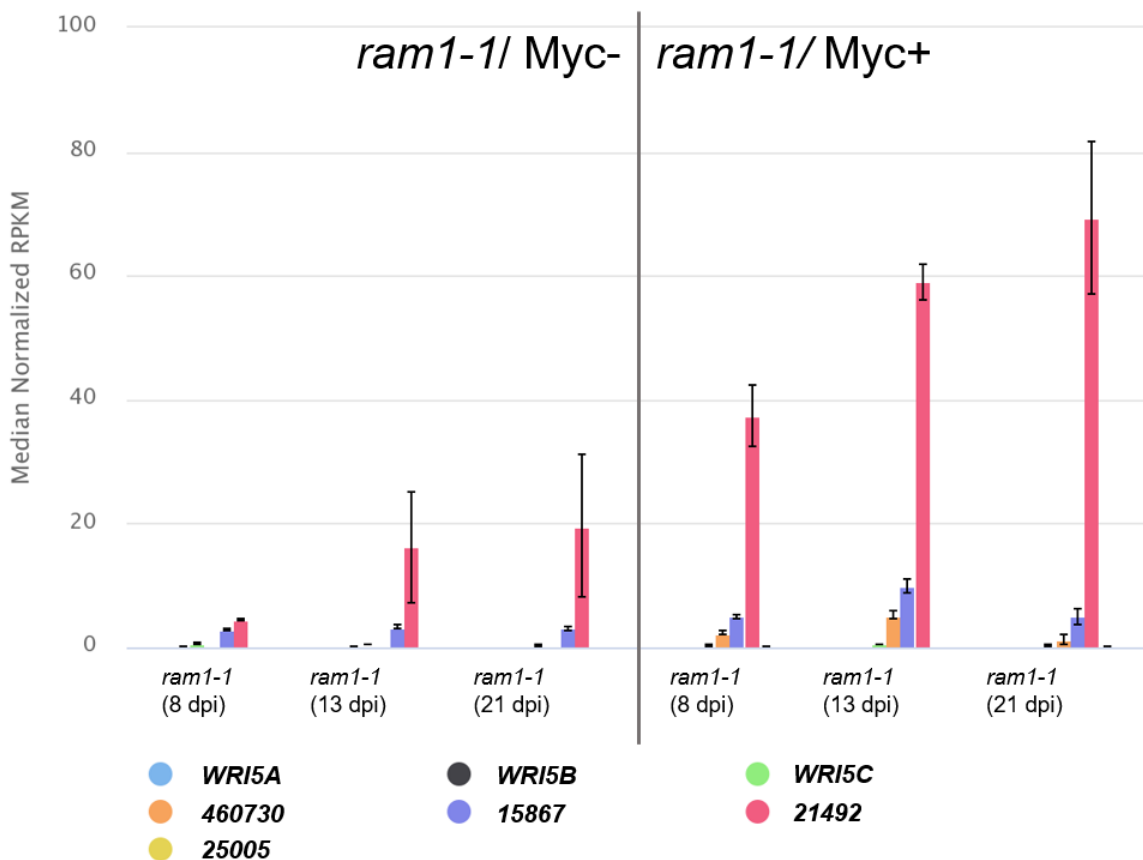


## Results

**Figure 15: Expression of five AM-related *ERF* TF genes are dependent on RAM1 and PT4.** Promoter activity of either *pWRI5A* (A-H), *pWRI5B* (I-P), *pWRI5C* (Q-X), *p460730* (Y-AF) and *p15867* (AG-AN) was analyzed under four different conditions: *ram1-1* mutant lines (first image column) and *pt4-2* mutant lines (second image column) compared to A17 Myc+ roots (third image column) and A17 Myc- roots (fourth image column), functioning as comparative control roots. In comparison to Myc+ control roots, *pWRI5A*, *pWRI5B*, *pWRI5C* and *p460730* do not show promoter activity in *ram1-1* as well as in *pt4-2* roots, indicating a dependency of RAM1 and PT4. Apart from displaying a similar dependency on PT4, *p15867* reveals slight promoter-activity in *ram1-1* mutant lines. Roots were harvested at the following time points: *pWRI5A*, *pWRI5B*, *p460730* and *p15867* at 42 dpi and *pWRI5C* at 49 dpi. Constructs *pWRI5B* and *pWRI5C* were designed and cloned by (Pallokat, 2013) and cloned by Agnes Krüger (Krüger, 2020).

The findings, that expression of either *pWRI5A*, *pWRI5B*, *pWRI5C*, *p460730* and *p15867* are RAM1-dependent, are in general conform to RNAseq data comparing non-mycorrhized with mycorrhized roots in a *ram1-1* background over time (Luginbuehl et al., 2017) (Figure 16). Interestingly, *15867* is steadily expressed on a low level in all conditions. This fits to the earlier described, weak *p15867-gus* induction in *ram1-1*.

The RNAseq data also include transcriptional activity of *21492* and *25005*, that were not studied by promoter-*gus* in *ram1-1* mutants. Whereas *25005* shows no activity at all in the *ram1-1* background, *21492* reveals increasing activity in the non-mycorrhized and even stronger increasing activity in the mycorrhized *ram1-1* roots. Since the *ram1-1* RNAseq data result from the earlier described dataset 4 (Luginbuehl et al., 2017) (Figure 11), transcription rates of *21492* in *ram1-1* and wild type roots can be compared to each other, showing a similar progression of transcriptional activity over time.



## Results

**Figure 16: RNAseq data, comparing all *ERF* TF expression in non-mycorrhized (Myc-) *ram1-1* and mycorrhized (Myc+) *ram1-1* roots.** Myc- and Myc+ roots were harvested at three different timepoints (t1= 8 dpi; t2= 13 dpi; t3= 27 dpi), transcripts were isolated and sequenced via RNAseq (Luginbuehl et al., 2017). Data were normalized and provided as RPKM values. *WRI5A*, *WRI5B*, *WRI5C* as well as *460730* and *25005* show nearly no transcription in Myc-/Myc+ roots over time, whereas *15867* displays low and *21492* steeply increasing transcriptional activity, especially in Myc+ *ram1-1* roots, compared to the other candidate genes. Mycorrhization was obtained via a carrot inoculum approach, leading to a fastened AMF colonization (taken and adapted from Luginbuehl et al., 2017).

The high increase of *21492* activity over time complicates exact analysis of the transcriptional activity of the remaining six *ERF* TF genes which display lower transcriptional rates. Therefore, RNAseq data were displayed without *21492* (Figure 17). It is evident that *WRI5A*, *WRI5B*, *WRI5C* and *25005* show nearly no transcriptional activity in the *ram1-1* background, independent of the roots' mycorrhization status. Contrastingly, transcription rates of *15867* show residual levels at each timepoint, where transcription of *15867* clearly increases. Interestingly, transcription rate of *460730* equally increases under this condition. In contrast to *15867*, no transcriptional activity of *460730* can be observed in non-mycorrhized *ram1-1* roots and, except from the 13 dpi timepoint, only low levels of transcription can be noticed at the other two timepoints in mycorrhized roots.

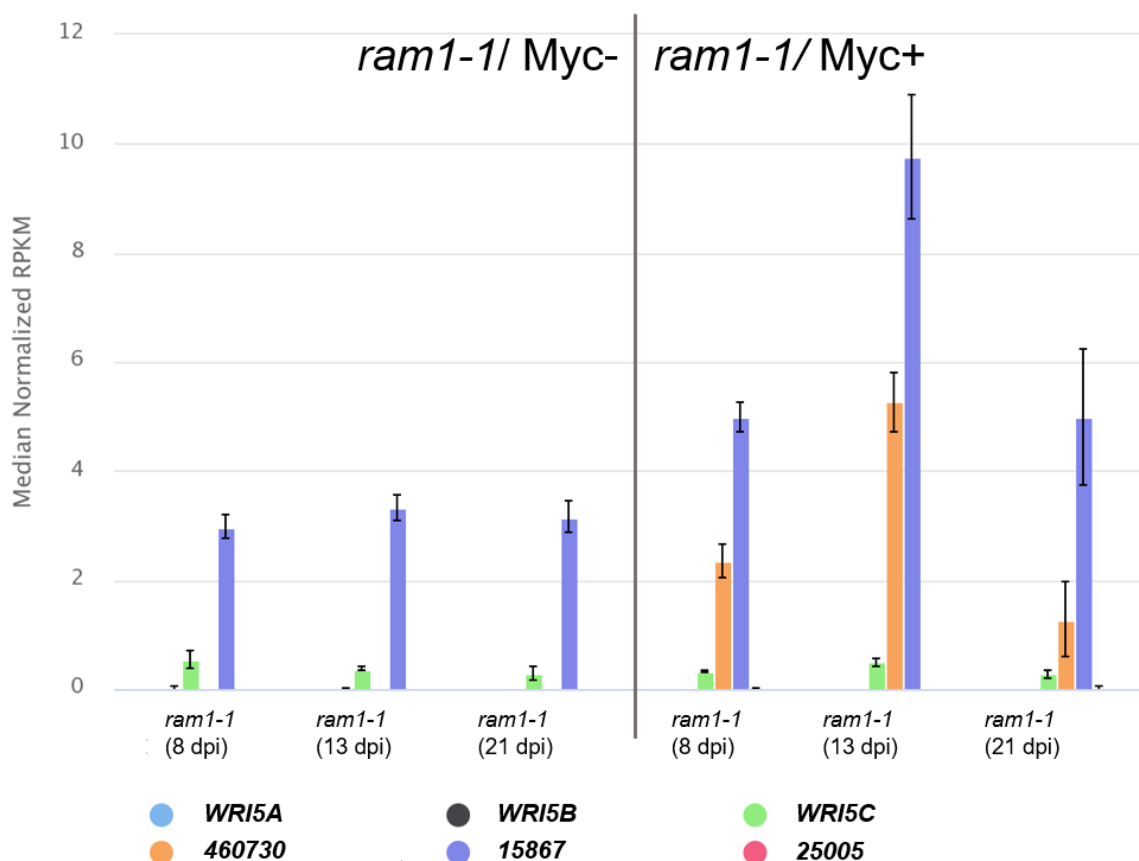


**Figure 17: RNAseq data, comparing *ERF* TF expression (lacking *21492*) in non-mycorrhized (Myc-) *ram1-1* and mycorrhized (Myc+) *ram1-1* roots.** Myc- and Myc+ roots were harvested at three different timepoints (t1= 8 dpi; t2= 13 dpi; t3= 27 dpi), transcripts were isolated and sequenced via RNAseq (Luginbuehl et al., 2017).

## Results

---

Data were normalized and provided as RPKM values. *WRI5A*, *WRI5B*, *WRI5C* as well as *460730* and *25005* show nearly no transcription in Myc-/Myc+ roots over time, whereas *15867* displays low transcriptional background activity, only increasing at 13 dpi (t2) in Myc+ roots. *460730* equally increases its transcription rate at this timepoint. The *ERF* TF candidate gene *21492* was left out in this figure to provide a clearer overview over the other six, less transcribed *ERF* TF candidate genes. Mycorrhization was obtained via carrot inoculum (taken and adapted from Luginbuehl et al., 2017).

### ***ERF* TF genes show diverging expression patterns, delimiting *WRI5A*, *WRI5B*, *WRI5C* and *25005* from the other candidate genes**

To summarize all findings from the promoter-*gus* (Figure 13, Figure 14, Figure 15) and RNAseq approaches (Figure 11, Figure 16) (Luginbuehl et al., 2017), all seven *ERF* TF candidate genes reveal AM-dependent promoter-activity, in most cases restricted to arbuscule-containing cells (Figure 18). Strong dependency of *WRI5A*, *WRI5B*, *WRI5C* and *25005* on RAM1 and PT4 in both approaches reveals a quite specific expression of these genes in functioning arbuscules. In contrast to this, *460730* shows – at least in the RNAseq dataset – transcriptional activity less dependent on RAM1. Nevertheless, these findings could not be observed in the corresponding promoter-*gus* approach, eventually due to differences in mycorrhizal inoculation techniques. Whereas the RNAseq time course summarized progression of the candidate genes' transcriptional activity, analyzed areas on roots containing promoter-*gus* constructs only reveal gene expression at a specific timepoint and restricted to a certain area. *21492* and *15867* show even lower dependency on RAM1, fitting in with the slight promoter-*gus* activity observed for *p15867* in mycorrhized *ram1-1* roots. *21492* expression seems to be relatively independent of RAM1 compared to the other *ERF* TF genes.

Regarding these data, it can be stated that *WRI5A*, *WRI5B*, *WRI5C* and *25005* show similar expression patterns in all expression analysis performed so far, whereas *460730*, *15867* and *21492* differ. Importantly, *15867* and *WRI5C* are the only *ERF* TF genes potentially active in AM stages with degrading arbuscules.

To further analyze the function of these seven candidate genes, RNAi-constructs of some of the genes were designed. Since all candidate genes are quite arbuscule-specific, this approach was supposed to shed light on the effects of *ERF* TF knockdown mutants, potentially showing effects on mycorrhization rates, arbuscular phenotypes and further target genes of these TFs measured via qRT-PCR.

## Results

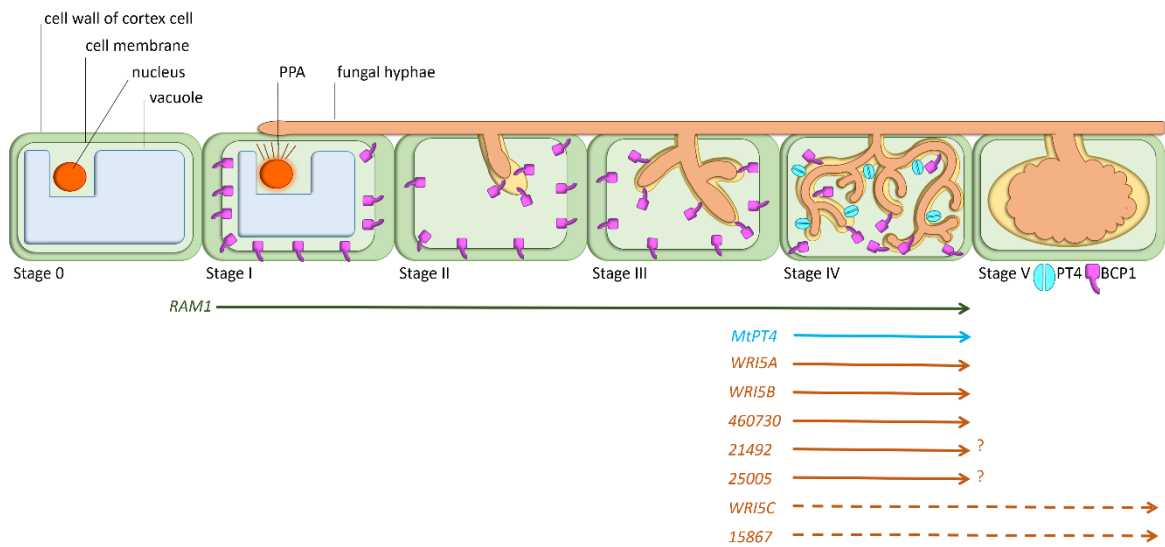


**Figure 18: Expression of all *ERF* TF candidate genes is activated in arbusculated cells, in dependence on *RAM1* and *PT4*.** During the developmental stages of arbuscules, beginning with the formation of a PPA (Stage 0) to the stage of degrading arbuscules (Stage IV), *RAM1* expression starts at the stage of PPA formation (Stage I), while *PT4* expression commences at stage IV. Due to the data presented, *WR15A*, *WR15B*, *WR15C*, *460730*, *15867*, *21492* and *25005* are specifically expressed in arbuscule-containing cells. Question marks indicate that *21492* and *25005* could not be further analyzed in the promoter-*gus* studies due to weak *gus*-staining. Areas of degrading arbuscules display fading to no *gus*-staining in *pWR15A*, *pWR15B* and *p460730* roots, whereas *pWR15C* and *p15867* roots still show strong *gus*-staining in these areas and might therefore be still active (indicated by dashed arrows) (adapted from Gutjahr, 2013).

### **RNAi knockdowns targeting *ERF* TF genes reveal effects on mycorrhization and AM-dependent FA biosynthesis genes**

Due to the arbuscule-specific expression of *ERF* TF gene promoters, RNAi knockdown constructs targeting some of the *ERF* candidate genes were designed to further analyze the effects of these genes on overall mycorrhization rate and fungal structures, as well as to identify potential target genes. Constructs were successfully cloned via Gateway cloning (Limpens et al., 2004) (Table 12). Plants were either infected with *A. rhizogenes* strains carrying RNAi knockdown constructs or an empty vector control, simultaneously mycorrhized and roots were harvested. After harvesting, each root system was split to perform qRT-PCR measurements as well as phenotypical analysis. RNA isolated individually from each root system was measured via qRT-PCR using gene-specific primers (Table 7). Transcript levels were compared between roots containing either the RNAi constructs or an empty vector control to calculate knockdown effects.

Four RNAi constructs revealed a sufficient reduction of transcript levels of their corresponding targets to be further analyzed. Two of them were designed and cloned by Phil Pallokat (Pallokat, 2013) (Table 42).

**Table 42: Overview of cloned RNAi-constructs and their effects on the corresponding *ERF* TF gene.** The six constructs 21492\_1, 21492i, 15867i, 1449\_1, 460730\_1 and 460730\_2 revealed transcript level reduction comparing empty vector controls to RNAi constructs and were further analyzed. Asterisks indicate constructs designed and cloned by Phil Pallokat (Pallokat, 2013).

Candidate gene targeted	RNAi-constructs designed	Calculated knockdown effect (%)	Harvesting time point (dpi)
<i>WR15A</i>	1449_1	98	49
<i>460730</i>	460730_2	66	49
<i>15867</i>	15867i*	73	63
<i>21492</i>	21492i*	83	63

The four RNAi constructs mediating decreased transcript levels of genes were used for further work (1449\_1, 460730\_2, 15867i and 21492i). At least eight RNAi knockdown roots from individual root systems and their corresponding eight empty vector control roots were analyzed in qRT-PCR measurements with three technical replicates for each biological sample (Figure 19). Each PCR plate contained *TRANSLATION-ELONGATION-FACTOR- $\alpha$*  (*MtTef $\alpha$* ) measurements for each measured sample. *MtTef $\alpha$*  is evenly expressed in roots and therefore used as a normalization for every measurement. As further controls, a *Glomus intraradices*  $\alpha$ -*TUBULIN* (*GiaTub*) and an AM marker gene (*MtPT4*), encoding an AM-specific phosphate transporter, were measured. Since *MtPT4* is an AM marker gene for functioning arbuscules (Javot et al., 2007), results of this measurement would reveal, if the nutritional exchange during AM symbiosis is disrupted.

## Results

*WRI5A* is known to play a role during FA biosynthesis and phosphate uptake (Jiang et al., 2018; Luginbuehl et al., 2017). In addition, further ERF TFs, like 460730 and 15867, being closely related to *LjCBX1* important for AM-dependent lipid synthesis and phosphate uptake in *L. japonicus*, might be involved in this process as well (Xue et al., 2018). Effects of 460730 and 15867 on the process of FA biosynthesis were therefore also studied.

Finally, these measurements include the important regulatory GRAS TF gene *RAM1* as well as some genes like *RAM2* or *FatM*, encoding components of to the AM-dependent FA-biosynthesis (Bravo et al., 2017) (Figure 4). At last, effects on some of the other *ERF* candidate genes were measured, providing insights into a regulatory network potentially mediating FA biosynthesis during AM.

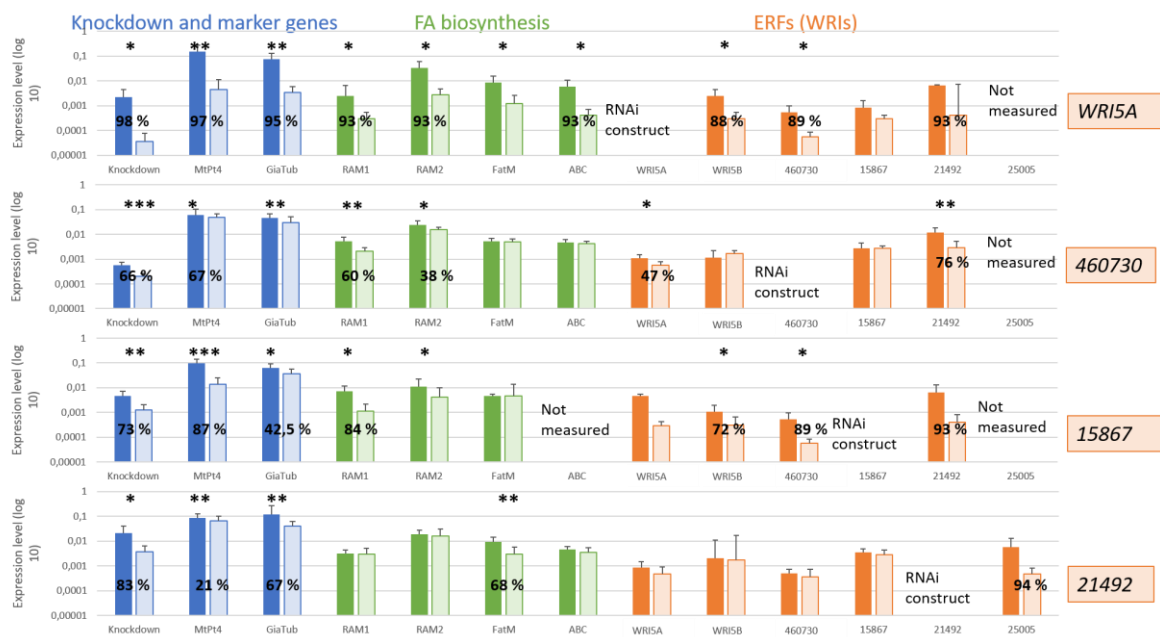


**Figure 19: qRT-PCR measurements of the four best working RNAi constructs reveal effects on overall mycorrhization, genes of the FA biosynthesis and other *ERF* TF genes.** Results of the RT-PCR measurements of RNAi-constructs targeting either *WRI5A*, *15867*, *21492* or *460730* were summarized. Darker columns (left part of column pair) show the mean of all eight measured empty vector control roots whereas lighter colored columns (right side of the column pair) are the mean of all eight measured RNAi constructs-containing roots. Each column is shown with the corresponding standard deviation and, if calculated, the statistical significance (\* $p=0,05$ , \*\* $p=0,01$ , \*\*\* $p=0,001$ ) of the measured transcript level reduction comparing empty vector control roots and corresponding RNAi construct-containing roots. All columns in blue belong to the knockdown effect/ marker gene group, green indicates transcript level measurements of genes belonging to AM-dependent FA biosynthesis and orange summarizes the results of effects on further *ERF* TF candidate genes.

In case of the *WRI5A* knockdown, the strongest knockdown achieved a 98 % reduction of the transcript level of *WRI5A*, severe reductions – in most cases over 90 % - on the group of AM marker genes, AM-dependent FA biosynthesis genes and *ERF* TF genes. Eviscerating the effects on *15867* and *21492*, all calculated effects showed a significant reduction. In case of those two *ERF* TF genes, the calculated RNAi-knockdown is not significant. In comparison to the results of the *WRI5A* knockdown, the knockdowns of *21492* and *15867* (83 % and 73 %) revealed less effects on the marker gene group and only partial

## Results

reductions in the group of FA biosynthesis genes and *ERF* TF genes. In the 15867 knockdown roots, transcript levels of *MtRAM1*, 460730, *WRI5B* and 21492 were reduced, whereas measurements with roots containing the 21492i RNAi construct only caused reduction of *FatM* and 25005 transcript levels.

The 460730 RNAi construct showed the weakest reduction of only 66 % of the transcript level comparing control roots versus RNAi roots. Nevertheless, slight but significant effects on *MtPT4* and *GiaTub* as well as on *MtRAM1*, *MtRAM2*, *WRI5A* and 21492 could be measured.

To put it in a nutshell: RNAi constructs targeting *WRI5A*, 460730, 15867 and 21492 all revealed effects on genes belonging to AM-dependent FA biosynthesis. In contrast to this, only *WRI5A* and 15867 RNAi constructs, revealing the strongest knockdown effects, showed decreased levels of *MtPT4* and *GiaTub*. Interestingly, all RNAi constructs displayed effects on further *ERF* TF genes, hereby showing contrasting target patterns. Together, these findings indicate a role of 15867, 460730 and 21492 in AM-dependent FA biosynthesis, besides the already stated role of *WRI5A* (Jiang et al., 2018; Luginbuehl et al., 2017). The downregulation of further *ERF* TF candidate genes might suggest a regulatory network of *ERF* TF genes regulating this process, potentially built in a hierarchical structure, and maybe including the already known regulator *RAM1* (Luginbuehl et al., 2017). The different patterns mentioned above are summarized in a heat map for a better overview of the RNAi knockdown dataset (Figure 20).

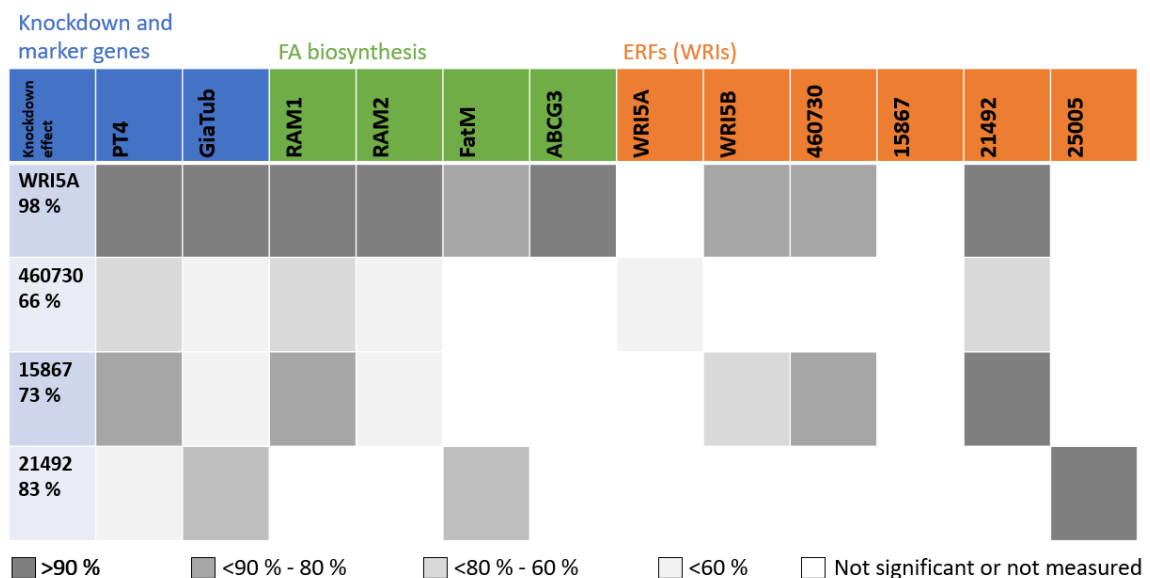


**Figure 20: Summary of qRT-PCR results as heat map.** Dark colored boxes indicate strong downregulation, lighter colors less downregulation of possible target genes whereas white boxes show no significant reduction or so far not measured results. First column shows the different knockdown constructs and their effects on the targeted genes. All columns in blue belong to the knockdown effect/ marker gene group, green indicates transcript level measurements of genes belonging to AM-dependent FA biosynthesis and orange summarizes the effects on further *ERF* TF genes.

## Results

Two independent knockdown approaches with the four selected constructs were performed, and resulted in RNAi-mediated knockdowns, which might indicate different efficiencies of the RNAi constructs. From former studies, it is known, that RNAi-knockdown constructs can show varying results in independent repetitions (Floß et al., 2008). The RNAi knockdown data presented here thus need careful evaluation. Since some of the constructs showed reduced amounts of *GiaTub*, the marker gene for the fungal mass, phenotypical analysis of the roots corresponding to the measured RNA were performed.

### Phenotyping of RNAi roots showed only slight effects on the fungal morphology

Roots containing the knockdown constructs targeting *21492*, *460730*, *15867* and *WRI5A* revealed the strongest knockdown effect and were therefore microscopically analyzed via Gridline intersection. This method reveals possible morphological changes of the fungal material and of the overall mycorrhization. In a blind study, overall mycorrhization, hyphal structures, vesicles, arbuscule-containing cells and the arbuscular phenotype (wild type or truncated, Figure 21) were taken into account (Figure 22, Figure 23, Figure 24, Figure 25). Results of the RNAi-construct containing roots were compared to the roots containing the corresponding empty vector control. To obtain first insights, the eight root systems that were measured in the qRT-PCR were pooled and 900 to 1200 (depending on the amount of material) gridlines were analyzed for this phenotyping approach.

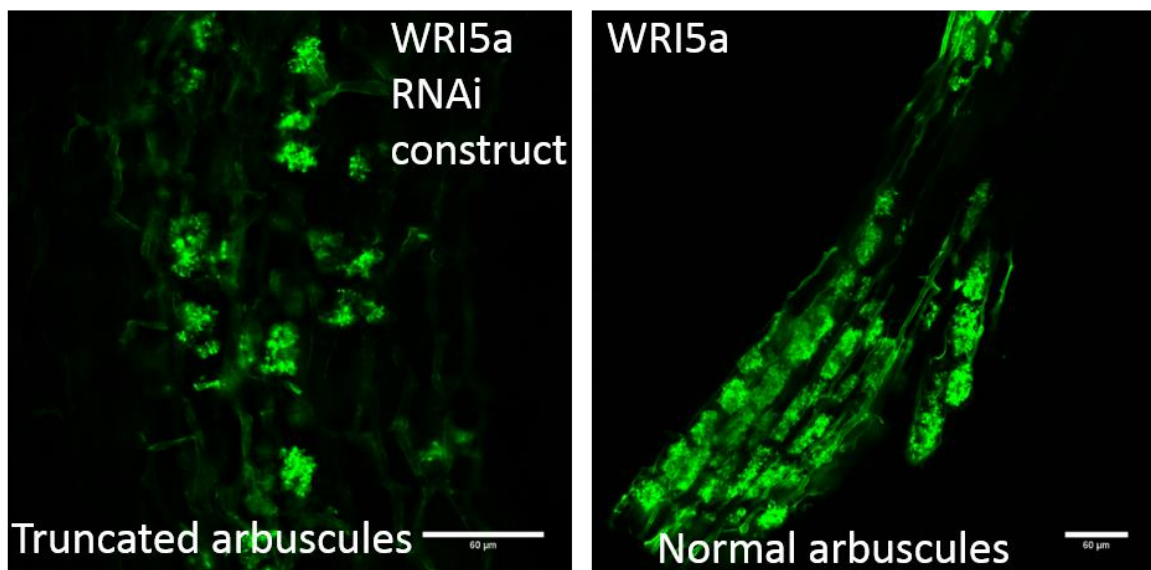


**Figure 21: Phenotype of truncated (left) versus normal looking arbuscules of the *WRI5A* RNAi-knockdown roots.** Phenotyping of RNAi knockdown roots revealed roots containing truncated arbuscules (left image) as well as roots containing normal looking (wild type) arbuscules. Normal looking arbuscules are characterized by a rectangular shape that resembles the cell shape of the roots whereas truncated arbuscules do not seem to fill the whole root cell, are often roundly shaped or even arrest in the bird foot stage. The two images are exemplary for the counts performed during Gridline intersection of all used RNAi knockdown roots, distinguishing between wild type and truncated roots. Hyphal structures were stained via WGA Alexa 488.



## Results

The phenotyping of knockdown roots revealed only slight differences between knockdown roots and control roots (Figure 22, Figure 23, Figure 24, Figure 25). Roots containing the *WR15A* construct only revealed differences in the arbuscular phenotype, showing 30 % truncated arbuscules compared to the 15 % truncated arbuscules in the control roots (Figure 22). Overall colonization as well as hyphal structures or vesicles did not differ between knockdown roots and empty vector control roots.

*460730\_2*-containing roots (*460730* knockdown) even retained more arbuscule-containing parts (17 % difference) and more normal looking arbuscules (80 %), when compared to the control roots (63 %) (Figure 23). Overall colonization, hyphal structures and vesicles did not differ between control roots and knockdown roots. The *460730* and *WR15A* knockdown roots and their corresponding controls were harvested at 49 dpi.

Roots containing the constructs *15867i* and *21492i* were harvested at 63 dpi (Figure 24, Figure 25). *15867* knockdown roots revealed an increase of vesicles in comparison to the control roots, but no differences in any other category, even displaying higher overall mycorrhization rates as control roots. *21492* RNAi knockdown roots (25 %) revealed less overall mycorrhization compared to their corresponding control roots (47 %) but did not differ in neither the hyphae nor the vesicle or arbuscule categories. Roots containing this construct even showed less truncated and more wild type arbuscule-containing cells. Nevertheless, *WR15A* and *21492* targeting RNAi roots at least revealed tendencies of either a higher amount of truncated arbuscules or a reduced overall mycorrhization rate.

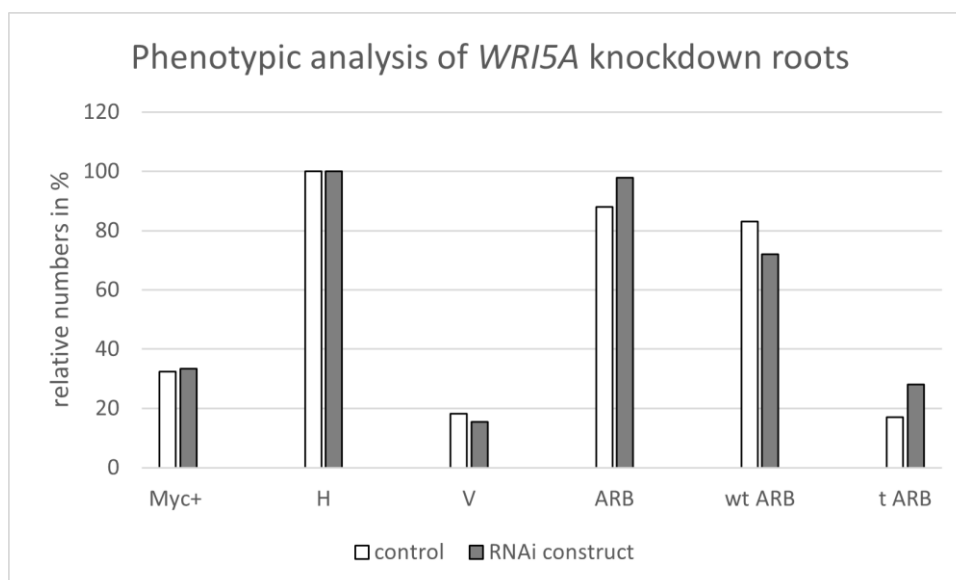


**Figure 22: RNAi-knockdown of *WR15A* leads to a higher amount of truncated arbuscules.** Parts of the eight root systems measured in the qRT-PCR measurement (Figure 19) were stained with WGA Alexa 488 and counted using Gridline intersection. Overall mycorrhization (Myc+) was counted and categorised into areas containing hyphae (H), vesicles (V) and arbuscules (ARB). ARB-containing areas were separately counted as either wild type arbuscules (wt ARB) or truncated arbuscules (t ARB). Roots were harvested at 49 dpi.

## Results

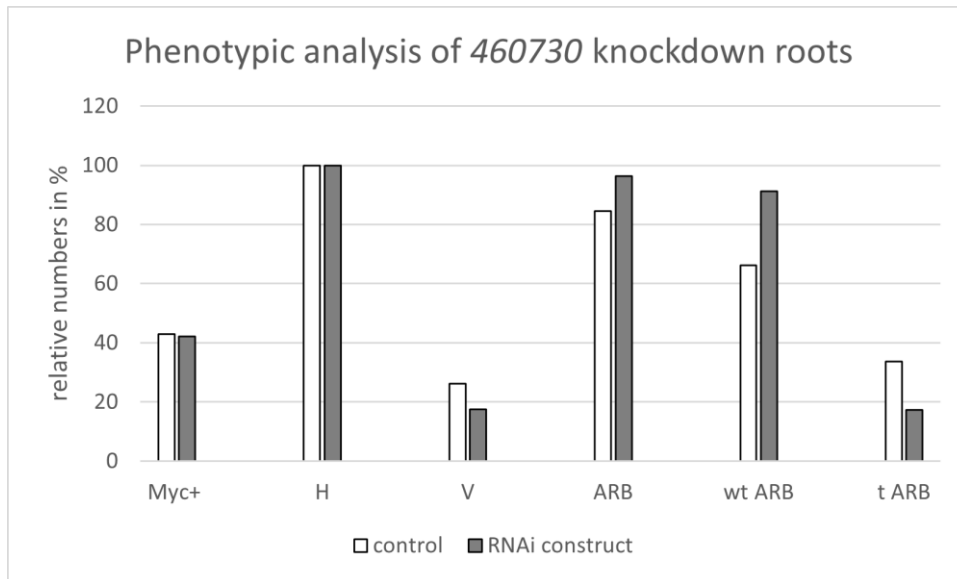


**Figure 23: RNAi-knockdown of 460730 results in a reduced amount of vesicles.** Parts of the eight root systems measured in the qRT-PCR measurement (Figure 19) were stained with WGA Alexa 488 and counted using Gridline intersection. Overall mycorrhization (Myc+) was counted and categorised into areas containing hyphae (H), vesicles (V) and arbuscules (ARB). ARB-containing areas were separately counted as either wild type arbuscules (wt ARB) or truncated arbuscules (t ARB). Roots were harvested at 49 dpi.

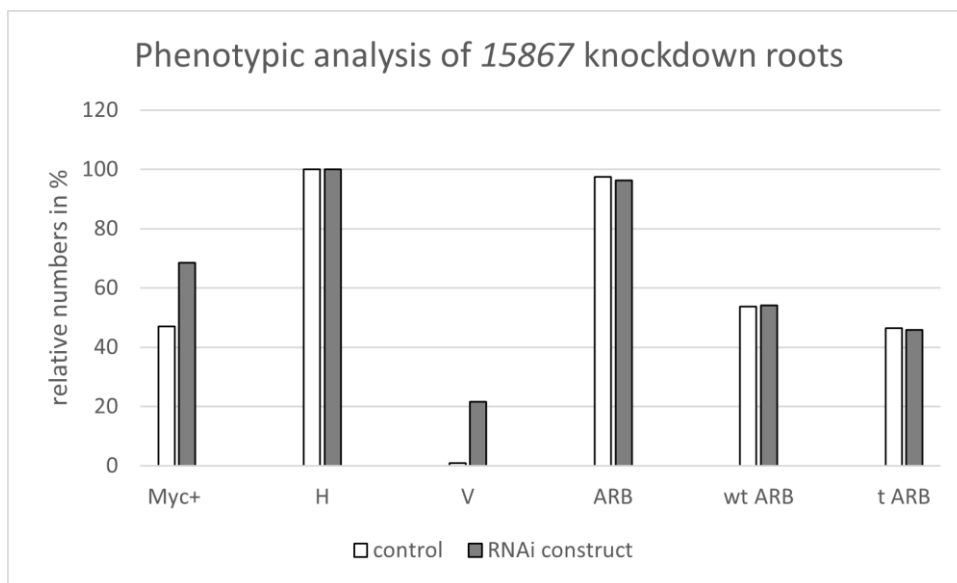


**Figure 24: RNAi-knockdown of 15867 roots display higher overall mycorrhization and higher amounts of vesicles.** Parts of the eight root systems measured in the qRT-PCR measurement (Figure 19) were stained with WGA Alexa 488 and counted using Gridline intersection. Overall mycorrhization (Myc+) was counted and categorised into areas containing hyphae (H), vesicles (V) and arbuscules (ARB). ARB-containing areas were separately counted as either wild type arbuscules (wt ARB) or truncated arbuscules (t ARB). Roots were harvested at 63 dpi.

## Results

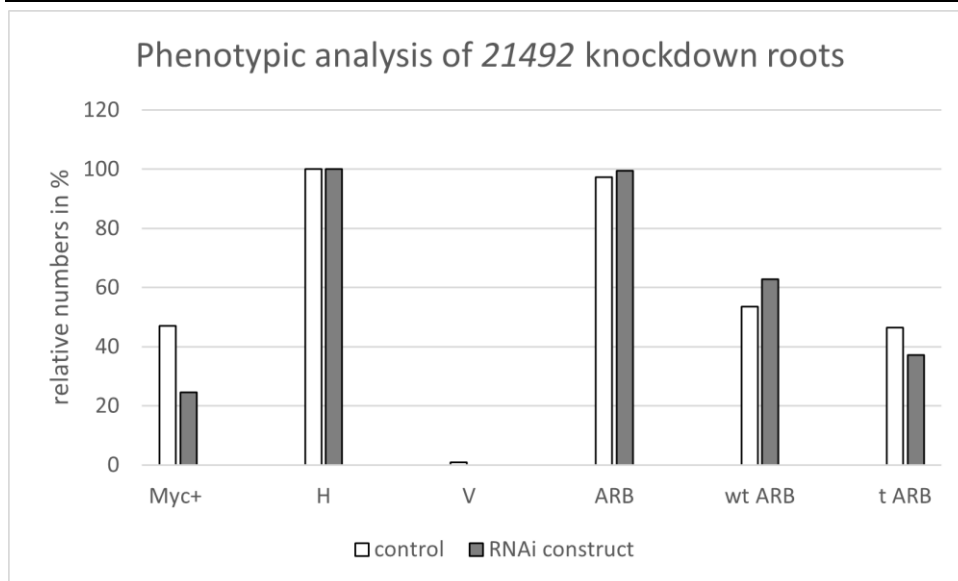


**Figure 25: RNAi-knockdown of 21492 leads to a reduced overall mycorrhization.** Parts of the eight root systems measured in the qRT-PCR measurement (Figure 19) were stained with WGA Alexa 488 and counted using Gridline intersection. Overall mycorrhization (Myc+) was counted and categorised into areas containing hyphae (H), vesicles (V) and arbuscules (ARB). ARB-containing areas were separately counted as either wild type arbuscules (wt ARB) or truncated arbuscules (t ARB). Roots were harvested at 63 dpi.

Taken together, these results were surprising, since they do not echo the high reduction of *GiaTub* (*WRI5A*: 97 % and *15867*: 87 %) measured by qRT-PCR dataset (Figure 19).

The late harvesting time points of all knockdown containing roots equate old time points concerning the overall symbiosis status and could therefore be a reason for the discrepancy between molecular and morphological phenotype. Whereas qRT-PCR measurements exhibit the transcript levels at a short time point, phenotypical analysis can be seen as a cumulative summary of developmental steps. Due to the late harvesting, the symbiosis in RNAi containing roots could have “caught up” with the symbiosis situation in control roots and morphological effects might have diminished by this situation.

On the other hand, *GiaTub* measurements in qRT-PCR should reflect the overall amount of transcriptionally active fungal material. A severe reduction of this marker gene should normally show less overall mycorrhization or severe effects on fungal structures like arbuscules.

Since ERF TFs probably play a regulatory role in the whole AM-dependent FA biosynthesis, the morphological effect of knockdowns would probably be on the arbuscular level. This would also fit in with findings of the promoter-*gus* studies that only revealed high promoter activities in arbuscule-containing cells for all the analyzed ERF promoters. A further effect could be on the number of vesicles as fungal lipid storage bodies. Reduced FA biosynthesis could lead to a reduction of those storage bodies.

The missing phenotypical differences might also be due to the fact that all *ERF* TF genes used in this study belong to the same TF family and are therefore structurally similar, in

## Results

---

addition to being similarly expressed. Missing phenological effects could be caused by redundancies of two or more ERF TFs that play a similar role in the regulation of FA biosynthesis. This could be further analyzed by a joint analysis of all ERF TFs possibly involved in this FA biosynthesis process.

---

**Y1H approaches reveal that ERF TFs and RAM1 regulate promoters of ERF TF and genes belonging to the FA biosynthesis**

The RNAi studies indicate several follow-up questions tackled in the upcoming chapters. The first two striking questions, targeted in this chapter are: Do the selected ERF TF candidates regulate each other and are thereby part of a larger regulatory network? Do further ERF TFs – apart from WRI5A, WRI5B and WRI5C – regulate AM-dependent FA biosynthesis and what are the potential target genes?

The regulation of downstream targets via TFs is often managed by the TFs' binding to the target genes' promoter. The resulting protein-DNA binding was analysed here via a Yeast-1-Hybrid (Y1H) approach. Hereby, yeast strains with promoters of interest integrated into the genome function as baits, whereas yeast strains, expressing the TF of interest function as preys. To construct the bait strains, the promoters of interest were ultimately cloned into two different vectors referred to as *pMWR2* and *pMWR3* via *Gateway* cloning (Deplancke et al., 2004; Fuxman Bass et al., 2016b) (Table 13). The two final vectors either contain a *HISTIDINE3* (*HIS3*; *pMWR2*) or a *lacZ* (*pMWR3*) reporter gene following the integrated target promoter gene sequence. The vector containing the *lacZ* gene further contains an *URACIL3* (*URA3*) gene expressed by an independently driven promoter. The *pMWR2* vector additionally contains a minimal *HIS3*-promoter necessary to provide sufficient *HIS* levels. The *pMWR2*- and *pMWR3*-constructs containing the same promoter sequences were simultaneously transformed into a suitable yeast strain (Table 4). Proper integration of the plasmids into the yeast genomes can be tested via plating the freshly transformed strains on SD-media plates lacking the components *HIS/URA* (referred to as SD *HIS/URA* media).

Yeast prey strains, which express the TF gene of interest were cloned into the *pGADT* vector (Table 14). This vector expresses *LEUCINE* (*LEU*), which helps to select correct strains after the yeast transformation. In contrast to the bait strains, prey strains do not integrate their plasmid into the yeast genome. Prey strains of all seven ERF candidate genes could be obtained, as well as *RAM1* expressing prey strains (Table 16).

Since *WRI5A*, *WRI5B* and *WRI5C* as well as *RAM1* are known to play a role during AM-dependent FA biosynthesis (Jiang et al., 2018; Luginbuehl et al., 2017), *RAM1*-expressing prey strains were also integrated into the upcoming interaction studies. Since the exact interactions between *WRI5* TFs and *RAM1* remain unclear, the Y1H approaches were thought to shed light on this question. Unfortunately, *pRAM1* could not be obtained for these experiments. Nevertheless, since *RAM1* could also interact with the promoter of other ERF TFs and thereby regulating FA biosynthesis during AM, interaction studies including ERF TFs and *RAM1* might shed light on this regulatory network.

### **Autoactivity tests reveal that all Y1H bait strains can be used for Y1H studies**

Autoactivation in bait strains can occur due to endogenous yeast TFs binding to the integrated bait promoters (Fuxman Bass et al., 2016b). In addition to this, bait strains from a single yeast transformation can display varying levels of autoactivation, depending on differing numbers of reporter cassette integrations from the *pMWR2* and *pMWR3* plasmids. Autoactivity of the resulting yeast bait strains must be tested with two different assays: a  $\beta$ -Galactosidase assay testing for *lacZ* autoactivation via a colorimetric assay and growth on SD HIS/URA media containing increasing levels of 3-AMINOTRIAZOL (3-AT) (Fuxman Bass et al., 2016a, 2016b) (Figure 26). 3-AT is a competitive inhibitor of HIS3. To overcome the inhibition on increasing amounts of 3-AT, promoter-driven *HIS3* expression is necessary to convey growth of yeast colonies. Higher amounts of 3-AT are required to repress yeast growth. The stronger the autoactivation of the examined yeast strain, the higher are the required levels of 3-AT. Therefore, this autoactivation test on 3-AT containing media helps to determine a baseline level for a suitable 3-AT concentration. Since 3-AT concentrations repressing autoactivity are unique for each bait strain, results of Y1H matings can only be compared within the group of the same bait construct.

Due to methodological issues, only six yeast bait strains, containing *pMWR:p15867*, *pMWR:p21492*, *PMWR:pRAM1*, *pMWR:pFatM*, *pMWR:pKASII* and *pMWR:pSTR* could be obtained.

## Results

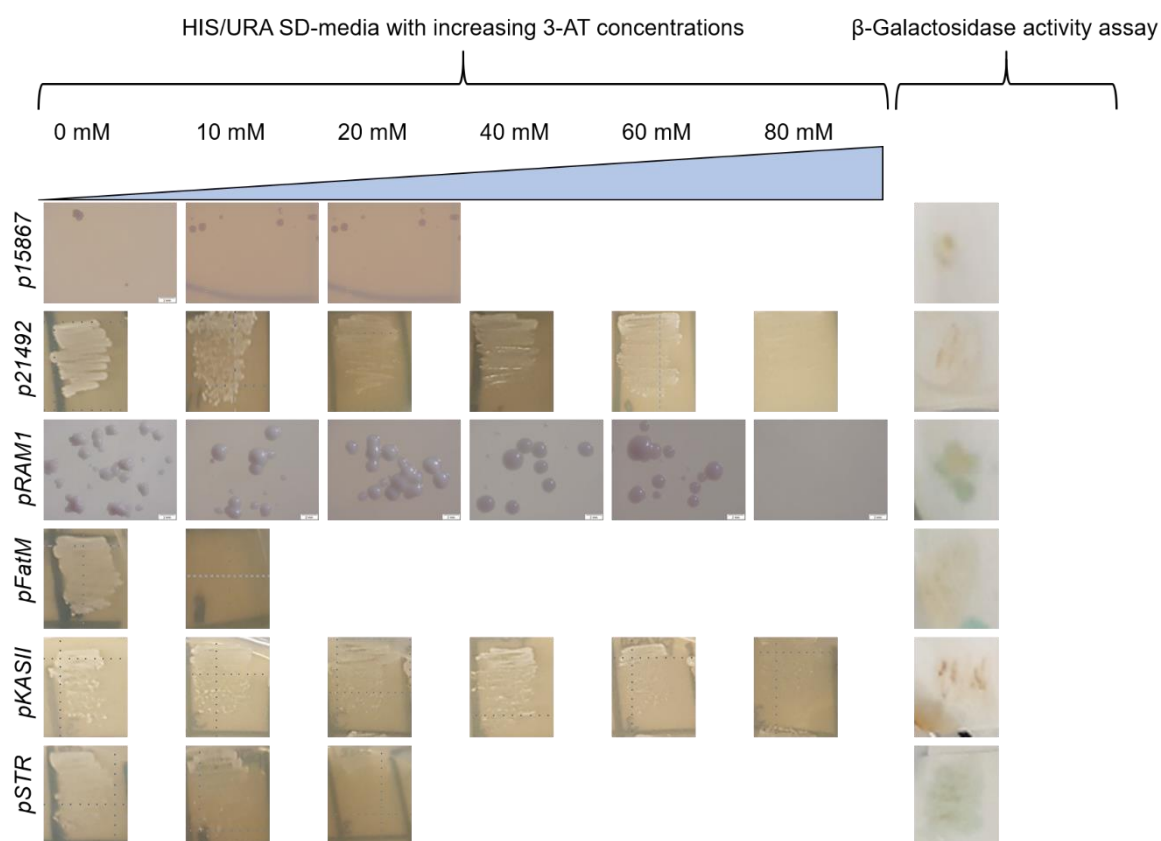


**Figure 26: Autoactivity tests of Y1H bait strains via HIS-autoactivity and  $\beta$ -Galactosidase assay reveal varying results in HIS autoactivation.** Yeast bait strains containing genome integrations of either *pMWR:p15867*, *pMWR:p21492*, *pMWR:pRAM1*, *pMWR:pFatM*, *pMWR:pKASII* or *pMWR:pSTR*, were tested on HIS/URA SD-media with increasing levels of 3-AT (0 mM – 120 mM) and colony lift colorimetric assay for  $\beta$ -galactosidase (Fuxman Bass et al., 2016a, 2016b). Blue staining in the colorimetric assay would indicate autoactivity, whereas white colonies indicate no autoactivity.

Most yeast bait strains, including *pMWR:p15867*, *pMWR:pFatM* and *pMWR:pSTR* show growth repression on low levels of 3-AT (10 mM – 20 mM), indicating a low level of autoactivation in the HIS-autoactivity test (Table 43). In contrast to this, bait strains containing *pMWR:p21492*, *pMWR:pRAM1* and *pMWR:pKASII* revealed a high HIS-autoactivity level. Neither of the six different bait strains showed autoactivity in the  $\beta$ -Galactosidase activity assay (Figure 26). Considering both types of autoactivity tests, all six yeast bait strain constructs can be used for further Y1H approaches, if 3-AT levels are adjusted accordingly.

**Table 43: Baseline levels for Y1H experiments in accordance with autoactivity tests.**

yeast strain	Baseline level of 3-AT concentration
<i>pMWR:p15867</i>	20 mM
<i>pMWR:p21492</i>	80 mM
<i>pMWR:pRAM1</i>	80 mM
<i>pMWR:pFatM</i>	10 mM
<i>pMWR:pKASII</i>	80 mM
<i>pMWR:pSTR</i>	20 mM

## Results

---

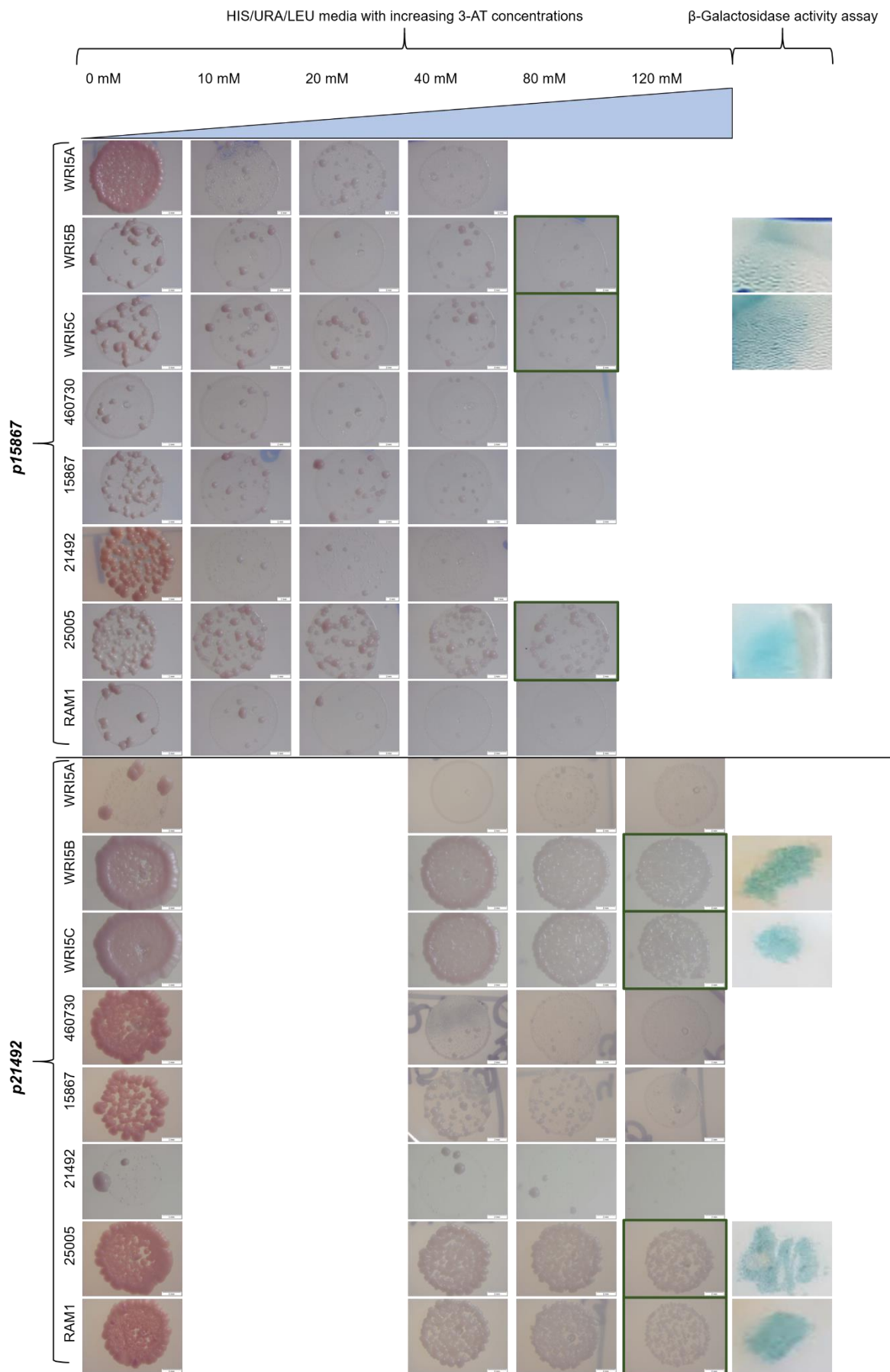
Unfortunately, the *pMWR:pRAM1* bait strain could not be used for further mating matrices since even the matings on HIS/URA/LEU SD-media with neither ERF TF nor the RAM1 prey strain did show results (data not shown in this work).

### **The promoter of 15867 and 21492 are targeted by ERF TFs and RAM1 in a Y1H approach**

To answer the question, whether ERF TFs regulate each other by binding to their promoters, yeast prey strains expressing either one of the seven ERF TFs were mated with yeast bait strains containing the *ERF* gene promoters *pMWR:p15867* or *pMWR:p21492* (Figure 27). A yeast prey strain expressing RAM1 was also included into the mating matrix to shed light on a potential regulatory network of FA biosynthesis including RAM1 in addition to ERF TFs.



# Results



## Results

**Figure 27: ERF promoters *p15867* and *p21492* are targeted by *WRI5B*, *WRI5C*, *25005* and, in case of *p21492*, also by *RAM1*.** Yeast bait strains containing genome integrations of either *pMWR:p15867* or *pMWR:p21492* were mated with yeast prey strains expressing one of the seven ERF TF candidate genes (*WRI5A*, *WRI5B*, *WRI5C*, *460730*, *15867*, *25005*, *21492*) or *RAM1*. Resulting matings were plated on HIS/URA/LEU SD-media with increasing levels of 3-AT (0 mM – 120 mM). Baseline levels of 3-AT concentrations were chosen according to the determined autoactivity levels (Table 43). Positive interactions (indicated by yeast colonies growing on higher 3-AT levels as the autoactivity baseline level) were framed in dark green. Colony lift colorimetric assay for  $\beta$ -galactosidase (Fuxman Bass et al., 2016a, 2016b) was used for further evaluation of potential interactions. Blue staining in the colorimetric assay indicates autoactivity, whereas white colonies indicate no autoactivity. Positive interactions were repeated at least 2-3 times.

*WRI5B*, *WRI5C* and *25005* interacted with the bait strains containing either *pMWR:p15867* or *pMWR:p21492* (Figure 27, Table 44). Furthermore, *pMWR:p21492* containing yeast strain also interacted with the *RAM1* expressing prey strain. These results indicate that ERF TFs target each other's promoters and are part of a larger regulatory network. In addition to this, *RAM1* seems to regulate the expression of some ERF TFs like *21492* via binding to the genes' promoters. Of course, *ERF* TF gene regulation is mediated by short motifs on targeted promoters, mostly including 10 - 20 bp. Some of these target motifs like the GCC box motive, the AW motive and the CTTC motive were already identified (Allen et al., 1998; Cheng et al., 2013; Jiang et al., 2018; Lee et al., 2004; Wu et al., 2007; Xu et al., 2016; Xue et al., 2018). The question what motive mediates ERF binding on *p15867* will be targeted in the upcoming chapter.

Interestingly, the upstream regulators are in both cases *WRI5B* and *WRI5C* as well as *RAM1*, TFs also linked to the process of FA biosynthesis (Jiang et al., 2018; Luginbuehl et al., 2017). Since these TFs regulate the promoters *p15867* and *p21492*, this suggests a role of those two genes in the whole process of AM-dependent lipid biosynthesis. The strong interactions between both bait strains and the *25005* expressing prey strain further indicate a regulatory role of *25005*, that could also be linked to FA biosynthesis. This idea will be further examined in the upcoming chapter by a Y1H approach mating ERF TF prey constructs with some bait strains carrying integrated promoters of FA biosynthesis structural genes.

**Table 44: Promoters of *15867* and *21492* are targeted by *WRI5B*, *WRI5C*, *25005* and *RAM1*.** Yeast bait strains *pMWR:p15867* and *pMWR:p21492* are listed in the first column whereas prey strains expressing *WRI5B*, *WRI5C*, *25005* and *RAM1* are listed in the table's first line. Positive interactions are marked in green, white fields indicate no interaction.

	<b>WRI5B</b>	<b>WRI5C</b>	<b>25005</b>	<b>RAM1</b>
<b><i>pMWR:p15867</i></b>				
<b><i>pMWR:p21492</i></b>				

### **Shortened promoter fragments of *p460730* and *p15867* reveal the promoter length needed to provide expression of *460730* and *15867* genes**

The chapters above showed that ERF TFs regulate each other by binding to their promoters. More precisely, *p15867* and *p21492* are regulated by WRI5A, WRI5B, WRI5C and – in case of *p21492* – by RAM1. This finding arises the question, which binding motif could mediate this DNA-protein interaction. As described in the introduction, there are three known binding motifs, mediating ER TF regulation: the AW-box, the GCC-box and the CTTC motive (Hao et al., 1998; Jiang et al., 2018; Liu et al., 2020). AW-box and CTTC-motifs could not be identified in the promoters studied here. As stated in literature, the GCC-box core motif of only seven bases (AGCCGCC) is sufficient for monomeric binding of an ERF TF (Hao et al., 1998). Within these seven bases (AGCCGCC), the bases shown in bold were found to be sufficient for binding of ERF TFs. Interestingly, *p460730* and *p15867* showed a GCC core motive (AGCCGCC), similar to the one (AGCCGCC) stated in previous publications (Hao et al., 1998). Comparing the stated GCC-box core motif and the predicted one in *p460730* and *p15867*, they show a difference in the sixth base (AGCCGGC), being a C in Hao, et al. 1998 and a G in the core motive found in *p460730* and *p15867*. The GCC-box core motifs in both *ERF* promoters were found approximately 250 bp to 150 bp upstream of the corresponding genes' start codon.

For the analysis of predicted GCC-box core motifs in *p460730* and *p15867*, two different approaches were performed: a reporter gene analysis and a Y1H assay using the *gusAint* as the reporter gene. The reporter gene experiment was hereby performed to shed light on the following questions: Which length of promoter is sufficient to drive gene expression of *460730* and *15867*? Are the promoters *p460730* and *p15867* still expressed, when containing a GCC-box motive?

The Y1H approach was performed to answer the following questions: Which promoter-fragment of *p460730* and *p15867* is necessary to provide binding of other ERF TFs? Is the predicted GCC-box core motive of *p460730* and *p15867* really a GCC-box motive or is binding by ERF TFs provided by another area of the promoter? To answer these questions, in total seven different promoter length of *p460730* and *p15867* were used. Exact length of these constructs as well as information about the contributors to the cloning process can be found Table 11 and Table 13. The *p460730* and *p15867* constructs used for the analysis of the promoter activity in the chapters before served as control constructs or control length in the Y1H approach, respectively. The length of the promoter region was then shortened, using a 1 kb (starting 1 kb upstream of the start codon) promoter fragment of each – *p460730* and *p15867* – as the next step. The promoter fragments *p460730\_250bp* and *p15867\_250bp* (starting 250 bp upstream of the start codon) both still contained the predicted GCC-box. In case of the promoter of *460730*, a 160 bp constructs (upstream of

## Results

---

the start codon) was cloned, still containing the GCC-box. The 160 bp constructs only start few bases before the predicted GCC-box, trying to shed light on the question, whether the area surrounding the GCC-box might as well play a role for the binding ability of the ERF TFs. As negative controls, constructs, not containing the predicted GCC-box core motif were designed, starting approximately 135 bp (*p460730*) and 180 bp (*p15867*) upstream of the genes' ATG.

### 250 bp of *p460730* and 1 kb of *p15867* are sufficient for the expression of the following genes

The five successively shortened promoter fragments of *p460730* and *p15867* were cloned into *pRR* and *M. truncatula* germlings could be infected with all seven constructs (Krüger, 2020) (Table 11). Infection of *M. truncatula* roots as well as mycorrhization, harvesting and staining was performed simultaneously to compare the promoter constructs belonging to either *p460730* or *p15867* with each other. Plants were harvested at 35 dpi (Figure 28, Figure 29).

Cloning of the five shortened versions of the promoter-*gus* constructs, as well as preparation of all transgenic plants, harvesting and staining of the roots was in part performed by Agnes Krüger (Krüger, 2020)

Promoter-*gus* images of roots containing one of the seven constructs were taken under the same conditions to enable comparison (Figure 28). Images of the stained roots were taken by Agnes Krüger (Krüger, 2020).

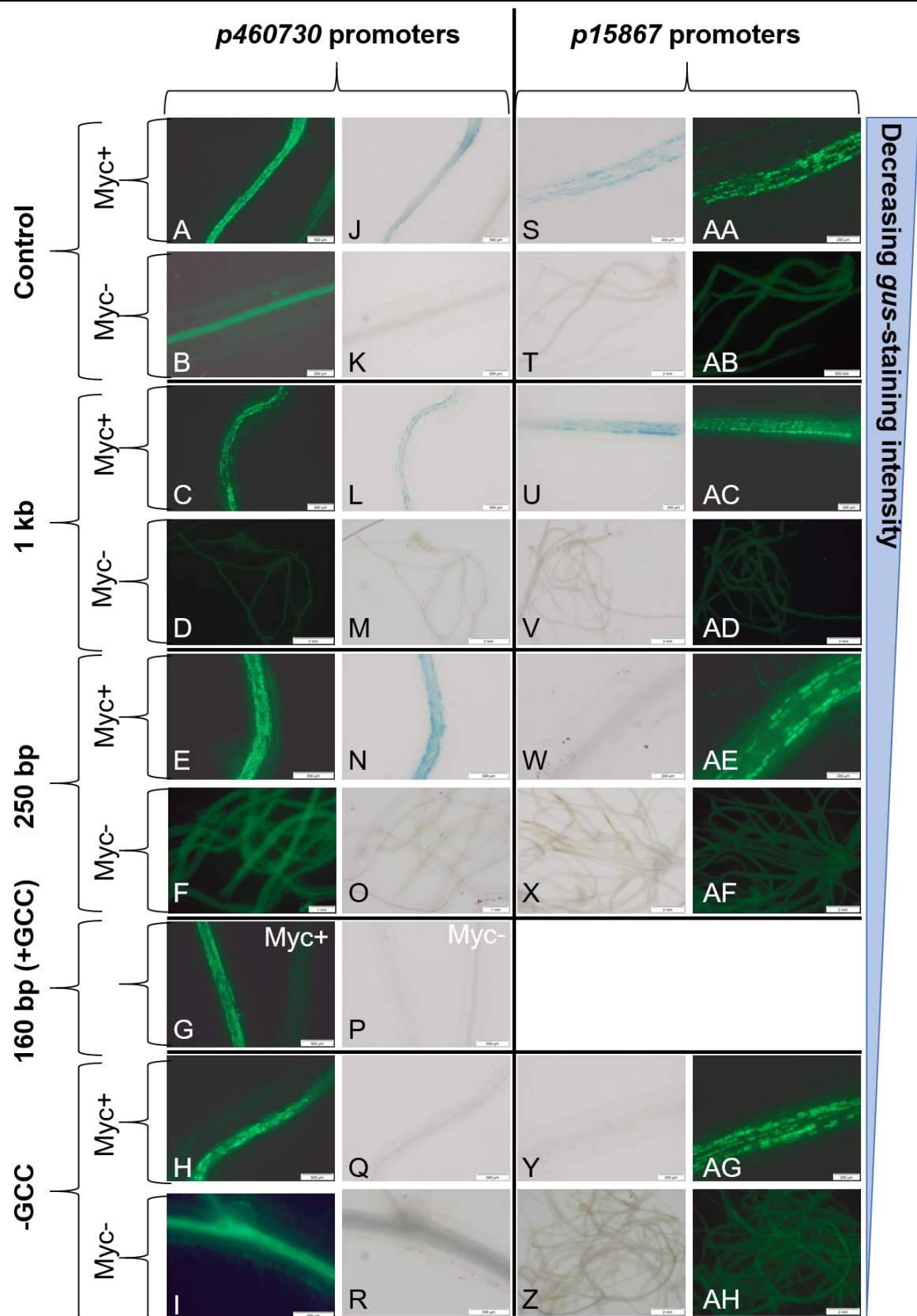


Figure 28: Promoter activity of *p460730* and *p15867* deletions show decreasing expression activity correlated with reduced length of the promoter-*gus* construct. *p460730* (A-R) and *p15867* (S-AH) constructs with decreasing length were expressed in mycorrhizal and non-mycorrhizal roots (Myc+ and Myc-) harvested at 35 dpi. Control constructs are already the *p460730* and *p15867*-constructs shown in Figure 13 and

## Results

---

Figure 14. The following constructs were used in this approach: 1 kb upstream of the ATG (1 kb construct), 250 bp upstream of the ATG (250 bp), 160 bp upstream of the ATG (160 bp), which all contain the potential GCC box and the -GCC (shortest promoter fragment, not including the GCC-box). Constructs were cloned and root images were taken by Agnes Krüger (Krüger, 2020).

Promoter activity of the *p460730* constructs can be observed until a promoter-fragment length of 250 bp, which still contains the predicted GCC-box core motive. The 160 bp long promoter-fragment as well as the shortest construct without the GCC-box do not show any expression of *460730*. This finding suggests that crucial elements necessary for gene expression such as enhancers might be missing in the shortest *p460730*-constructs.

Gene expression of *15867* could only be observed in the promoter-*gus* constructs containing the longest (control) fragment and the 1 kb fragment. Elements, necessary for gene expression of *15867* are thus probably placed in the promoter region 1 kb to 250 bp upstream of the start codon. Therefore, no promoter activity could be observed in the 250 bp construct and the construct not containing the GCC-box. For better comparison of all the *p460730* and *p15867* constructs, stained roots (35 dpi) of all promoter sets were placed next to each other (Figure 29).

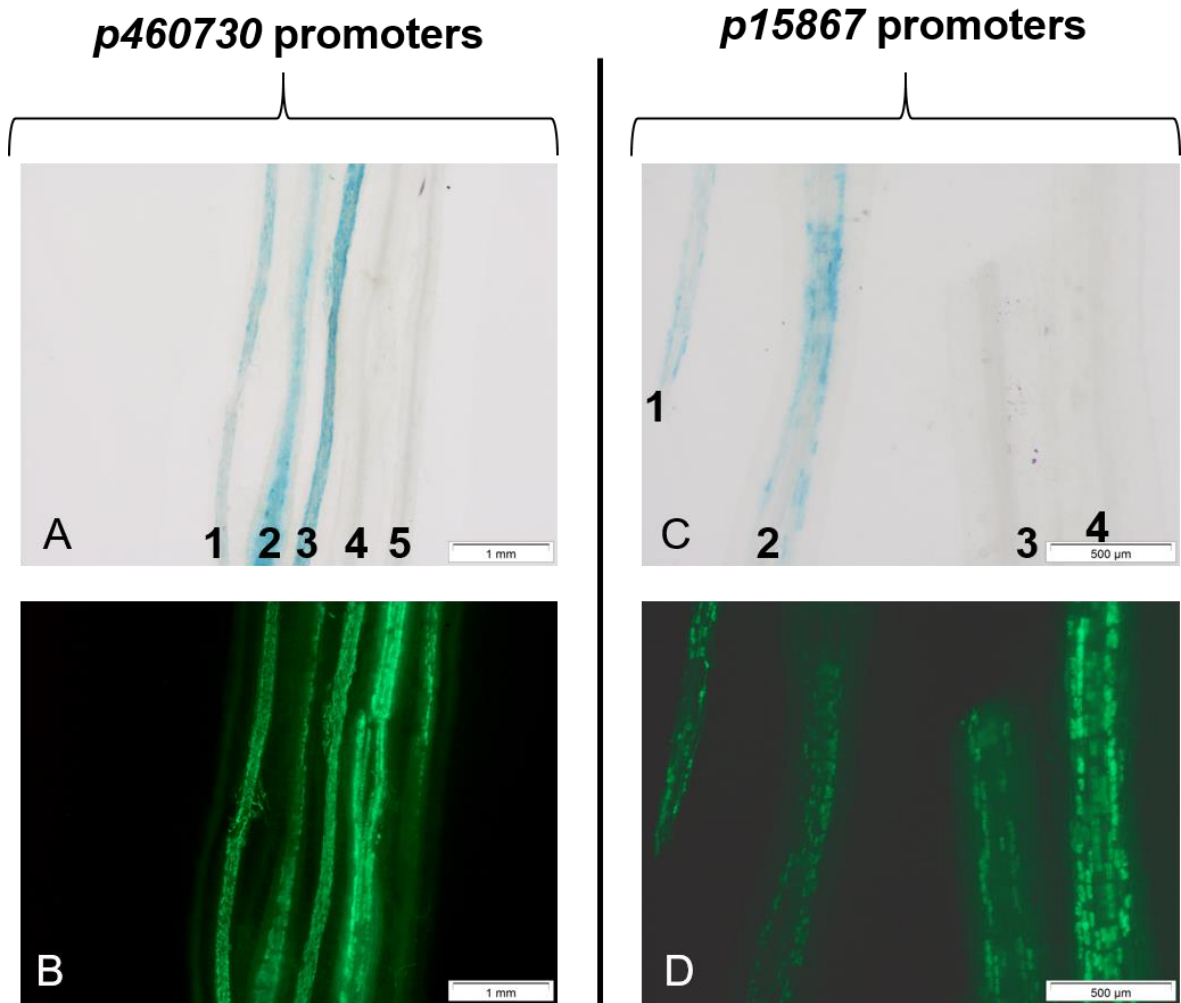


**Figure 29: Staining activity of the evaluated promoter-*gus* constructs decreases with reduced length of promoter-*gus* constructs.** Image A and B show the five different promoter-*gus* constructs *p460730* (1), *p460730-1kb* (2), *p460730-250bp* (3), *p460730-160bp* (4) and *p460730-GCC* (5). Image C and D show all promoter-*gus* constructs containing *p15867*-fragments: *p15867* (1), *p15867-1kb* (2), *p15867-250bp* (3), *p460730-160bp* (4) and *p460730-GCC* (5). A and C show promoter-*gus* staining, whereas B and D show corresponding WGA488 Alexa staining. Images were taken by Agnes Krüger (Krüger, 2020).

## Results

---

### Y1H approaches with the promoter-fragments of *p460730-250bp* and *p460730-GCC-* did not show any interactions with ERF TFs or RAM1

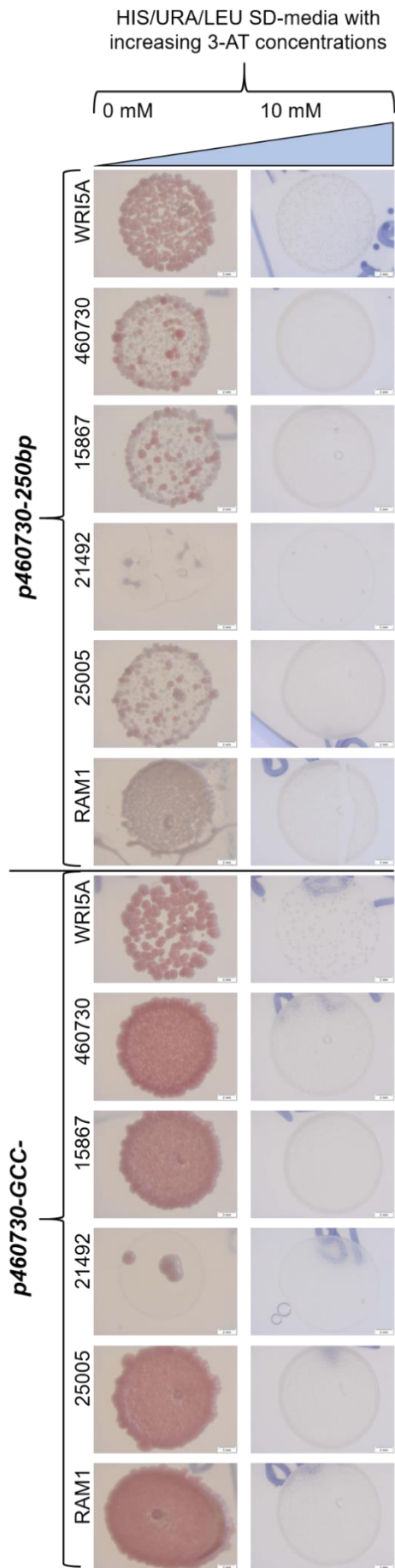
The Y1H constructs containing the seven different promoter fragments of *p460730* and *p15867* could be successfully cloned into the *pMWR2* and *pMWR3* (see Table 13 for information about the contributors and the exact length of each construct). Transformation of the yeast strains resulted in few to no colonies in most cases, only allowing for a few interaction studies concerning the *p15867* and *p460730* containing Y1H strains (see Table 15 for an overview over all yeast strains available for Y1H).

The inefficient transformation of Y1H strains could be due to the needed double integration of the *pMWR2* and *pMWR3* construct into the yeast genome, already discussed in literature (Fuxman Bass et al., 2016b). Besides this, ingredients like the carrier DNA needed for the process of transformation were changed during experiments, leading to even less successful transformations of the yeast strains.

Nevertheless, yeast strains containing integration of either *p460730-250bp* and *p460730-GCC-* were obtained, allowing comparison of ERF TFs and RAM1 interactions with either *p460730* bait strains containing the predicted GCC-box versus a construct not containing the GCC-box (Figure 30). Although the matings in this Y1H experiment worked, no growth on media plates with increasing 3AT levels (10 mM) could be observed. Apart from technical issues, this could be due to the fact that the two fragments (250 bp and 136 bp long) are not regulated by any of the tested TFs, or that boxes mediating this regulation are located more upstream and are therefore not included in the *p460730* fragments tested.



# Results



## Results

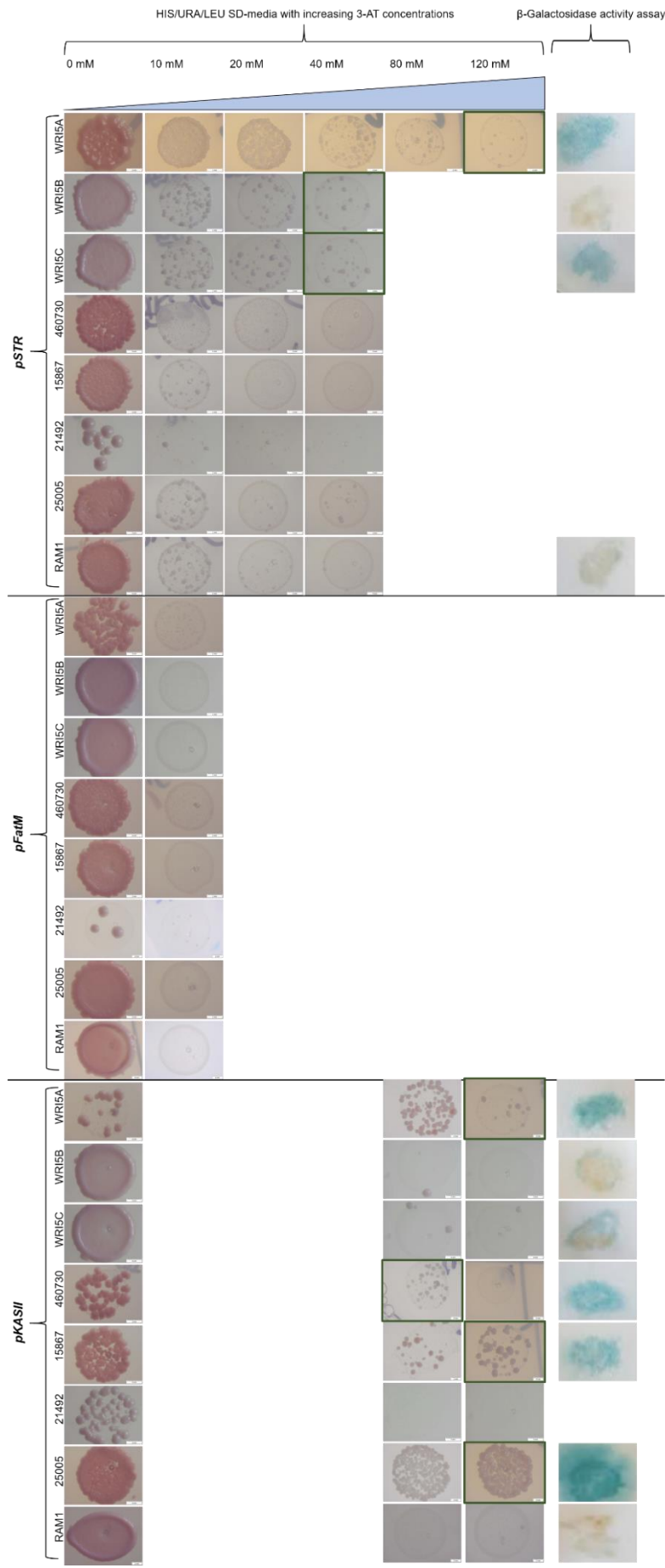
---

**Figure 30: Y1H approach comparing the interaction of ERF TFs with *p460730* yeast strains containing the predicted GCC-box versus a non-GCC-box do not show any interactions at all.** Y1H bait strains either containing *pMWR:p460730-250bp* or *pMWR:p460730-GCC* were tested against prey strains either containing WRI5A, 460730, 15867, 21492, 25005 or RAM1. The interactions were tested on media containing no to 10 mM 3AT concentrations. Due to time limitation, the tests could not be repeated three times.

### **Genes of the FA biosynthesis are regulated via promoter binding of ERF TF in an Y1H approach**

To answer the questions if – apart from the already known WRI5A, WRI5B and WRI5C – there are more ERF TFs involved in AM-dependent FA biosynthesis, yeast bait strains containing genome integrations of either *pMWR:pSTR*, *pMWR:pFatM* or *pMWR:pKASII* were mated with one of the ERF TFs or RAM1 expressing prey strains (Figure 31). The resulting matrix also helps identifying potential downstream targets regulated by WRI5A, WRI5B or WRI5C.

# Results



## Results

**Figure 31: Promoters of structural genes belonging to the AM-dependent FA biosynthesis are targeted by ERF TFs.** Yeast bait strains containing genome integrations of either *pMWR:pSTR*, *pMWR:pFatM* or *pMWR:pKASII* were mated with yeast prey strains expressing one of the seven ERF TF candidate genes (*WRI5A*, *WRI5B*, *WRI5C*, *460730*, *15867*, *25005*, *21492*) or *RAM1*. Resulting matings were plated on SD-media (lacking HIS/URA/LEU) with increasing levels of 3-AT (0 mM – 120 mM). Baseline levels of 3-AT concentrations were chosen according to the determined autoactivity levels (Table 43). Positive interactions (indicated by yeast colonies growing on higher 3-AT levels as the autoactivity baseline level) were framed in dark green. Colony lift colorimetric assay for  $\beta$ -galactosidase activity (Fuxman Bass et al., 2016a, 2016b) was used for further evaluation of potential interactions. Blue staining in the colorimetric assay indicates autoactivity, whereas white colonies indicate no autoactivity.

The promoter of *pSTR* is targeted by *WRI5A*, *WRI5B* and *WRI5C*, although *WRI5B* reveals the weakest interaction, not showing blueish staining in the colony lift colorimetric assay for  $\beta$ -galactosidase activity. In contrast to this, *pKASII* seems to be targeted by *WRI5A*, *460730*, *15867* and *25005*, but not by *WRI5B* and *WRI5C* (Table 45). Since the *pKASII*-containing bait strain tolerates relatively high 3-AT concentration level, thus showing strong auto activity, results of all the matings with this bait must be carefully compared to each other. Due to growth on media containing the highest 3-AT concentration level (120 mM) and the bluish staining of colonies, displayed in the  $\beta$ -galactosidase activity assay, yeast strains expressing the TFs *WRI5A*, *15867* and *25005* nevertheless show convincing interactions with *pKASII*-containing bait strains. Although matings of *460730*-expressing prey strains with this bait strain only grow on SD-media (lacking HIS, URA and LEU) up to a maximum of 80 mM 3-AT, the bluish staining of the colonies in the colorimetric assay indicates that interaction between *460730* and *pKASII* takes place.

The yeast strain containing a *pFatM* integration did not show any interaction with neither an *ERF* TF gene expressing prey strains nor the strain expressing *RAM1*, indicating a regulation of the promoter by other TFs.

Nevertheless, matings of *pMWR:pKASII*-containing bait strains support the ideas that besides *WRI5A*, *WRI5B* and *WRI5C* there might be more ERF TFs, namely *460730*, *15867* or *25005* regulating AM-dependent FA biosynthesis. Comparing the interactors targeting *pSTR* to the ones targeting *pKASII*, this matrix also reveals those structural genes belonging to the same pathway are probably regulated individually (Table 45).

**Table 45: Promoters of *STR* and *KASII* are regulated by different ERF TFs via DNA-protein interaction.** Yeast bait strains *pMWR:pSTR*, *pMWR:FatM* and *pMWR:pKASII* are listed in the first column, whereas prey strains expressing *WRI5A*, *WRI5B*, *WRI5C*, *460730*, *15867* and *25005* are listed in the table's first line. Positive interactions are marked in green, light green indicates weaker interactions whereas white fields indicate no interaction.

	<b>WRI5A</b>	<b>WRI5B</b>	<b>WRI5C</b>	<b>460730</b>	<b>15867</b>	<b>25005</b>
<b><i>pSTR</i></b>						
<b><i>pFatM</i></b>						
<b><i>pKASII</i></b>						

### **In Y2H studies, ERF TFs interact with either NF-Y subunits or RAM1**

Due to the results of the Y1H and RNAi studies described in the previous chapters, seven ERF TF regulate each other's genes expression as well as structural genes related to AM-dependent FA biosynthesis. These results reveal first insights into a complex regulatory network of TFs mediating FA biosynthesis in AM.

An additional central regulator of this FA biosynthesis identified in previous studies is the GRAS TF RAM1 (Jiang et al., 2018; Luginbuehl et al., 2017).

Since RAM1 is known to heterodimerize with other GRAS TFs like DIP1, RAD1 and NSP2 in order to regulate AM in different plant species including *O. sativa*, *L. japonicus* and *M. truncatula*, it might also interact with ERF TFs on a protein-protein level, mediating regulation of downstream promoters (Gobbato et al., 2012; Xue et al., 2015). This interaction would not be surprising, since TFs of the AP2/ERF family are known to interact with members of the GRAS TF family to regulate different processes such as wound defence in *A. thaliana* (Heyman et al., 2016, 2018; Son et al., 2012).

Not only members of the GRAS TF family, also members of the NF-Y family of TFs are known to interact with AP2/ERF TFs (Bai et al., 2016; Romier et al., 2003; Sun et al., 2014; Zhiguo et al., 2018). As described in these studies, the three NF-Y subunits hereby build a heterotetramer with AP2/ERF TFs to e.g., regulate endosperm development in *O. sativa*. To solve the question, whether ERF TFs are able to interact with members of the NF-Y or the GRAS TF family to potentially regulate FA biosynthesis or other processes during AM, Y2H approaches were performed.

The question, if seven ERF TF might interact with each other on a protein-protein level could not be solved, due to the fact that ERF TFs did not work when cloned as prey yeast strains. This could be explained by the AD added to the ERF TF prey constructs, which differs from the BD added to the ERF TF bait constructs. The two domains are structurally different, and the AD of the prey constructs might hinder the proper protein folding the ERF TFs.

### **Bait strains expressing the proteins RAM1, 460730, 15867 and 21492 display autoactivation**

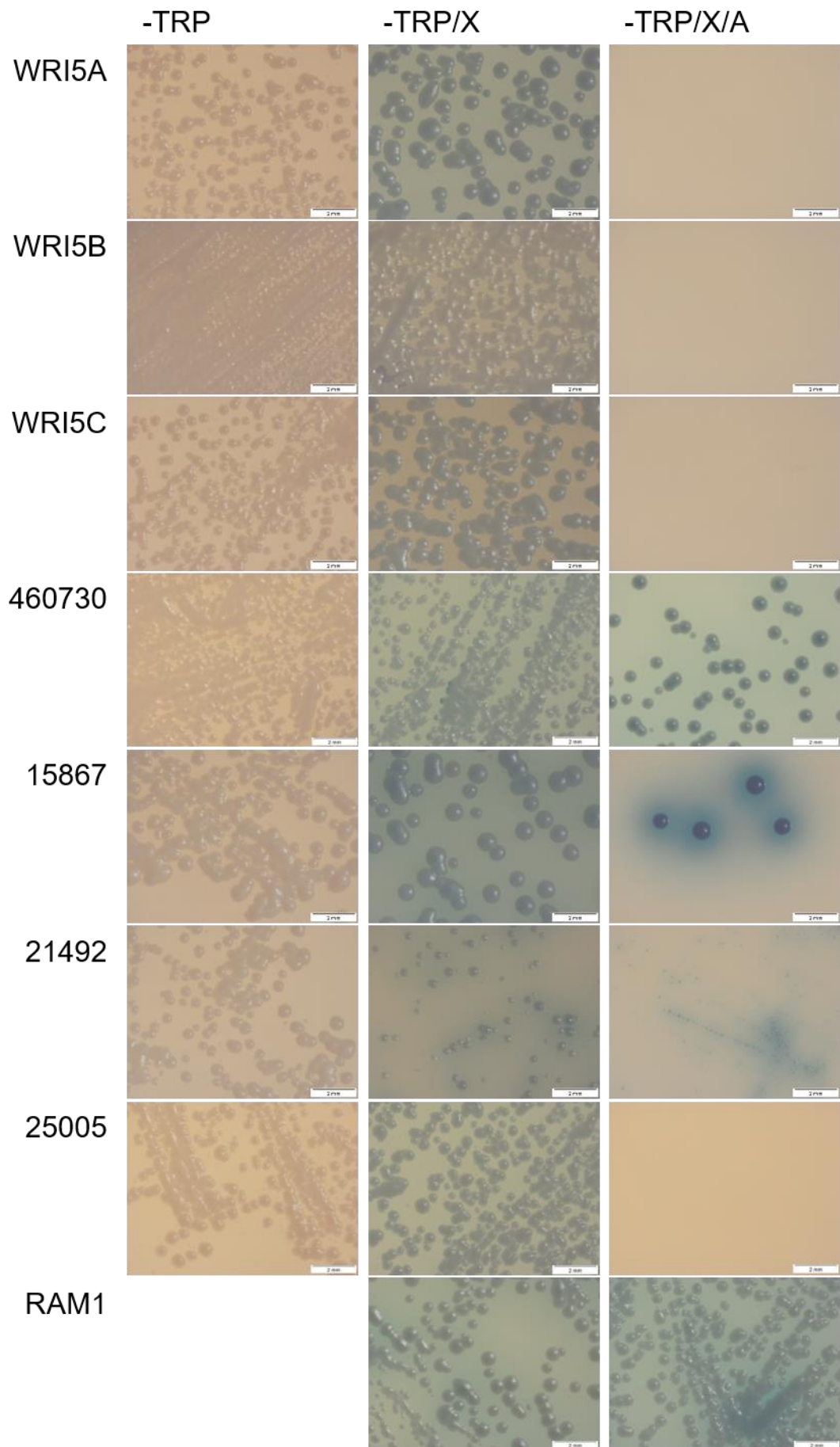
To identify interaction partners of the seven ERF TF candidates, the coding sequence (CDS) of the seven *ERF* TF genes was amplified and cloned into bait and prey vectors (Table 14). Bait and prey constructs were transformed in two different yeast strains (Table 4).

The Y2H approach is based on the principle that each protein is fused to a domain of the GALACTOSIDASE4 TRANSCRIPTIONAL ACTIVATOR (GAL4), the prey interactor to the ACTIVATION DOMAIN (AD) and the bait interactor to the BINDING Domain (BD) (Fields & Song, 1989; Kew & Douglas, 1976). Protein-protein interaction of bait and prey in transgenic

## Results

---

yeast cells results in an expression of marker genes like AA auxotrophy, galactosidase activity and resistance against fungicides such as aureobasidin (A). The yeast prey strains used in this approach are the same as in the Y1H experiments, expressing LEU to compensate leucine auxotrophy in yeast. The yeast bait strains express Tryptophan (TRP) to overcome TRP auxotrophy. Auto activity of the Y2H bait strains must be tested prior to Y2H mating experiments, using increasing levels of stringency (Figure 32). The three stringency levels are thereby SD media (lacking TRP each) as well as testing for  $\alpha$ -galactosidase activity (X) on the last two and for aureobasidin (A) on the highest stringency level. They are therefore referred to as TRP, TRP/X, and TRP/X/A.



## Results

---

**Figure 32: Autoactivity tests of Y2H on increasing stringency media reveals autoactivity of 460730-, 15867- and 21492- bait strains.** Yeast bait strains containing plasmids expressing either of the seven *ERF* TF candidate genes or *RAM1* were tested on SD-media lacking TRP (-TRP), -TRP SD-media containing X- $\alpha$ -Gal (-TRP/X) and -TRP SD media containing X- $\alpha$ -Gal and the yeast and fungi targeting biocide Aureobasidin (-TRP/X/A). Autoactivity of bait strains is indicated via blue colonies and growth on the Aureobasidin-containing media plates. Yeast bait strains expressing the proteins WRI5A, WRI5B, WRI5C, 460730, 15867, 21492, 25005 or *RAM1* were tested.

Due to the performed autoactivity tests for the bait strains, only bait constructs expressing the proteins WRI5A, WRI5B, WRI5C or 25005 could be used. The other tested bait constructs showed high levels of autoactivity, growing on the SD-media lacking TRP and even on media containing aureobasidin (-TRP/X/A). Consequently, they should therefore not be used in further Y2H approaches.

### **ERF TFs interact with AM-upregulated members of the NF-Y TFs**

To target the question, whether ERF TFs interact with NF-Ys on a protein-protein level, the remaining ERF bait constructs expressing WRI5A, WRI5B, WRI5C and 25005 were mated with prey constructs expressing NF-Y subunit A, B and C proteins, being upregulated during AM (Hogekamp et al., 2011; Hogekamp & Küster, 2013; Krüger, LUH, unpublished data) (NF-Y constructs were cloned and transformed by Steven Krüger (Krüger, LUH, unpublished data); all Y2H constructs and their contributors used in this approach are listed in Table 14 and Table 16). Interestingly, NF-Y A and NF-Y B subunits showed interactions with ERF TFs in these experiments (Figure 33).



## Results

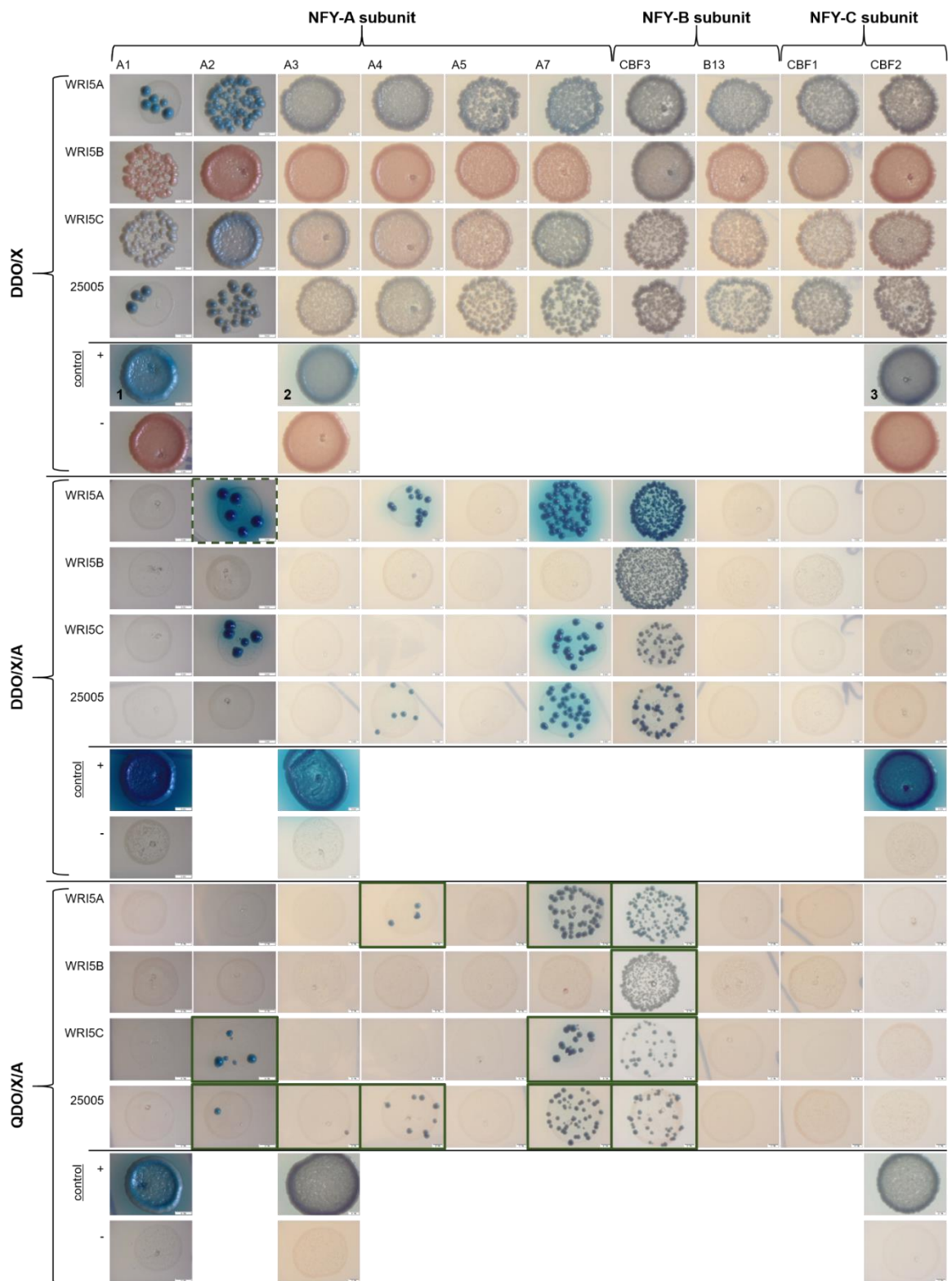


**Figure 33: WRI5A, WRI5C and 25005 interact with NF-YA and NF-YB subunits on a protein-protein level.** Yeast strains expressing the proteins WRI5A, WRI5B, WRI5C and 25005 were mated with prey strains expressing TFs NF-YA (A2, A3, A4, A5, A7), NF-YB (CBF3) and NF-YC (CBF1, CBF2) subunits and plated on increasing stringency media (top to bottom) Double Dropout (DDO/X, lacking TRP and LEU and containing  $\alpha$ -galactosidase), DDO/X/A and finally Quadruple Dropout (QDO/X/A, lacking ADE and HIS besides TRP and LEU and containing  $\alpha$ -galactosidase and aureobasidin). Positive and negative interaction controls 1 (for A2 and A3), 2 (for A4, A5, A7, B13, CBF1) and 3 (for CBF3 and CBF2) are used as a reference for the strength of interaction and as stringency controls to avoid using plates with insufficient levels of aureobasidin. Positive interaction between bait and prey strains is marked via growth of blue yeast colonies on DDO/X/A and, even better, on

## Results

QDO/X/A media. Potential interaction on QDO/X/A media are highlighted via images framed in dark green (in case of the A2/WRI5A with dashed lines).

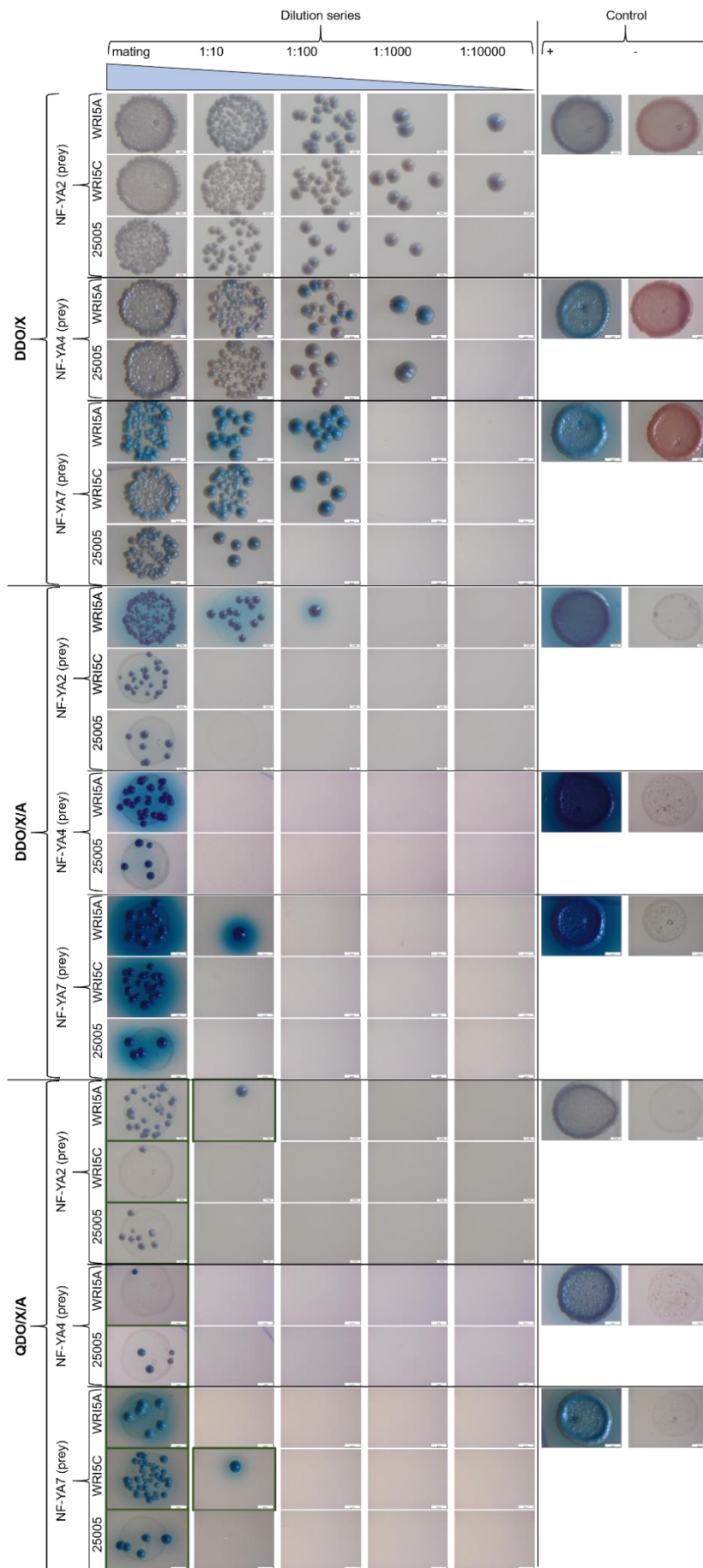
In a first Y2H approach, NF-Y A (A2, A3, A4 and A7) and NF-Y B subunits (NF-Y B7 = CBF3) CBF3 interacted with WRI5A, WRI5B, WRI5C and 25005 (Table 46). In the matrix shown, NF-Y subunits were cloned as preys, whereas ERF TFs were cloned as bait constructs. Interestingly, the reverse approach using ERF TF prey strains and NF-Y bait strains did not show positive interactions on the highest stringency level, but only on DDO/X/A plates (data not shown here, preparation and analyzation of the matrix was performed by Steven Krüger, LUH, unpublished data). These results could be due to the fusion of either an AD or a BD to the ERF TFs, thereby hindering the proper folding of the analysed proteins.

**Table 46: ERF TFs interact with NF-Y A and NF-Y B subunits in the initial Y2H approach.** Results of the initial Y2H approach are listed in this table, positive interactions are marked in green. The NF-Y A2 WRI5A interaction is also included in this table because the mating grew on DDO/X/A (Figure 33).

	<b>WRI5A</b>	<b>WRI5B</b>	<b>WRI5C</b>	<b>25005</b>
<b>NF-Y A2</b>				
<b>NF-Y A3</b>				
<b>NF-Y A4</b>				
<b>NF-Y A7</b>				
<b>CBF3 (NF-Y B7)</b>				

To verify the results of the obtained positive interactions and to evaluate the strength of each interaction, Y2H results were tested in a dilution series on increasing stringency media (Figure 34 and Figure 35). For each interaction, two independent dilution series were tested, to obtain at least three repetitions in total for each positive interaction.

# Results



## Results

---

**Figure 34: WRI5A, WRI5C and 25005 interact with NF-YA subunits A2, A4, A7.** Yeast strains expressing the bait proteins WRI5A, WRI5C and 25005 were mated with prey strains expressing NF-YA (A2, A4, A7) subunits and were diluted (mating, 1:10, 1:100, 1:1000, 1:10000) and plated on increasing stringency media (top to bottom). Double Dropout (DDO/X, lacking TRP and LEU), DDO/X/A and finally Quadruple Dropout (QDO/X/A, lacking ADE and HIS besides TRP and LEU). Positive and negative interaction controls are used as a reference for the strength of interaction and as stringency controls to avoid using plates with insufficient levels of aureobasidin (A). Positive interaction between bait and prey strains is marked via growth of blue yeast colonies on DDO/X/A and, even better, on QDO/X/A media. Potential interaction on QDO/X/A media are highlighted via dark green framed images.

Interactions between the ERF TFs WRI5A, WRI5B, WRI5C or 25005 and either NF-Y A2, NF-Y A4 or NF-Y A7 could be verified in both dilution series, even growing on the highest stringency plate QDO/X/A (Figure 34). In contrast, the dilution series of NF-Y A3 interacting with 25005 turned out to be negative (data not shown) and was therefore excluded from further studies. The CBF3 interaction with ERF TFs were equally tested in two independent dilution series (Figure 35).

## Results

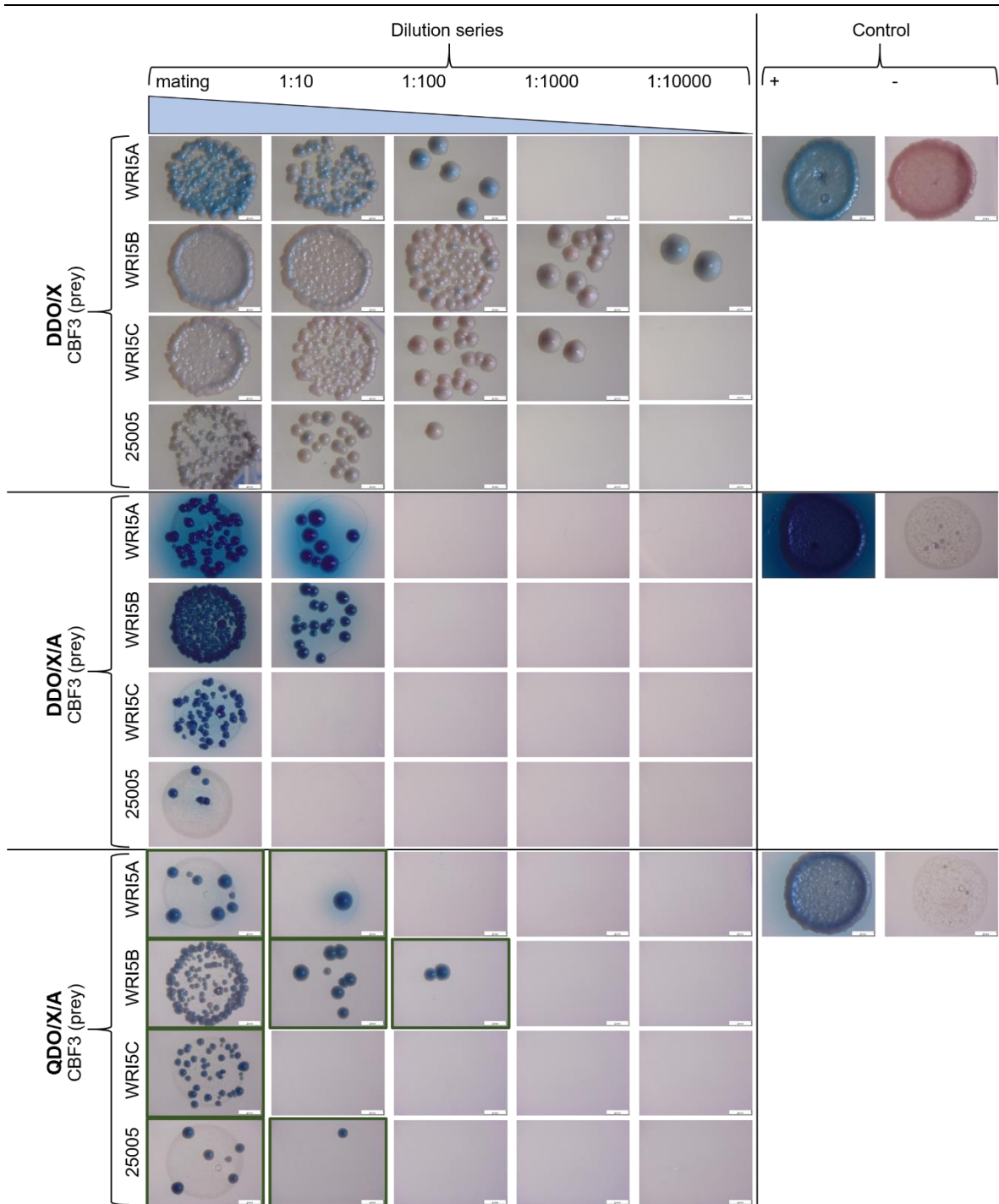


**Figure 35: WRI5A, WRI5B, WRI5C and 25005 interact with the NF-YB subunit CBF3 (NF-Y B7).** Yeast strains expressing the TFs WRI5A, WRI5B, WRI5C and 25005 were mated with prey strains expressing NF-YB subunit CBF3 and were diluted (mating, 1:10, 1:100, 1:1000, 1:10000) and plated on increasing stringency media (top to bottom). Double Dropout (DDO/X, lacking TRP and LEU), DDO/X/A and finally Quadruple Dropout (QDO/X/A, lacking ADE and HIS besides TRP and LEU). Positive and negative interaction controls are used as a reference for the strength of interaction and as stringency controls to avoid using plates with insufficient levels of aureobasidin. Positive interaction between bait and prey strains is marked via growth of blue yeast colonies on DDO/X/A and, even stronger, on QDO/X/A media. Potential interactions on QDO/X/A media are highlighted via dark green framed images.

The positive interaction between either of the ERF TFs and CBF3 could be repeated in the two independent dilution series, although mating efficiencies varied. To further verify the

## Results

positive protein-protein interactions between ERF TFs and either NF-Y A or NF-Y B subunits, a Bimolecular Fluorescence Complementation (BiFC) approach (Walter et al., 2004) was prepared (NF-Y A and B subunits were cloned and transformed by Steven Krüger, LUH, unpublished data). Although interactions between ERF TFs and NF-Y A and B subunits could be demonstrated convincingly in the Y2H approach (Figure 33, Figure 34, Figure 35, Table 47), this approach did not lead to the identification of positive interactions (data not shown here).

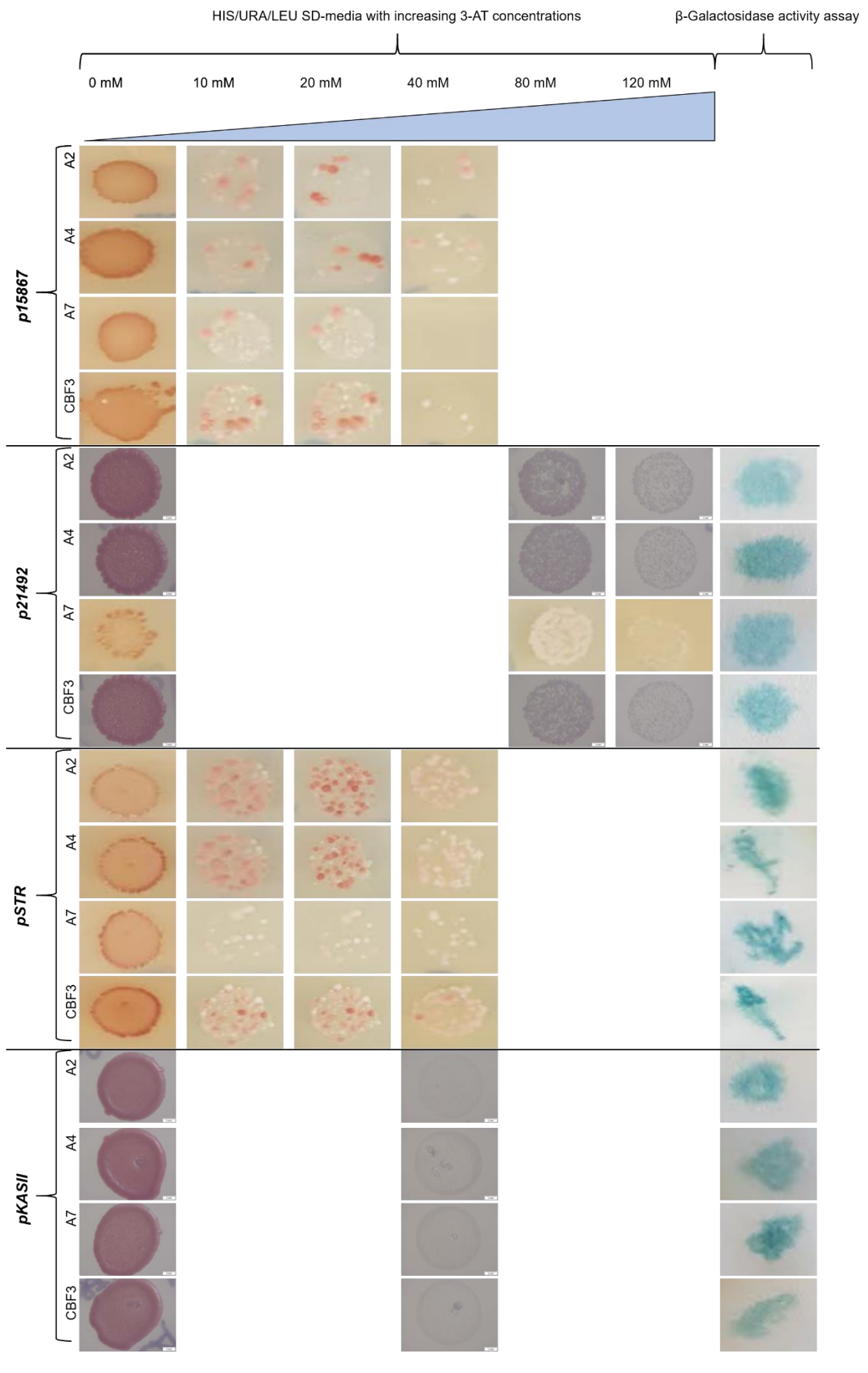
**Table 47: Refined table of ERF TFs interacting with NF-Y A and NF-Y B subunits in a Y2H approach.** Results of the initial Y2H approach are listed in this table, positive interactions are marked in green.

	<b>WRI5A</b>	<b>WRI5B</b>	<b>WRI5C</b>	<b>25005</b>
<b>NF-Y A2</b>				
<b>NF-Y A4</b>				
<b>NF-Y A7</b>				
<b>CBF3</b>				

### **AM-upregulated NF-Y subunits A and B are involved in the regulation of FA biosynthesis**

As described in the introduction, ERF TFs are known to build heterotetrameric interactions with NF-Y A, B and C in order to regulate downstream targets (Bai et al., 2016; Laloum et al., 2013; Sun et al., 2014; Zhiguo et al., 2018), the NF-Y interactors identified in the Y2H approach in the chapter before (namely NF-Y A2, NF-Y A4, NF-Y A7 and CBF3) were tested in a Y1H approach using the available Y1H bait strains that were already tested concerning their auto activity levels (Table 43). In these experiments, Y1H approaches showed positive results for some Y1H interactions (Figure 36).

# Results



## Results

**Figure 36: NF-YA and NF-YB TFs also bind to the promoters of *ERF* TF genes and structural genes of AM-dependent FA biosynthesis.** Yeast bait strains containing genome integrations of either *pMWR:p15867*, *pMWR:p21492*, *pMWR:pSTR* or *pMWR:pKASII* were mated with yeast prey strains expressing the TFs NF-YA2, NF-YA4, NF-YA7 or CBF3. Resulting matings were plated on SD-media (lacking HIS/URA/LEU) with increasing levels of 3-AT (0 mM – 120 mM). Baseline levels of 3-AT concentrations were chosen in accordance with the determined autoactivity levels (Table 43). Positive interactions were framed in dark green. Colony lift colorimetric assay for  $\beta$ -Galactosidase activity (Fuxman Bass et al., 2016a, 2016b) was used for further evaluation of potential interactions. Blue staining in the colorimetric assay indicates autoactivity, whereas white colonies indicate no autoactivity. Positive interactions were at least repeated once to verify positive interactions. Due to time constraints, colony lift assays were not performed for each interaction tested.

Positive interactions between prey strains expressing NF-Y subunit A and B and bait strains with either *pSTR*, *p15867* or *p21492* could be observed (Table 48). Interestingly, these promoters are also targets of ERF TFs and RAM1 (Table 44 and Table 45). The promoter of *KASII* did not show interactions with neither of the tested NF-Y subunits, but revealed blueish staining in the colony lift assay, probably pointing to autoactivity of Y1H bait strains containing *pKASII*. This allows to conclude that both ERF TF and NF-Y TFs can bind to the same promoters related either to AM-dependent FA biosynthesis genes or the group of *ERF* TF genes.

**Table 48: NF-Y A and B subunits that interact with ERF TFs on a protein-protein level also interact with their potential promoter targets in a Y1H approach.** Positive interactions are marked in green. Darker green colour indicates stronger interactions.

	<i>p15867</i>	<i>p21492</i>	<i>pSTR</i>
<b>NF-Y A2</b>			
<b>NF-Y A4</b>			
<b>NF-Y A7</b>			
<b>CBF3 (NF-Y B7)</b>			

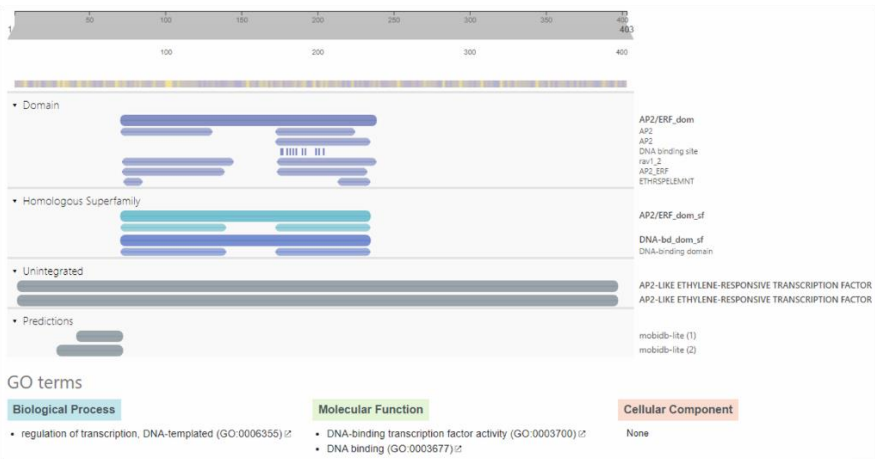
### **ERF TFs do not interact with NF-Y TFs via known protein interacting domains**

Since ERF TFs can interact on a protein-protein level, the CDS of WRI5A, WRI5B, WRI5C and 25005 was translated into an AA sequence and analysed using Interpro-Scan to identify potential protein interaction domains (EMBL-EBI, InterPro, used in December 2020, <https://www.ebi.ac.uk/interpro/search/sequence/>) (Figure 37). Interestingly, sequence analysis of all CDS only revealed AP2 DNA-binding domains in all four sequences, but no protein-protein interaction domains. This leads to the question, how and via what region the four ERF TF proteins interact with e.g. members of the NF-Y A and B subunits.



# Results

WIR5A



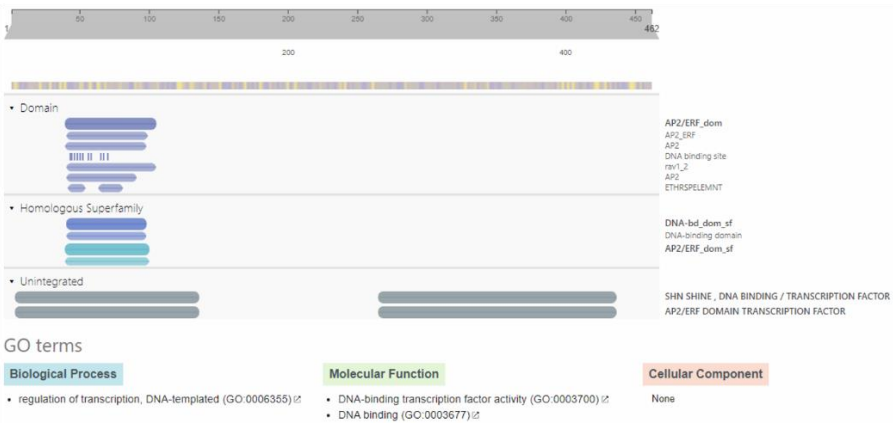
WIR5B



WIR5C



25005



## Results

**Figure 37: Sequence analysis of WRI5A, WRI5B, WRI5C and 25005 revealed AP2 binding domains, but did not show any domains mediating protein-protein interaction.** Sequence scans of the AA sequence of the CDS of WRI5A, WRI5B, WRI5C and 25005 linked the four proteins to the family of AP2 ERF TFs via their two (WRI5A, WRI5B, WRI5C) or one (25005) AP2 binding domain mediating DNA-binding (shown in blue and purple colour). The sequence scan was performed using Interproscan (EMBL-EBI, InterPro, used in December 2020 <https://www.ebi.ac.uk/interpro/search/sequence/>).

### RAM1 forms a heterodimer with either WRI5A or WRI5C in Y2H and BiFC approaches

Since GRAS TFs are shown to heterodimerize and interact with ERF TFs (Heyman et al., 2016, 2018; Son et al., 2012), also described in the introduction chapter, ERF TF bait strains were tested against AM-upregulated ERF TFs in an Y2H approach (Figure 38). GRAS TF prey strains used in this Y2H matrix were cloned by Rico Hartmann (Hartmann et al., 2019). Information about the cloned constructs and the contributors are provided in the Material and Methods section (Table 14 and Table 16).

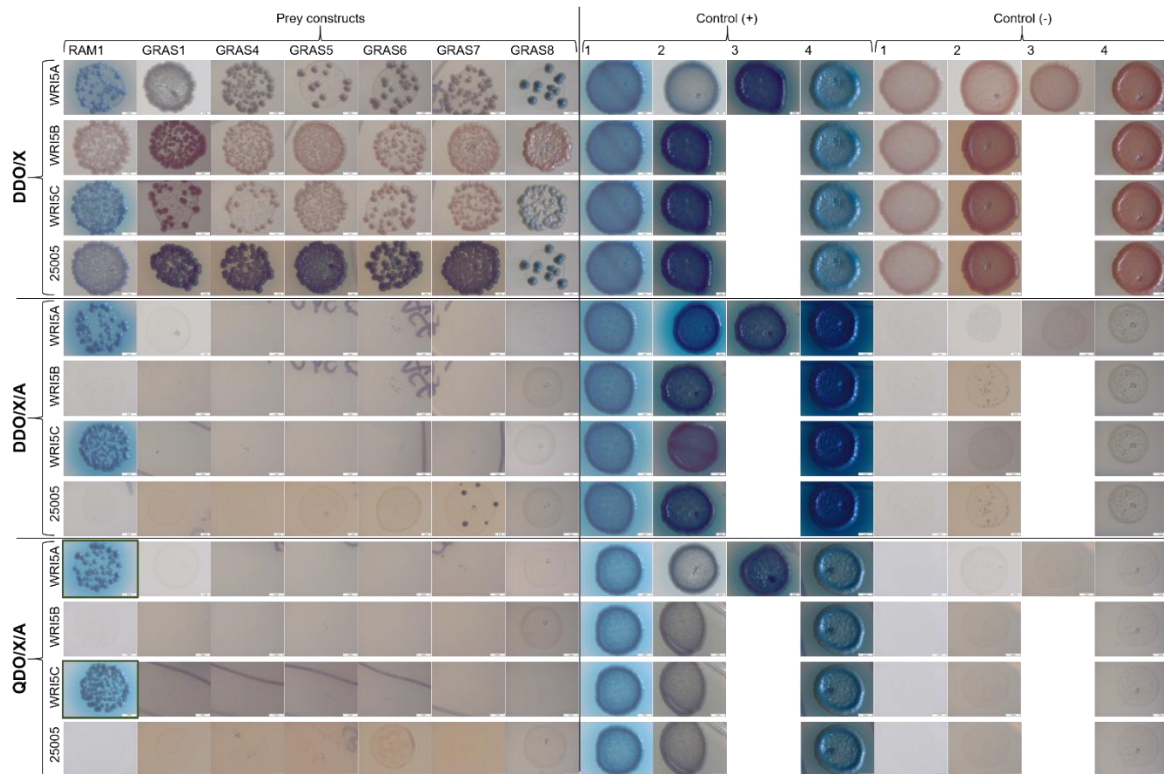


**Figure 38: WRI5A and WRI5C each build a heterodimer with RAM1.** Yeast strains expressing the TFs WRI5A, WRI5B, WRI5C and 25005 were mated with prey strains expressing GRAS TFs (RAM1, GRAS1, GRAS4, GRAS5, GRAS6, GRAS7, GRAS8) and plated on increasing stringency media (top to bottom): Double Dropout (DDO/X, lacking TRP and LEU), DDO/X/A and finally Quadruple Dropout (QDO/X/A, lacking ADE and HIS besides TRP and LEU). Positive and negative interaction controls 1 (for RAM1), 2 (for GRAS1-7; except in the matings with WRI5A bait: GRAS1) 3 (GRAS4-7 in the matings with WRI5A bait) and 4 (for GRAS8) are used as a reference for the strength of interaction and as stringency controls to avoid using plates with insufficient levels of aureobasidin. Positive interaction between bait and prey strains is marked via growth of blue yeast colonies on DDO/X/A and, even better, on QDO/X/A media. Potential interaction on QDO/X/A media are highlighted via dark green framed images.

In a first Y2H approach, RAM1, cloned as prey strain, interacted with WRI5A and WRI5C. No further of the here tested GRAS TFs interacted with WRI5A, WRI5B, WRI5C or 25005. To verify the results of the obtained positive interactions and furthermore evaluate the strength of each interaction, Y2H results were tested in a dilution series on increasing

## Results

stringency media (Figure 39). For each interaction, two independent dilution series were tested to obtain at least three repetitions in total for each positive interaction.

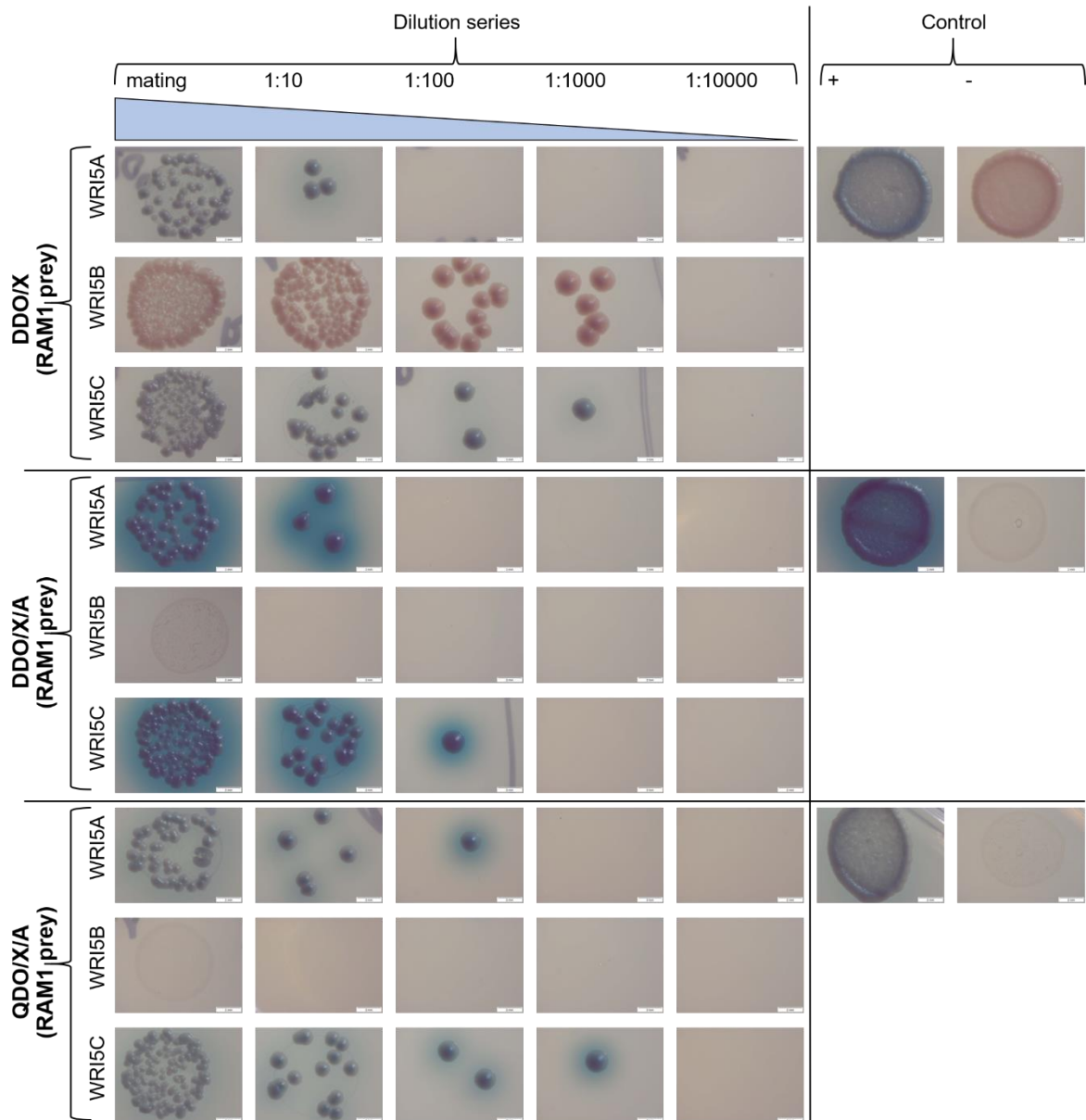


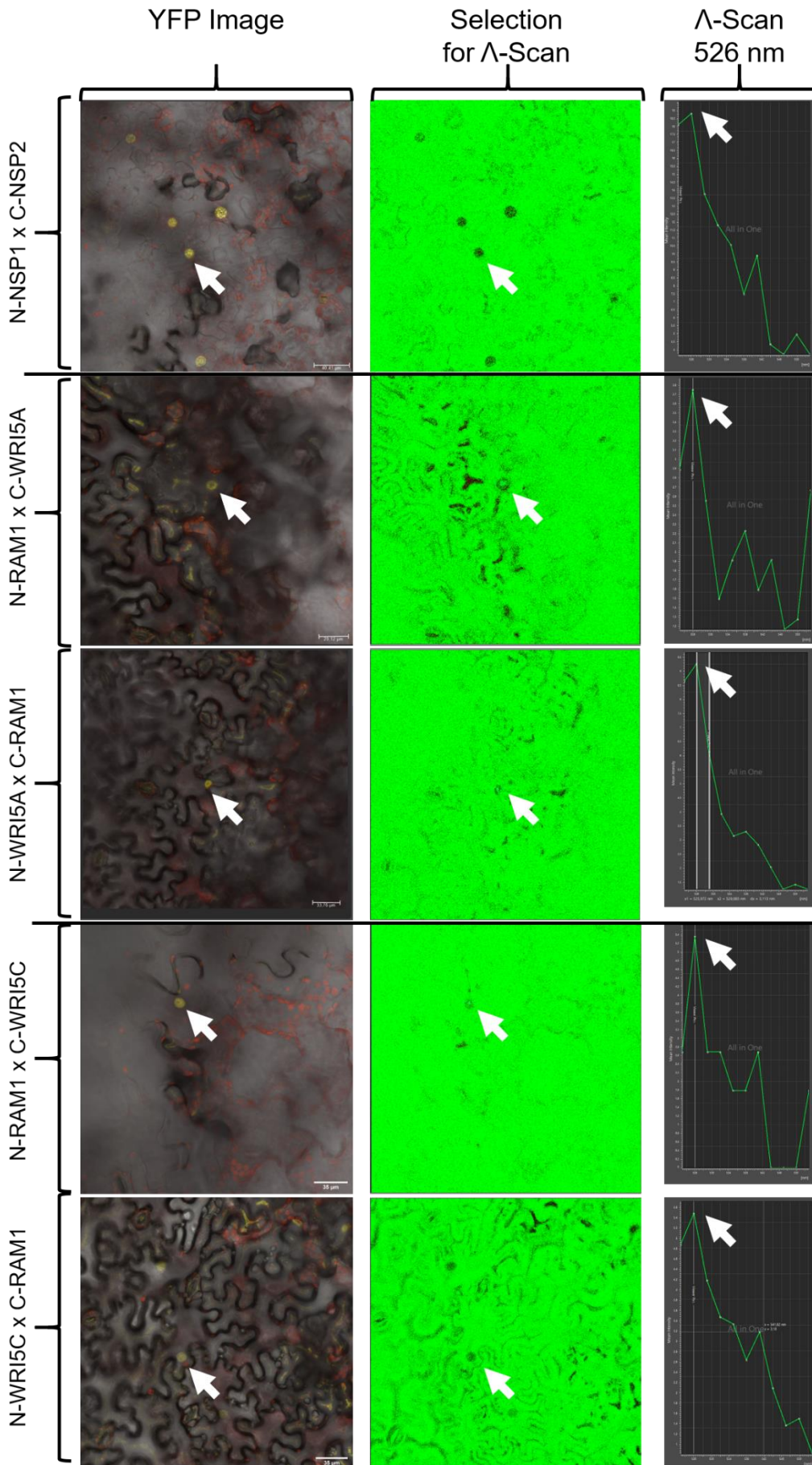
**Figure 39: RAM1 heterodimerizes with WRI5A or WRI5C.** Yeast strains expressing the TFs WRI5A, WRI5B and WRI5C were mated with prey strains expressing RAM1 and were diluted (mating, 1:10, 1:100, 1:1000, 1:10000) and plated on increasing stringency media (top to bottom). Double Dropout (DDO/X, lacking TRP and LEU), DDO/X/A and finally Quadruple Dropout (QDO/X/A, lacking ADE and HIS besides TRP and LEU). Positive and negative interaction controls are used as a reference for the strength of interaction and as stringency controls to avoid using plates with insufficient levels of aureobasidin. Positive interaction between bait and prey strains is marked via growth of blue yeast colonies on DDO/X/A and, even better, on QDO/X/A media. Positive interactions were tested at least two times in independent experiments in a dilution series.

The positive interaction of RAM1 with either WRI5A or WRI5C could be verified in the Y2H dilution series (Table 49). To further verify this positive interaction *in planta*, BiFC (Walter et al., 2004) experiments were performed (Figure 40). Hereby, plasmids containing either a N-terminal (*pSPYNE*) or a C-terminal (*pSPYCE*) fusion of the protein of interest were constructed. Subsequently, *A. tumefaciens* was transformed with the proteins of interest. *A.*

## Results

---

*tumefaciens* strains expressing genes encoding the proteins of interest were mixed and *N. benthamiana* leaves were transfected with this mixture. Hereby, it is important that the mixture contains a C-terminally and an N-terminally fused protein to test their interaction *in planta*.



## Results

**Figure 40: Interactions of RAM1 with either WRI5A or WRI5C were confirmed in a BiFC experiment.** *A. tumefaciens* strains containing either *pSPYCE:WRI5A* (C-WRI5A, second line), *pSPYNE:WRI5A* (N-WRI5A, third line), *pSPYCE:WRI5C* (C-WRI5C, fourth line) or *pSPYNE:WRI5C* (N-WRI5C, fifth line) were either tested against *pSPYNE:RAM1* (N-RAM1) or *pSPYCE:RAM1* (C-RAM1), respectively. *pSPYNE:NSP1* (N-NSP1) versus *pSPYCE:NSP2* (C-NSP2, first line) was used as a positive control to monitor handling and furthermore served as a reference for observed interactions. First column always shows a positive interaction in the cellular environment. Images were taken with the corresponding fluorescence channel. White arrows mark positive interactions in the nuclei. The second column was used to choose potential positive interactions further tested in the  $\lambda$ -Scan (selected nuclei tested in  $\lambda$ -Scan are marked by white arrows). Third column shows the corresponding  $\lambda$ -Scan. These columns prove that the showed fluorescence belongs to YFP having its extinction at a 526 nm (white arrows highlight the YFP maximum at 526 nm). All positive interactions were repeated at least once. Constructs containing *RAM1* were provided by Arne Petersen (A. Petersen, unpublished data, LUH).

The performed BiFC experiments confirmed the results of the Y2H approaches. The positive interaction of RAM1 with either WRI5A or WRI5C could hereby be observed with combinations using a C-terminally fused RAM1 as well as a N-terminal fused RAM1 with the corresponding WRI5A or WRI5C constructs. Since RAM1, WRI5A and WRI5C are all TF located in the nucleus, positive interactions could be observed via yellow-fluorescent nuclei. The interaction data suggest that RAM1 heterodimerizes with WRI5A and WRI5C to regulate potential downstream targets such as FA biosynthesis genes, which will be further analyzed in the discussion. Interestingly, RAM1 exclusively interacts with WRI5A and WRI5C, but not with WRI5B (Table 49), suggesting a differing regulatory role of WRI5B, which will be discussed in the following chapters.

**Table 49: RAM1 interacts with WRI5A or WRI5C, but not with WRI5B on a protein-protein level.** Positive interactions are marked in green. Table summarizes the results of the Y2H and the BiFC approaches.

	WRI5A	WRI5B	WRI5C
RAM1			

## Discussion

### **Seven ERF TFs play a role in the regulatory network of AM-dependent FA biosynthesis**

Formation and establishment of AM between *M. truncatula* and *R. irregularis* is directed by a core set of genes that regulate transcriptional reprogramming of the root cortex cells during the process of symbiosis (Czaja et al., 2012; C. Hogekamp et al., 2011; Hogekamp & Küster, 2013; Hohnjec et al., 2015). This transcriptional reprogramming is regulated by TFs like ERF TFs, GRAS TFs, and NF-Y TFs. One of the major regulators for AM in *M. truncatula* is the GRAS TF RAM1, regulating processes crucial for AM like FA biosynthesis and phosphate uptake, via binding to its target promoters (Gobbato et al., 2012; Jiang et al., 2018; Luginbuehl et al., 2017; Park et al., 2015). RAM1 is thought to bind as a heterodimer, establishing protein-protein interactions with e.g. other GRAS TFs to regulate AM-related gene expression (Gobbato et al., 2012; Xue et al., 2015).

Not only GRAS TFs, but also ERF TFs are important regulators of the AM symbiosis in many different organism like *L. japonicus* or *M. truncatula* (Jiang et al., 2018; Luginbuehl et al., 2017; Xue et al., 2018). Interestingly, ERF TFs are not only linked to the process of AM-dependent FA biosynthesis, but also to the AM-dependent phosphate uptake in *L. japonicus* as well as in *M. truncatula*. Regulation of these processes via ERF TFs in *M. truncatula* was first discovered by studying three specific ERF TFs, namely WRI5A, WRI5B and WRI5C. Due to the RAM1-dependent expression of the corresponding genes and their important role for the C16-FA (precursor of production TAG), shown in tobacco leaves, they were primarily linked to the process of AM-dependent FA biosynthesis (Jiang et al., 2018; Luginbuehl et al., 2017). Besides the proposed regulation via RAM1 and the WRI5 TFs, the exact regulatory network of AM-dependent FA biosynthesis and AM-dependent phosphate in *M. truncatula* is still poorly understood.

In this thesis, seven AM upregulated *ERF* TF genes (*WRI5A*, *WRI5B*, *WRI5C*, *460730*, *15867*, *21492* and *25005*) were therefore analysed to gain deeper understanding of the exact regulatory roles of the encoded ERF TFs during *M. truncatula* AM symbiosis (Table 40). To obtain detailed insights into the regulatory network of AM mediated by ERF TFs, different experimental approaches, including *in situ* expression analysis, RNAi-knockdown experiments and interaction studies were performed.

---

**Expression of AM-upregulated ERF TF genes is dependent on a functioning arbuscule**

Phosphate homeostasis and the resulting Pi nourishment of the plant via interaction with *R. irregularis* is pivotal for the maintenance of the AM symbiosis (Javot et al., 2007). Expression of the AM-dependent phosphate transporter gene *MtPT4*, crucial for Pi supply during AM, seems to be dependent on RAM1, indicating the central role of RAM1 for a functioning arbuscule (Luginbuehl et al., 2017; Park et al., 2015). To understand gene expression of the seven ERF TFs selected for this thesis, reporter gene fusion constructs using the  $\beta$ -glucuronidase gene were analysed in transgenic *M. truncatula* roots. All seven ERF TF genes showed an AM-specific upregulation in *R. irregularis* colonized *M. truncatula* roots (Figure 13, Figure 14). More precisely, the expression of ERF TF genes could be linked to a functioning arbuscule, shown by an absent expression in *ram1-1* and *pt4-2* mutant lines, lacking the GRAS TF RAM1 and the AM-specific phosphate transporter PT4, respectively (Figure 15). The observed expression of the seven ERF candidate genes is widely mirrored in RNAseq data, measuring the expression of ERF TF genes in either *M. truncatula* mycorrhized wild type roots or mycorrhized *ram1-1* versus mock-inoculated control roots (Luginbuehl et al., 2017) (Figure 11, Figure 16).

Strikingly, the only exceptions are the 15867 and 21492 genes, behaving differently when comparing the RNAseq data with the results from promoter analysis (Luginbuehl et al., 2017). These two genes still show expression in the myc- RNAseq data (Figure 11), but expression is decreased compared to the Myc+ background. Furthermore, ERF TF genes 15867 and 21492 show transcription over time in the *ram1-1* background (Figure 16). However, transcription of 15867 and 21492 is still decreased in the myc- background compared to the myc+ background as well as in the *ram1-1* background. These findings underline the idea that all seven ERF TFs analysed in this thesis are dependent on a functioning arbuscule. These observations are also reflected in the promoter-*gus* studies. Interestingly, the expression pattern observed in promoter-*gus* experiments is similar for all seven ERF TF genes, revealing an arbuscule-specific expression that is dependent on MtRAM1 as well as on MtPT4 (Figure 41). The arbuscule-specific expression of *WRI5A*, *WRI5B*, *WIR5C*, *460730* and *15867* observed in this thesis is in line with findings of Luginbuehl et al., 2017. This observation points, as already mentioned, to a role in the functioning arbuscule, potentially during processes connected to nutritional exchange like the AM-dependent FA biosynthesis or the AM-dependent phosphate uptake of the plant. This conclusion is supported by the findings of recent publications in *M. truncatula* and *L. japonicus*, linking the TFs *WRI5A*, *WRI5B* and *WRI5C* or *CBX1*, respectively, to the AM-dependent processes of lipid transfer and phosphate uptake during AM (Jiang et al., 2018;



## Discussion

Liu et al., 2020; Luginbuehl et al., 2017; Xue et al., 2018). Nevertheless, the finding that seven ERF TFs might all play a regulatory role in the same AM-dependent processes suggests – at least partially – a functional redundancy. This idea is supported by results from recent publications, showing that even a triple knockdown of *WR15A*, *WR15B* and *WR15C* was not sufficient to completely block mycorrhization and arbuscule development in *M. truncatula* (Jiang et al., 2018). The idea of a functional redundancy of the seven ERF TFs will be further discussed in the upcoming chapters.

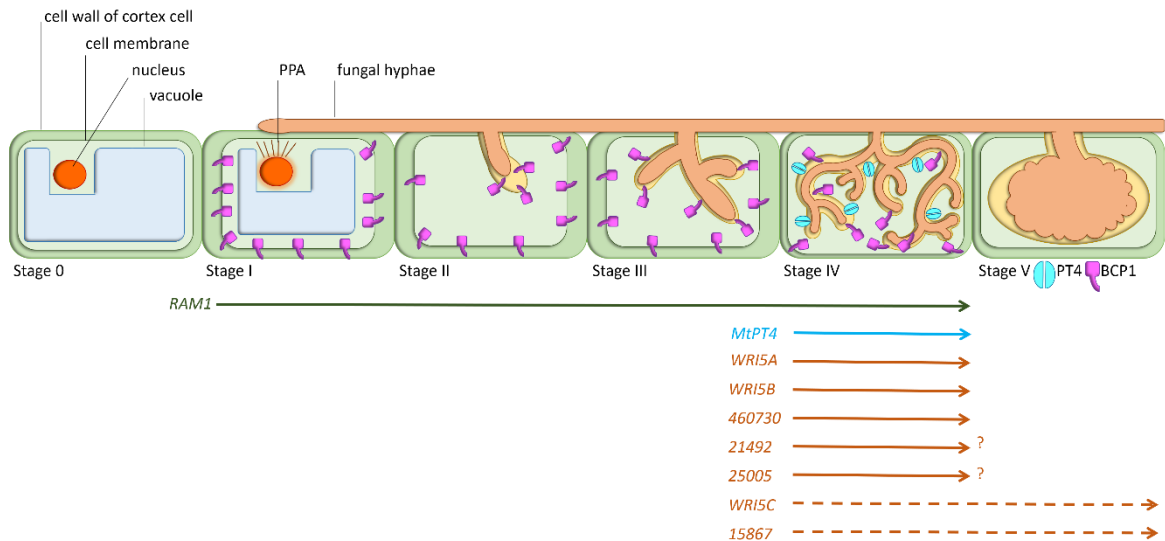


**Figure 41: Seven analysed *ERF* TF genes display a redundant expression pattern, showing a dependency on *RAM1* and *MtPT4*.** Due to the results of the reporter gene analysis, the encoded ERF TFs could be linked to a functioning arbuscule, underlined by the absent promoter activities in *ram1-1* and *pt4-2* mutant lines. Orange arrows indicate, where *ERF* TF genes are expressed in wild type AM roots. Orange arrows indicate the expression of *ERF* TF genes and blue arrows indicate the expression of *MtPT4*, respectively. The green arrow denotes the activity of *RAM1* from stage I to stage IV.

---

**Seven AM-upregulated TFs form regulatory networks of ERF TFs**

The observed strong expression of ERF TFs in arbusculated cells as well as a successful knockdown of *WRI5B*, resulting in truncated arbuscules, (Devers et al., 2013) led to the question whether RNAi-knockdowns of single *ERF TF* genes have an effect on mycorrhization, other *ERF TF* genes or genes of the Am-dependent FA biosynthesis. In this thesis, RNAi-knockdowns for *WRI5A*, *460730*, *15867* and *21492* could be achieved (Figure 19). Thereby, *WRI5A* displayed the strongest knockdown, showing negative effects on the expression of *MtPT4*, *GiaTub*, *RAM1*, *FatM*, *RAM2* and also on *ERF TF* genes like *WRI5B*, *460730* and *21492*. Expressional reduction of fungal marker genes, *ERF TF* and FA biosynthesis genes could also be observed in plant roots expressing *460730*-, *15867*- or *21492*-RNAi constructs albeit to a lesser extent. Contrasting to this is the finding that only slight phenotypical effects on mycorrhization could be observed (Figure 22, Figure 23, Figure 24, Figure 25). Here, the *WRI5A*-knockdown construct showed a higher amount of truncated arbuscules, whereas the *21492*-knockdown mildly reduced overall mycorrhization. Knockdown constructs of *460730* and *15867* did not show any effects on a phenotypical level.

All in all, the mild or missing effects of *WRI5A*-, *460730*-, *15867*- and *21492*-knockdowns on mycorrhization phenotypes contradict the results obtained with the *WRI5B*-knockdown reported by Devers et al. (2013).

However, results of the *WRI5B*-knockdown cannot be directly compared to the experiments performed in this thesis. First of all, the amiRNA-construct targeting *WRI5B* was driven by the mycorrhiza-specific *pMtPT4* (Devers et al., 2013; Pumplin et al., 2012). In this thesis, the general but weaker *p35S* was used. Furthermore, the leech inoculum used for mycorrhization in earlier publications differs from the mycorrhization technique used in this thesis (Devers et al., 2013). Leech inoculum allows a faster and more synchronised mycorrhization of *M. truncatula* roots, allowing an earlier harvesting time point (21 dpi) compared to the much older root systems harvested here (49 dpi – 63 dpi). In addition to this, the *WRI5B*-amiRNA construct targets the 640 bp region downstream of the genes' ATG. This region is part of the second AP2-ERF domain of *WRI5B* (Figure 37). Since the AP2 ERF domain is a highly conserved motive in the *AP2/ERF TF* gene family, a knockdown construct targeting this area could possibly downregulate expression of further *ERF TF* genes, resulting in a stronger effect on conditions redundantly regulated by these genes e.g., mycorrhization (Sakuma et al., 2002).

It is therefore more fitting to compare the results of the RNAi approach shown in this thesis to the results obtained by the constructed *WRI5A*, *WRI5B*, *WRI5C* triple knockdown (Jiang et al., 2018). Although these three regulators of AM were downregulated, the resulting

construct only revealed slight effects on total mycorrhization (20 % reduction compared to control roots), mild effects on fully developed arbuscules, and a minor increase of truncated arbuscules. The authors therefore hypothesized a redundant function of ERF TFs during AM symbiosis, which is also stated in this thesis.

Nevertheless, the observed effects on the transcription of *RAM1* as well as on structural genes of the FA biosynthesis and *PT4* point to an important role of *WRI5A*, *WRI5B*, *WRI5C*, *460730*, *15867* and *21492* during the regulation of AM symbiosis. These results could only partially be obtained in publications examining AM symbiosis in *M. truncatula* as well as in *L. japonicus* (Jiang et al., 2018; Luginbuehl et al., 2017; Xue et al., 2018). In contrast to this thesis, former publications dealing with AM symbiosis in *M. truncatula* only examined the role of *WRI5A*, *WRI5B* and *WRI5C* TFs, whereas the other four ERF TFs *460730*, *15867*, *21492* and *25005* were not studied. The presented data here on these genes however suggest an interesting addition to the regulatory tasks of ERF TFs during AM-related processes like FA biosynthesis. Moreover, these additional four TFs underline the theory of redundantly functioning ERF TFs which regulate e.g., FA biosynthesis during AM.

The observation that ERF TFs function partially redundant in order to regulate symbiosis is an already known pattern. During rhizobial symbiosis, the functional homologues *ERN1* and *ERN2*, as well as their antagonist *ERN3* act in a regulatory network to control the expression of *MtENOD11*, a gene that is pivotal for the progression of rhizobial infection (Andriankaja et al., 2007; Cerri et al., 2012, 2016; Middleton et al., 2007).

The observed knockdown effects of *ERF TF* genes on *RAM1* are equally reflected in other publications, indicating a positive feedback loop between the examined ERF TFs and *RAM1* (Jiang et al., 2018; Luginbuehl et al., 2017). The connection between ERF TFs and *RAM1* was analysed in the interaction studies in this thesis and will be discussed in the upcoming chapters. Equally interesting are the effects of some ERF TF knockdowns on *MtPT4*. Since *MtPT4* presents the key phosphate transporter importing phosphate into cortical root cells during AM, it plays a pivotal role, reflected in the formation of truncated arbuscules when knocked down (Breuillin-Sessoms et al., 2015; Pumplin et al., 2012). A regulatory effect of ERF TFs on *MtPT4* expression would be possible, since *CBX1*, an ERF TF functioning during AM in *L. japonicus*, mediates expression of *LjPT4* via binding to the promoters' CTTC and AW box motive (Liu et al., 2020; Xue et al., 2018). Furthermore, the RT PCR measurements presented in this work suggest a real network of ERF TFs -and potentially *RAM1*. ERF TFs and *RAM1* seem to influence each other's expression and thereby regulate processes like AM-dependent FA biosynthesis and phosphate uptake. A regulatory network of ERF TFs seems to be a conserved mode of action of these TFs, reflected in many different processes, not only in *M. truncatula* but also in *A. thaliana*, where a group of

AP2/ERF TFs e.g. regulates wound control (Cerri et al., 2012, 2016; Heyman et al., 2016, 2018; Son et al., 2012).

### **ERF TFs directly control each other as well as genes of the AM-dependent FA biosynthesis**

The recently stated *de novo* linear FA biosynthesis pathway supplying AMF with TAG precursors during AM is very well established, including key enzymes like KASII, RAM2 or FatM as well as the ABC-transporters STR/STR2, needed for the TAG precursor import into the PAI (Bravo et al., 2017; Jiang et al., 2017; Kamel et al., 2017; Keymer et al., 2017; Trépanier et al., 2005; Wewer et al., 2014). Nevertheless, the regulation of this elaborated pathway, taking part in different cellular compartments of root cortex cells, is not fully understood (Figure 4). Although WRI5 TFs and RAM1 are stated as major regulators of this process in *M. truncatula*, the targets as well as the potential regulatory networks including these TFs are only partially understood (Jiang et al., 2018; Luginbuehl et al., 2017).

Besides WRI5A, WRI5B and WRI5C, four more TFs (460730, 15867, 21492, 25005) could be identified in this thesis, potentially taking part in the regulatory network. The questions that were therefore addressed by a Y1H approach included the following: Do ERF TFs regulate the expression of other *ERF TF* genes in the regulatory network of FA biosynthesis? If this is the case, which are the promoter motifs mediating *ERF TF* gene regulation? Which target genes are regulated by the seven ERF TFs during FA biosynthesis?

To address the first question, it is necessary to understand that ERF TFs are widely known to regulate biotic stress response in regulatory networks, including not only one but more ERF TFs to control expression of target genes (Andriankaja et al., 2007; Cerri et al., 2012; Cerri et al., 2016; Heyman et al., 2016, 2018; Middleton et al., 2007; Son et al., 2012; Zhiguo et al., 2018). This regulatory interplay of ERF TFs can thereby be in a cooperative or antagonistic manner, as seen in the regulation of *MtENOD11* via ERN1, ERN2 and ERN3, where the two manners are realized in parallel to regulate rhizobial symbiosis (Andriankaja et al., 2007; Cerri et al., 2012; Cerri et al., 2017).

In case of the regulation of AM-dependent FA biosynthesis, there are seven ERF TFs potentially regulating this pathway besides RAM1 (Jiang et al., 2018; Luginbuehl et al., 2017). The results obtained in a Y1H approach, where WRI5B, WRI5C and 25005 interact with *p15867* and *p21492* strongly suggest that ERF TFs regulate each other to enhance each other's gene expression in a positive feedback loop. Additionally, ERF TF's might hereby act in a hierarchical manner (Figure 27, Table 44). The Y1H data furthermore suggest a regulation of *p21492* via RAM1. Unfortunately, the *pRAM1* could not be included in this dataset, although it would have been interesting to analyse a possible regulation of

*pRAM1* via ERF TFs. This would shed light on the recently suggested idea that ERF TFs and RAM1 increase each other's expression to regulate FA biosynthesis (Jiang et al., 2018; Luginbuehl et al., 2017).

A follow-up question to the ERF TF mediated regulation of *p15867* and *p21492* was, which motive on the TF gene's promoters could convey binding of WRI5B, WRI5C or 25005. Three motifs – conserved in different plants like *A. thaliana*, *L. japonicus* or *M. truncatula* - mediating ERF TF binding could hereby potentially play a role: the AW box motive, the GCC box motive or the CTTC Cre (Allen et al., 1995; Cerri et al., 2016; Hao et al., 1998; Jiang et al., 2018; Xue et al., 2018). The GCC-box-like AGCCGGC motifs located on *p15867* and *p460730* (150 bp to 250 bp upstream of the genes' startcodon) were therefore chosen for further analysis (Figure 30). Due to experimental limitations, only the *p460730-250bp* and the *p460730-GCC* could be analysed via Y1H, which did not show any regulation by one of the seven ERF TFs or RAM1. These data either indicate that *460730* expression might not be regulated by the tested ERF TFs or RAM1, or that the stated GCC-box-like motive does not mediate binding of one of the ERF TFs. Interestingly, *460730* is downregulated by *WR5A* and *15867* knockdown constructs, suggesting at least an indirect effect of those genes on *460730* expression. Including the RNAseq dataset (Luginbuehl et al., 2017) and the results from the reporter gene-assay performed in this thesis, *460730* seems to be dependent on RAM1, as well (Figure 15).

Remarkably, the *p460730-250bp* fragment seems to be sufficient to drive expression of the gene in a reporter gene analysis (Figure 28, Figure 29). This suggests that this fragment length is sufficient for gene expression, containing all the necessary elements like enhancers or binding motifs of important regulators. Taken into account the Y1H data on this promoter, regulation via ERF TFs alone might be more upstream and obviously not mandatory for the genes' expression. In contrast to this, a 1 kb fragment of *p15867* was required for *15867* gene expression, suggesting that important regulators and enhancers of the gene might be upstream of the 250 bp – located GCC-like box. Since *15867* was downregulated in roots containing a *WRI5A* knockdown and displayed a dependency on RAM1, it is worth examining this promoter in further Y1H approaches to shed light on WRI5B, WRI5C and 25005 as potential regulators of this gene.

Since WRI5B, WRI5C and 25005 also interacted with *p21492*, it might be worth searching for potential AW box, CTTC Cre or GCC-box motifs on this promoter as well. An AW box motive (5'-[CnTnG]<sub>n</sub>[CG]-3') could also be an interesting choice. This motive is known in the regulatory context of FA biosynthesis, not only during AM in *M. truncatula* or *L. japonicus* but also in the context of FA biosynthesis in *A. thaliana*, where it mediates binding of AtWR11 to *pAtKASI* (Jiang et al., 2018; Maeo et al., 2009; Xue et al., 2018). Besides this, WRI5A binding to the AW-box of *pSTR* is necessary for the genes' expression during AM-

dependent FA biosynthesis in *M. truncatula* (Jiang et al., 2018). These data could be confirmed in a further Y1H approach in this thesis, targeting the promoters of enzymes and transporters important for supplying the AMF with a TAG precursor (Bravo et al., 2017; Jiang et al., 2017; Kamel et al., 2017; Keymer et al., 2017; Trépanier et al., 2005; Wewer et al., 2014) (Figure 31, Table 45).

Remarkably, *pSTR* is not only bound by WRI5A, but also by WRI5B and WRI5C, which was also suggested by findings in recent publications (Jiang et al., 2018). In contrast to this, WRI5A, 460730, 15867 and 25005 seem to interact with *pKASII*, revealing a differing regulatory pattern compared to the *pSTR* regulation. WRI5A regulation of *pKASII* has already been stated in former publications, using overexpression constructs of WRI5A (Jiang et al., 2018). The regulation of *pKASII* via 460730, 15867 and 25005 provides an interesting addition to the regulatory network of AM-dependent FA biosynthesis, definitely placing these genes within the already established network. The proposed regulation of *FatM* expression via WRI5A overexpression could not be observed via Y1H. This might indicate that *FatM* expression is only indirectly dependent on WRI5A, but that the gene is not a direct regulatory target of the ERF TF. Interaction of further ERF TFs or RAM1 with *pFatM* could not be observed in the Y1H approach presented here, suggesting a different regulator of *FatM*.

The observed regulatory pattern of *pSTR* and *pKASII* again underlines the idea of redundantly functioning ERF TF factors during AM (Jiang et al., 2018; Luginbuehl et al., 2017). Due to the fact that *p21492* is also regulated by WRI5B, WRI5C and 25005, all seven ERF TFs could be -included directly or indirectly- into the regulatory network of AM-dependent FA biosynthesis in *M. truncatula*. This regulatory network might follow a hierarchical structure e.g., indicated by the finding that the expression of *ERF TF* genes like 15867 or 21492 is regulated by other ERF TFs. Alternatively, this finding might suggest feedback loops, positively enhancing expression of ERF TF in order to regulate FA biosynthesis.

---

**ERF TF interact with NF-Ys and RAM1 on a protein-protein level**

It is known from previous studies that ERF TFs can interact with members of the GRAS TF and the NF-Y TF families, respectively, to control various developmental or abiotic stress processes like endosperm development in *O. sativa* or wound defense control in *A. thaliana* (Bai et al., 2016; Heyman et al., 2016, 2018; Laloum et al., 2013; Son et al., 2012; Sun et al., 2014; Zhiguo et al., 2018). Results from these studies rise the question, if the ERF TFs studied in this thesis might function in protein-protein complexes with other TFs, in order to regulate FA biosynthesis. Y2H and BiFC data provided in this thesis suggest that the analysed ERF TFs indeed interact with members of the NF-Y TF family and with the GRAS TF RAM1 on the protein level (Figure 34, Figure 35, Figure 39, Figure 40).

The GRAS TF RAM1 could already be placed in the regulatory network of ERF TFs (Jiang et al., 2018; Luginbuehl et al., 2017; Park et al., 2015), a finding that could be underlined by the data suggested in this thesis. Nevertheless, the finding of this thesis, that RAM1 dimerizes with either WRI5A or WRI5C might have solved the open question how ERF TFs and RAM1 conjointly regulate AM-dependent FA biosynthesis.

The observed dimerization of RAM1 with WRI5A or WRI5C thereby underlined the finding that the GRAS TF RAM1 is probably not able to bind its regulatory targets on its own, but needs a dimerization partner (Gobbato et al., 2012; Park et al., 2015; Xue et al., 2015). In these studies, RAM1 dimerized with the DIP1, NSP2 or RAD1 GRAS TFs to provide regulation of AM in *L. japonicus*, *M. truncatula* and *O. sativa*, respectively.

Besides RAM1-WRI5A and RAM1-WRI5C dimers, ERF TFs could also be shown to interact in a tetrameric complex consisting of a trimeric NF-YA, NF-YB and NF-YC complex and an ERF TF (WRI5A, WRI5B, WRI5C or 25005). The finding that NF-Ys upregulated during AM also regulate AM-dependent FA biosynthesis genes like *STR* or potential regulators of the process like *15867* or *21492* definitely places the involved NF-Y subunits (NF-Y A2, A3, A4, A7 and CBF3, also referred to as NF-Y B7) in the regulatory network of AM-dependent FA biosynthesis (Figure 36, Table 48). These data also suggest a conserved function of ERF TFs and NF-Ys in FA biosynthesis, since members these TF families are also known to regulate oil accumulation in seeds of *Z. mays* and *A. thaliana* (Baud et al., 2007; Maeo et al., 2009; Mu et al., 2008; Rangan et al., 1996; Roder et al., 1997; Santos-Mendoza et al., 2008; Schweizer et al., 2002; Shen et al., 2010). However, the finding that TFs of the NF-Y TF family might function during AM-dependent FA biosynthesis is a novel finding, revealing an even more complex underlying regulatory pattern.

Interestingly, sequence analyses of WRI5A, WRI5B WRI5C and 25005 could reveal at least one AP2 binding domain in each TF, mediating ERF TF binding to the DNA, but no

commonly known protein-protein interaction domain. It would therefore be a future task to identify the protein-protein interaction domain of these ERF TFs.

Finally, it could be discussed if WRI5A or WRI5C together with RAM1 and the trimeric NF-Y complex build a pentameric complex in order to regulate common targets like *pSTR* or *p21492* (Figure 42). WRI5A (or WRI5C) would hereby function as an adapter between RAM1 and the trimeric NF-Y complex, since RAM1 could not be shown to interact directly with one of the NF-Y subunits in a Y2H approach (Steven Krüger, LUH, unpublished data).

Somehow contradicting to this hypothesis are findings from earlier studies, that dealt with the role of ERF TFs and GRAS TFs in wound defence of *A. thaliana* or endosperm development in *O. sativa* regulated by ERF TFs and NF-Y TFs (Bai et al., 2016; Heyman et al., 2016, 2018; Laloum et al., 2013; Son et al., 2012; Sun et al., 2014; Zhiguo et al., 2018). In these studies, ERF TFs interacted with one GRAS TF or with the NF-Y B and NF-Y C subunit to control the already mentioned processes. The results suggest that no further factors are associated to control wound defence or endosperm development. Remarkably, the suggested protein-protein interactions between NF-Y subunits and ERF TFs (Bai et al., 2016; Sun et al., 2014; Xu et al., 2016; Zhiguo et al., 2018) somehow differ compared to the findings in this thesis. Whereas data presented in this thesis show that ERF TFs interact with the A and the B subunit of NF-Y TFs, ERF TFs analysed in the studies mentioned above interacted with the B and the C subunit of NF-Y TFs.

In conclusion, the protein-protein interaction data presented in this thesis strongly suggest a regulatory network of ERF TFs, NF-Y TFs and RAM1 that work conjointly to orchestrate AM-dependent FA biosynthesis.



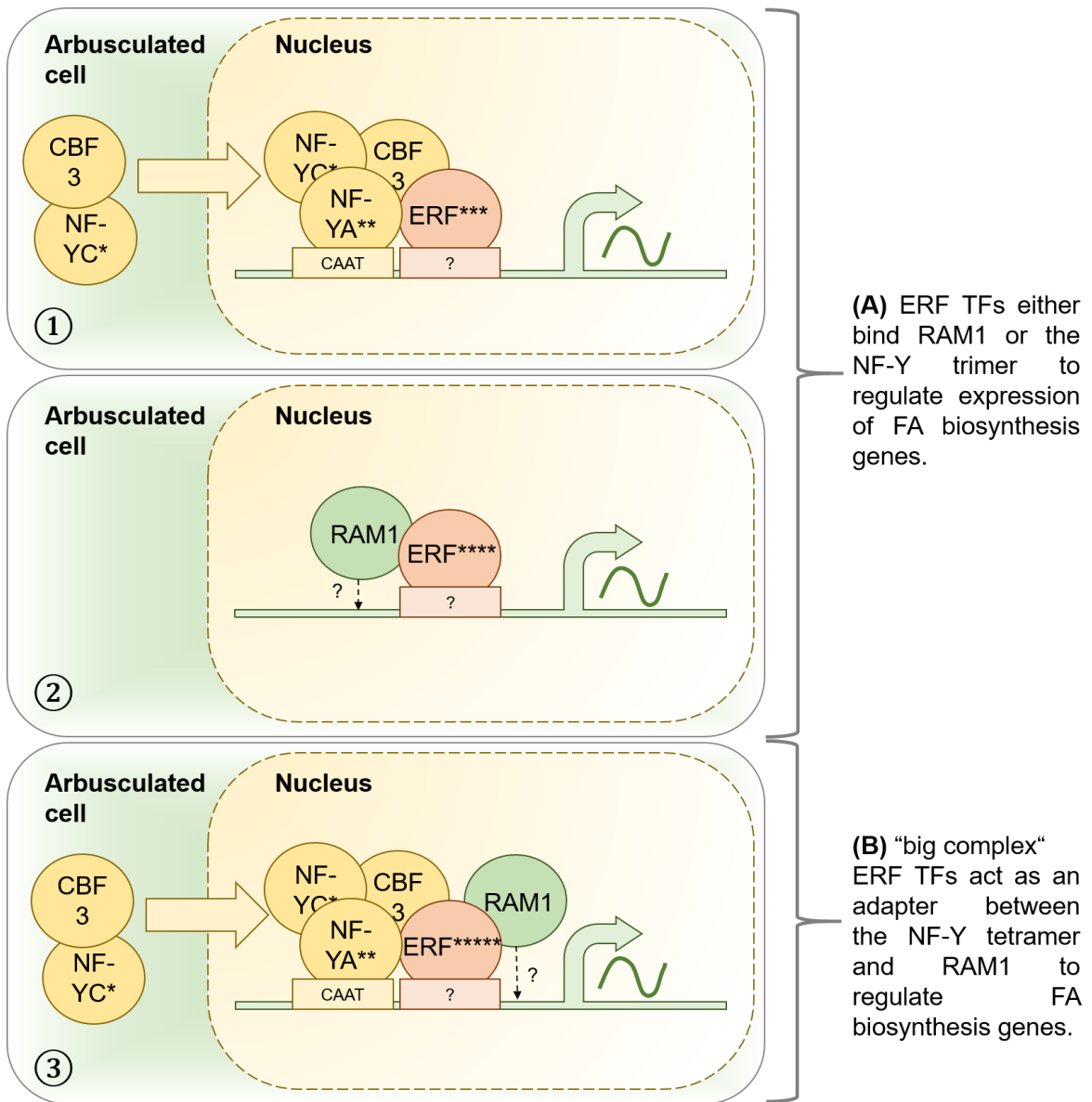


**Figure 42: ERF TFs interact with varying NF-Y trimers and RAM1 to regulate expression of FA biosynthesis genes.** (A) Y2H and BiFC data, obtained in this thesis suggest that ERF TFs interact with a tetrameric NF-Y complex (1) or RAM1 (2) in order to regulate FA biosynthesis genes. (1) CBF3 (NF-Y B7) and the NF-YC subunit build a dimeric complex in the cytoplasm and are transported into the nucleus afterwards. There, a heterotetrameric complex consisting of CBF3, NF-Y A and NF-Y C and an ERF TF is built. In this heterotetramer, NF-Y A and CBF3 can potentially interact with the ERF TF. Protein-DNA interaction is conducted by the ERF TF and the NF-Y A subunit. Whereas the motive mediating DNA binding of the ERF TF remains unclear (indicated by a questions mark), NF-Y A binds its targeted DNA via a CAAT box motive. (2) ERF TFs also interact with RAM1 in order to regulate FA biosynthesis genes. DNA binding motifs of the ERF TFs as well as direct binding of RAM1 with the targeted DNA thereby remain unclear (indicated by questions marks). (B) Data provided in this thesis could also suggest a pentameric “big complex” of the NF-Y trimer as well as an ERF TF and RAM1. The ERF TF would hereby function as an adapter between the NF-Y complex and RAM1. (Due to the data suggested in the Y2H and BiFC approaches: NF-Y C\*: CBF1 and CBF2 could be part of this complex; NF-Y A\*\*: NF-Y A2, A3, A4 and A7 could be part of this complex; ERF\*\*\*: WRI5A, WRI5C and 25005 could be part of this complex, WRI5B only interacted with CBF3; ERF\*\*\*\*: WRI5A and WRI5C interacted with RAM1; ERF\*\*\*\*\*: only WRI5A and WRI5C could be part of this hypothetical pentameric complex)

---

**ERF TFs, together with RAM1 and NF-Y TFs, conjointly regulate AM-dependent FA biosynthesis in *M. truncatula***

The stated AM-dependent regulatory network controlling AM-dependent FA biosynthesis is potentially modulated by ERF-RAM1 and ERF-NF-Y TFs complexes (Figure 43). Analysed members of the ERF as well as NF-Y TF families thereby show redundant regulatory patterns allowing variable ERF-NF-Ys TF complexes for the regulation of the very same targets. The findings of ERF-NF-Ys complexes presented in this thesis add an unknown regulatory complex to the already stated regulation of AM-dependent FA biosynthesis via RAM1 and ERF TFs (Jiang et al., 2018; Luginbuehl et al., 2017).

Equally important is the described observation of WRI5A-RAM1 and WRI5C-RAM1 regulatory complexes since they shed light on the previously asked question how RAM1 and ERF TFs conjointly regulate FA biosynthesis. Surprisingly, the regulatory complexes of ERF-RAM1 and ERF-NF-Ys not only regulate genes of the FA biosynthesis but additionally enhance expression of other ERF TFs genes like *15867* and *21492*. These data indicate a positive feedback loop to increase ERF TF gene expression, thereby also increasing expression of FA biosynthesis genes.

Besides the stated complexes, the regulation of *pKASII* via ERF TFs observed in this thesis suggests that the regulatory complexes might not control gene expression of all AM-dependent FA biosynthesis genes. Contrastingly, these data might suggest that ERF TFs alone are sufficient for the regulations of some FA biosynthesis genes.

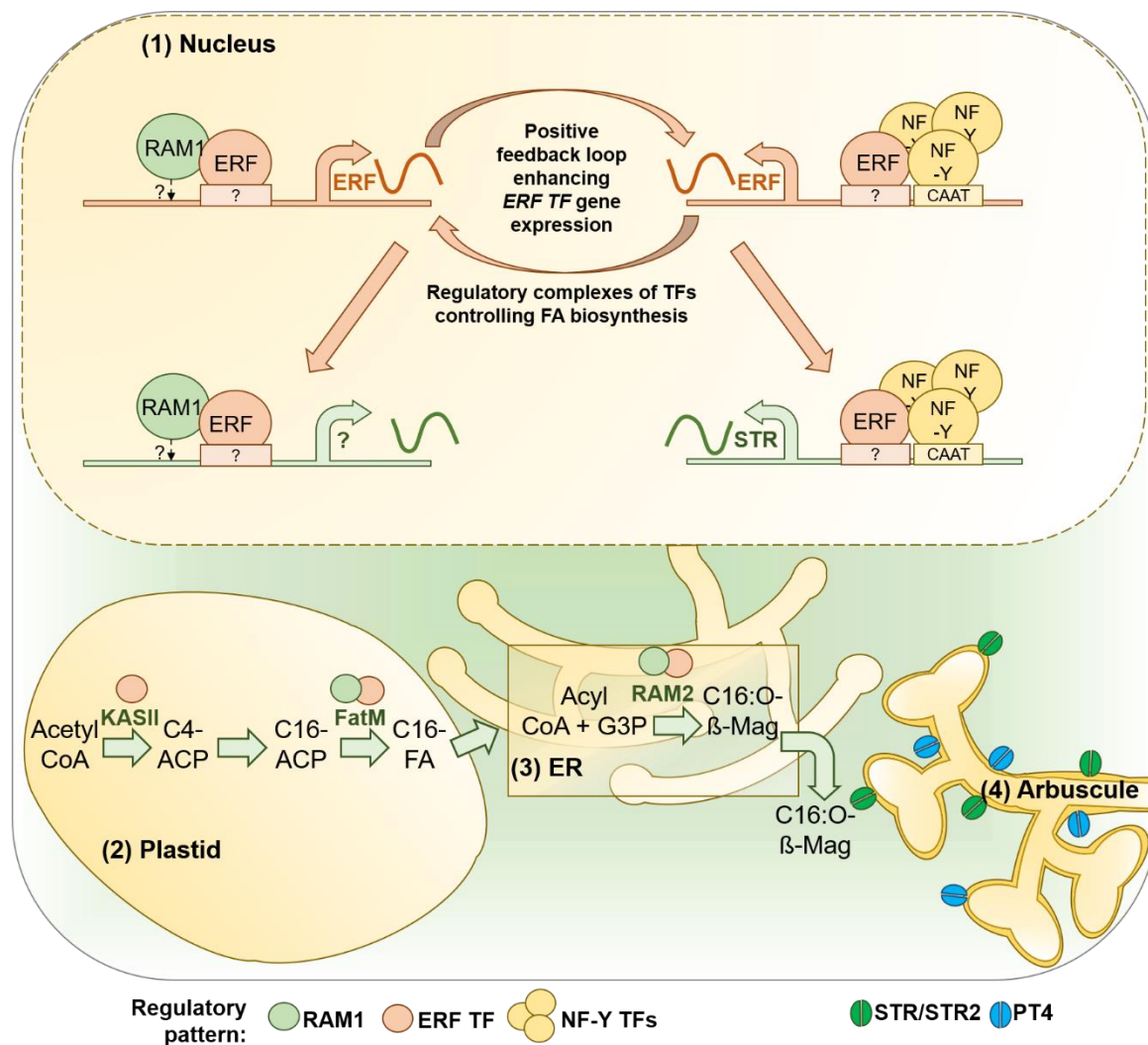


**Figure 43: Model of the AM-dependent FA biosynthesis regulated by ERF-RAM1 and ERF-NF-Y TF complexes.** (1) In the nucleus TF complexes consisting of either ERF-RAM1 or ERF-NF-Ys regulate the expression of other ERF TFs, potentially in a positive feedback loop. The very same TF complexes might also regulate gene expression of FA biosynthesis genes like *KASII*, *FatM*, *RAM2* or *STR/STR2*. In case of the ERF-NF-Y complexes the ABC-transporter gene *STR* could be identified as a direct target. In case of the ERF-RAM1 complex, direct regulatory targets still need to be identified (indicated by the question mark). (2) Potential regulatory targets of the identified regulatory complexes could be the enzymes *KASII* and *FatM*, stepwise converting Acetyl-CoA to C-16-FA in the plastids. (3) Another regulatory target, possibly regulated by an ERF-RAM1 complex is *RAM2* (the GPAT enzyme), that attaches C16:0-FA to the second carbon of glycerol-3-phosphate to make C16:0 β-MAG. (4) The ABC-transporter gene *STR* was analyzed as a target of ERF-NF-Y TF complexes, whereas the regulatory complex of the second gene encoding for the transporter *STR/STR2* transporting C16:0 β-MAG into the PAI, *STR2*, remains unclear. Regulation of *STR* via ERF TFs binding to the promoter is potentially mediated by an AW box, at least in case of *WRI5A* (indicated by a question mark in (1)). Suggested regulators for enzymes important for AM-dependent FA biosynthesis, summarizing results of this thesis as well as results from previous studies are indicated via circles over the enzymes' names (Jiang et al., 2018; Luginbuehl et al., 2017).

The direct regulators of genes like *FatM*, *RAM2* or *STR2* still remain unclear. Although previous studies indirectly show gene expression of these genes in *RAM1* as well as *WRI5A* overexpression backgrounds, further direct approaches must be conducted to identify the direct regulators (Jiang et al., 2018; Luginbuehl et al., 2017).

## Discussion

---

As shown for *15867* and *21492*, ERFs also seem to regulate each other's gene expression. It would therefore be remarkably interesting to test, whether the other five ERF TFs analysed in this thesis are also regulated by ERF-RAM1 or ERF-NF-Ys TF complexes.

An important force for the establishment and maintenance of AM symbiosis is the Pi status of the plant, with MtPT4 being pivotal for this homeostasis (Javot et al., 2007). During AM symbiosis of *L. japonicus*, ERF TF CBX1 could be identified as a main regulator of *LjPT4* and *LjHA1*, both being essential for important for phosphate transport from the AMF to the plant (Liu et al., 2020; Xue et al., 2018). This might indicate a possible regulation of AM-dependent phosphate intake via ERF TFs in *M. truncatula*. Since *MtPT4* expression is highly dependent on *RAM1* expression, the regulatory network of this AM-dependent process might include ERF TFs in addition to RAM1 (Park et al., 2015; Pimprikar et al., 2016). In addition to their regulatory role during FA biosynthesis, ERF TF might thus also be involved in the fine-tuning of phosphate transport during AM.

## References

- Allen, E. B., Allen, M. F., Helm, D. J., Trappe, J. M., Molina, R., & Rincon, E. (1995). Patterns and regulation of arbuscular and ectomycorrhizal plant and fungal diversity: a hypothesis. *Plant and Soil*, *170*, 47–62.
- Allen, M. D., Yamasaki, K., Ohme-Takagi, M., Tateno, M., & Suzuki, M. (1998). A novel mode of DNA recognition by a  $\beta$ -sheet revealed by the solution structure of the GCC-box binding domain in complex with DNA. *The EMBO Journal*, *17*(18), 5484–5496.
- Andriankaja, A., Boisson-Dernier, A., Frances, L., Sauviac, L., Jauneau, A., Barker, D. G., & De Carvalho-Niebel, F. (2007). AP2-ERF transcription factors mediate nod factor-dependent Mt ENOD11 activation in root hairs via a novel cis-regulatory motif. *Plant Cell*, *19*(9), 2866–2885.
- Bai, A. N., Lu, X. D., Li, D. Q., Liu, J. X., & Liu, C. M. (2016). NF-YB1-regulated expression of sucrose transporters in aleurone facilitates sugar loading to rice endosperm. *Cell Research*, *26*(3), 384–388.
- Balestrini, R., Berta, G., & Bonfante, P. (1992). The plant nucleus in mycorrhizal roots: positional and structural modifications. *Biology of the Cell*, *75*(1), 235–243.
- Barker, D. G., Bianchi, S., Blondon, F., Duc, G., Essad, S., Flament, P., Gdnier, G., Guy, P., Muel, X., Ddnarid, J., & Huguet, T. (1990). *Medicago truncatula*, a model plant for studying the molecular genetic of the rhizobium-legume symbiosis. *Plant Molecular Biology Reporter*, *8*(1), 40–49.
- Baud, S., Mendoza, M. S., To, A., Harscoët, E., Lepiniec, L., & Dubreucq, B. (2007). WRINKLED1 specifies the regulatory action of LEAFY COTYLEDON2 towards fatty acid metabolism during seed maturation in *Arabidopsis*. *Plant Journal*, *50*(5), 825–838.
- Baudin, M., Laloum, T., Lepage, A., Rípodas, C., Ariel, F., Frances, L., Crespi, M., Gamas, P., Blanco, F. A., Zanetti, M. E., de Carvalho-Niebel, F., & Niebel, A. (2015). A phylogenetically conserved group of nuclear factor-Y transcription factors interact to control nodulation in legumes. *Plant Physiology*, *169*(4), 2761–2773.
- Blancaflor, E. B., Zhao, L., & Harrison, M. J. (2001). Microtubule organization in root cells of *Medicago truncatula* during development of an arbuscular mycorrhizal symbiosis with *Glomus versiforme*. *Protoplasma*, *217*(4), 154–165.
- Bonfante, P., & Genre, A. (2010). Mechanism underlying beneficial plant-fungus interactions in mycorrhizal symbiosis. *Nature Communications*, *1*, 1–11.

## References

---

- Bravo, A., Brands, M., Wewer, V., Dörmann, P., & Harrison, M. J. (2017). Arbuscular mycorrhiza-specific enzymes FatM and RAM2 fine-tune lipid biosynthesis to promote development of arbuscular mycorrhiza. *New Phytologist*, *214*(4), 1631–1645.
- Breullin-Sessoms, F., Floss, D. S., Gomez, S. K., Pumplin, N., Ding, Y., Levesque-Tremblay, V., Noar, R. D., Daniels, D. A., Bravo, A., Eaglesham, J. B., Benedito, V. A., Udvardi, M. K., & Harrison, M. J. (2015). Suppression of arbuscule degeneration in *Medicago truncatula* phosphate transporter4 mutants is dependent on the ammonium transporter 2 family protein AMT2;3. *Plant Cell*, *27*(4), 1352–1366.
- Brundrett, M., Bougher, N., Dell, B., Grove, T. & Malajczuk, N. (1996). Working With Mycorrhizas in Forestry and Agriculture. *ACIAR Monograph Series*.
- Bucher, M. (2007). Functional biology of plant phosphate uptake at root and mycorrhiza interfaces. *New Phytologist*, *173*(1), 11–26.
- Bucher, M., Hause, B., Krajinski, F., & Küster, H. (2014). Through the doors of perception to function in arbuscular mycorrhizal symbioses. *New Phytologist*, *204*(4), 833–840.
- Cairney, J. W. G. (2000). Evolution of mycorrhiza systems. *Naturwissenschaften*, *87*(11), 467–475.
- Caretti, G., Motta, M. C., & Mantovani, R. (1999). NF-Y Associates with H3-H4 Tetramers and Octamers by Multiple Mechanisms. *Molecular and Cellular Biology*, *19*(12), 8591–8603.
- Carling, D., & Brown, M. (1982). Anatomy and physiology of vesicular-arbuscular nonmycorrhizal roots. *Phytopathology*, *72*, 1108–1114.
- Cernac, A., & Benning, C. (2004). WRINKLED1 encodes an AP2/EREB domain protein involved in the control of storage compound biosynthesis in *Arabidopsis*. *Plant Journal*, *40*(4), 575–585.
- Cerri, M. R., Frances, L., Laloum, T., Auriac, M.-C., Niebel, A., Oldroyd, G. E. D., Barker, D. G., Fournier, J., & de Carvalho-Niebel, F. (2012). *Medicago truncatula* ERN Transcription Factors: Regulatory Interplay with NSP1/NSP2 GRAS Factors and Expression Dynamics throughout Rhizobial Infection. *Plant Physiology*, *160*(4), 2155–2172.
- Cerri, M. R., Frances, L., Kelner, A., Fournier, J., Middleton, P. H., Auriac, M. C., Mysore, K. S., Wen, J., Erard, M., Barker, D. G., Oldroyd, G. E., & de Carvalho-Niebel, F. (2016). The symbiosis-related ERN transcription factors act in concert to coordinate

## References

---

- rhizobial host root infection. *Plant Physiology*, 171(2), 1037–1054.
- Cerri, M. R., Frances, L., Laloum, T., Auriac, M. C., Niebel, A., Oldroyd, G. E. D., Barker, D. G., Fournier, J., & de Carvalho-Niebel, F. (2012). Medicago truncatula ERN transcription factors: Regulatory interplay with NSP1/NSP2 GRAS factors and expression dynamics throughout rhizobial infection. *Plant Physiology*, 160(4), 2155–2172.
- Cerri, M. R., Wang, Q., Stolz, P., Folgmann, J., Frances, L., Katzer, K., Li, X., Heckmann, A. B., Wang, T. L., Downie, J. A., Klingl, A., de Carvalho-Niebel, F., Xie, F., & Parniske, M. (2017). The ERN1 transcription factor gene is a target of the CCaMK/CYCLOPS complex and controls rhizobial infection in Lotus japonicus. *New Phytologist*, 215(1), 323-337.
- Chabaud, M., Genre, A., Sieberer, B. J., Faccio, A., Fournier, J., Novero, M., Barker, D. G., & Bonfante, P. (2011). Arbuscular mycorrhizal hyphopodia and germinated spore exudates trigger Ca<sup>2+</sup> spiking in the legume and nonlegume root epidermis. *New Phytologist*, 189(1), 347–355.
- Chen, Y. F., Etheridge, N., & Schaller, G. E. (2005). Ethylene signal transduction. *Annals of Botany*, 95(6), 901–915.
- Cheng, M. C., Liao, P. M., Kuo, W. W., & Lin, T. P. (2013). The arabidopsis ETHYLENE RESPONSE FACTOR1 Regulates abiotic stress-responsive gene expression by binding to different cis-acting elements in response to different stress signals. *Plant Physiology*, 162(3), 1566–1582.
- Combiér, J. P., Frugier, F., De Billy, F., Boualem, A., El-Yahyaoui, F., Moreau, S., Vernié, T., Ott, T., Gamas, P., Crespi, M., & Niebel, A. (2006). MtHAP2-1 is a key transcriptional regulator of symbiotic nodule development regulated by microRNA169 in Medicago truncatula. *Genes and Development*, 20(22), 3084–3088.
- Coustry, F., Maity, S. N., Sinha, S., & De Crombrugghe, B. (1996). The transcriptional activity of the CCAAT-binding factor CBF is mediated by two distinct activation domains, one in the CBF-B subunit and the other in the CBF-C subunit. *Journal of Biological Chemistry*, 271(24), 14485–14491.
- Czaja, L. F., Hogekamp, C., Lamm, P., Maillet, F., Martinez, E. A., Samain, E., Dénarié, J., Küster, H., & Hohnjec, N. (2012). Transcriptional responses toward diffusible signals from symbiotic microbes reveal MtNFP- and MtDMI3-dependent reprogramming of host gene expression by arbuscular mycorrhizal fungal lipochitooligosaccharides.

## References

---

- Plant Physiology*, 159(4), 1671–1685.
- Daniell, T. J., Hodge, A., Peter, J., Young, W., & Fitter, A. (1999). How many fungi does it take to change a plant community? *Trends in Plant Science*, 4(3), 81–82.
- de Bary, A. (1879). Die Erscheinung der Symbiose. *De Gruyter*, 5-30.
- Deplancke, B., Dupuy, D., Vidal, M., & Walhout, A. J. M. (2004). A Gateway-Compatible Yeast One-Hybrid System. *Cold Spring Harbor Protocols*, 14(508), 2093–2101.
- Devers, E. A., Teply, J., Reinert, A., Gaude, N., & Krajinski, F. (2013). An endogenous artificial microRNA system for unraveling the function of root endosymbioses related genes in *Medicago truncatula*. *BMC Plant Biology*, 13(1), 82.
- Di Laurenzio, L., Wysocka-Diller, J., Malamy, J. E., Pysh, L., Helariutta, Y., Freshour, G., Hahn, M. G., Feldmann, K. A., & Benfey, P. N. (1996). The SCARECROW gene regulates an asymmetric cell division that is essential for generating the radial organization of the *Arabidopsis* root. *Cell*, 86(3), 423–433.
- Dolfini, D., Gatta, R., & Mantovani, R. (2012). NF-Y and the transcriptional activation of CCAAT promoters. *Critical Reviews in Biochemistry and Molecular Biology*, 47(1), 29–49.
- Donati, G., Gatta, R., Dolfini, D., Fossati, A., Ceribelli, M., & Mantovani, R. (2008). An NF-Y-dependent switch of positive and negative histone methyl marks on CCAAT promoters. *PLoS ONE*, 3(4).
- Fields, S., & Song, O. K. (1989). A novel genetic system to detect protein-protein interactions. *Nature*, 340(6230), 245–246.
- Fiorilli, V., Catoni, M., Miozzi, L., Novero, M., Accotto, G. P., & Lanfranco, L. (2009). Global and cell-type gene expression profiles in tomato plants colonized by an arbuscular mycorrhizal fungus. *New Phytologist*, 184(4), 975–987.
- Floß, D. S., Hause, B., Lange, P. R., Küster, H., Strack, D., & Walter, M. H. (2008). Knock-down of the MEP pathway isogene 1-deoxy-d-xylulose 5-phosphate synthase 2 inhibits formation of arbuscular mycorrhiza-induced apocarotenoids, and abolishes normal expression of mycorrhiza-specific plant marker genes. *Plant Journal*, 56(1), 86–100.
- Floss, D. S., Levy, J. G., Lévesque-Tremblay, V., Pumplin, N., & Harrison, M. J. (2013). DELLA proteins regulate arbuscule formation in arbuscular mycorrhizal symbiosis. *PNAS*, 110(51), E5025-E5034.



## References

---

- Focks, N., & Benning, C. (1998). Wrinkled 1: A novel, low-seed-oil mutant of arabidopsis with a deficiency in the seed-specific regulation of carbohydrate metabolism. *Plant Physiology*, 118(1), 91–101.
- Forsburg, S. L., & Guarente, L. (1989). Identification and characterization of HAP4: a third component of the CCAAT-bound HAP2/HAP3 heteromer. *Genes & Development*, 3(8), 1166–1178.
- Frank, A. B. (1885). Über die auf Wurzelsymbiose beruhende Ernährung gewisser Bäume durch unterirdische Pilze. *Berlin Deutsche Botanische Gesellschaft*, 3, 128–145.
- Fuxman Bass, J. I., Reece-Hoyes, J. S., & Walhout, A. J. M. (2016a). Colony lift colorimetric assay for  $\beta$ -Galactosidase activity. *Cold Spring Harbor Protocols*, 2016(12), 1110–1112.
- Fuxman Bass, J. I., Reece-Hoyes, J. S., & Walhout, A. J. M. (2016b). Generating Bait Strains for Yeast One-Hybrid Assays. *Cold Spring Harbor Protocols*, 12(5), 139–148.
- Fuxman Bass, J. I., Reece-Hoyes, J. S., & Walhout, A. J. M. (2016c). Zymolyase-treatment and polymerase chain reaction amplification from genomic and plasmid templates from yeast. *Cold Spring Harbor Protocols*, 2016(12), 1113–1115.
- Gao, M. J., Li, X., Huang, J., Gropp, G. M., Gjetvaj, B., Lindsay, D. L., Wei, S., Coutu, C., Chen, Z., Wan, X. C., Hannoufa, A., Lydiate, D. J., Gruber, M. Y., Chen, Z. J., & Hegedus, D. D. (2015). SCARECROW-LIKE15 interacts with HISTONE DEACETYLASE19 and is essential for repressing the seed maturation programme. *Nature Communications*, 6.
- Gao, M. J., Parkin, I. A. P., Lydiate, D. J., & Hannoufa, A. (2004). An auxin-responsive SCARECROW-like transcriptional activator interacts with histone deacetylase. *Plant Molecular Biology*, 55(3), 417–431.
- Gao, Z., Chen, Y. F., Randlett, M. D., Zhao, X. C., Findell, J. L., Kieber, J. J., & Schaller, G. E. (2003). Localization of the Raf-like Kinase CTR1 to the Endoplasmic Reticulum of Arabidopsis through Participation in Ethylene Receptor Signaling Complexes. *Journal of Biological Chemistry*, 278(36), 34725–34732.
- Gatta, R., & Mantovani, R. (2011). NF-Y affects histone acetylation and H2A.Z deposition in cell cycle promoters. *Epigenetics*, 6(4), 526–534.
- Gatta, R., & Mantovani, R. (2013). Erratum: NF-Y substitutes H2A-H2B on active cell-cycle promoters: Recruitment of CoREST-KDM1 and fine-tuning of H3 methylations (Nucleic

## References

---

- Acids Research (2008) 36 (6592-6607) DOI: 10.1093/nar/gkn699). *Nucleic Acids Research*, 41(19), 9208.
- Gaude, N., Bortfeld, S., Duensing, N., Lohse, M., & Krajinski, F. (2012b). Arbuscule-containing and non-colonized cortical cells of mycorrhizal roots undergo extensive and specific reprogramming during arbuscular mycorrhizal development. *Plant Journal*, 69(3), 510–528.
- Gemoll, W. (1908). *Griechisch-Deutsches Schul-und Handwörterbuch*. Tempsky, Wien.
- Genre, A., Chabaud, M., Balzergue, C., Puech-Pagès, V., Novero, M., Rey, T., Fournier, J., Rochange, S., Bécard, G., Bonfante, P., & Barker, D. G. (2013). Short-chain chitin oligomers from arbuscular mycorrhizal fungi trigger nuclear Ca<sup>2+</sup> spiking in *Medicago truncatula* roots and their production is enhanced by strigolactone. *New Phytologist*, 198(1), 190–202.
- Genre, A., Chabaud, M., Timmers, T., Bonfante, P., & Barker, D. G. (2005). Arbuscular mycorrhizal fungi elicit a novel intracellular apparatus in *Medicago truncatula* root epidermal cells before infection. *Plant Cell*, 17(12), 3489–3499.
- Gnesutta, N., Saad, D., Chaves-Sanjuan, A., Mantovani, R., & Nardini, M. (2017). Crystal Structure of the *Arabidopsis thaliana* L1L/NF-YC3 Histone-fold Dimer Reveals Specificities of the LEC1 Family of NF-Y Subunits in Plants. *Molecular Plant*, 10(4), 645–648.
- Gobbato, E., Marsh, J. F., Vernié, T., Wang, E., Maillet, F., Kim, J., Miller, J. B., Sun, J., Bano, S. A., Ratet, P., Mysore, K. S., Dénarié, J., Schultze, M., & Oldroyd, G. E. D. (2012). A GRAS-type transcription factor with a specific function in mycorrhizal signaling. *Current Biology*, 22(23), 2236–2241.
- Gomez, S. K., Javot, H., Deewatthanawong, P., Torres-Jerez, I., Tang, Y., Blancaflor, E. B., Udvardi, M. K., & Harrison, M. J. (2009). *Medicago truncatula* and *Glomus intraradices* gene expression in cortical cells harboring arbuscules in the arbuscular mycorrhizal symbiosis. *BMC Plant Biology*, 9(10).
- Govindarajulu, M., Pfeffer, P. E., Jin, H., Abubaker, J., Douds, D. D., Allen, J. W., Bücking, H., Lammers, P. J., & Shachar-Hill, Y. (2005). Nitrogen transfer in the arbuscular mycorrhizal symbiosis. *Nature*, 435(7043), 819–823.
- Grant, S. G. N., Jessee, J., Bloom, F. R., & Hanahan, D. (1990). Differential plasmid rescue from transgenic mouse DNAs into *Escherichia coli* methylation-restriction mutants. *PNAS*, 87(12), 4645–4649.

## References

---

- Gutjahr, C., & Parniske, M. (2013). Cell and developmental biology of arbuscular mycorrhiza symbiosis. *Annual Review of Cell and Developmental Biology*, 29, 593–617.
- Handa, Y., Nishide, H., Takeda, N., Suzuki, Y., Kawaguchi, M., & Saito, K. (2015). RNAseq Transcriptional Profiling of an Arbuscular Mycorrhiza Provides Insights into Regulated and Coordinated Gene Expression in *Lotus japonicus* and *Rhizophagus irregularis*. *Plant and Cell Physiology*, 56(8), 1490–1511.
- Hao, D., Ohme-Takagi, M., & Sarai, A. (1998). Unique mode of GCC box recognition by the DNA-binding domain of ethylene-responsive element-binding factor (ERF domain) in plant. *Journal of Biological Chemistry*, 273(41), 26857–26861.
- Harrison, M. J. (2002). A Phosphate Transporter from *Medicago truncatula* Involved in the Acquisition of Phosphate Released by Arbuscular Mycorrhizal Fungi. *The Plant Cell Online*, 14(10), 2413–2429.
- Harrison, M. J., & Buuren, M. L. Van. (1995). A phosphate transporter from the mycorrhizal fungus *Glomus versiforme*. *Letters to Nature*, 378(12), 626-629.
- Hartmann, R. M., Schaepe, S., Nübel, D., Petersen, A. C., Bertolini, M., Vasilev, J., Küster, H., & Hohnjec, N. (2019). Insights into the complex role of GRAS transcription factors in the arbuscular mycorrhiza symbiosis. *Scientific Reports*, 9.
- Heckmann, A. B., Lombardo, F., Miwa, H., Perry, J. A., Bunnewell, S., Parniske, M., Wang, T. L., & Downie, J. A. (2006). *Lotus japonicus* nodulation requires two GRAS domain regulators, one of which is functionally conserved in a non-legume. *Plant Physiology*, 142(4), 1739–1750.
- Heyman, J., Canher, B., Bisht, A., Christiaens, F., & De Veylder, L. (2018). Emerging role of the plant ERF transcription factors in coordinating wound defense responses and repair. *Journal of Cell Science*, 131(2).
- Heyman, J., Cools, T., Canher, B., Shavialenka, S., Traas, J., Vercauteren, I., Van Den Daele, H., Persiau, G., De Jaeger, G., Sugimoto, K., & De Veylder, L. (2016). The heterodimeric transcription factor complex ERF115-PAT1 grants regeneration competence. *Nature Plants*, 2(10), 1–7.
- Hirsch, S., Kim, J., Muñoz, A., Heckmann, A. B., Downie, J. A., & Oldroyd, G. E. D. (2009). GRAS Proteins Form a DNA Binding Complex to Induce Gene Expression during Nodulation Signaling in *Medicago truncatula*. *Plant Cell*, 21(2), 545–557.
- Hoffmann, B., Trinh, T. H., Leung, J., Kondorosi, A., & Kondorosi, E. (1997). A new

## References

---

- Medicago truncatula line with superior in vitro regeneration, transformation, and symbiotic properties isolated through cell culture selection. *Molecular Plant-Microbe Interactions*, 10(3), 307–315.
- Hogekamp, C., Arndt, D., Pereira, P. A., Becker, J. D., Hohnjec, N., & Küster, H. (2011). Laser Microdissection Unravels Cell-Type-Specific Transcription in Arbuscular Mycorrhizal Roots, Including CAAT-Box Transcription Factor Gene Expression Correlating with Fungal Contact and Spread. *Plant Physiology*, 157(4), 2023–2043.
- Hogekamp, C., & Küster, H. (2013). A roadmap of cell-type specific gene expression during sequential stages of the arbuscular mycorrhiza symbiosis. *BMC Genomics*, 14(1), 306.
- Hohnjec, N., Czaja-Hasse, L. F., Hogekamp, C., & Küster, H. (2015). Pre-announcement of symbiotic guests: Transcriptional reprogramming by mycorrhizal lipochitooligosaccharides shows a strict co-dependency on the GRAS transcription factors NSP1 and RAM1. *BMC Genomics*, 16(1).
- Huang, Y., Li, H., Hutchison, C. E., Laskey, J., & Kieber, J. J. (2003). Biochemical and functional analysis of CTR1, a protein kinase that negatively regulates ethylene signaling in Arabidopsis. *Plant Journal*, 33(2), 221–233.
- Ivanov, S., Austin, J., Berg, R. H., & Harrison, M. J. (2019). Extensive membrane systems at the host–arbuscular mycorrhizal fungus interface. *Nature Plants*, 5(2), 194–203.
- Javot, H., Penmetsa, R. V., Terzaghi, N., Cook, D. R., & Harrison, M. J. (2007). A Medicago truncatula phosphate transporter indispensable for the arbuscular mycorrhizal symbiosis. *Proc Natl Acad Sci U S A*, 104(5), 1720–1725.
- Jiang, Y., Wang, W., Xie, Q., Liu, N., Liu, L., Wang, D., Zhang, X., Yang, C., Chen, X., Tang, D., & Wang, E. (2017). Plants transfer lipids to sustain colonization by mutualistic mycorrhizal and parasitic fungi. *Science*, 356(6343), 1172–1173.
- Jiang, Y., Xie, Q., Wang, W., Yang, J., Zhang, X., Yu, N., Zhou, Y., & Wang, E. (2018). Medicago AP2-Domain Transcription Factor WRI5a Is a Master Regulator of Lipid Biosynthesis and Transfer during Mycorrhizal Symbiosis. *Molecular Plant*, 11(11), 1344–1359.
- Ju, C., Yoon, G. M., Shemansky, J. M., Lin, D. Y., Ying, Z. I., Chang, J., Garrett, W. M., Kessenbrock, M., Groth, G., Tucker, M. L., Cooper, B., Kieber, J. J., & Chang, C. (2012). CTR1 phosphorylates the central regulator EIN2 to control ethylene hormone signaling from the ER membrane to the nucleus in Arabidopsis. *PNAS*, 109(47), 19486–19491.

## References

---

- Kaló, P., Gleason, C., Edwards, A., Marsh, J., Mitra, R. M., Hirsch, S., Jakab, J., Sims, S., Long, S. R., Rogers, J., Kiss, G. B., Downie, J. A., & Oldroyd, G. E. D. (2005). Nodulation signaling in legumes requires NSP2, a member of the GRAS family of transcriptional regulators. *Science*, *308*(5729), 1786–1789.
- Kamel, L., Keller-Pearson, M., Roux, C., & Ané, J. M. (2017). Biology and evolution of arbuscular mycorrhizal symbiosis in the light of genomics. *New Phytologist*, *213*(2), 531–536.
- Kendrick, M. D., & Chang, C. (2008). Ethylene signaling: new levels of complexity and regulation. *Current Opinion in Plant Biology*, *11*(5), 479–485.
- Kew, O. M., & Douglas, H.C. (1976). Genetic Co-Regulation of Galactose and Melibiose Utilization in *Saccharomyces*. *Journal of Bacteriology*, *125*(1), 9.
- Keymer, A., Pimprikar, P., Wewer, V., Huber, C., Brands, M., Bucerius, S. L., Delaux, P. M., Klingl, V., von Röpenack-Lahaye, E., Wang, T. L., Eisenreich, W., Dörmann, P., Parniske, M., & Gutjahr, C. (2017). Lipid transfer from plants to arbuscular mycorrhiza fungi. *ELife*, *6*(29107).
- Kieber, J. J., Rothenberg, M., Roman, G., Feldmann, K. A., & Ecker, J. R. (1993). CTR1, a negative regulator of the ethylene response pathway in arabidopsis, encodes a member of the Raf family of protein kinases. *Cell*, *72*(3), 427–441.
- Kobae, Y., & Hata, S. (2010). Dynamics of periarbuscular membranes visualized with a fluorescent phosphate transporter in arbuscular mycorrhizal roots of rice. *Plant and Cell Physiology*, *51*(3), 341–353.
- Kobae, Y., Tamura, Y., Takai, S., Banba, M., & Hata, S. (2010). Localized expression of arbuscular mycorrhiza-inducible ammonium transporters in soybean. *Plant and Cell Physiology*, *51*(9), 1411–1415.
- Kosuta, S., Hazledine, S., Sun, J., Miwa, H., Morris, R. J., Downie, J. A., & Oldroyd, G. E. D. (2008). Differential and chaotic calcium signatures in the symbiosis signaling pathway of legumes. *Proceedings of the National Academy of Sciences*, *105*(28), 9823–9828.
- Kosuta, S., Chabaud, M., Loughnon, G., Gough, C., Dénarié, J., Barker, D. G., & Bécard, G. (2003). A diffusible factor from arbuscular mycorrhizal fungi induces symbiosis-specific MtENOD11 expression in roots of *Medicago truncatula*. *Plant Physiology*, *131*(3), 952–962.

## References

---

- Kuhn, H., Küster, H., & Requena, N. (2010). Membrane steroid-binding protein 1 induced by a diffusible fungal signal is critical for mycorrhization in *Medicago truncatula*. *New Phytologist*, *185*(3), 716–733.
- Lacey, R. F., & Binder, B. M. (2014). How plants sense ethylene gas - The ethylene receptors. *Journal of Inorganic Biochemistry*, *133*, 58–62.
- Laffont, C., Rey, T., André, O., Novero, M., Kazmierczak, T., Debelle, F., Bonfante, P., Jacquet, C., & Frugier, F. (2015). The CRE1 cytokinin pathway is differentially recruited depending on *Medicago truncatula* root environments and negatively Regulates resistance to a pathogen. *PLoS ONE*, *10*(1), 1–19.
- Laloum, T., De Mita, S., Gamas, P., Baudin, M., & Niebel, A. (2013). Erratum to: “CCAAT-box binding transcription factors in plants: Y so many?”. [Trends in Plant Science 18 (2013), 157-166]. *Trends in Plant Science*, *18*(10), 594–595.
- Lee, J. H., Hong, J. P., Oh, S. K., Lee, S., Choi, D., & Woo, T. K. (2004). The ethylene-responsive factor like protein 1 (CaERFLP1) of hot pepper (*Capsicum annuum* L.) interacts in vitro with both GCC and DRE/CRT sequences with different binding affinities: Possible biological roles of CaERFLP1 in response to pathogen infection a. *Plant Molecular Biology*, *55*(1), 61–81.
- Lee, J. Y., Colinas, J., Wang, J. Y., Mace, D., Ohler, U., & Benfey, P. N. (2006). Transcriptional and posttranscriptional regulation of transcription factor expression in *Arabidopsis* roots. *PNAS*, *103*(15), 6055–6060.
- Limpens, E., Ramos, J., Franken, C., Raz, V., Compaan, B., Franssen, H., Bisseling, T., & Geurts, R. (2004). RNA interference in *Agrobacterium rhizogenes*-transformed roots of *Arabidopsis* and *Medicago truncatula*. *Journal of Experimental Botany*, *55*(399), 983–992.
- Liu, F., Xu, Y., Wang, H., Zhou, Y., Cheng, B., & Li, X. (2020). APETALA 2 transcription factor CBX1 is a regulator of mycorrhizal symbiosis and growth of *Lotus japonicus*. *Plant Cell Reports*, *39*(4), 445–455.
- Liu, W., Kohlen, W., Lillo, A., Op den Camp, R., Ivanov, S., Hartog, M., Limpens, E., Jamil, M., Smaczniak, C., Kaufmann, K., Yang, W.-C., Hooiveld, G. J. E. J., Charnikhova, T., Bouwmeester, H. J., Bisseling, T., & Geurts, R. (2011). Strigolactone Biosynthesis in *Medicago truncatula* and Rice Requires the Symbiotic GRAS-Type Transcription Factors NSP1 and NSP2. *The Plant Cell*, *23*(10), 3853–3865.
- Lotan, T., Ohto, M. A., Matsudaira Yee, K., West, M. A. L., Lo, R., Kwong, R. W., Yamagishi,

## References

---

- K., Fischer, R. L., Goldberg, R. B., & Harada, J. J. (1998). Arabidopsis LEAFY COTYLEDON1 is sufficient to induce embryo development in vegetative cells. *Cell*, 93(7), 1195–1205.
- Loth-Pereda, V., Orsini, E., Courty, P. E., Lota, F., Kohler, A., Diss, L., Blaudez, D., Chalot, M., Nehls, U., Bucher, M., & Martin, F. (2011). Structure and expression profile of the phosphate pht1 transporter gene family in mycorrhizal *Populus trichocarpa* 1spi. *Plant Physiology*, 156(4), 2141–2154.
- Luginbuehl, L. H., Menard, G. N., Kurup, S., Van Erp, H., Radhakrishnan, G. V., Breakspear, A., Oldroyd, G. E. D., & Eastmond, P. J. (2017). Fatty acids in arbuscular mycorrhizal fungi are synthesized by the host plant. *Science*, 356(6343), 1175–1178.
- Maeo, K., Tokuda, T., Ayame, A., Mitsui, N., Kawai, T., Tsukagoshi, H., Ishiguro, S., & Nakamura, K. (2009). An AP2-type transcription factor, WRINKLED1, of Arabidopsis thaliana binds to the AW-box sequence conserved among proximal upstream regions of genes involved in fatty acid synthesis. *Plant Journal*, 60(3), 476–487.
- Maere, S., De Bodt, S., Raes, J., Casneuf, T., Van Montagu, M., Kuiper, M., & Van De Peer, Y. (2005). Modeling gene and genome duplications in eukaryotes. *PNAS*, 102(15), 5454–5459.
- Maillet, F., Poinot, V., André, O., Puech-Pagés, V., Haouy, A., Gueunier, M., Cromer, L., Giraudet, D., Formey, D., Niebel, A., Martinez, E. A., Driguez, H., Bécard, G., & Dénarié, J. (2011). Fungal lipochitooligosaccharide symbiotic signals in arbuscular mycorrhiza. *Nature*, 469(7328), 58–64.
- Mantovani, R. (1999). The molecular biology of the CCAAT-binding factor NF-Y. *Gene*, 239, 15–27.
- Mantovanis, R., Li, X., Pessaràn, U., Huisjdijnenll, R. H. Van, Benoist, C., & Mathis, D. (1994). Dominant negative analogs of NF-YA \* NF-YA. *Journal of Biological Chemistry*, 269(32), 20340–20346.
- Middleton, P. H., Jakab, J., Penmetsa, R. V., Starker, C. G., Doll, J., Kaló, P., Prabhu, R., Marsh, J. F., Mitra, R. M., Kereszt, A., Dudas, B., VandenBosch, K., Long, S. R., Cook, D. R., Kiss, G. B., & Oldroyd, G. E. D. (2007). An ERF transcription factor in *Medicago truncatula* that is essential for Nod factor signal transduction. *The Plant Cell*, 19(4), 1221–1234.

## References

---

- Moreau, S., Fromentin, J., Vailleau, F., Vernié, T., Huguet, S., Balzergue, S., Frugier, F., Gamas, P., & Jardinaud, M. F. (2014). The symbiotic transcription factor MtEFD and cytokinins are positively acting in the *Medicago truncatula* and *Ralstonia solanacearum* pathogenic interaction. *New Phytologist*, *201*, 1343-1357.
- Morton, J. B., & Benny, G. L. (1990). Revised classification of arbuscular mycorrhizal fungi (Zygomycetes): a new order, Glomales, two new suborders, Glomineae and Gigasporineae, and two new families, Acaulosporaceae and Gigasporaceae with an emendation of Glomaceae. *Mycotaxon*, *37*, 471–1491.
- Mu, J., Tan, H., Zheng, Q., Fu, Y., Liang, Y., Zhang, J., Yang, X., Wang, T., Chong, K., Wang, X. J., & Zuo, J. (2008). LEAFY COTYLEDON1 is a key regulator of fatty acid biosynthesis in *Arabidopsis*. *Plant Physiology*, *148*(2), 1042–1054.
- Mukherjee, A., & Ané, J. M. (2011). Germinating spore exudates from arbuscular mycorrhizal fungi: Molecular and developmental responses in plants and their regulation by ethylene. *Molecular Plant-Microbe Interactions*, *24*(2), 260–270.
- Nagy, R., Karandashov, V., Chague, V., Kalinkevich, K., Tamasloukht, M., Xu, G., Jakobsen, I., Levy, A. A., Amrhein, N., & Bucher, M. (2005). The characterization of novel mycorrhiza-specific phosphate transporters from *Lycopersicon esculentum* and *Solanum tuberosum* uncovers functional redundancy in symbiotic phosphate transport in solanaceous species. *Plant Journal*, *42*(2), 236–250.
- Oláh, B., Brière, C., Bécard, G., Dénarié, J., & Gough, C. (2005). Nod factors and a diffusible factor from arbuscular mycorrhizal fungi stimulate lateral root formation in *Medicago truncatula* via the DMI1/DMI2 signalling pathway. *Plant Journal*, *44*(2), 195–207.
- Paracer, S., & Ahmadjian, V. (1986). *Symbiosis: An Introduction to Biological Associations*. (1st ed.), Oxford University Press.
- Park, H. J., Floss, D. S., Levesque-Tremblay, V., Bravo, A., & Harrison, M. J. (2015). Hyphal branching during arbuscule development requires reduced arbuscular mycorrhiza. *Plant Physiology*, *169*(4), 2774–2788.
- Peng, J., Carol, P., Richards, D. E., King, K. E., Cowling, R. J., Murphy, G. P., & Harberd, N. P. (1997). The *Arabidopsis* GAI gene defines a signaling pathway that negatively regulates gibberellin responses. *Genes and Development*, *11*(23), 3194–3205.



## References

---

- Pimprikar, P., Carbonnel, S., Paries, M., Katzer, K., Klingl, V., Bohmer, M. J., Karl, L., Floss, D. S., Harrison, M. J., Parniske, M., & Gutjahr, C. (2016). A CCaMK-CYCLOPS-DELLA complex activates transcription of RAM1 to regulate arbuscule branching. *Current Biology*, 26(8), 987–998.
- Poulin, R. (2007). Evolutionary ecology of parasites. (2nd ed.) *Princeton University Press*.
- Pumplin, N., & Harrison, M. J. (2009). Live-Cell Imaging Reveals Periarbuscular Membrane Domains and Organelle Location in *Medicago truncatula* Roots during Arbuscular Mycorrhizal Symbiosis. *Plant Physiology*, 151(2), 809–819.
- Pumplin, N., Zhang, X., Noar, R. D., & Harrison, M. J. (2012). Polar localization of a symbiosis-specific phosphate transporter is mediated by a transient reorientation of secretion. *Proceedings of the National Academy of Sciences of the United States of America*, 109(11), 665–672.
- Pysh, L. D., Wysocka-Diller, J. W., Camilleri, C., Bouchez, D., & Benfey, P. N. (1999). The GRAS gene family in *Arabidopsis*: Sequence characterization and basic expression analysis of the SCARECROW-LIKE genes. *Plant Journal*, 18(1), 111–119.
- Quandt, H., Pühler, A., & Broer, I. (1993). Transgenic root-nodules of *vicia-hirsuta* - a fast and efficient system for the study of gene-expression in indeterminate-type nodules. *Molecular Plant-Microbe Interactions*, 6(6), 699–704.

## References

---

- Raikhel, N. (1992). Nuclear targeting in plants. *Plant Physiology*, *100*(4), 1627–1632. <https://doi.org/10.1104/pp.100.4.1627>
- Rangan, V. S., Oskouian, B., & Smith, S. (1996). Identification of an inverted CCAAT box motif in the fatty-acid synthase gene as an essential element for mediation of transcriptional regulation by cAMP. *Journal of Biological Chemistry*, *271*(4), 2307–2312. <https://doi.org/10.1074/jbc.271.4.2307>
- Rich, M. K., Schorderet, M., Bapaume, L., Falquet, L., Morel, P., Vandenbussche, M., & Reinhardt, D. (2015). The petunia GRAS transcription factor ATA/RAM1 regulates symbiotic gene expression and fungal morphogenesis in arbuscular mycorrhiza. *Plant Physiology*, *168*(3), 788–797. <https://doi.org/10.1104/pp.15.00310>
- Roder, K., Wolf, S. S., Beck, K. F., Sickinger, S., & Schweizer, M. (1997). NF-Y binds to the inverted CCAAT box, an essential element for cAMP-dependent regulation of the rat fatty acid synthase (FAS) gene. *Gene*, *184*(1), 21–26. [https://doi.org/10.1016/S0378-1119\(96\)00568-9](https://doi.org/10.1016/S0378-1119(96)00568-9)
- Romier, C., Cocchiarella, F., Mantovani, R., & Moras, D. (2003). The NF-YB/NF-YC structure gives insight into DNA binding and transcription regulation by CCAAT factor NF-Y. *Journal of Biological Chemistry*, *278*(2), 1336–1345. <https://doi.org/10.1074/jbc.M209635200>
- Ropars, J., Toro, K. S., Noel, J., Pelin, A., Charron, P., Farinelli, L., Marton, T., Krüger, M., Fuchs, J., Brachmann, A., & Corradi, N. (2016). Evidence for the sexual origin of heterokaryosis in arbuscular mycorrhizal fungi. *Nature Microbiology*, *1*(6). <https://doi.org/10.1038/nmicrobiol.2016.33>
- Sakuma, Y., Liu, Q., Dubouzet, J. G., Abe, H., Yamaguchi-Shinozaki, K., & Shinozaki, K. (2002). DNA-binding specificity of the ERF/AP2 domain of Arabidopsis DREBs, transcription factors involved in dehydration- and cold-inducible gene expression. *Biochemical and Biophysical Research Communications*, *290*(3), 998–1009. <https://doi.org/10.1006/bbrc.2001.6299>
- Santos-Mendoza, M., Dubreucq, B., Baud, S., Parcy, F., Caboche, M., & Lepiniec, L. (2008). Deciphering gene regulatory networks that control seed development and maturation in Arabidopsis. *Plant Journal*, *54*(4), 608–620. <https://doi.org/10.1111/j.1365-313X.2008.03461.x>
- Schwarzott, D., & Walker, C. (2001). A new fungal phylum, the Glomeromycota: phylogeny and evolution \*. *Mycol. Res.*, *105*(12), 1413–1421.

## References

---

- Schweizer, M., Roder, K., Zhang, L., & Wolf, S. S. (2002). Transcription factors acting on the promoter of the rat fatty acid synthase gene. *Biochemical Society Transactions*, 30(6), 1070–1072. <https://doi.org/10.1042/BST0301070>
- Shen, B., Allen, W. B., Zheng, P., Li, C., Glassman, K., Ranch, J., Nubel, D., & Tarczynski, M. C. (2010). Expression of ZmLEC1 and ZmWRI1 increases seed oil production in maize. *Plant Physiology*, 153(3), 980–987. <https://doi.org/10.1104/pp.110.157537>
- Siefers, N., Dang, K. K., Kumimoto, R. W., Bynum IV, W. E., Tayrose, G., & Holt, B. F. (2009). Tissue-specific expression patterns of Arabidopsis NF-Y transcription factors suggest potential for extensive combinatorial complexity. *Plant Physiology*, 149(2), 625–641. <https://doi.org/10.1104/pp.108.130591>
- Sinha, S., Kim, I. S., Sohn, K. Y., de Crombrughe, B., & Maity, S. N. (1996). Three classes of mutations in the A subunit of the CCAAT-binding factor CBF delineate functional domains involved in the three-step assembly of the CBF-DNA complex. *Molecular and Cellular Biology*, 16(1), 328–337. <https://doi.org/10.1128/mcb.16.1.328>
- Solano, R., Stepanova, A., Chao, Q., & Ecker, J. R. (1998). Nuclear events in ethylene signaling: A transcriptional cascade mediated by ETHYLENE-INSENSITIVE3 and ETHYLENE-RESPONSE-FACTOR1. *Genes and Development*, 12(23), 3703–3714. <https://doi.org/10.1101/gad.12.23.3703>
- Son, G. H., Wan, J., Kim, H. J., Nguyen, X. C., Chung, W. S., Hong, J. C., & Stacey, G. (2012). Ethylene-responsive element-binding factor 5, ERF5, is involved in chitin-induced innate immunity response. *Molecular Plant-Microbe Interactions*, 25(1), 48–60. <https://doi.org/10.1094/MPMI-06-11-0165>
- Sun, J., Miller, J. B., Granqvist, E., Wiley-Kalil, A., Gobbato, E., Maillet, F., Cottaz, S., Samain, E., Venkateshwaran, M., Fort, S., Morris, R. J., Ané, J. M., Dénarié, J., & Oldroyd, G. E. D. (2015). Activation of symbiosis signaling by arbuscular mycorrhizal fungi in legumes and rice. *Plant Cell*, 27(3), 823–838. <https://doi.org/10.1105/tpc.114.131326>
- Sun, X., Ling, S., Lu, Z., Ouyang, Y. dan, Liu, S., & Yao, J. (2014). OsNF-YB1, a rice endosperm-specific gene, is essential for cell proliferation in endosperm development. *Gene*, 551(2), 214–221. <https://doi.org/10.1016/j.gene.2014.08.059>
- Tang, N., San Clemente, H., Roy, S., Bécard, G., Zhao, B., & Roux, C. (2016). A Survey of the gene repertoire of Gigaspora rosea unravels conserved features among glomeromycota for obligate biotrophy. *Frontiers in Microbiology*, 7(3).

## References

---

- <https://doi.org/10.3389/fmicb.2016.00233>
- Tian, C., Wan, P., Sun, S., Li, J., & Chen, M. (2004). Genome-wide analysis of the GRAS gene family in rice and Arabidopsis. *Plant Molecular Biology*, *54*(4), 519–532. <https://doi.org/10.1023/B:PLAN.0000038256.89809.57>
- Tisserant, E., Malbreil, M., Kuo, A., Kohler, A., Symeonidi, A., Balestrini, R., Charron, P., Duensing, N., Frei dit Frey, N., Gianinazzi-Pearson, V., Gilbert, L. B., Handa, Y., Herr, J. R., Hijri, M., Koul, R., Kawaguchi, M., Krajinski, F., Lammers, P. J., Masclaux, F. G., ... Martin, F. (2013). Genome of an arbuscular mycorrhizal fungus provides insight into the oldest plant symbiosis. *PNAS*, *110*(50), 20117–20122. <https://doi.org/10.1073/pnas.1313452110>
- Tong, H., Jin, Y., Liu, W., Li, F., Fang, J., Yin, Y., Qian, Q., Zhu, L., & Chu, C. (2009). DWARF and LOW-TILLERING, a new member of the GRAS family, plays positive roles in brassinosteroid signaling in rice. *Plant Journal*, *58*(5), 803–816. <https://doi.org/10.1111/j.1365-313X.2009.03825.x>
- Trépanier, M., Bécard, G., Moutoglis, P., Willemot, C., Gagné, S., Avis, T. J., & Rioux, J. A. (2005a). Dependence of arbuscular-mycorrhizal fungi on their plant host for palmitic acid synthesis. *Applied and Environmental Microbiology*, *71*(9), 5341–5347. <https://doi.org/10.1128/AEM.71.9.5341-5347.2005>
- Vernie, T., Moreau, S., de Billy, F., Plet, J., Combiér, J.-P., Rogers, C., Oldroyd, G., Frugier, F., Niebel, A., & Gamas, P. (2008). EFD Is an ERF Transcription Factor Involved in the Control of Nodule Number and Differentiation in *Medicago truncatula*. *The Plant Cell Online*, *20*, 2696–2713. <https://doi.org/10.1105/tpc.108.059857>
- Walder, F., Brulé, D., Koegel, S., Wiemken, A., Boller, T., & Courty, P. E. (2015). Plant phosphorus acquisition in a common mycorrhizal network: Regulation of phosphate transporter genes of the Pht1 family in sorghum and flax. *New Phytologist*, *205*(4), 1632–1645. <https://doi.org/10.1111/nph.13292>
- Walter, M., Chaban, C., Schütze, K., Batistic, O., Weckermann, K., Näke, C., Blazevic, D., Grafen, C., Schumacher, K., Oecking, C., Harter, K., & Kudla, J. (2004). Visualization of protein interactions in living plant cells using bimolecular fluorescence complementation. *Plant Journal*, *40*(3), 428–438. <https://doi.org/10.1111/j.1365-313X.2004.02219.x>
- Wang, E., Schornack, S., Marsh, J. F., Gobbato, E., Schwessinger, B., Eastmond, P., Schultze, M., Kamoun, S., & Oldroyd, G. E. D. (2012). A common signaling process

## References

---

- that promotes mycorrhizal and oomycete colonization of plants. *Current Biology*, 22(23), 2242–2246. <https://doi.org/10.1016/j.cub.2012.09.043>
- Wenkel, S., Turck, F., Singer, K., Gissot, L., Le Gourrierec, J., Samach, A., & Coupland, G. (2006). CONSTANS and the CCAAT box binding complex share a functionally important domain and interact to regulate flowering of Arabidopsis. *Plant Cell*, 18(11), 2971–2984. <https://doi.org/10.1105/tpc.106.043299>
- Wewer, V., Brands, M., & Dörmann, P. (2014). Fatty acid synthesis and lipid metabolism in the obligate biotrophic fungus *Rhizophagus irregularis* during mycorrhization of *Lotus japonicus*. *Plant Journal*, 79(3), 398–412. <https://doi.org/10.1111/tpj.12566>
- Wilson, E. (1975). *Sociobiology: The New Synthesis*. Harvard University Press.
- Wu, L., Chen, X., Ren, H., Zhang, Z., Zhang, H., Wang, J., Wang, X. C., & Huang, R. (2007). ERF protein JERF1 that transcriptionally modulates the expression of abscisic acid biosynthesis-related gene enhances the tolerance under salinity and cold in tobacco. *Planta*, 226(4), 815–825. <https://doi.org/10.1007/s00425-007-0528-9>
- Xie, Z., Li, X., Glover, B. J., Bai, S., Rao, G. Y., Luo, J., & Yang, J. (2008). Duplication and functional diversification of HAP3 genes leading to the origin of the seed-developmental regulatory gene, LEAFY COTYLEDON1 (LEC1), in nonseed plant genomes. *Molecular Biology and Evolution*, 25(8), 1581–1592. <https://doi.org/10.1093/molbev/msn105>
- Xing, Y., Zhang, S., Olesen, J. T., Rich, A., & Guarente, L. (1994). Subunit interaction in the CCAAT-binding heteromeric complex is mediated by a very short  $\alpha$ -helix in HAP2. *PNAS*, 91(8), 3009–3013. <https://doi.org/10.1073/pnas.91.8.3009>
- Xu, J. J., Zhang, X. F., & Xue, H. W. (2016). Rice aleurone layer specific OsNF-YB1 regulates grain filling and endosperm development by interacting with an ERF transcription factor. *Journal of Experimental Botany*, 67(22), 6399–6411. <https://doi.org/10.1093/jxb/erw409>
- Xue, L., Cui, H., Buer, B., Vijayakumar, V., Delaux, P. M., Junkermann, S., & Bucher, M. (2015). Network of GRAS transcription factors involved in the control of arbuscule development in *Lotus japonicus*. *Plant Physiology*, 167(3), 854–871. <https://doi.org/10.1104/pp.114.255430>
- Xue, L., Klinnawee, L., Zhou, Y., Saridis, G., Vijayakumar, V., Brands, M., Dörmann, P., Gigolashvili, T., Turck, F., & Bucher, M. (2018). AP2 transcription factor CBX1 with a specific function in symbiotic exchange of nutrients in mycorrhizal *Lotus japonicus*.

## References

---

- PNAS*, 115(39), E9239–E9246. <https://doi.org/10.1073/pnas.1812275115>
- Yamasaki, K., Kigawa, T., Seki, M., Shinozaki, K., & Yokoyama, S. (2013). DNA-binding domains of plant-specific transcription factors: structure, function, and evolution. *Trends in Plant Science*, 18(5), 267–276. <https://doi.org/10.1016/j.tplants.2012.09.001>
- Yang, S. Y., Grønlund, M., Jakobsen, I., Grotemeyer, M. S., Rentsch, D., Miyao, A., Hirochika, H., Kumar, C. S., Sundaresan, V., Salamin, N., Catausan, S., Mattes, N., Heuer, S., & Paszkowski, U. (2012). Nonredundant regulation of rice arbuscular mycorrhizal symbiosis by two members of the PHOSPHATE TRANSPORTER1 gene family. *Plant Cell*, 24(10), 4236–4251. <https://doi.org/10.1105/tpc.112.104901>
- Yoneyama, K., Xie, X., Kusumoto, D., Sekimoto, H., Sugimoto, Y., Takeuchi, Y., & Yoneyama, K. (2007). Nitrogen deficiency as well as phosphorus deficiency in sorghum promotes the production and exudation of 5-deoxystrigol, the host recognition signal for arbuscular mycorrhizal fungi and root parasites. *Planta*, 227(1), 125–132. <https://doi.org/10.1007/s00425-007-0600-5>
- Zhang, G., Chen, M., Li, L., Xu, Z., Chen, X., Guo, J., & Ma, Y. (2009). Overexpression of the soybean GmERF3 gene, an AP2/ERF type transcription factor for increased tolerances to salt, drought, and diseases in transgenic tobacco. *Journal of Experimental Botany*, 60(13), 3781–3796. <https://doi.org/10.1093/jxb/erp214>
- Zhang, J. Y., Broeckling, C. D., Blancaflor, E. B., Sledge, M. K., Sumner, L. W., & Wang, Z. Y. (2005). Overexpression of WXP1, a putative *Medicago truncatula* AP2 domain-containing transcription factor gene, increases cuticular wax accumulation and enhances drought tolerance in transgenic alfalfa (*Medicago sativa*). *Plant Journal*, 42(5), 689–707. <https://doi.org/10.1111/j.1365-313X.2005.02405.x>
- Zhang, Q., Blaylock, L. A., & Harrison, M. J. (2010). Two *Medicago truncatula* half-ABC transporters are essential for arbuscule development in arbuscular mycorrhizal symbiosis. *Plant Cell*, 22(5), 1483–1497. <https://doi.org/10.1105/tpc.110.074955>
- Zhao, X. C., & Schaller, G. E. (2004). Effect of salt and osmotic stress upon expression of the ethylene receptor ETR1 in *Arabidopsis thaliana*. *FEBS Letters*, 562(1–3), 189–192. [https://doi.org/10.1016/S0014-5793\(04\)00238-8](https://doi.org/10.1016/S0014-5793(04)00238-8)
- Zhiguo, E., Li, T., Zhang, H., Liu, Z., Deng, H., Sharma, S., Wei, X., Wang, L., Niu, B., & Chen, C. (2018). A group of nuclear factor y transcription factors are sub-functionalized during endosperm development in monocots. *Journal of Experimental Botany*, 69(10), 2495–2510. <https://doi.org/10.1093/jxb/ery087>

## References

---

Zhou, C., Zhang, L., Duan, J., Miki, B., & Wu, K. (2005). Histone Deacetylase19 is involved in jasmonic acid and ethylene signaling of pathogen response in Arabidopsis. *Plant Cell*, 17(4), 1196–1204. <https://doi.org/10.1105/tpc.104.028514>

## **Theses**

Krüger, A. (2020). Expressions- und Funktionsanalysen von ERF Transkriptionsfaktor-  
genen in der arbuskulären Mykorrhiza. B.Sc. Thesis (LUH)

Pallokat, P. (2016). Funktionelle Analyse von ERF Transkriptionsfaktor-Genen in der  
arbuskulären Mykorrhiza-Symbiose von *Medicago truncatula*. M.Sc. Thesis (LUH)

Hartmann, R. (2018). Functional analysis of arbuscular mycorrhiza-related GRAS  
transcription factor genes of *Medicago truncatula*. PhD Thesis (LUH)

## Abbreviations

°C	degree Celsius
µg	microgram
µl	microliter
µM	micromolar
A	Aureobasidin
ABC	ATP-binding cassette
AD	GAL4 activation domain
Ade	Adenine
AM	arbuscular mycorrhiza
AMF	arbuscular mycorrhiza fungi
amiRNA	artificial micro RNA
Ap	ampicillin
Appr.	approximately
Arb	arbuscule
ATP	adenosine triphosphate
BD	GAL4 DNA binding domain
BLAST	basic local alignment search tool
Bp	base pairs
BSA	bovine serum albumin
BiFC	Bimolecular fluorescence complementation
C	carbon
Ca	calcium
CBF	CAAT-box binding factor
CDS	codon determining sequence
CFP	cyan fluorescent protein
Cm	centimeter
COs	chitooligosaccharides
CP	cytoplasm
Ctr	copper transporter
Cu	copper
DDO	double dropout medium
Dm	dry matter
DMSO	dimethylsulfoxide
DNA	deoxyribonucleic acid
Dpi	days post inoculation



## Abbreviations

---

dsRed	<i>discosoma</i> Red
DTT	dithiothreitol
e. g.	<i>exemplii gratia</i>
EDTA	ethylene-diamine-tetra-acetate
ER	endoplasmatic reticulum
ERF	ethylene-responsive factor
et al.	<i>et alii</i>
Fe	ferrum
g	gramm
GRAS	gibberellin-insensitive ( <u>G</u> AI), repressor of gal1-3 ( <u>R</u> GA), or scarecrow ( <u>S</u> CR)
GPAT	glycerole phosphate-O-acyltransferase
GUS	$\beta$ -glucuronidase
h	hours
His	Histidine
ID	identifier
IPTG	isopropyle- $\beta$ -D-thiogalactopyranoside
LB	left border
K	potassium
Km	Kanamycin
Leu	Leucine
LCOs	lipo-chitooligosaccharides
LiAc	Lithium acetate
LMPC	Laser microdissect and pressure catapulting
M	molar
m	milli
Mg	magnesium
ml	milliliter
mM	millimolar
Mn	manganese
MOPS	3-Morpholinopropane-1-sulfonic acid
mRNA	messenger RNA
Mt	<i>Medicago truncatula</i>
Myc-factor	factor for mycorrhization
Myk-	not mycorrhized
Myk+	mycorrhized
n	number of biological replicates

## Abbreviations

---

N	nitrogen
NF-Y	Nuclear factor Y
Ng	nanogram
nm	nanometer
Nod-factor	factor for nodulation
p	promoter
P	phosphate
PA	Penassay
PAM	periarbuscular membrane
PAS	periarbuscular space
PBS	physiologically buffered saline
PCR	polymerase chain reaction
pH	<i>pondus hydrogenii</i>
PPA	pre-penetration apparatus
QDO	quadruple dropout media
RAM1	reduced arbuscular mycorrhization 1
RB	right border
RFP	red fluorescent protein
RNA	ribonucleic acids
RNAi	RNA interference
rpm	rounds per minute
RT	reverse transcription
RT-PCR	Reverse transcription polymerase chain reaction
SD	single dropout
sec	seconds
Spec	Spectomycin
Strep	Streptomycin
t	time
TA	Tris acetate
TF	transcription factor
Trp	Tryptophan
TY	tryptone yeast
U	units
UTR	untranslated region
vs	versus
w/v	weight per volume

## Abbreviations

---

WGA	wheat germ agglutinin
Wt	wild type
Y1H	Yeast-1-Hybrid
Y2H	Yeast-2-Hybrid
YPDA	yeast peptone dextrose adenine hemisulfate
Zn	zinc
$\beta$ -MAG	$\beta$ -monoacyl glycerol

## **Acknowledgement**

I received a great deal of support and assistance throughout performing and writing this thesis.

I would first like to thank my supervisor, Professor Dr. Helge Küster, for the opportunity to work on this interesting and challenging project. Your expertise was invaluable in formulating the research questions and methodology. Furthermore, you always took your time to discuss open questions and new experiments adding an interesting story to this thesis.

I would also like to thank my supervisor, Dr. Natalija Hohnjec, for your valuable guidance throughout my studies. You introduced me into the methods used in the AG Küster and participated in a lot of discussions concerning the data I obtained and further experiments. I wish to thank the Deutsche Forschungsgemeinschaft for financial support in frame of DFG Research Training Group GRK1798 "Signaling at the Plant-Soil Interface".

Special thanks to Professor Dr. Debener and Dr. Offermann for taking on the role of chairman and examiner.

Many thanks to the whole team of the AG Küster who contributed to this thesis with advice and interesting discussions. Hereby, I especially want to thank Steven Krüger with whom I shared an office (and later a lab). Together, we performed these nice interaction studies showing a connection between NF-Y and ERF TFs that gave my results an interesting spin. I also want to thank Dr. Marian Uhe and Dr. Rico Hartmann for their introduction into the methods used in the lab and a lot of interesting discussions. Furthermore, I want to thank Arne Petersen for discussion and advice (especially on the BiFC experiments). Special thanks also to Natascha Köppens for her help throughout my time in the lab.

I want to thank the whole GRK 1798 for interesting discussions, conferences, and the social events. I had a great time with all of you and enjoyed being part of this DFG funded group. Finally, I would like to thank my family and my partner Robert for their love and support during this thesis.

## Curriculum Vitae

Lisa Hartung

Nationality: German

Date of birth: 13.12.1989

Place of birth: Bamberg

### work experiences

since 12/2020

Medical Content Developer at CAST PHARMA, Dresden

10/2016 – 09/2020

doctoral researcher in the Institute of Plant genetics, Leibniz Universität Hannover (Graduate school 1798, DFG funded)

Topic: Ethylen responsive transcription factors orchestrating AM-dependent fatty acid biosynthesis act in complexes with Nuclear Factor-Y TFs and the key AM regulator RAM1

10/2015 - 09/2016

research assistant in the teaching innovations project „*GENau nachgefragt!* - *Gentechnik, Ethik, Natur an der TU Braunschweig*“ (gene technologies, ethics and nature at the TU Braunschweig) in the department of fungal genetics, TU Braunschweig

Tasks: teaching and administration of a student initiative, conception of a teaching module (ethic in natural sciences for biologists), organization of excursions and roundtable discussions, planning and moderation of public appearances, creating and maintaining of a website/ blog

12/2011 - 04/2014

research assistant

Tasks: preparation and supervision of the B.Sc. biology lab course in genetics

### Education

10/2013 - 12/2015

*Master of Science*, biology (TU Braunschweig) with a focus on genetics, cell biology and infection biology

10/2010 – 09/2013

*Bachelor of Science*, biology (TU Braunschweig) with a focus on molecular biology and chemistry

06/2009

German Abitur (at Wigbertschule Hünfeld)

### stays abroad

09/2009 – 03/2010

work and travel in Spain (intensive language training, entertainer at a hotel in Fuerteventura, language assistant for English in Madrid)

**further qualifications**

further training:

GMP certification

*Projektleiterkurs nach § 15 (4) der Gentechnik-Sicherheitsverordnung* (Safety Aspects in Genetic Engineering for project leaders and inspectors for biological safety, related to § 15 GenTSV)

certificate „*Basisqualifizierung in der Lehre*“ (qualification in teaching basics at TU Braunschweig; teach4TU)

certificate *Promotion+plus qualifiziert* (add-on qualification during this thesis with an emphasis on career planning, professional key competences, management competences)

**Publication list**

06/2019

Schumann, M. R., Brandt, U., Adis, C., Hartung, L., Fleißner, A. (2019): The penta-EF-hand protein PEF1 of *Neurospora crassa* promotes plasma membrane integrity during cell-cell fusion and in response to pore-forming drugs. *Genetics* 213(1):195-211